Assessing the biogeochemical role and controls of nitrogen fixation in the Eastern Tropical South Pacific

Dissertation
zur Erlangung des
Doktorgrades der Naturwissenschaften

– Dr. rer. nat. –

der **Mathematisch-Naturwissenschaftlichen Fakultät**
der **Christian-Albrechts-Universität zu Kiel**

vorgelegt von

Leila Richards Kittu

Kiel, Juli 2023

Die vorliegende Doktorarbeit wurde in der Zeit von Januar 2019 bis Juli 2023 im Forschungsbereich 2 Marine Biogeochemie, in der Abteilung Biologische Ozeanographie am GEOMAR Helmholtz Zentrum für Ozeanforschung Kiel angefertigt.

Hauptbetreuer und erster Gutachter:	**Prof. Dr. Ulf Riebesell** GEOMAR Helmholtz Zentrum für Ozeanforschung, Kiel
Zweite Gutachterin:	**Prof. Dr. Maren Voss** Leibniz Institute of Baltic Sea Research, Warnemünde.

Abgabe beim Promotionsbüro:	10.07.2023
Tag der mündlichen Prüfung:	07.09.2023
Genehmigt zum Druck:	07.09.2023

To the women in my family, whose boundaries I break, whose wildest dreams I encapsulate, and whose limitations fuel my passions and aspirations!

Table of contents

Summary

The Eastern Tropical South Pacific (ETSP), hosts an extensive Oxygen Minimum Zone (OMZ) in the water column which has a major imprint on local and global marine biogeochemistry. Due to the low oxygen conditions within the OMZ, microbial processes of nitrogen (N) loss, such as anammox and denitrification are sustained in the water column. These processes result in a pronounced N deficit which reduces bioavailable N for primary productivity and thus influences fisheries production in the region. To maintain a balanced marine N inventory regionally in ETSP, the N deficit would have to be compensated by N inputs via upwelling or N_2 fixation. A classical assumption is that N_2 fixation is favoured by iron (Fe) availability and a surplus of inorganic phosphate relative to inorganic nitrogen (this relativity is defined as P*), both conditions are present in the ETSP. Over the past decades, this assumption has been integrated into most coupled circulation and N-cycle biogeochemical models. These models indicate that there is a close spatial link between areas of high N loss, generally confined to OMZs and N_2 fixation. On the contrary, other biogeochemical models have revealed that a close spatial link between N loss and N_2 fixation in the OMZ may give rise to run-away loss of fixed N in the ETSP, ultimately destabilizing the regional marine N inventory. A run-away N loss could have far-reaching consequences for primary productivity in the region, with potential negative cascading effects on the trophic system.

At the onset of this thesis in 2019, there was already a good understanding of the magnitudes and spatial distribution of microbial N loss processes in the ETSP. However, a limited and poor spatial resolution of N_2 fixation rates challenged our understanding of its relevance in the ETSP. Thus, the model results suggesting a spatial coupling between N_2 fixation and N loss in the ETSPs' OMZ are yet to be validated. In particular, it was unclear whether the magnitude of N_2 fixation provide sufficient N inputs required to replenish the local N loss and sustain the high primary productivity in the ETSP. This largely unassessed ecological and biogeochemical role of N_2 fixation impedes a proper assessment of the marine N inventory locally in the ETSP.

The primary objective of this doctorate dissertation was to assess the spatial distribution and biogeochemical relevance of N_2 fixation rates in the ETSP, with a specific focus on the Humboldt Upwelling System (HUS) off the coast of Peru. The first manuscript of this dissertation (Chapter 2), assessed the spatial coupling hypothesis by deciphering the spatial distribution and magnitudes of N_2 fixation in the HUS and the relationship with estimates of N loss. Additionally, I quantified the contribution of coastal N_2 fixation as a new N source for phytoplankton productivity. The study encompassed the North to South region of the HUS from 8°S to 16°S. We covered various intensities of the OMZ, N deficit and gradients in physical and biogeochemical environmental factors including O_2, macro and micronutrients and primary productivity. This study presents the first comprehensive dataset on coastal N_2 fixation rates in the northern HUS. We identified a latitudinal gradient in N_2 fixation rates, with higher rates observed in southern productive waters compared to the northern low-productivity

region. This latitudinal pattern mirrored the intensity of the OMZ, N deficits and nitrite maxima, which are indicative of microbial N loss processes. My results reveal that in austral summer, the HUS is not a hotspot of N_2 fixation due to detectable but low rates measured from coastal euphotic waters, and their further decrease with depth and distance from the coast.

In this dissertation work, I provide a comprehensive synthesis by incorporating N_2 fixation datasets collected from various seasons and years during cruises conducted as part of the Collaborative Research Centre 754 (SFB754). These in-situ measurements allowed us to derive robust conservative estimates of N_2 fixation rates and assess their spatiotemporal distribution in the ETSP. Generally low N_2 fixation rates of less than 5 nmol N L^{-1} d^{-1} were consistently observed across seasons and years. Nonetheless, higher N_2 fixation rates were observed during austral summer, with a significant degree of variability due to sporadic and patchy occurrences of a few high rates above 10 nmol N L^{-1} d^{-1}. When integrated and extrapolated to the entire ETSP, these conservative estimates demonstrate that in-situ N_2 fixation rates are lower than model-predicted estimates, challenging the characterization of the region as a hotspot of N_2 fixation. Overall, this analysis indicates that even during austral summer when coastal N_2 fixation rates are at their peak, they are still lower than model estimates and they contribute only a minor fraction (~0.4%) of the total primary productivity in the coastal HUS. Comparing the estimates of N_2 fixation to the high N loss rates currently observed in the ETSP, it becomes evident that across all seasons, N_2 fixation rates are insufficient to fully replenish local N losses. Thus, from a biogeochemical perspective, our findings suggest that N_2 fixation and N loss in the ETSP are spatially decoupled necessitating higher N_2 fixation in other regions to replenish the N loss occurring in the ETSP.

Insufficient knowledge of the environmental factors that regulate and constrain N_2 fixation has presented challenges in reconciling field observations with model estimates. To address this gap, I went a step further to assess the relationships and interactions between N_2 fixation and environmental predictors influencing its distribution (Chapters 2 & 3). In Chapter 3 of this dissertation, a novel aspect is presented. I highlight the potential for trace metal colimitation involving Fe, cobalt (Co) and nickel (Ni) in regulating N_2 fixation in the HUS. Contrary to the traditional perspective, we demonstrate that N_2 fixation in this region exhibits a weak response to the presence of P* and high Fe conditions along the coast (Chapters 2 and 3). Additionally, we emphasize that the regulation of N_2 fixation in the HUS may involve nonlinear interactions among various environmental factors such as trace metals and phytoplankton-associated organic matter due to the prevalence of non-cyanobacterial diazotrophs (NCDs). Therefore, relying solely on Fe and P concentrations to predict N_2 fixation in the ETSP, without considering other potential interconnected factors may have led to an overestimation of its role in the region. Chapter 3 presents an updated perspective on other potential controls for N_2 fixation in the HUS, which may have been overlooked and require further investigation. Overall, this dissertation work provides valuable insights for future field studies and experiments on the regulation of N_2 fixation in OMZs.

In Chapter 4, I explore nitrate availability from upwelled deep water as a primary nitrogen source for primary productivity in the ETSP. The study focused on understanding how gradients in nitrate concentration and light regulate phytoplankton nitrate and carbon uptake, thereby influencing primary productivity within the HUS. The direct response of natural phytoplankton communities to changes in light and nitrate conditions remains understudied in the HUS. This knowledge gap poses challenges in accurately parameterizing phytoplankton responses within biogeochemical models, which aim to predict the fate of this ecosystem under climate change. My findings reveal that nitrate uptake is limited by nitrate concentrations only under high light intensities, whereas carbon uptake is predominantly nitrate-limited. However, regenerative nitrogen sources such as ammonium may contribute substantially to carbon uptake. Notably, at low nitrate concentrations, carbon uptake was decoupled from nitrate uptake resulting in an above-Redfield uptake ratio of carbon to nitrogen. This non-Redfield behaviour was observed in conjunction with the presence of a mixotrophic phytoplankton community. Consequently, primary productivity in the HUS cannot be simply predicted from light attenuation and concentrations of upwelled nitrate and chlorophyll *a.* The influence of regenerative nutrient uptake and non-Redfield productivity may play a large role in sustaining primary productivity, particularly in mixotrophy-dominated phytoplankton communities. These results have important implications for the parameterisation of phytoplankton responses to light and nutrients used in satellite-based approaches for estimating primary productivity in the HUS.

As we contemplate the future of marine N cycling in the ETSP, it is imperative to understand the current dynamics of N inputs and losses. This dissertation work serves to update our current understanding of the distribution and magnitudes of N_2 fixation and its contribution to primary productivity and the replenishment of N loss in the ETSP. Furthermore, the measured rates enhance the spatial resolution on which large-scale extrapolations of N_2 fixation in the ETSP are based. By elucidating the distribution of N_2 fixation across physicochemical gradients and examining the sensitivity of N_2 fixation rates to changes in Fe and P concentrations within an understudied yet biogeochemically and ecologically significant region (Chapters 2 and 3), this dissertation work contributes to our evolving comprehension of the factors governing N_2 fixation in OMZs. We highlight that the disparity between in-situ N_2 fixation rates and model predictions in the ETSP may largely stem from a limited consideration of other biogeochemical factors that potentially regulate N_2 fixation as well as insufficient knowledge regarding the physiology of non-cyanobacterial N_2 fixers that dominate the ETSP. Furthermore, the notion of N_2 fixation being primarily regulated by Fe and P as widely recognized in the global ocean, may have been overstated for the ETSP. Thus, these findings serve as a valuable foundation for future research on the regulation of marine N_2 fixation especially in the ETSP. Moreover, this dissertation provides insights for parameterisations of N_2 fixation in forthcoming modelling studies that assess the marine nitrogen cycle and its vulnerability to climate change.

Zusammenfassung

Im östlichen tropischen Südpazifik (ETSP) befindet sich eine ausgedehnte Sauerstoffminimumzone (OMZ) in der Wassersäule, die einen erheblichen Einfluss auf die lokale und globale marine Biogeochemie besitzt. Aufgrund der sauerstoffarmen Bedingungen innerhalb der OMZ werden mikrobielle Prozesse des Stickstoffverlustes, wie Anammox und Denitrifikation, in der Wassersäule verstärkt. Diese Prozesse führen zu einem ausgeprägten Stickstoffdefizit, welches die Bioverfügbarkeit des Stickstoffs für die Primärproduktivität und somit die Produktivität der Fischerei insgesamt reduziert. Damit ein ausgewogenes Stickstoffinventar im ETSP lokal aufrechterhalten wird, müsste dieses Stickstoffdefizit durch andere Stickstoffquellen, wie den Auftrieb von Tiefenwasser oder N_2-Fixierung, ausgeglichen werden. Eine weit verbreitete Annahme ist, dass die N_2-Fixierung begünstigt wird durch die Verfügbarkeit von Eisen (Fe) sowie einen Überschuss an anorganischem Phosphat (P) im Verhältnis zum anorganischen Stickstoff (N) (dieses Verhältnis wird als P* definiert), wobei beide Bedingungen im ETSP vorliegen. In den letzten Jahrzehnten wurde diese Annahme in die meisten gekoppelten, biogeochemischen Zirkulations- und Stickstoffzyklusmodelle integriert. Gemäß diesen Modellen besteht ein enger räumlicher Zusammenhang zwischen Bereichen mit hohem Stickstoffverlust, welche sich im Allgemeinen auf die OMZs begrenzen und Bereichen, in denen die N_2-Fixierung stattfindet. Im Gegensatz dazu haben andere biogeochemische Modelle gezeigt, dass ein räumlicher Zusammenhang zwischen einem Stickstoffverlust und der N_2-Fixierung in der OMZ zu einem unkontrollierten Verlust von fixiertem N im ETSP führen könnte, was letztlich das lokale marine Stickstoffinventar destabilisiert. Ein unkontrollierter Verlust von N könnte weitreichende Folgen für die Primärproduktivität in dem Gebiet haben, mit möglichen weiterführenden, negativen Effekten auf das Nahrungsnetz.

Zu Beginn dieser Arbeit im Jahr 2019 hatte man bereits ein gutes Verständnis über die Größenordnung sowie die räumliche Verteilung des mikrobiellen Stickstoffverlustes im ETSP. Andererseits warf aber auch die begrenzte Datenlage und das damit einhergehende unzureichende Wissen über die räumliche Auflösung der N_2-Fixierungsraten Fragen über deren Bedeutung für den ETSP auf. So steht eine Validierung der Ergebnisse der Modelle, die eine räumliche Kopplung zwischen der N_2-Fixierung und dem Stickstoffverlust in der OMZ im ETSP zeigen, derzeit noch aus. Insbesondere blieb dabei ungeklärt, ob das Ausmaß an N_2-Fixierung ausreicht, um die lokalen Stickstoffverluste auszugleichen und damit die hohe Primärproduktivität im ETSP aufrechtzuerhalten. Diese weitgehend unerforschte ökologische und biogeochemische Rolle der N_2-Fixierung erschwert eine angemessene Untersuchung des marinen Stickstoffinventars lokal im ETSP.

Das Hauptziel dieser Dissertation bestand darin, die räumliche Verteilung sowie die ökologische und biogeochemische Bedeutung der N_2-Fixierungraten im ETSP genauer zu untersuchen, wobei der Fokus spezifisch auf dem Auftriebsgebiet des Humboldt-Stroms (HUS) vor der Küste Perus lag. Im ersten Manuskript (Kapitel 2) dieser Dissertation wurde die Hypothese zur räumlichen Kopplung untersucht, indem im HUS die räumliche Verteilung und die Menge der

N_2-Fixierung in Bezug zu dem geschätzten Stickstoffverlust aufgeschlüsselt wurde. Zudem habe ich den Beitrag der küstennahen N_2-Fixierung als Stickstoffquelle für die Produktivität des Phytoplanktons quantifiziert. Die Studie erstreckte sich auf den Bereich von 8° bis zu 16° südlicher Breite (°S). Wir haben dabei verschiedene Intensitäten der OMZ, des Stickstoffdefizits sowie Gradienten von physikalischen und biogeochemischen Umweltfaktoren, einschließlich Sauerstoff (O_2), Makro- und Mikronährstoffen und die Primärproduktivität erfasst. Mit dieser Studie liegt der erste umfassende Datensatz zu den küstennahen N_2-Fixierungraten im nördlichen HUS vor. Dabei konnten wir einen Gradienten bzgl. der Breitengrade in den N_2-Fixierungsraten identifizieren, wobei höhere Raten in den produktiven Gewässern des Südens im Vergleich zur nördlichen Region mit geringerer Produktivität beobachtet wurden. Dieses Muster in der regionalen Verteilung spiegelte die Intensität der OMZ, des Stickstoffdefizits und der Nitrit-Maxima wider, die auf mikrobielle Prozesse des Stickstoffverlustes hinweisen. Unsere Beobachtungen zeigen, dass die N_2-Fixierungsraten in küstennahen, nährstoffreichen Gewässern nachweisbar, jedoch relativ niedrig sind und mit zunehmender Tiefe und Entfernung von der Küste weiter abnehmen.

In dieser Dissertationsarbeit liefere ich eine umfassende Synthese, indem ich die Datensätze zur N_2-Fixierung aus verschiedenen Jahren und Jahreszeiten zusammenführe, welche während der Ausfahrten im Rahmen des Collaborative Research Centre 754 (SFB754) gesammelt wurden. Diese in-situ-Messungen ermöglichten es uns robuste, konservative Schätzungen der N_2-Fixierungraten und ihrer räumlichen und zeitlichen Verteilung im ETSP abzuleiten. Im Allgemeinen wurden über die Jahre und die Jahreszeiten hinweg konsistent relativ niedrige N_2-Fixierungraten mit weniger als 5 nmol N L^{-1} d^{-1} beobachtet. Jedoch wurden auch während der Sommermonate der Südhemisphäre höhere N_2-Fixierungsraten festgestellt, die aufgrund des vereinzelten und punktuellen Auftretens einiger weniger hoher Raten über 10 nmol N L^{-1} d^{-1} ein erhebliches Maß an Variabilität aufwiesen. Wenn diese konservativen Schätzungen integriert und auf den gesamten ETSP extrapoliert werden, zeigt sich, dass die N_2-Fixierungraten in-situ niedriger sind als die von den Modellen vorhergesagten Schätzungen, was die Charakterisierung der Region als Hotspot der N_2-Fixierung in Frage stellt. Insgesamt deutet diese Analyse darauf hin, dass selbst, wenn die küstennahen N_2-Fixierungraten ihren Höhepunkt in den Sommermonaten erreichen, sie immer noch geringer ausfallen als die Modellschätzungen und sie nur einen geringen Anteil (etwa 0,4%) der gesamten Primärproduktivität des küstennahen HUS‘s ausmachen. Vergleicht man diese Schätzungen der niedrigen N_2-Fixierung mit den hohen Raten an Stickstoffverlust, welche derzeit im ETSP beobachtet werden, so wird deutlich, dass die N_2-Fixierungraten nicht ausreichen, um die lokalen Stickstoffverluste vollständig auszugleichen. Aus biogeochemischer Sicht legen unsere Ergebnisse daher nahe, dass die N_2-Fixierung und der Stickstoffverlust im ETSP räumlich entkoppelt sind und eine höhere N_2-Fixierung in anderen Regionen stattfinden muss, um den im ETSP auftretenden Stickstoffverlust auszugleichen.

Das unzureichende Wissen über die Umweltfaktoren, die die N_2-Fixierung beeinflussen und beschränken, hat es schwierig gemacht, die Feldbeobachtungen mit den Modellschätzungen in

Einklang zu bringen. Um diese Lücke zu schließen, bin ich einen Schritt weiter gegangen und habe die Zusammenhänge und Wechselwirkungen zwischen der N_2-Fixierung und Umweltfaktoren, welche deren Verteilung beeinflussen, untersucht (Kapitel 2 und 3). In Kapitel 3 dieser Arbeit wird dazu ein neuer Aspekt vorgestellt. Dabei hebe ich die potenzielle Ko-Limitierung von Spurenmetallen wie Fe, Cobalt (Co) und Nickel (Ni) auf die N_2-Fixierung im HUS hervor. Im Gegensatz zur bisherigen Auffassung können wir zeigen, dass die N_2-Fixierung in diesem Bereich nur schwach auf das Vorliegen von P* und einen hohen Fe-Gehalt entlang der Küste reagiert (Kapitel 2 und 3). Darüber hinaus betonen wir, dass aufgrund des Vorkommens von nicht-cyanobakteriellen mikrobiellen Stickstofffixierern (NCDs), nicht-lineare Wechselwirkungen zwischen verschiedenen Umweltfaktoren wie Spurenmetallen und Phytoplankton-assoziierten organischen Stoffen einen Einfluss auf die N_2-Fixierung haben können. Wenn man sich also nur auf die Konzentration von Fe und P stützt, um die N_2-Fixierung im ETSP vorherzusagen, ohne diese sich wechselseitig beeinflussenden Faktoren zu berücksichtigen, kann dies zu einer Überschätzung der Rolle und des Beitrags der N_2-Fixierung in dieser Region führen. In Kapitel 3 wird somit ein neuer Blick auf potenzielle Einflussgrößen auf die N_2-Fixierung im HUS geworfen, welche möglicherweise bislang übersehen wurden und einer weiteren Untersuchung bedürfen. Insgesamt liefert diese Dissertation nützliche Erkenntnisse für zukünftige Feldstudien und Experimente zu den Einflussgrößen auf die N_2-Fixierung in OMZs.

In Kapitel 4 untersuche ich die Verfügbarkeit von Nitrat, welche aus dem Auftrieb von Tiefenwasser hervorgeht, als primäre Stickstoffquelle für die Primärproduktivität im ETSP. Die hierzu durchgeführte Studie konzentrierte sich darauf zu verstehen, wie Gradienten sowohl in der Nitratkonzentration als auch in der Lichtintensität die Nitrat- und Kohlenstoffaufnahme des Phytoplanktons verändern und dadurch die Primärproduktivität innerhalb des Systems beeinflussen. Die direkte Reaktion natürlicher Phytoplanktongemeinschaften auf Veränderungen der Licht- und Nitratverhältnisse ist im HUS nach wie vor wenig erforscht. Diese Wissenslücke stellt eine Herausforderung dar, wenn es darum geht, die Reaktionen des Phytoplanktons in biogeochemischen Modellen, die darauf abzielen das Schicksal dieses Ökosystems im Zuge des Klimawandels vorherzusagen, genau zu parametrisieren. Meine Ergebnisse zeigen, dass die Nitrataufnahme nur unter hoher Lichtintensität durch die Nitratkonzentration beschränkt ist, wohingegen die Kohlenstoffaufnahme allgemein durch die Nitratkonzentration beeinflusst wird. Es ist allerdings auch so, dass regenerative Stickstoffquellen wie Ammonium die Kohlenstoffaufnahme erhöhen können. Bemerkenswerterweise zeigte sich, dass bei niedrigen Nitratkonzentrationen die Kohlenstoffaufnahme von der Nitrataufnahme entkoppelt war, was zu einem Aufnahmeverhältnis von Kohlenstoff zu Stickstoff über dem Redfield-Wert führte. Dieses Verhalten, welches nicht dem Redfield-Verhältnis entspricht, wurde im Zusammenhang mit der Gegenwart einer mixotrophen Phytoplanktongemeinschaft beobachtet. Folglich kann die Primärproduktivität im HUS nicht einfach anhand der durch den Auftrieb entstehenden Nitrat-, Chlorophyllkonzentrationen und der Lichtabschwächung vorhergesagt werden. Der Einfluss der regenerativen Nährstoffaufnahme und dieser Nicht-Redfield-Produktivität könnte

insbesondere in Phytoplankton-Gemeinschaften, die durch Mixotrophie gekennzeichnet sind, eine große Rolle bei der Aufrechterhaltung der Primärproduktivität spielen. Diese Ergebnisse besitzen wichtige Implikationen für die Parametrisierung der Reaktionen des Phytoplanktons auf Licht und Nährstoffe, welche bei der satellitenbasierten Schätzung der Primärproduktivität im HUS verwendet werden.

Wenn man über die Zukunft des marinen Stickstoffkreislaufs im ETSP nachdenkt, ist es unerlässlich, die gegenwärtige Dynamik der Stickstoffzuwächse und -verluste zu verstehen. Diese Dissertation dient dem Zweck, unser Verständnis der Verteilung und der Größenordnung der N_2-Fixierung im ETSP auf einen aktuellen Stand zu bringen und so ihren Beitrag zur Primärproduktivität und zum Ausgleich des Stickstoffverlusts bewerten zu können. Des Weiteren tragen die erfassten N_2-Fixierungraten zu einer verbesserten Auflösung bei, auf welcher die Extrapolationen der N_2-Fixierung im ETSP im großen Maßstab beruhen. Durch die Analyse der Verteilung der N_2-Fixierung über physikochemische Gradienten hinweg und die Untersuchung der Sensitivität der N_2-Fixierungsraten auf Veränderungen der Konzentration von Fe und P in einer noch wenig erforschten, aber biogeochemisch und ökologisch bedeutsamen Region (Kapitel 2 und 3), trägt diese Arbeit zu einem wachsenden Verständnis der Faktoren bei, die die N_2-Fixierung in den OMZs beeinflussen. Wir heben hervor, dass die Diskrepanz zwischen den N_2-Fixierungsraten in-situ und den Vorhersagen aus Modellen im ETSP größtenteils auf die unzulängliche Berücksichtigung anderer biogeochemischer Faktoren, die potenziell die N_2-Fixierung beeinflussen, zurückzuführen sein könnte sowie auf unzureichende Kenntnisse über die Physiologie der nicht-cyanobakteriellen N_2-Fixierer, welche im ETSP dominant vorkommen. Darüber hinaus könnte die Ansicht, dass die N_2-Fixierung hauptsächlich durch Fe und P beeinflusst wird, welche in Bezug auf den globalen Ozean weithin anerkannt ist, gerade in Hinblick auf den ETSP, überbewertet worden sein. Diese Ergebnisse bilden somit eine wertvolle Grundlage für zukünftige Forschungsvorhaben zu den Einflussgrößen auf die marine N_2-Fixierung. Zusätzlich liefert diese Dissertation Erkenntnisse für die Parametrisierung der N_2-Fixierung in zukünftigen Modellierungsstudien, welche die marinen Stickstoffkreisläufe und ihre Anfälligkeit für den Klimawandel untersuchen.

Chapter 1

Introduction

1.1 General Introduction

1.1.1 The interlinking carbon and nitrogen cycles: Importance of bioavailable nitrogen for primary production in the ocean

Marine primary productivity accounts for ~ 50% of the annual primary production globally (Behrenfeld et al., 2001; Field et al., 1998). It makes up the foundation of the marine food web, where trophic interactions mediate the transfer of energy to higher trophic levels (Falkowski, 1997; Messié and Chavez, 2015). The productivity of marine ecosystems primarily relies on the availability and supply of nutrients. Among these, bioavailable nitrogen and dissolved inorganic phosphorus (P) are the major nutrients, essential for the formation of biomolecules and cellular components such as nucleic acids, proteins, and amino acids. Bioavailable or fixed nitrogen (N) encompasses various oxidized and reduced inorganic and organic nitrogen forms, including nitrate (NO_3^-), nitrite (NO_2^-), ammonium (NH_4^+), urea and dissolved organic nitrogen (DON), henceforth collectively simplified to "bioavailable or fixed N". Phytoplankton assimilate (forward reaction) bioavailable N, P and dissolved carbon dioxide (CO_2) to organic matter, and respire (reverse reaction) organic matter following a stoichiometric relationship defined as the 'Redfield ratio' as depicted in Equation. 1 (Redfield, 1958). This ratio implies a strong connection between macronutrient availability, phytoplankton productivity, and carbon cycling. In the case of silicifying phytoplankton, such as diatoms, Silica (Si) also serves as an essential element. Furthermore, phytoplankton also require trace amounts of other micronutrients like Iron (Fe), Cobalt (Co), and Zinc (Zn), among others to function (Morel and Price, 2003). Consequently, the biogeochemical cycling of macro and micronutrients in the ocean plays a vital role in driving marine productivity.

$$106CO_2 + 16HNO_3 + H_3PO_4 + 122H_2O \underset{\rightleftharpoons}{light} (CH_2O)_{106}(NH_3)_{16}(H_3PO_4) + 138O_2 \quad (1)$$

Liebig's Law of the Minimum states that the maximum yield of phytoplankton is determined by the nutrient that is present in the least quantity relative to the demands for phytoplankton growth (Liebig, 1855). In the present ocean, on timescales ranging from years to centuries, productivity can be locally and temporarily limited by the availability and supply of bioavailable N (Tyrrell, 1999). This N limitation becomes evident through an immediate increase in primary productivity when fixed N is added to the surface ocean. Therefore, the processes that supply bioavailable N to the surface ocean play a crucial ecological role in regulating marine productivity and the export of carbon to the deep ocean (Gruber, 2004).

Phytoplankton production is primarily influenced by external N sources, referred to as "new N", resulting from the upwelling and vertical diffusion of NO_3^- enriched waters (Raimbault and Garcia, 2008) as well as microbial nitrogen fixation (henceforth N_2 fixation), and to a lesser extent through atmospheric deposition of nitrogenous compounds, groundwater and river runoff (Gruber, 2008; Jickells et al., 2017). This external nitrogen supports the growth of

phytoplankton, known as “new production”. On the other hand, a significant but relatively minor fraction of total primary production, termed “regenerated production” is sustained by the recycling or regeneration of N within the euphotic zone in the form of NH_4^+, NO_2^-, urea or DON, (Dugdale and Goering, 1967). However, only new N can alleviate N limitation and significantly impact organic matter export at magnitudes significant for CO_2 uptake (Karl et al., 2002).

Over annual timescales, the export of sinking organic matter from surface waters balances new production, thereby sustaining the role of the biological carbon pump in CO_2 uptake. In other words, the metabolism of phytoplankton N is coupled with carbon (C) cycling, ecosystem functioning, and the efficiency of CO_2 uptake. Assuming parallel C and N cycling, if bioavailable N limits primary productivity, it also constrains the effectiveness of CO_2 uptake by marine primary producers. Therefore, significant changes in the marine N inventory, which is known to be sensitive to climatic conditions can have feedback effects on climate by reducing the efficiency of the biological carbon pump due to N limitation on phytoplankton productivity (Voss et al., 2013).

1.1.2 The marine nitrogen cycle in a snapshot.

The biogeochemical processes within the marine N cycle are highly dependent on and sensitive to changes in dissolved oxygen (O_2) levels in the environment. As a result of sharp gradients between oxic and anoxic/hypoxic (zero/low O_2) conditions, both water columns and marine sediments exhibit a complex N cycle involving a diverse range of assimilatory and dissimilatory microbial processes (Canfield et al., 2010). Throughout these processes, bioavailable N is either oxidized or reduced, leading to the production of N-related compounds that can either accumulate or be lost from the environment. The intricate transformations involved in this cycle are illustrated in Figure 1 and described in detail below.

Despite the abundance of nitrogen in the Earth’s atmosphere (78%), it exists primarily as inert nitrogen gas (N_2). Through a process called **N_2 fixation**, inert N_2 dissolved in seawater is microbially converted to NH_4^+, thus becoming bioavailable for marine organisms. The **assimilation of NH_4^+** and **NO_3^-** by marine phytoplankton is the dominant process in the marine N cycle. NH_4^+ is the preferred form of N for phytoplankton and macro-algae because it occurs in the most reduced state, making its consumption more energy efficient (Galloway et al., 2004).

In oxygenated conditions, an alternative process influencing **NH_4^+**, called **ammonium oxidation/ nitrification** occurs, where NH_4^+ is sequentially oxidized to NO_2^- and then to NO_3^-. Under anoxic/hypoxic conditions, this dissimilatory process can result in the intermediate production of nitrous oxide (N_2O), a potent greenhouse gas with a higher global warming potential than CO_2 (Canfield et al., 2010). Furthermore, in anoxic conditions, N_2O is also generated as an intermediate product during the stepwise microbial process of denitrification,

involving **nitrite reduction** (Eqn. 2a). However, the production of N_2O while spatially variable is only considered a minor sink of bioavailable N globally (Bianchi et al., 2012; Voss et al., 2013).

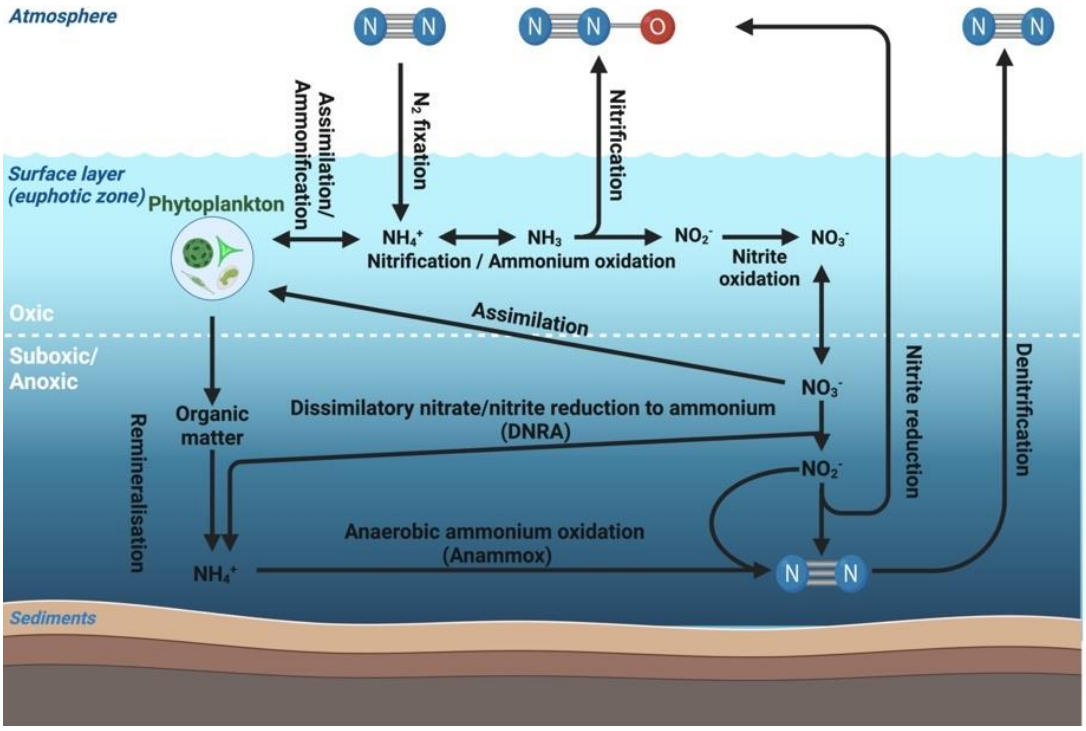

Figure 1.1 A simplified schematic illustration of the marine nitrogen cycle and its microbial pathways and transformations. Of particular importance are nitrogen (N_2) fixation and denitrification which are mainly responsible for mediating large and long-term changes in the marine N inventory. *Figure created with BioRender.com*.

In O_2 depleted (anoxic to hypoxic) conditions, NO_3^- is preferentially used as an alternative electron acceptor for the degradation of organic matter during the process of **Denitrification.** In this process, heterotrophic anaerobic bacteria sequentially reduce, NO_3^- to N_2 via NO_2^- and N_2O consumes NO_3^- during organic matter remineralization (Eqn.2a,b) and has long been considered the primary pathway for NO_3^- reduction in the marine environment (Falkowski, 1997). Depending on the extent of anoxia, denitrification can be complete (fully anoxic) with N_2 as the end product or incomplete (suboxic), thereby producing NO_2^-. Significant advancements in understanding the N cycle have recognized the importance of **dissimilatory nitrate/nitrite reduction to ammonium (DNRA)** carried out by autotrophic and heterotrophic bacteria. DNRA provides an alternative pathway through which bioavailable N can be retained in the environment in the form of NH_4^+ (Canfield et al., 2005).

Sequential denitrification reaction

$$NO_3^- \rightarrow NO_2^- \rightarrow NO + N_2O \rightarrow N_2 \quad (2a)$$

Redox denitrification reaction

$$2NO_3^- + 10e^- + 12H^+ \rightarrow N_2 + 6H_2O \quad (2b)$$

For decades, oceanographers were puzzled by the low to non-detectable NH_4^+ concentrations in low O_2 environments. It was hypothesized that NH_4^+ in these environments might undergo anaerobic oxidation to N_2, using either NO_3^- or NO_2^- as electron acceptors (Richards et al., 1965). Evidence for such a pathway was first discovered in a wastewater treatment plant in 1995 (van de Graaf et al., 1995). Subsequently, autotrophic anaerobic bacteria were found to mediate the loss of bioavailable N in marine environments such as anoxic shelf sediments, semi-enclosed basins, and the water column of Oxygen Minimum Zones (OMZs), through the process of **anaerobic oxidation of ammonium (anammox),** (Thamdrup and Dalsgaard, 2002; Kuypers et al., 2003, 2005). During anammox, ammonium is oxidized using NO_2^- (Eqn. 3) and the process is considered less sensitive to O_2 than denitrification (Kalvelage et al., 2011). While the quantitative significance of anammox on a global scale remains debated, regionally it is considered the dominant pathway for N loss in the Oman shelf and OMZs associated with major upwelling systems off Namibia, Peru and Chile (Thamdrup et al., 2006; Jensen et al., 2011; Kuypers et al., 2005; Hamersley et al., 2007). Nonetheless, from a geochemical perspective, both denitrification and anammox (hereafter N loss) are responsible for the removal of bioavailable N from the marine system, although they differ in their stoichiometry (Paulmier et al., 2009).

$$\mathrm{NH_4^+ + NO_2^- \rightarrow N_2 + 2H_2O} \quad (3)$$

The ocean is a large reservoir of bioavailable N, which constitutes about 6% of all the dissolved N in seawater. In general, these microbially-mediated reduction-oxidation (redox) reactions that occur within the water column and sediments regulate the inventory of N in the global ocean. Of these processes, **N_2 fixation and denitrification** are characterized by rate-limiting feedback that primarily regulate the marine N inventory. Hence, on long-time scales, they are ultimately responsible for large deviations in the bioavailable N inventory and consequently influence bioavailable nitrogen availability, rates of primary production and export of organic carbon to the deep ocean (Galloway et al., 2004).

1.2 Marine nitrogen fixation

1.2.1 The evolutionary process of fixing nitrogen.

Atmospheric nitrogen gas (N_2) is composed of two nitrogen atoms that are strongly bound by a triple bond (N≡N), making it difficult and energetically costly to break. As a result, most organisms are unable to assimilate N_2 once it is dissolved in water. However, a specialized group of diverse bacteria and archaea called diazotrophs possess the nitrogenase enzyme complex which catalyzes the enzymatic reduction of N_2 gas into bioavailable forms such as ammonia (Capone and Carpenter, 1982). Nonetheless, even for these specialized organisms, N_2 fixation is an energetically demanding process, requiring the consumption of 16 adenosine triphosphate (ATP) units for every N_2 molecule reduced.

Despite the energetic cost associated with N_2 fixation, the ability to fix N_2 is widespread across the Tree of Life. The evolutionary origin of Nitrogenases is believed to trace back to a reduced atmosphere and ocean (low O_2), approximately 3.5 billion years ago when early thermophilic methanogens evolved the capacity to fix N_2 as a means to circumvent a severe N limitation in their environment (Kasting and Siefert, 2001). Today, nitrogenase is responsible for catalyzing the production of up to half of the bioavailable N on Earth (Falkowski, 1997). The overall reaction of the nitrogenase enzyme complex is summarized in Equation 2 below.

$$\mathrm{N_2 + 8H^+ + 8e^- + 16ATP \rightarrow 2NH_3 + H_2 + 16ADP + 16P_i} \quad (4)$$

The primary form of nitrogenase that is extensively studied is the molybdenum (Mo)-dependent nitrogenase which is encoded by the *nifHDK* gene, made up of two subunits. The *nifH* subunit encodes the dinitrogenase reductase, (an iron protein) while the *nifDK* subunit encodes the dinitrogenase (an Iron-Mo protein). Hereafter I refer to *nifHDK* as *nifH*: the functional marker gene for N_2 fixation. *nifH* gene is the preferred biomarker in the study of diazotrophic diversity because it is highly conserved and widespread in bacteria and archaea phyla (Raymond et al., 2004; Zehr et al., 2003; Turk-Kubo et al., 2012; Jayakumar et al., 2012). Nitrogenases are therefore considered metalloenzymes, utilizing trace metal cations as a cofactor in their active site. These metal centres, particularly for iron (Fe), confer diazotrophs higher Fe requirements compared to non-diazotrophs (Kustka et al., 2002).

Due to the evolutionary history of nitrogenases in low and potentially transient O_2 conditions, all nitrogenases are sensitive to O_2 and are permanently inhibited by its presence (Robson and Postgate, 1980). However, diazotrophs have developed species-specific mechanisms to protect themselves from oxygen damage. Examples include temporal separation of N_2 fixation and oxygenic photosynthesis in *Crocosphaera* spp and enzymatic oxygen scavenging in *Trichodesmium* spp (Berman-Frank et al., 2001b; Inomura et al., 2019). Thus, it has long been assumed that diazotrophs are sensitive to redox conditions and associated impacts on Fe availability in their environment (Gruber, 2004).

The dependence of nitrogenase on Fe is perhaps an evolutionary relic of the Archaean Ocean when Fe was soluble and highly abundant relative to Mo (Anbar and Knoll, 2002). Apart from Fe, the evolution of nitrogenases was also influenced by changes in the availability of other trace metals in the ocean, which were associated with shifts in the oceans' oxidative state (Anbar and Knoll, 2002). The availability of cobalt (Co) in Archaean times played a crucial role in the proper functioning and assembly of the nitrogenase enzyme complex. Thus, links have been established between earlier sulphidic/euxinic ocean conditions and N_2 fixation (Zerkle et al., 2006; Boyle et al., 2013; Anbar and Knoll, 2002), as sulphidic conditions influence the bioavailability of redox-sensitive bio-essential trace metals like Co and Fe in the ocean (Silva et al., 2001). Over time, alternative forms of molybdenum-free nitrogenases emerged such as those containing vanadium (*vnfDK*) or only iron (*anfDK*) in their active site (Hales et al., 1986; Chisnell et al., 1988; Boyd et al., 2011). Therefore, the varied trace element requirements and

selection imprinted in common and alternative nitrogenases reflect the oceanic redox states and associated trace metal availability in seawater throughout the evolution of the nitrogenases (Zerkle et al., 2006, 2005; Dupont et al., 2006).

Hence the changing redox chemistry of the ocean connects the activity of diazotrophs to the availability of trace metals (Zerkle et al., 2005). Therefore, one may question whether modern N_2 fixation would be possible without the early forms enabled by Fe, Mo, Co and other bioavailable trace metals. Consequently, although the primary role of Fe in diazotrophy has long been assumed, understanding the impact of other transition metal availabilities on the functionality and diversity of diazotrophs can provide insights into what may control diazotrophy in a changing ocean. Regardless of the specific pathway for the evolution of N_2 fixation, it is evident that its evolution over time was driven by environmental changes in which early life forms encountered a nitrogen crisis. These changes in the environments, including variations in the ocean's oxygenation state, influenced the availability of trace metals that play a crucial role in the structure and reactivity of nitrogenases and thus the relevance of diazotrophs in the environment (Boyd and Peters, 2013).

Considering that environmental controls like Fe and phosphorus (P) are currently used to parameterise the biogeography of N_2 fixation in the modern ocean, but do not fully explain the observed patterns of N_2 fixation, it is important to explore other potential factors (Luo et al., 2014; Ward et al., 2013; Monteiro et al., 2011; Berman-Frank et al., 2005; Romero et al., 2013). The evolutionary pathways and metabolic flexibility of diazotrophs, which have enabled them to survive and function in transient ocean redox states and other environmental conditions should therefore not be ignored as marine biogeochemists ascertain the controls of nitrogen fixation in the modern ocean. In the face of a changing ocean, it is therefore crucial to consider the potential for this metabolic flexibility and adaptability in environmental conditions such as trace metal utilization by diazotrophs. It is plausible that short- to long-term changes in the ocean's redox state and associated environmental conditions could create favourable conditions under which N_2 fixation in dynamic environments could be enhanced even if temporarily. Thus, understanding the metabolic plasticity of diazotrophs in response to varying environmental conditions, whether transient or permanent is essential to predicting N_2 fixation in a changing ocean.

1.2.2 Traditional and changing perspectives of marine nitrogen fixation, its Protagonists and Drivers

The majority of N_2 fixation in the ocean has traditionally been attributed to photoautotrophic cyanobacterial diazotrophs, particularly the filamentous and non-heterocystous *Trichodesmium* spp (Capone et al., 1997), as well as diatom symbionts like *Richelia* (Karl et al., 2012). *Trichodesmium* spp are commonly found in warm (20°C – 24°C) and highly stratified nitrogen-depleted sub-surface waters with high light intensities (Capone et al., 1997, 2005; Karl and Letelier, 2008; Luo et al., 2014). Their ecological success is often demonstrated by large

blooms occurring in oligotrophic tropical and sub-tropical surface waters in the North Atlantic North Pacific oceans and the Arabian Sea (Benavides and Voss, 2015; Capone and Carpenter, 1982; Dore et al., 2008). The high light intensities in surface waters are beneficial for photoautotrophic diazotrophs to meet the high energy demands of N_2 fixation (Luo et al., 2014). Additionally, warm temperatures are partly associated with high respiration rates, which are essential for maintaining an anoxic cellular environment for diazotrophs in highly oxygenated surface waters (Breitbarth et al., 2007).

Due to the high energy demand associated with N_2 fixation, diazotrophs were traditionally believed to fix N_2 only when it provides a competitive advantage over assimilating bioavailable N forms such as NO_3^-, which require relatively more energy (Howarth et al., 1988). As a result, the deficiency of NO_3^- in oligotrophic waters favoured diazotrophs to outcompete faster-growing non-diazotrophic organisms (Arrigo, 2005). In oligotrophic waters, NO_3^- deficit is also tied to inorganic nitrogen and phosphorus (P) ratios (N:P) being lower than the Redfield ratio of 16:1, enabling P to become available for diazotrophs once all the bioavailable N is depleted at a relatively faster rate by non-diazotrophic phytoplankton (Sohm and Capone, 2006).

Diazotrophs require ~ 5 -100 fold more Fe than non-diazotrophs due to Fes' role in *nifH* (Kustka et al., 2003; Berman-Frank et al., 2001a; Hutchins and Boyd, 2016). Hence, blooms of *Trichodesmium* spp in the North Atlantic have been associated with a high input of Fe to the surface ocean through aeolian dust deposition (Moore et al., 2009; Langlois et al., 2008). However, the evidence for large-scale Fe limitation of N_2 fixation in the global ocean is largely circumstantial, as results from Fe addition experiments have either yielded inconclusive or no relationship between N_2 fixation and Fe concentrations (Hood et al., 2000).

Thus, the concept of a diazotrophic niche in the oligotrophic ocean has been shaped by these observations of diazotrophs and the surrounding environmental conditions (Luo et al., 2014). For these reasons, *Trichodesmium* spp has been used as a model organism to parameterize diazotrophy in most global and regional ecological and biogeochemical models of N_2 fixation in the ocean (Luo et al., 2014; Ward et al., 2013; Monteiro et al., 2011). However, currently, *Trichodesmium* spp is estimated to contribute ~60-80 Tg N yr^{-1}, accounting for only 25 – 50% of the geochemically estimated N_2 fixation rates globally (Mahaffey et al., 2005; Gruber and Sarmiento, 1997). This implies a missing N source potentially originating from other less considered or unknown organisms. Nonetheless, in comparison to *Trichodesmium* spp, the ecophysiologies of other potentially significant marine diazotrophs are currently less understood.

Ongoing advancements in molecular techniques and integrative genome analyses, along with the use of imaging data, have led to more accurate explorations of the diversity, abundance, distribution and controls of diazotrophs in the ocean (Zehr et al., 2003; Karlusich et al., 2021). *nifH* genes have been observed in diverse marine environments outside the traditional niche. Currently, *nifH* genes have been recovered from arctic waters and nutrient-rich upwelling

regions and aphotic environments (Fernández-Méndez et al., 2016; Sipler et al., 2017; von Friesen and Riemann, 2020; Bonnet et al., 2013; Dekaezemacker et al., 2013; Bonnet et al., 2013). These observations are therefore challenging the notion of a diazotrophic niche confined to the tropical and subtropical oligotrophic ocean.

Moreover, the traditional perception of *Trichodesmium* spp as the predominant diazotroph in the global ocean is being reconsidered as new genetic datasets and molecular techniques from global expeditions have broadened their reach and expanded our knowledge. Unicellular cyanobacteria such as UCYN-A1, UCYN-A2, UCYN-B, UCYN-C, and diatom symbionts such as *Calothrix* (Cornejo-Castillo and Zehr, 2021), as well as non-cyanobacterial diazotrophic species (NCDs) are gaining recognition. Cultured UCYN-B, specifically *Crocosphaera spp*, has been shown to make a significant contribution to the nitrogen budget in the North Pacific and Atlantic Oceans (Montoya et al., 2004; Zehr et al., 1998). Some NCDs, which are mostly heterotrophic and were previously unknown, have been discovered to possess and express the *nifH* gene in oxygenated waters, cold upwelling systems (<17°C), OMZs, and aphotic mesopelagic waters indicating their ubiquity and potential importance in diverse environments (Bonnet et al., 2013; Farnelid et al., 2013; Löscher et al., 2014; Dekaezemacker et al., 2013; Fernandez et al., 2011; Halm et al., 2012; Jayakumar et al., 2012; Riemann et al., 2010, 2022).

Current progress is also being made in incorporating these less-represented diazotrophic taxa into biogeochemical models, which has improved the characterization of N_2 fixation distribution in the ocean (Luo et al., 2014; Tang et al., 2019b; Tang and Cassar, 2019). Our understanding of large-scale physical and biogeochemical controls, including inputs and availability of phosphorus (P), bioavailable N and Fe, is also advancing across ocean basins and regions (Weber and Deutsch, 2014; Sohm et al., 2011). *Trichodesmium* spp and *Crocosphaera* spp among other diazotrophs have demonstrated the ability to utilise alternative P sources such as dissolved organic phosphorus (DOP), and exhibit plasticity in their carbon-to-phosphorus ratio, allowing for low cellular P quotas (Filella et al., 2022; Dyhrman et al., 2006; Karl and Björkman, 2015). This suggests that while P is necessary for N_2 fixation, it may not be the primary driver for diazotrophs distribution and activity in other parts of the ocean (Moutin et al., 2008; Fu et al., 2005; Mulholland et al., 2002).

Although it has been traditionally assumed that N_2 fixation benefits from a deficit of NO_3^-, accumulating evidence from field studies and culture work has demonstrated diazotrophs presence, growth, and activity under modest concentrations of NO_3^- and NH_4^+ concentrations (Knapp, 2012; Shiozaki et al., 2018; Inomura et al., 2018; Turk-Kubo et al., 2018; Dekaezemacker and Bonnet, 2011). This suggests that N_2 fixation may not be as sensitive to inorganic nitrogen as previously believed. Perhaps a threshold of inorganic N availability exists below which N_2 fixation can still take place if P is available. Nonetheless, the proportion of N to P (N:P ratio) may play a critical role, as high concentrations of inorganic N can offset N_2 fixation rates even when P is replete (Knapp, 2012).

Furthermore, high Fe availability is suggested to create co-limiting conditions for other biochemical trace metals such as Nickel (Ni) and Co in some diazotrophs like *Trichodesmium* (Middag et al., 2020; Ho, 2013). This raises the question of whether other trace metals beyond Fe may exert control on marine N_2 fixation at regional scales (Tuo et al., 2020). In general, all these findings challenge the classical niche concept for diazotrophs and highlight our limited understanding of the factors and mechanisms that regulate marine N_2 fixation in the ocean.

The roles, quantitative significance, and success of the diverse assemblage of diazotrophs in their local environment are a function of physiological adaptations in their environment and the ecological conditions that promote and maximize their growth and activity (Zehr and Capone, 2020). Our view of the controls on N_2 fixation in the ocean is evolving to consider the diversity and metabolic flexibility of diazotrophs in local marine environments and their interactions with other plankton. Dissolved organic matter has been shown to stimulate heterotrophic diazotrophs in aphotic environments and coastal productive waters (Rahav et al., 2013; Bonnet et al., 2013; Bentzon-Tilia et al., 2015). Additionally, the interior of carbon-rich particles in euphotic oxygenated waters favour the growth and activity of heterotrophic diazotrophs (Moisander et al., 2017). Notably, NCDs are active within organic-rich particles that create micro-niches with restricted O_2 diffusion, protecting NCDs from O_2 damage (Chakraborty et al., 2021; Pedersen et al., 2018). Top-down control from zooplankton grazing has also been proposed to play a role in the regulation of N_2 fixation patterns globally (Wang et al., 2019; Landolfi et al., 2021).

While the concept of a diazotrophic niche seems to hold for a large part of the oligotrophic ocean, these emerging patterns in marine N_2 fixation are challenging traditional paradigms of N_2 fixation in the ocean. These examples highlight that N_2 fixation occurs in a much wider range of environments, and the diversity of diazotrophs and the environmental controls on N_2 fixation in the ocean extends beyond our current understanding. Therefore, these advancements indicate that there is a complex interplay between physical, chemical, and biotic factors that govern the distribution and activity of diazotrophs in the ocean that is yet to be fully understood. One may expect that at local to regional scales, depending on the specific species, different constellations of these factors may be involved in the regulation of N_2 fixation. However, assessing the local and global distributions of diazotrophic species remains a challenging task, which presents significant research challenges for accurately quantifying the importance of N_2 fixation in the ocean. The ecology and N_2 fixing mechanisms of NCDs are still largely unknown owing to the difficulty in isolating marine isolates for experimental work. As a result, obtaining robust direct estimates of N_2 fixation from NCDs and incorporating them in the global N inventory is still a challenge (Bombar et al., 2016; Turk-Kubo et al., 2014). These uncertainties contribute to the discrepancies between observed and model-predicted N_2 fixation rates in the ocean and have implications for the assessment of the marine N inventory (Codispoti, 2007). One of the key insights from these advancements is that a comprehensive understanding of the dynamics of the ocean N inventory requires considering the full diversity of marine diazotrophs, improving N_2 fixation rate measurements and their accuracy, and

gaining a better understanding of the range of environmental conditions and mechanisms that regulate marine N_2 fixation.

1.2.3 The Conundrum of a balanced marine nitrogen budget and associated feedback

The marine N inventory is kept in balance by the processes releasing N (as N_2, N_2O) back into the atmosphere (anammox and denitrification) and the inputs of bioavailable N (N_2 fixation). This has been the focus of several previous studies, which have yielded conflicting results on whether these processes are in equilibrium.

Models estimating N_2 fixation can be categorised into three groups based on their considerations of spatial patterns and timescales. The first group of models, using geochemical gradients and deviations in N:P ratios from the Redfield ratio (excess phosphorus and nitrate deficits - P*, N*), suggest that the marine N inventory is stabilized by negative feedback mechanisms emanating from the spatial separation of N_2 fixation and N loss as shown in Figure 1.2a (Gruber, 2004). In these models, denitrification is the dominant N loss process in coastal sediments and OMZ waters, such as those found in the eastern tropical South Pacific, southwest Africa, and the Arabian Sea. On the other hand, the majority of N_2 fixation occurs in subtropical and tropical oligotrophic gyres of the Northern Hemisphere, where high concentrations of Fe are deposited from dust (Codispoti et al., 2001).

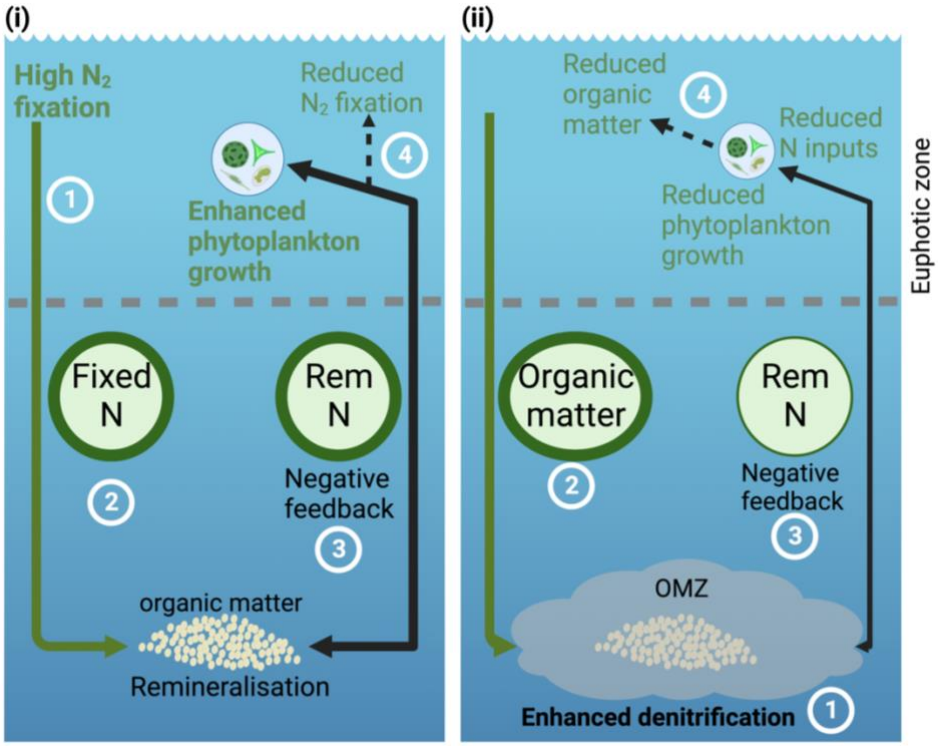

Figure 1.2a. The spatial separation paradigm shows the biogeochemical negative feedback preventing large shifts in the marine N cycle. (i) and (ii) indicate the negative stabilizing

feedbacks (feedback 3 and 4) that ensue when N_2 fixation and N loss are spatially separated. In (i), N_2 fixation is self-limiting due to the supply of excess bioavailable nitrogen once the organic matter is remineralized (Rem N) and in (ii) denitrification generates nitrogen deficits which reduces the amount of bioavailable N for non-diazotrophic phytoplankton, hence a decline in organic matter export. *Adapted from Landolfi et al (2013). Figure created with BioRender.com*

Robust estimates from these geochemical extrapolations indicate an imbalanced oceanic N budget emanating from denitrification being more than N_2 fixation (Codispoti, 2007; Voss et al., 2013; Gruber and Galloway, 2008; Gruber, 2008; Falkowski, 1997). Marine N_2 fixation is estimated at 140 ± 50 Tg N yr^{-1} (Voss et al., 2013 and references therein) whereas marine N loss is estimated at 350 - 450 Tg N yr^{-1} due to relatively higher estimates of sedimentary denitrification (~ 300 Tg N yr^{-1}) than in the water column (~ 150 Tg N yr^{-1}), (Codispoti, 2007; Lam and Kuypers, 2011; Brandes and Devol, 2002). Plausible reasons for this imbalance include either unidentified N inputs through organisms not covered by existing direct and geochemical methods, limited spatiotemporal coverage of N_2 fixation measurements i.e. N_2 fixation is underestimated (White et al., 2020), or that denitrification is overestimated (Brandes and Devol, 2002). Some models also assert an imbalance due to the assumption of inflexible elemental ratios used in many model parameterisations (Wang et al., 2019; Weber and Deutsch, 2014). Furthermore, inaccurate estimation of global marine N_2 fixation due to the different methods employed in N_2 fixation assays, some of which underestimate N_2 fixation rates potentially contributes to this imbalance (White et al., 2020; Mohr et al., 2010; Großkopf et al., 2012).

The second group of models, based on indirect estimates obtained through inverse modelling approaches suggest that strong stabilizing feedback maintains the stability of the marine N inventory through a tight spatial and temporal coupling of N_2 fixation and N loss (Deutsch et al., 2007; Moore and Doney, 2007; Tyrrell, 1999). Deutsch et al. (2007) hypothesized that this feedback is particularly relevant in upwelling areas adjacent to zones of intense N loss such as OMZs (Figure 1.2b). The mechanism is presumed to operate as follows: denitrified OMZ waters with low inorganic N:P ratios (relative to Redfield 16:1) are upwelled to the surface, promoting the growth and activity of diazotrophs once all the bioavailable N has been consumed by other phytoplankton, and assuming other elements such as P and Fe are non-limiting (Figure 1.2b).

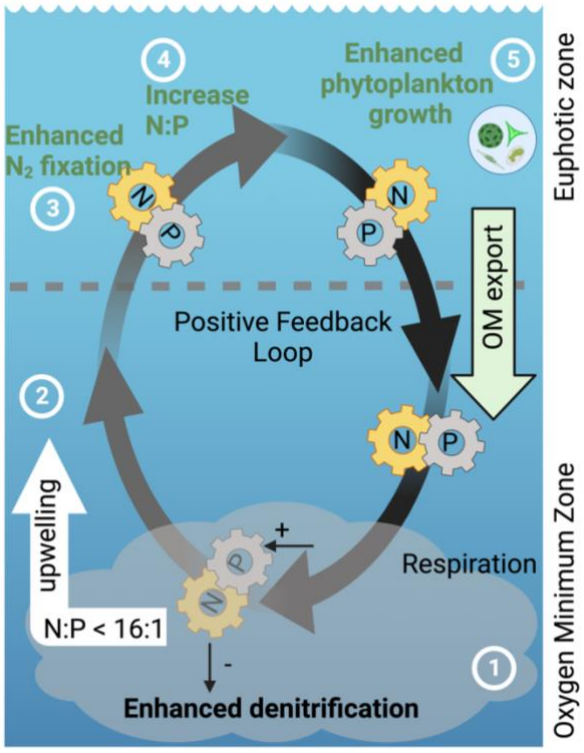

Figure 1.2b. Schematic of a spatial coupling between N_2 fixation and denitrification (N loss) in OMZs close to upwelling systems as predicted by Deutsch et al. (2007). Due to intense denitrification in the OMZ (1), waters with N:P ratios lower than the Redfield ratio (16:1) are upwelled into the euphotic zone (2) thereby stimulating N_2 fixation (3). Diazotrophs drawdown P and add new N to fuel more productivity thus restoring the N:P ratio towards Redfield (4) and enhancing organic matter export to the OMZ (5). In this scenario, N_2 fixation and N loss sustain each other in a positive feedback loop. Gears indicate the transformation of N:P ratios by the uptake and release activities of phytoplankton, diazotrophs, and denitrifiers. *Figure adapted from White et al. (2013).*

Regionally in OMZs, testing the spatial coupling hypothesis is underpinned by challenges in obtaining accurate estimates of N_2 fixation rates due to a low number of observations and limited geographical range and known controls for N_2 fixation in these regions (Zehr and Capone, 2020). Another key uncertainty in the rates of N_2 fixation is the high spatial and temporal variability which is closely linked to the variability (spatial and temporal) in the supply of its model-based biogeochemical controls N, P, and Fe (Ward et al., 2013; Fowler et al., 2013). Interestingly, the recent re-evaluation of global N_2 fixation supports the dominance of high N_2 fixation in oligotrophic subtropical gyres rather than in upwelling regions (Wang et al., 2019). Hence, it is still not clear whether N_2 fixation rates in OMZs such as the ETSP can occur at magnitudes enough to replenish the N loss as hypothesized by Deutsch et al. (2007).

The third set of biogeochemical models indicates that strong homeostatic controls have kept the marine N inventory stable over the last 5000 years (Gruber, 2004; Altabet, 2007). These contrasting arguments indicate that both the timescales and control mechanisms

underpinning N_2 fixation and N loss at regional, basin and global scales are not well understood. Nonetheless, an alluded imbalance cannot be ignored, since an imbalanced N inventory cannot be sustained over time and would therefore have major implications for marine primary productivity, which is largely limited by bioavailable N (Moore et al., 2013; Bopp et al., 2013). Moreover, positive and negative feedback that regulate carbon turnover may either amplify or mitigate changes in the ocean that are tightly coupled to the nitrogen cycle. This demands a re-evaluation of discrete measurements of N_2 fixation and N loss at local and basin scales and the techniques used to extrapolate these measurements to the global scale.

In general, all methods of estimating basin-and global scale N_2 fixation have considerable biases and assumptions. In addition, there are large variations between models concerning the magnitude and spatial pattern of diazotrophy regionally. Nevertheless, the distribution of nutrients and their ratios remains to be the best way for estimating N_2 fixation at the basin to global scale. On much smaller regional scales, methodological errors underestimating direct N_2 fixation measurements limit their comparability temporally within regions or between regions (Mohr et al., 2010; Großkopf et al., 2012). Hence currently the relative balance of bioavailable N inputs and removal, and the coupling of these processes at regional, basin and global scales are yet to be conclusively resolved, leaving oceanographers on a persistent search for the missing Tgs' of N. Considering the many fluxes and pathways in the marine N cycle, extensive measurements especially on N_2 fixation are still required to constrain their range of values and reduce the high uncertainty. In light of this, there is no better time than the present to quantify N_2 fixation and assess the factors that control the temporal and spatial distribution of N_2 fixation rates at all spatial scales. The focus of this dissertation is to assess N_2 fixation, its magnitudes, and controls, and elucidate its biogeochemical role in one of the most relevant environments for the marine N cycle, the OMZ in the northern Humboldt Upwelling System (HUS) off Peru.

1.3 Study area: The Northern Humboldt Upwelling System

1.3.1 Physical Conditions, biogeochemistry, and system variability

This dissertation will focus on one region highly susceptible to ocean deoxygenation: the OMZ associated with the HUS. The HUS is located in the Eastern Tropical South Pacific (ETSP) off the coast of Peru between 5°S and 20°S (Figure 1.3a). It is one of the four eastern Boundary Upwelling systems (EBUS; California, Canary, and Benguela systems) located on the western side of the major continents.

Within the HUS, the prevailing wind direction is parallel to the coast, due to a large-scale pressure difference between the South American continent and the Southeast Pacific Ocean. As a result, equatorward winds blow along the west coast of the South American continent, generating equatorward currents on the Peruvian coast as illustrated in Figure 1.3a below (Karstensen and Ulloa, 2009). These currents consist of the Peru Coastal Current (PCC), located

near the coast at ~ 100 km with a vertical extent of up to 50 m from the surface (Huyer et al., 1991). Further offshore, beyond 180 km, the Peru Current (PC), also known as the Humboldt Current flows at depths of up to 500 m between 15°S and 20°S. The equatorward wind stress generated by these currents, primarily the PCC, leads to an offshore transport of water to the left of the wind direction in the Southern Hemisphere called Ekman transport (Brink et al., 1983). This offshore divergence of surface waters results in a process called upwelling, where cold nutrient-rich deep waters from below 150 m are transported to the surface along the coast (Karstensen and Ulloa, 2009). In addition to the Ekman transport, another process, Ekman pumping occurs offshore, which refers to the vertical velocity induced by the Ekman transport and also triggers an upward flux of nutrients through coastal upwelling (Kämpf and Chapman, 2016).

Two major southward flowing currents are associated with these upwelled waters in the HUS (Fig. 1.3a): the surface Peru-Chile Counter current (PCCC) and the subsurface Peru-Chile Undercurrent (PCUC). PCUC predominantly flows along the coast at 100 m depth, with a vertical extent of 300 m – 400 m (Chaigneau et al., 2013). It is mainly fed by the Pacific Equatorial Undercurrent (EUC) and transports warm, saline, low-O_2, and nutrient-rich waters southward, serving as the main source of coastal upwelled waters (Tsuchiya and Talley, 1998). The PCUC particularly intensifies between 8°S and 16°S, which covers most of the Peruvian coast (northern HUS) and weakens south of 16°S. Within the Peruvian coast, the PCUC is strongest between 9°S and 12°S during summer and weakens in winter (Chaigneau et al., 2013; Brink et al., 1983). Additionally, at 100 – 300 km offshore of the Peruvian coast, between the two equatorward currents, the other poleward flowing current, the PCCC also transports equatorial warm and saline waters poleward (Tsuchiya and Talley, 1998).

Upwelled nutrient-rich waters trigger seasonally variable high phytoplankton productivity at the coast dominated by large diatom blooms (Franz et al., 2012). This high surface phytoplankton productivity makes the region exceptionally productive in secondary production and consequently supports one of the most economically significant single-species fisheries in the world, the anchovy fishery (Chavez et al., 2008; Pauly and Christensen, 1995). The rich biological productivity of the HUS generates high organic matter which sinks to depth triggering changes in water column biogeochemistry due to the creation of a unique feature called the oxygen minimum zone.

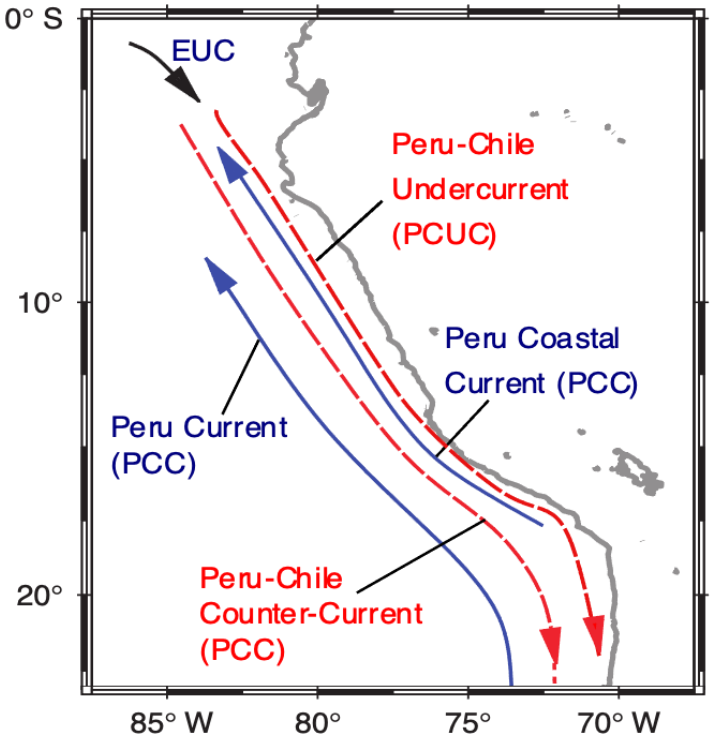

Figure 1.3a. Schematic of the northern Humboldt Upwelling system indicating the main cold surface (blue) and warm subsurface currents (red) and the Pacific Equatorial Undercurrent (EUC, black) that feeds the PCUC. Currents not drawn to scale. Figure *modified from Karstensen and Ulloa (2009)*.

Due to its proximity to the Equatorial Pacific, the HUS is impacted by strong interannual variability associated with the El Niño Southern Oscillation (ENSO) and the Pacific Decadal Oscillation (PDO), (Stramma et al., 2020). ENSO is characterized by warm El Niño and cold La Niña phases on a two-to-seven-year cycle (Penven et al., 2005). El Niño conditions are associated with reduced upwelling, a deep thermocline, high sea surface temperatures (SST), and nutrient limitation in surface waters which results in low primary productivity. During La Niña, the thermocline shallows, trapping nutrients in euphotic waters resulting in higher phytoplankton productivity (Barber and Chavez, 1983).

1.3.2 The oxygen minimum zone (OMZ) and its role in the marine N cycle

The Peruvian OMZ associated with the HUS is the shallowest and most intense OMZ globally (Bettencourt et al., 2015), (Figure 1.3b). It is estimated to cover ~34% of the total OMZ area worldwide, defined by anoxic-hypoxic waters with dissolved O_2 concentrations of < 20 μmol Kg^{-1} / 0.5 ml L^{-1} (Karstensen et al., 2008; Stramma et al., 2008; Helly and Levin, 2004). The core of the OMZ extends about 1000 km into the open ocean. The upper OMZ boundary is situated between ~25 – 100 m water depth and can extend into the euphotic zone in certain areas of the ETSP, thickening depth-wise by ~300 - 700 m in depth (Fuenzalida et al., 2009). Water

masses and currents in the area regulate the thickness of the OMZ which is thickest between 5°S and 13°S and shows a distinct narrowing where the PCUC develops along the coastline (15°S – 20°S, Figure 1.3b). The lower OMZ boundary exhibits distinct latitudinal variations due to the influence of a mid-depth circulation system in the region.

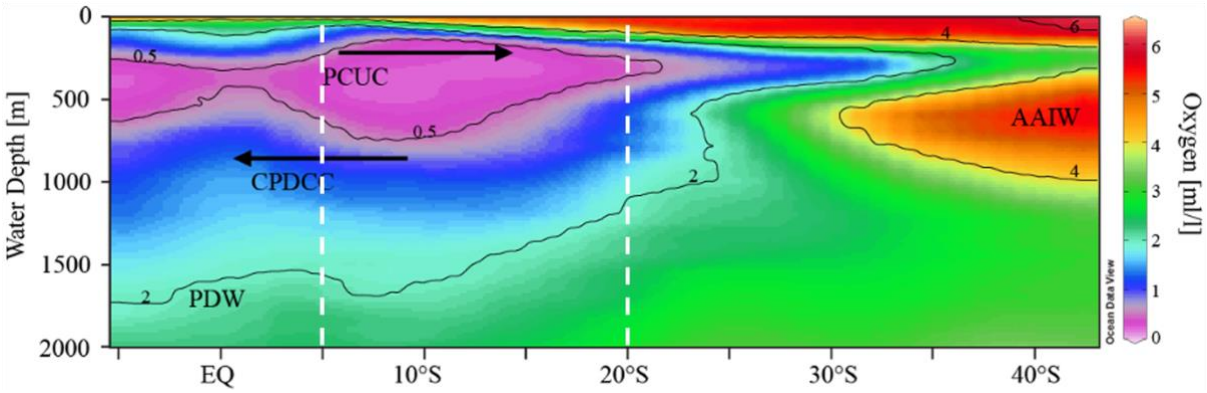

Figure 1.3b. Example of a latitudinal transect at 80°W showing the dissolved O_2 concentrations from the World Ocean Data, WOD13 (Boyer et al., 2013), and primary water masses in the HUS. (PCUC: Peru-Chile Undercurrent, CPCDCC: Chile-Peru Deep Coastal Current, AAIW: Antarctic Intermediate Water, and PDW: Pacific Deep Water). 1 ml L^{-1} = 45 μmol Kg^{-1}. White dotted lines demarcate the Peruvian OMZ.

The formation and maintenance of the Peruvian OMZ is a combination of complex physical and biogeochemical processes, that are considered to interact threefold; (1) the rich biological productivity of the HUS generates high organic matter whose remineralization consumes O_2 as it sinks to depth, (2) a sharp permanent pycnocline limits vertical mixing between the oxygenated surface mixed layer and subsurface waters (Fiedler and Talley, 2006) and (3) a weak deep circulation impedes advection of oxygenated waters from below the pycnocline (Fiedler and Talley, 2006; Helly and Levin, 2004). These low O_2 conditions impact nitrogen cycling and ecosystem productivity (Figure 1.2b). NO_3^- (which is energetically the next favourable and predominant electron acceptor after O_2) is preferentially respired from organic matter through denitrification resulting in a loss of bioavailable N and the formation of a secondary NO_2^- maxima under incomplete denitrification (Lam and Kuypers, 2011). This NO_2^- fuels anammox, another N loss pathway prevalent in the Peruvian OMZ (Dalsgaard et al., 2012). Thus, the strong secondary NO_2^- maxima, found at depths of 30 m to 400 m and extending 300 km offshore between 10°S and 20°S is usually interpreted to be an active sign of N loss (Codispoti, and Packard, 1980). A scientific debate regarding the contribution of denitrification and anammox in the Peruvian OMZ is still ongoing. Recent work suggests however that anammox is the dominant pathway for water column N loss in the ETSP, often taking place in sinking organic matter particles and OMZ bottom waters (Karthäuser et al., 2021; Lam et al., 2009). In general N loss in the ETSP OMZ is well understood and estimated to account for ~25% of global water column N loss albeit with significant temporal variability associated with ENSO and PDO (Bianchi et al., 2012; Codispoti, 2007).

While the OMZ may be a net sink of N, it represents a major source of dissolved inorganic phosphorus (P) due to its proximity to the continental shelf. P associated with metal oxides such as iron (Fe) oxides buried in sediments is released back into the water column under reducing conditions (Figure 1.4), resulting in surplus phosphate (P*), (Ingall and Jahnke, 1994). Therefore P* is simultaneously accompanied by large amounts of bioavailable Fe (Noffke et al., 2012). Hence nutrient-rich upwelling source waters from the OMZ feature inorganic N:P ratios lower than Redfield often expressed as an N-deficit relative to P concentrations (N*=N-16.P). This N:P stoichiometry of upwelled OMZ waters in addition to the reduced O_2 levels are both proposed to provide a niche for diazotrophs in the OMZ of the ETSP (Deutsch et al., 2007). This has been the basis on which a spatial coupling between N loss and N_2 fixation has been hypothesized for OMZs proximate to upwelling regions (Deutsch et al., 2007).

1.4 Motivation and Objectives

The ratio of N_2 fixation and N loss controls the inventory of bioavailable N for marine primary productivity in the global ocean. The hypothesis of Deutsch et al. (2007) of a close spatial link between N_2 fixation and nitrogen loss and therefore the prediction of high N_2 fixation rates in the ETSP is antagonistic to the traditional paradigm for a stable marine N inventory (Gruber, 2004), which is based on an inter-basin separation of the two processes (Figure 1.2a). Therefore understanding the magnitudes and distribution of N_2 fixation and N loss in the HUS system is essential to assessing potential feedback, the sensitivity of the local N inventory to climate-related changes, and potential cascading effects on dependent ecosystem components and functions such as primary productivity.

A critique of the hypothesis proposed by Deutsch et al. (2007) is based on a theoretical stoichiometric discrepancy between N_2 fixation and N loss (Paulmier et al., 2009). The denitrification of newly fixed organic matter consumes bioavailable N (NO_3^-) at a higher inorganic N:P ratio (N:P 120:1) compared to N_2 fixation inputs which are assumed to occur under Redfield conditions (N:P 16:1), (Paulmier et al., 2009). The location and magnitude of N_2 fixation relative to zones and magnitude of denitrification in OMZ waters are therefore of biogeochemical significance. Under this imbalanced stoichiometry, the denitrification of organic matter associated with newly fixed N in OMZ waters would generate a much greater loss of bioavailable N than is fixed through N_2 fixation (Canfield, 2006; Landolfi et al., 2013). This in turn stimulates N_2 fixation due to the upwelling of waters with low N:P ratios and high Fe close to the coast. The increased N_2 fixation rates would support more organic matter inputs which further sustain denitrification and amplify the N deficit, thus initiating a vicious cycle composed of self-sustaining feedback (Fig. 1.2b). If this cycle persists, accumulating N deficits may result in runaway N loss in the ETSP as hypothesized by Landolfi et al (2013).

The maintenance of the OMZ and N loss involves a combination of processes, including the supply of N for primary productivity, fluxes of organic matter that support microbial respiration, and the intensity of mixing and ventilation (Karthäuser et al., 2021; Duteil and

Oschlies, 2011; Ganeshram et al., 1995). Among these, only the organic matter fluxes would be potentially influenced by N_2 fixation at the regional scale. Hence a proposed coupling between N_2 fixation and N loss requires that the magnitudes of N_2 fixation are sufficient to enhance productivity and sustain organic matter export to the zones of denitrification. To allow for stabilizing feedback in the N inventory, Landolfi et al. (2013) hypothesised that fixed N could be transformed and packaged in forms such as dissolved organic nitrogen that are less bioavailable and readily advected away from OMZ waters. Otherwise, N_2 fixation and associated organic matter may need to be spatially separated from sites of denitrification to avoid a runaway N loss.

The ecological, biogeochemical and economic dynamics of the northern HUS are closely linked. The fisheries yield is tightly coupled to the primary production (Messié and Chavez, 2015). Hence the strong reliance of the economy on the fisheries sector makes marine productivity a key component of the economic dynamics (Messié and Chavez, 2015; Christensen et al., 2014; Pauly and Christensen, 1995). As bioavailable N is the key nutrient limiting primary productivity in marine systems, the productivity of the northern HUS scales with the availability of bioavailable N (Messié et al., 2009). A runaway N loss as hypothesized by Landolfi et al. (2013) threatens nutrient availability for primary productivity in the northern HUS. Hence understanding the inputs and outputs of nitrogen in the system is essential in evaluating large-scale, cascading effects on ecosystem productivity.

To date, the majority of studies conducted in the HUS have primarily focused on elucidating the pathways of N loss, with limited attention given to N inputs via N_2 fixation. Thus, the understanding of N loss processes in the region is relatively well-established, with estimates suggesting that it contributes ~1/3 of the global N loss (Dalsgaard et al., 2012; Bianchi et al., 2012; Chang et al., 2010; Codispoti, and Packard, 1980; Gruber and Sarmiento, 1997). Thus, the lack of a comprehensive dataset that resolves N_2 fixation rates in both space and time constraints our understanding of the spatial distribution and importance of N_2 fixation in the HUS. There is also limited empirical data from the region supporting a direct clear link between N_2 fixation rates, and the availability of Fe and P, deemed primary conditions regulating N_2 fixation in the ocean (Ward et al., 2013). Thus, there is an incomplete understanding of what controls N_2 fixation in the ETSP. This has hindered the accurate assessment of the regional marine N inventory, potential feedback mechanisms, and their impact on N turnover and productivity.

Therefore, the main objective of this doctoral dissertation was to investigate the spatial distribution of N_2 fixation relative to N loss in the ETSP. We aimed to assess whether coastal water masses above and within the OMZ serve as hotspots for N_2 fixation in order to determine the potential for positive feedback on regional N cycling. Increasing the measurements of N_2 fixation and elucidating its relation to environmental conditions in the HUS is crucial for advancing our understanding of its biogeochemical significance locally, as well as in the global

ocean. By doing so significant strides can be made in comprehending and evaluating the fate of N_2 fixation in an ocean ridden by climate change. The specific aims were to:

(a) Explore the spatial distribution of the N_2 fixation rates in relation to the OMZ and N loss signal, coastal–offshore, and meridional gradients in environmental parameters (Chapter 2), in order to identify biogeochemical and physical conditions associated with the presence of N_2 fixation.
(b) Quantify the role of N_2 fixation in supplying new N for primary productivity and compensating the regional N deficit in the OMZ of the HUS (Chapter 2)
(c) Test the sensitivity and response of N_2 fixation to environmental conditions, including N:P supply ratios and excess phosphorus in upwelled waters and trace metal availability (Chapters 2 and 3)
(d) Evaluate how nitrate availability and light irradiance regulate nitrate and carbon uptake in the ETSP (Chapter 4).

1.5 Chapter Synopsis and author contributions

This doctoral dissertation is part of the "Humboldt Tipping" project, which is a subproject of the BioTip research focus funded by the German Federal Ministry of Education (BMBF). The project ran from 2019 – 2023 with the aim of assessing the risk of reduced productivity in the Humboldt upwelling system (HUS) off the west coast of Peru. The participating institutes were GEOMAR Helmholtz Centre for Ocean Research, Christian-Albrechts University (CAU-Kiel), The University of Hamburg, The University of Bremen, Leibniz Centre for Tropical Marine Research, Instituto del Mar del Perú, Group for the Analysis of Development (GRADE) and The Pontifical Catholic University of Peru.

This dissertation is part of work package 1 (WP1): Biogeochemical and ecological tipping points of the HUS focusing on evaluating the spatial distribution and biogeochemical role of N_2 fixation in the Humboldt Upwelling System, related biogeochemical feedbacks on the nitrogen cycle and cascading effects on regional primary production. The upcoming three chapters of this doctoral dissertation (Chapters 2- 4) are based on a scientific cruise (MSM80) conducted during the Austral summer of December 2018 – January 2019 and focusing on coastal upwelling systems in a changing Ocean.

Chapter 2: Published manuscript

Kittu, L. R., Paul, A. J., Fernández-Méndez, M., Hopwood, M. J., & Riebesell, U. (2023). **Coastal N_2 fixation rates coincide spatially with N loss in the Humboldt Upwelling System off Peru.** *Global Biogeochemical Cycles*, https://doi.org/10.1029/2022GB007578.

Chapter 3 presents the first spatially resolved dataset of N_2 fixation rates from the Eastern Tropical South Pacific (ETSP). Insitu N_2 fixation rate measurements were conducted across six onshore-offshore transects covering three-quarters of the Peruvian coast. N_2 fixation rates

were measured from the euphotic oxic waters to subsurface OMZ waters to include gradients in physical and biogeochemical environmental conditions. Alongside rate measurements, physical and biogeochemical environmental variables were also measured. As a novelty of this study that sets it apart from previous studies on N_2 fixation from the region, total dissolved trace metals concentrations including Fe were measured directly from the N_2 fixation incubations to determine in-situ Fe availability at the onset of incubations. This manuscript, therefore, reports on the magnitude, ecological (new N inputs for primary production), and biogeochemical (replenishing of local nitrogen loss) role of N_2 fixation rates in the HUS and potential environmental controls.

Chapter 3: Submitted manuscript

Kittu, L. R., Hopwood, M. J., Paul, A. J., Fernández-Méndez, M., Bach, L. T., Achterberg, E. P & Riebesell, U. (2023). **Cobalt and nickel moderate N_2 fixation rates in the Eastern Tropical South Pacific.** *Submitted to Science Advances*.

Chapter 3 reports results from a combination of a machine-learning statistical model (Boosted regression trees) on the observation dataset reported in Chapter 2 and bioassay experiments where key biogeochemical variables were manipulated to observe their influence on N_2 fixation rates. Two models were run where in addition to other variables, the role of Fe as a trace metal was investigated (Fe model) versus the inclusion of other trace metals such as Nickel (Ni), Cobalt (Co), Zinc (Zn), and Copper (Co) and the relative ratio of Co to Fe (TM model). At one offshore and coastal station on the Peruvian coast, bioassay experiments were conducted to investigate the response of N_2 fixation rates to different phosphorus concentrations in upwelled waters, Fe, Co, and Ni additions (added through mineral leachate) in incubations. Combining the results from these methods, this chapter demonstrates the weak response of N_2 fixation to Fe and P. As a novel part of this dissertation work, I show the potential for Co and Ni in regulating N_2 fixation in the ETSP and hypothesise the pathways through which this regulation may take place.

Chapter 4: Draft manuscript

Kittu, L. R., Fernández-Méndez, M., Paul, A. J., & Riebesell, U. (2023). **The impact of nitrate and light availability on nitrate and carbon uptake rates in the Humboldt Upwelling System off Peru.** *In preparation for Limnology and oceanography*

Chapter 5 presents results from nitrate and carbon assimilation experiments conducted at five stations along the Peruvian coast. Under different nitrate concentrations, nitrate uptake and its contribution to carbon uptake under variable light conditions were investigated using ^{15}N and ^{13}C isotopes. Furthermore, we conducted pigment composition analyses via high-performance liquid chromatography (HPLC) to assess the distribution of phytoplankton at the respective stations. My results indicate that in a mixotrophic-dominated phytoplankton

community under low nitrate concentrations, carbon and nitrate uptake are decoupled. Thus, we propose the role of regenerated nutrients in maintaining primary productivity in the ETSP.

Table 1. Author contributions

Chapter 2	
Conceptualization:	Allanah J. Paul, Ulf Riebesell, Mar Fernandez-Mendez, Leila R. Kittu, Mark J. Hopwood
Sample collection and analysis:	**Leila R. Kittu**, Allanah J. Paul, Mar Fernandez-Mendez, Mark J. Hopwood
Data analysis:	**Leila R. Kittu**
Writing – Original Draft preparation:	**Leila R. Kittu**
Writing - Review & Editing:	**Leila R. Kittu**, Allanah J. Paul, Mark J. Hopwood, Mar Fernandez-Mendez, Ulf Riebesell
Chapter 3	
Conceptualization:	Allanah J. Paul, Mar Fernandez-Mendez, **Leila R. Kittu**, Mark J. Hopwood, Lennart T. Bach
Sample collection and analysis:	Leila R. Kittu, Allanah J. Paul, Mar Fernandez-Mendez, Mark J. Hopwood
Data analysis:	**Leila R. Kittu**
Writing – Original Draft preparation:	**Leila R. Kittu**
Writing - Review & Editing:	**Leila R. Kittu**, Mark J. Hopwood, Allanah J. Paul, Mar Fernandez-Mendez, Eric P. Achterberg, Ulf Riebesell
Chapter 4	
Conceptualization:	Mar Fernandez-Mendez, Allanah J. Paul, **Leila R. Kittu**
Sample collection and analysis:	**Leila R. Kittu**, Mar Fernandez-Mendez, Allanah J. Paul
Data analysis:	**Leila R. Kittu**,
Writing – Original Draft preparation:	**Leila R. Kittu**
Writing - Review & Editing:	**Leila R. Kittu**, Mar Fernandez-Mendez, Allanah J. Paul, Ulf Riebesell

List of co-authored publications not included in this dissertation

Massig, J. C., Schukat, A., Auel, H., Auch, D., **Kittu, L. R.,** Arteaga, E. L., Acosta, J. C., Hagen, W. (2022). Toward a solution of the "Peruvian puzzle": Pelagic Food-Web structure and Trophic Interactions in the Northern Humboldt Upwelling System off Peru. *Frontiers in Marine Science*, https://doi.org/10.3389/fmars.2021.759603.

Shao et al. (2023). Version 2 of the global oceanic diazotrophic database. *Accepted for publication in Earth System science data.*

Auch, D., Steinen, V., Steckhan, L., Koppelmann, R., Yari, S., Mohrholz, V., Schukat, A., Fernández-Méndez, M., **Kittu. L. R.,** Myron Arms Peck (2022). Oceanographic structuring of the mucous-mesh grazer community in the Humboldt Current off Peru. *Under review in Marine Ecology Progress Series*.

Thielecke, A., Fernández-Méndez, M., Arístegui, A, Baumann, M., Behncke, J., Georgieva, S, Goldenberg, S., Gomez-Saez, G. V., Graco, M., Heene, T., **Kittu. L. R**, Krause, J, Ludwig, A., Meyer, J., Mohrholz, V., Ortiz, J., Schulz, K., Smith, A., Spilling, K., Sswat, M., Taucher, J., Varmanen, P., Riebesell, U (2023). The influence of light and upwelled nutrients on primary productivity, phytoplankton biomass, and carbon export during a mesocosm experiment off-shore Callao in February-March 2020. *To be submitted to Biogeosciences*.

Kittu, L. R, Paul, A. J., Löscher, C. R., Meyer, J., & Riebesell, U. (2023). Weak response of N_2 fixation activity to low N:P stoichiometry observed during a simulated upwelling event off the coast of Peru. *To be submitted to Biogeosciences*

Fernández-Méndez, M., Georgieva, S., **Kittu. L. R.,** Paul. A. J., Yari, S., Mohrholz, V., Riebesell, U (2023). Upwelling intensity modulates primary productivity and phytoplankton community composition in the Peruvian upwelling system. *In preparation*

Hopwood, M. J., Gledhill. M., Achterberg. E., Gu. Y., Al-Hasham. A., **Kittu. L.R.,** Krisch. S., Rapp. I (2023). Similar nickel distributions in the Peruvian, Benguela and Mauritania Oxygen Minimum Zones with potential implications for plankton physiology. *In preparation*

Chapter 2: Manuscript I

Magnitudes and Spatial distribution of N_2 fixation in the HUS

Coastal N_2 fixation rates coincide spatially with N loss in the Humboldt Upwelling System off Peru

L. R. Kittu[1*], A. J. Paul[1], M. Fernández-Méndez[1,2], M. J. Hopwood[1,3], U. Riebesell[1]

Published in *Global Biogeochemical Cycles*

https://doi.org/10.1029/2022GB007578

[1]Marine Biogeochemistry, GEOMAR Helmholtz Centre for Ocean Research Kiel, Düsternbrooker Weg 20, D-24105, Kiel, Germany

[2]Now at Alfred Wegner Institute Helmholtz Centre for Polar and Marine Research, Am Handelshafen 12, 27570, Bremerhaven

[3]Now at Southern University of Science and Technology, 1088 Xueyuan Avenue, 518055, Shenzhen, China

*Corresponding author:

Leila Kittu (lkittu@geomar.de)

**Manuscript format in journal style

Key points

- A north-to-south pattern in N_2 fixation rates was observed implying increased N turnover between 12°S and 16°S where N loss was pronounced.
- The highest N_2 fixation rates were measured in coastal productive waters above and within the OMZ, showing no clear relationship with Fe or P.
- The magnitude of N_2 fixation was low compared to predictions, estimated to account for ~0.3% of primary production and <2% of local N loss.

Abstract

Marine nitrogen (N_2) fixation supports significant primary productivity in the global ocean. However, in one of the most productive regions of the world ocean, the northern Humboldt Upwelling System (HUS), the magnitude and spatial distribution of this process remains poorly characterized. This study presents a spatially resolved dataset of N_2 fixation rates across six coastal transects of the northern HUS off Peru (8°S – 16°S) during austral summer. N_2 fixation rates were detected throughout the waters column including within the OMZ between 12°S and 16°S. N_2 fixation rates were highest where the subsurface Oxygen Minimum Zone (OMZ, O_2 <20 µmol L^{-1}) was most intense and estimated nitrogen (N) loss was highest. There, rates were measured throughout the water column. Hence the vertical and spatial distribution of rates indicates colocation of N_2 fixation with N loss in the coastal productive waters of the northern HUS. Despite high phosphate and total dissolvable iron (TdFe) concentrations throughout the study area, N_2 fixation was still generally low (1.19 ± 3.81 nmol L^{-1} d^{-1}) and its distribution could not be directly explained by these two factors. Our results suggest that the distribution was likely influenced by a complex interplay of environmental factors including phytoplankton biomass and organic matter availability, and potentially iron, or other trace metal (co)-limitation of both N_2 fixation and primary production. In general, our results support previous conclusions that N_2 fixation in the northern HUS plays a minor role as a source of new N and replenishes the regional N loss.

Plain Language Summary

High phytoplankton productivity in the Humboldt Upwelling System (HUS) is underpinned by a rich supply of nutrients, such as nitrate, brought to shelf surface waters from depth. However, marine microbes use up some of the nitrate in low-oxygen waters converting it back into nitrogen gas (N_2). Future climate change projections indicate that nitrate availability may decline in the surface ocean. Less phytoplankton growth in the HUS due to reduced nitrate supply could impact ocean services like fish production and biological carbon drawdown. Previous studies hypothesize that biological nitrogen fixation by microbes is present in the HUS. Here we studied the distribution and amount of nitrogen fixation in this region in relation to environmental conditions, to better understand if the inputs and losses of nitrogen are balanced. Our results indicate that nitrogen fixation rates are too low to counterbalance the

local nitrogen loss and do not contribute significantly to the nitrogen supply for phytoplankton growth. The availability of phosphate and iron is thought to control biological N_2 fixation rates on a global scale, but within the HUS we are unable to find evidence for this suggesting that other environmental factors, such as organic matter availability, control biological nitrogen fixation.

2.1 Introduction

Bioavailable nitrogen such as nitrate, nitrite, or ammonium, limits marine primary productivity in surface waters due to fast phytoplankton uptake relative to the supply (Moore et al., 2013). Therefore, processes that supply nitrogen (N) to the surface ocean are key to regulating marine productivity and the associated export of carbon to the deep ocean (Gruber, 2004). In the marine environment, the uptake of dinitrogen gas (N_2) by nitrogen-fixing microbes (diazotrophs) is widely recognized as a significant source of new bioavailable N (Gruber & Galloway, 2008). Therefore, diazotrophy has the potential to regulate marine productivity and influence the strength of the biological carbon pump (Karl et al., 2012). An understanding of the spatial distribution of N_2 fixation and the factors that regulate the growth of diazotrophs is essential to comprehending past and future changes in bioavailable N and the associated ecosystem services.

At a steady state and a global scale, inputs of bioavailable N to the oceans should be at equilibrium with loss of N through microbially mediated processes such as denitrification and anammox (anaerobic ammonium oxidation). To keep the global marine N inventory at equilibrium, stabilizing feedback mechanisms between N gain and N loss processes are thereby required. Inputs of bioavailable N are thought to be spatially separated from losses due to factors such as iron (Fe) limitation, temperature, and macronutrient availability which constrain diazotrophy and influence diazotrophs' response to the local N loss (Gruber, 2004). Whilst N_2 fixation is primarily known to take place in surface waters of open ocean environments, about a third of the global ocean N loss is ascribed to Oxygen Minimum Zones (OMZs, Karstensen et al., 2008). In these zones, oxygen (O_2) concentrations are low enough (OMZ is loosely defined herein as O_2 <20 µmol L^{-1}, Supplementary Info, Text. S1) for both N loss mechanisms, denitrification, and anammox to take place (DeVries et al., 2012). The OMZ in the Eastern Tropical South Pacific (ETSP) is one such region where a substantial portion of global N loss is known to occur (Hamersley et al., 2007; Kalvelage et al., 2013). As a result of the low O_2 concentrations in subsurface waters of the ETSP, preferential N loss over phosphate (P) results in surplus P conditions over available nitrate in the water column (P*, defined using the Redfield N:P ratio of 16, Deutsch et al., 2007; Redfield, 1958). In addition, and of direct relevance to diazotrophs given the high Fe requirement of the N_2 fixing enzyme nitrogenase, there is a pronounced release of Fe from shelf sediments into the water column (Kustka et al., 2003; Noffke et al., 2012). These conditions of increased phosphate relative to N, and high iron availability should theoretically favour the growth of diazotrophs. As a result, biogeochemical models have predicted that high N_2 fixation in the ETSP could potentially replenish the intense N loss taking place in subsurface coastal waters (Deutsch et al., 2007). However, contrasting

observational and biogeochemical evidence for spatial separation of N_2 fixation and N loss in the ETSP suggests that the regional N inventory in the ETSP could be balanced by external N inputs through high N_2 fixation rates observed in the Western Tropical South Pacific (Bonnet et al., 2017; Wang et al., 2019). There is uncertainty concerning the role of N_2 fixation in the ETSP and to what extent it may balance the regional N loss.

A biogeochemical model by Landolfi et al. (2013) demonstrated that colocation of N_2 fixation and N loss as hypothesized for the ETSP OMZ (Deutsch et al., 2007), could result in a self-sustaining destabilizing feedback in the N cycle. This emanates from a stoichiometric imbalance, whereby the denitrification of newly fixed organic matter occurs at a higher inorganic N:P ratio (120:1) than N_2 fixation inputs under Redfield conditions (N: P~16:1, Paulmier et al., 2009). This results in an enhanced N deficit which could stimulate more N_2 fixation. A vicious cycle can ensue if this feedback persists, whereby complete remineralization of organic matter associated with newly fixed N via N_2 fixation would lead to a net loss of bioavailable N from the system. To date, this hypothesized feedback and its implications on the local and global marine N inventory have yet to be assessed. Due to a scarcity of data, and a limited geographical range of observations, N_2 fixation estimates from regions with intensive N loss are mainly based on a few measurements extrapolated to large regions. Given the high spatial and temporal variability of diazotrophic abundances, activities, and species distributions (Gradoville et al., 2017), especially across dynamic shelf regions, these extrapolations have considerable uncertainties. For the ETSP in particular, it is still unclear for example how temporal patterns of N_2 fixation may be influenced by long-term climate variability and environmental changes associated with the El Niño-Southern Oscillation dynamics on which N loss processes like denitrification have been shown to respond sensitively to (Yang et al., 2017).

Furthermore, there is an ongoing debate concerning the extent to which N_2 fixation rates are controlled by environmental conditions such as in situ O_2, temperature, organic matter, phosphate, and iron availabilities (Knapp et al., 2016; Luo et al., 2014; Wang et al., 2019). Currently, there is only limited evidence to support a clear link between excess phosphate and Fe availability as primary regulators of N_2 fixation rates within the OMZ of the ETSP (Bonnet et al., 2013; Chang et al., 2019; Dekaezemacker et al., 2013; Fernandez et al., 2015; Löscher et al., 2014; Selden et al., 2021; Wang et al., 2019), despite these factors being widely attributed to determining the spatial niche in which diazotrophy can occur (Ward et al., 2013). However, a confounding factor in assessing the role, particularly of Fe, on diazotrophy is that trace metal concentrations are rarely measured in parallel with N_2 fixation rates partly due to high chances of sample contamination. This could be a contributing factor to the apparent lack of a clear relationship between Fe and measured rates. Herein, to investigate the distribution and magnitude of N_2 fixation in relation to environmental conditions in the ETSP, we conducted measurements across 6 transects from north to south of the northern HUS off the Peruvian coast. We measured N_2 fixation across gradients of latitude, and physical and biogeochemical conditions, including Fe concentrations within the incubations used to determine N_2 fixation rates. We aimed to evaluate the distribution of N_2 fixation in relation to environmental

conditions and assess the potential colocation of N_2 fixation and estimates of bioavailable N loss in the northern HUS.

2.2 Materials and Methods

2.2.1 Study area and hydrographic sampling

The cruise took place during a warm austral summer (December 23, 2018, to January 30, 2019) characterized by ~ 0.7 – 0.8 °C above average sea surface temperatures (SSTs) and weak southeast trade winds during an El Niño. We measured N_2 fixation rates, nutrient concentrations, and hydrographic data from 26 stations in the ETSP onboard RV Maria S Merian (cruise MSM 80). Sampling extended along six transects (Figure 1) off Peru from 8° 30'S to 16° 30'S at distances of 4 to 293 km from the shore. Our sampling strategy was optimized to cover spatial and vertical gradients of O_2, micro- and macronutrients, primary productivity, and light and upwelling intensities.

At each station, vertical depth profiles of temperature, salinity, dissolved oxygen (O_2), photosynthetically-active radiation (PAR), chlorophyll *a* fluorescence, and turbidity were obtained using a Seabird (SBE-911 plus, Seabird-Electronics, USA) conductivity-temperature-depth (CTD) profiler equipped with double temperature (SBE 3) and O_2 sensors (SBE43), a LI-COR Bio spherical PAR sensor and a Wet Labs ECO-FLNTURTD chlorophyll-turbidity sensor. O_2 concentrations from discrete water samples (Winkler titration) were used to calibrate the CTD oxygen sensor. The CTD and sensors were mounted on a 21×10 L Niskin bottle rosette water sampler from which discrete water samples were collected.

Satellite-derived MODIS Chl *a* (NASA Ocean Biology Processing Group, 2017) and SSTs (NASA/JPL, 2020) were downloaded as 8-day composites covering the dates each transect was sampled: Transect 1 (27-31 December 2018), Transect 2 and 3 (1 – 8 January 2019), Transect 4 and 5 (9 – 16 January 2019) and Transect 6 (17 – 24 January 2019).

2.2.2 N_2 fixation incubations and particulate matter isotopic composition

Seawater samples from each station were collected from four to six depths distributed from the surface (~ 5 – 10 m) to a maximum of 300 m covering the OMZ (O_2 <20 µmol L^{-1}). A subsample (0.4 – 1.5 L), was immediately filtered (GF75, Advantec, 25 mm Ø, 0.3 µm nominal pore size) for natural abundance of particulate organic carbon and nitrogen concentrations (POC/N) and isotopic compositions ($\delta^{13}C_{POC}/\delta^{15}N_{PON}$).

N_2 fixation rates were determined from triplicate incubations following the modified ^{15}N-N_2 dissolution technique (Großkopf et al., 2012; Mohr et al., 2010). 2.3 L Nalgene transparent polycarbonate bottles were pre-cleaned with 10% HCL and rinsed three times to minimize trace metal contamination before filling with seawater samples. Oxygen contamination during seawater collection was minimized by filling the bottles gently and bubble-free from the

bottom with a tube, allowing the overflow of about half the bottle volume before closing the headspace of the bottle free with septa-fitted caps. This same method was applied for collecting Winkler samples that were used for CTD calibration. Incubation bottles were amended with 100 mL of ^{15}N-N_2-enriched seawater (Supplementary Info, Text S2) yielding an average dissolved N_2 isotope abundance (^{15}N atom %) of 3.90 ± 0.02 atom % (mean ± SD) in the incubation bottle. Blank incubations using atmospheric air instead of ^{15}N-N_2 isotope addition were performed to track any natural changes in the $\delta^{15}N$ that may not have been a result of ^{15}N-N_2 addition. The use of air for the blank incubation introduced small amounts of dissolved O_2 changes against background concentrations calculated to range between 0 – 0.6 % in OMZ incubations and 0 – 0.14% in euphotic zone incubations. Bottles were incubated for 24 h in on-deck incubators with a continuous flow of surface seawater. Incubators were shaded to receive 100, 40%, 30%, 15%, 5%, and 0% (Lagoon blue neutral density light screens, Lee light filters) of incoming PAR corresponding to approximate *in-situ* PAR conditions of sampled depths. After 24 hrs, entire incubation bottles or, in cases of high biomass, subsamples from individual incubations (range of PON on filter 4.73 – 177.02 μg/filter) were filtered under gentle pressure (200 mbar) onto pre-combusted GF75 (Advantec, 25 mm Ø, 0.3 μm nominal pore size) and treated with acid (1M HCl for 2 minutes) to remove particulate inorganic carbon. Filters were oven-dried overnight at 60°C, packed in tin capsules, and pelleted for further analysis. All filters were analyzed for POC/N concentration and isotopic composition ($\delta^{13}C_{POC}$/$\delta^{15}N_{PON}$) on an elemental analyzer (Flash EA, ThermoFisher) connected to a mass spectrometer (Delta V Advantage Isotope Ratio MS, ThermoFisher) with the ConFlo IV interface (ThermoFisher).

2.2.3 N_2 fixation rates, limits of detection, and error analysis

Volumetric absolute N_2 fixation rates were computed as shown in equation (1) according to Montoya et al. (1996)

$$N_2 \text{ fixation rate} = \frac{A_{PON}^{t=f} - A_{PON}^{t_f=i}}{A_{N_2} - A_{PON}^{t_f=i}} \times \frac{[PON]}{\Delta t} \quad (1)$$

Whereby A_{PON} represents the isotope abundance (^{15}N atom %) of PON in the natural abundance samples ($t = 0$), blank ($t_f = i$) and final (t = f) incubations respectively. A_{N_2} represents the isotope abundance of the dissolved inorganic N_2 pool (added + ambient) available to N_2 fixers calculated according to White et al (2020), and Δt represents the incubation period. The concentration of added $^{15}N_2$ gas in the enriched water was estimated from ideal gas law and the ambient N_2 gas was estimated using gas solubility equations adapted from Weiss. (1970) (Supplementary Text S2). Following a Wilcoxon test for paired samples between the blank incubation and the natural abundance, we observed a significant difference in the isotope abundance of the PON between the two sets of samples (Supplementary Info, Figure S1) indicating that natural changes were taking place in the incubations, independent of isotope addition. Hence, we used the ^{15}N atom% enrichment from the blank incubation rather than the natural abundance for our calculation to ensure that detectable changes in the

$\delta^{15}N$ isotope signal from our amended incubations account for naturally occurring changes and bottle effects that were not associated with $^{15}N_2$ tracer addition.

For each station, volumetric rates were trapezoidal depth-integrated (areal rates) from the surface through to the maximum depth sampled per station (depth range = 20 – 250 m). To integrate rates, we assumed that N_2 fixation rates were constant from the surface (0 m) to the depth of the shallowest rate (often 5 – 10 m and always within the surface mixed layer depth). POC concentrations were also integrated to similar depths as N_2 fixation rates.

Limits of detection (LOD) were calculated as described by White et al. (2020) using standard propagation of errors based on observed variability between triplicate samples (Bevington & Robinson, 2002; Gradoville et al., 2017). Any measured N_2 fixation rates below the limit of detection for each respective measurement were assumed to be equal to 0 nmol N L^{-1} d^{-1} before any further statistical analysis was done. See Supplementary Info, Text S3 for detailed explanations concerning LOD calculations.

2.2.4 Inorganic nutrients, Chl a, and Trace metal analyses

Unfiltered samples for dissolved inorganic nitrogen (nitrate (NO_3^-), nitrite (NO_2^-) and ammonium (NH_4^+), hereafter DIN), phosphate (PO_4^{3-} or DIP), and silicate ($Si(OH)_4$) were collected in triplicate. Concentrations were measured onboard using an autosampler (XY-2 autosampler, SEAL Analytical) and a continuous flow analyzer (QUAAtro Autoanalyzer, SEAL Analytical) according to Holmes et al., 2011; Morris & Riley, 1963; Murphy & Riley, 1962. The LOD was calculated from blank measurements as blank + 3 times the standard deviation of the blank during each measurement (LOD NO_3^- = 0.133 μmol L^{-1}, NO_2^- = 0.011 μmol L^{-1}, NH_4^+ = 0.040 μmol L^{-1}, $Si(OH)_4$ = 0.130 μmol L^{-1}, PO_4^{3-} = 0.009 μmol L^{-1}). The precision of the measurements was estimated from the average standard deviation between triplicate measurements (NO_3^- = 0.028 μmol L^{-1}, NO_2^- = 0.018 μmol L^{-1}, NH_4^+ = 0.029 μmol L^{-1}, $Si(OH)_4$ = 0.013 μmol L^{-1}, PO_4^{3-} = 0.003 μmol L^{-1}). Dissolved organic phosphorus (DOP) was measured using the persulfate oxidation approach outlined in Hansen & Koroleff, 1999 with an oxidizing decomposition reagent (Merck, Germany). P* was calculated from DIN (NO_3^- +NO_2^- + NH_4^+) and DIP measurements after Deutsch et al. (2007) using equation (2) where $R_{16:1}$ is the integrated ratio of DIN and DIP in seawater and organic matter (Redfield, 1958).

$$P^* = \left[PO_4^{3-}\right] - \frac{[NO_3^-]+[NH_4^+]+[NO_2^-]}{R_{16:1}} \quad (2)$$

To measure total dissolvable (Td) trace metal concentrations available within our N_2 fixation incubations, seawater samples were taken unfiltered from the Niskin bottle where N_2 fixation samples were collected. Samples were retained in 125 ml low-density polyethene sample bottles (Nalgene) which had been pre-cleaned (Mucasol®, followed by 1 week in 3 M HCl and 1 week in 3 M HNO_3 with 3 deionized water rinses after each stage). Plasticware for sampling was cleaned similarly. Sample bottles were pre-rinsed three times with a few millilitres of the

sample before filling. Sample bottles were stored double-sealed in sample bags. Total dissolved trace metal concentrations were determined via inductively coupled plasma mass spectrometry (ICPMS) after preconcentration, per Rapp et al. (2017). Samples were acidified with ultrapure hydrochloric acid (UpA grade, Romil) to pH 1.9 and left sitting for >6 months, subjected to 4 h UV irradiation in 30 mL fluorinated ethylene propylene bottles, preconcentrated offline using a SeaFAST system (Elemental Scientific Inc), and then analyzed on an Element XR ICPMS (Thermo Finnigan). The trace metal reference material CASS-6 was also analyzed to assess the accuracy of the analytical procedure (Supplementary Info. Table 1).

As the main purpose of measuring total dissolvable iron (TdFe) was to ascertain the Fe available to diazotrophs as incubated, which may diverge from ambient concentrations, some degree of contamination would not detract from the purpose of the study. At 3 stations which were 6, 9, and 234 km from the coast, triplicate samples were taken to check for data reproducibility (Supplementary Info, Figure S2a). The similarity of triplicate TdFe samples (Supplementary Info, Figure S2a) suggests a limited degree of random contamination, and concentrations are in the range of Total particulate Fe and dissolved Fe concentrations determined on a prior cruise (Hopwood et al., 2021) with a GEOTRACES compliant trace metal clean rosette system and clean lab (Supplementary Info, Figure S2b). Due to a benthic Fe source in this region, the extremely high TdFe concentrations are realistic for coastal shallow stations (Chever et al., 2015) and would likely mask any modest degree of Fe contamination during handling (Supplementary Info, Figure S2b)

To assess trace metal and macronutrient coupling, we calculated a diagnostic tracer as a measure of Fe colimitation with PO_4^{3-} ($TdFe_P$*) using equation (3), (Parekh et al., 2005; Tang, Wang et al., 2019). $R_{Fe:P}$ represents average phytoplankton uptake requirements for multiple nutrient availabilities based on the extended Redfield ratio $(C_{7.75}N_1Si_1P_{0.0626})_{1000}Fe_{0.469}$ (Moore, 2016). Positive values for $TdFe_P$* suggest Fe is in excess relative to measured PO_4^{3-}, while negative values indicate Fe deficiency.

$$TdFe_P^* = [TdFe] - R_{Fe:P} \times \left[PO_4^{3-}\right] \quad (3)$$

2.2.5 Estimating fixed nitrogen loss

To estimate water column N loss, a DIN deficit (N_{def}) method, as described originally by Codispoti et al. (2001) was used. N_{def} estimates the amount of fixed nitrogen removed from a parcel of water integrated over space and time assuming no mixing. N_{def} was estimated as the difference between the expected DIN (N_{exp}) considering N loss was absent and observed DIN (N_{obs}) from our study according to equation (4) by Chang et al. (2010). N_{exp} was calculated considering Redfield (Redfield, 1958) organic matter respiration regenerating a local average inorganic N:P ratio of 15.8 for waters outside the ETSP OMZ where anaerobic DIN loss is assumed to be 0. The value 0.3 µmol L^{-1} denotes the concentration of PO_4^{3-} remaining when

DIN is zero in the N:P relationship. Based on this definition, positive values of N_{def} estimate DIN loss that has occurred in a water mass within in the Peruvian OMZ.

$$N_{def} = 15.8\left[PO_4^{3-} - 0.3\right] - \left[NO_3^- + NH_4^+ + NO_2^-\right] \quad (4)$$

2.2.6 Statistical analyses

Across the entire dataset of N_2 fixation, a Spearman's rank correlation was used to examine the potential relationships between N_2 fixation rates and physical, biogeochemical, and biological parameters across the northern HUS.

Gradients in biogeochemical variables could influence the magnitude and distribution of N_2 fixation rates in the water column, Therefore, three water column depth horizons were identified based on PAR/fluorescence and O_2 concentrations: the euphotic zone (oxic waters within the euphotic zone), the oxic zone (describing all sampled depths below the euphotic zone with O_2 concentrations >20 µmol L^{-1}) and the OMZ zone (describing deeper depths where O_2 concentrations were <20 µmol L^{-1}). See Supplementary Info, Text S1 for further details of how depth horizons were delimited. Measurements of N_2 fixation rates, and physical and biogeochemical variables were then grouped based on the depth horizons. To test for the differences in the distribution of N_2 fixation rates and physical and biogeochemical variables between the three depth horizons, a non-parametric one-way analysis of variance (ANOVA) with Kruskal-Wallis test was performed. A Dunns multiple comparison test was applied post hoc to analyze differences between every pair of groups. By applying these two techniques we increased the chance to reveal relationships that may not follow a linear distribution.

The spatial distribution of some environmental variables such as measured O_2, satellite-derived SSTs, and surface Chl *a* from MODIS were interpolated using the Akima package in R (code (TOMS 760 et al., 2021). All statistical analysis and data visualizations were performed with R studio version 1.3.959.

2.3. Results

2.3.1 Oceanographic conditions

Our cruise took place in the northern HUS, covering almost half of the Peruvian coast from north to south (Figure 1a). Our stations encompassed coastal locations where the lower boundary of the OMZ is ~600 m, and offshore locations where the lower boundary of the OMZ is >600 m (Kalvelage et al., 2013). Transects 1 and 2 were located on a wide shelf area off northern Peru where mean MODIS SSTs ranged from 21°C to 24°C (Figure 1a) with averages of 22.12 ± 1.82°C (Supplementary Info, Table 2). Vertical temperature and salinity distribution at the time of sampling exhibited a typical upwelling pattern of low surface temperatures (~ 20°C) and a reduced vertical temperature gradient close to shore with low salinity waters (<35.1, Supplementary Info, Figures S3, and S4). A pronounced subsurface salinity maximum developed past the shelf edge probably as a result of offshore drift of high salinity waters. In

addition, a thick (~70 m depth), well-oxygenated water layer was observed in all stations from the northern transects (Figure 2). The upper boundary of the OMZ (O_2 = 20 µmol L^{-1}) extended from 51 m to 150 m and O_2 concentrations were below the detection limit (2 – 3 µmol L^{-1}) in deeper waters between 200 and 650 m depth. In all stations above the shelf from Transects 1 and 2, O_2 concentrations were consistently above 50 µmol L^{-1} and an upward shoaling of oxyclines was also observed in stations above the shelf edge, indicating the influence of enhanced mixing and advection in coastal subsurface waters.

Transect 3 covered the central shelf at 12°S off Callao, marking a transition between the north and south of the HUS. Cool mean MODIS SSTs (~ 19°C) at the coast and salinity gradients indicated active or recent upwelling (Figure 1a). Surface waters were associated with elevated mean MODIS Chl *a* (Figure 1b) and increased turbidity (Supplementary Info, Table 3, Figure S6). In contrast to the northern shelf transects, salinity was in general slightly lower and homogenous throughout the water column (35.05) showing a weak subsurface salinity maximum (Supplementary Info, Figure S4). Towards oceanic waters at the transect edge, SSTs slightly increased to 24°C. All stations sampled from Transect 3 were coastal with an OMZ thickness ranging between 80 and 420 m (Figure 2). A shallow OMZ was observed where the upper boundary of the OMZ ranged between 20 and 70 m and O_2 concentrations were below detection between 100 m and 550 m.

On the southern Peruvian coast where the shelf is relatively narrow, hydrographic features between 14.5°S and 16°S indicated that upwelling was active during our sampling. A signal of low O_2, nutrient-rich waters appeared at the surface (Figure 2, Figure 4a). Low SST (~ 18°C) was observed close to the coast accompanied by upward shoaling of oxyclines very close to the coast at 14.4°S (Figure 2, Supplementary Info, Table 2, Figure S3). In offshore stations, mean MODIS SSTs reached a maximum of ~22°C and vertical O_2 and temperature profiles indicated a shallow (~20 m thick, Supplementary Info, Figure S3) well-oxygenated layer of warm surface water. Absolute temperatures and vertical gradients decreased eastwards towards the coastal stations in all southern transects (Transects 4-6). Around 15°S (Transect 5), local vertical shoaling of isotherms was observed above the shelf. High Chl *a* and POC concentrations (Figure 1) were observed in surface waters of coastal stations in the southern transects consistent with a narrow surface turbidity layer at 15.3°S (Supplementary Info, Figure S6). Additionally, a narrow-oxygenated surface water layer was observed, mostly separated from a shallow OMZ by the 17°C isotherm, although O_2 concentrations were still lower than the northern transects (Supplementary Info. Table 2). In the southern part of the study area, the upper boundary of the OMZ ranged from 4 m - 58 m. Between 50 m and 735 m across all stations from Transects 4 - 6, O_2 was below detection.

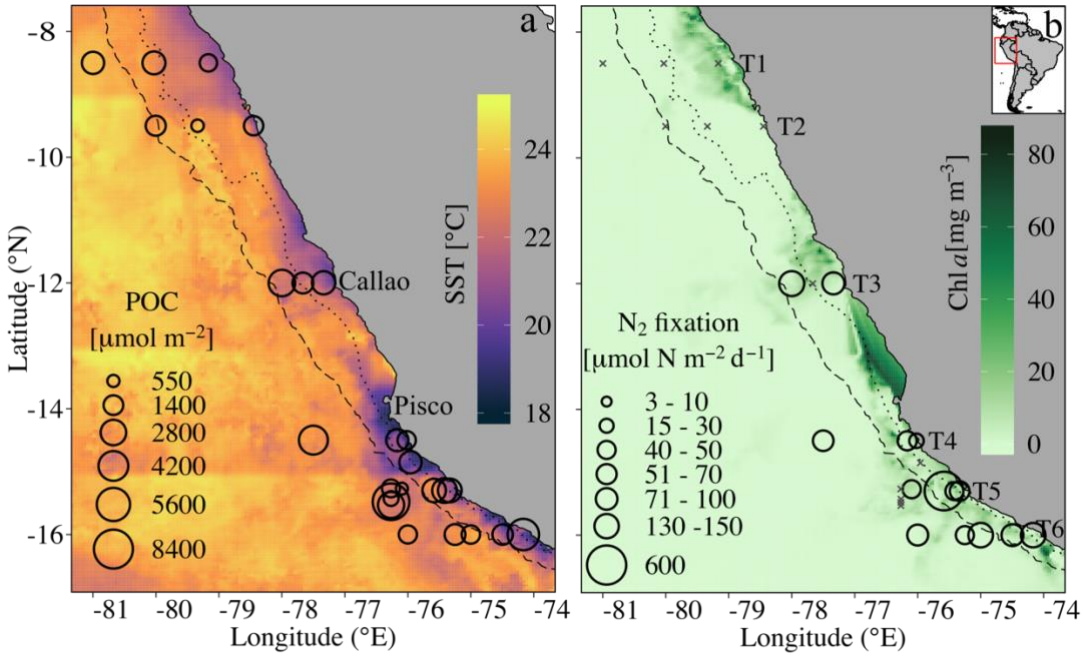

Figure 1. (a) Mean MODIS (NASA/JPL, 2020) sea surface temperature (SST) in the study area overlain by depth-integrated Particulate Organic Carbon (POC) concentrations at each station. (b) Mean MODIS (NASA Ocean Biology Processing Group, 2017) surface Chlorophyll *a* concentration (Chl a) overlain by integrated N_2 fixation rates (µmol N m^{-2} d^{-1}) for each station along the six across-shelf transects (T1-T6). Crosses on (b) indicate rates below detection. 8-day average products of SST and Chl *a* covering the dates each transect was sampled were used to generate figures a and b respectively. Black dotted and dashed lines show 200 m and 2000 m bathymetry to indicate the edge of the shelf and shelf slope, respectively.

2.3.2 N_2 fixation rates

Measured N_2 fixation rates showed a latitudinal trend, on average increasing from north to south of the Peruvian coast (Figure 2). This trend was consistent with significant latitudinal differences in SSTs, PO_4^{3-}, P*, DIN:P, N*def*, turbidity, POC, and PON (Supplementary Info. Table 2). Rates ranged between undetectable in the two northern transects (Transect 1 and 2) to a maximum of 30.97 nmol N L^{-1} d^{-1} at Transect 5 with an overall average and standard deviation of 1.19 ± 3.81 nmol N L^{-1} d^{-1} (n=103 measurements). Detectable N_2 fixation rates between 12°S to 16°S (Transects 3 – 6), were measured above the shelf (range 0.38 – 30.97 nmol N L^{-1} d^{-1} n= 75 measurements) corresponding to waters with DIN:DIP ratios below 16 (Figure 3a).

Considering the depth distribution of the rates, the highest mean N_2 fixation rates (1.73 ± 4.82 nmol N L^{-1} d^{-1}, n=62) were measured in warm (19.3 ± 2.22 °C), oxic waters (>20 µmol L^{-1}) within the euphotic zone (12 – 73 m) albeit with high variability between depths (Supplementary Info. Table 3). The second average rates, 0.45 ± 0.59 nmol N L^{-1} d^{-1} were measured within cooler waters of the OMZ where O_2 concentrations were lowest and P* and $\mathrm{Td}Fe_P^*$ were highest (Supplementary Info. Table 3) while the lowest average rates were measured from oxic waters

(0.12 ± 0.40 nmol N L^{-1} d^{-1}). A Kruskal-Wallis one-way analysis of variance testing for the null hypothesis that the distribution of N_2 fixation rates between the depth horizons has identical medians was insignificant (Kruskal-Wallis p>0.05, Supplementary Info. Table 3).

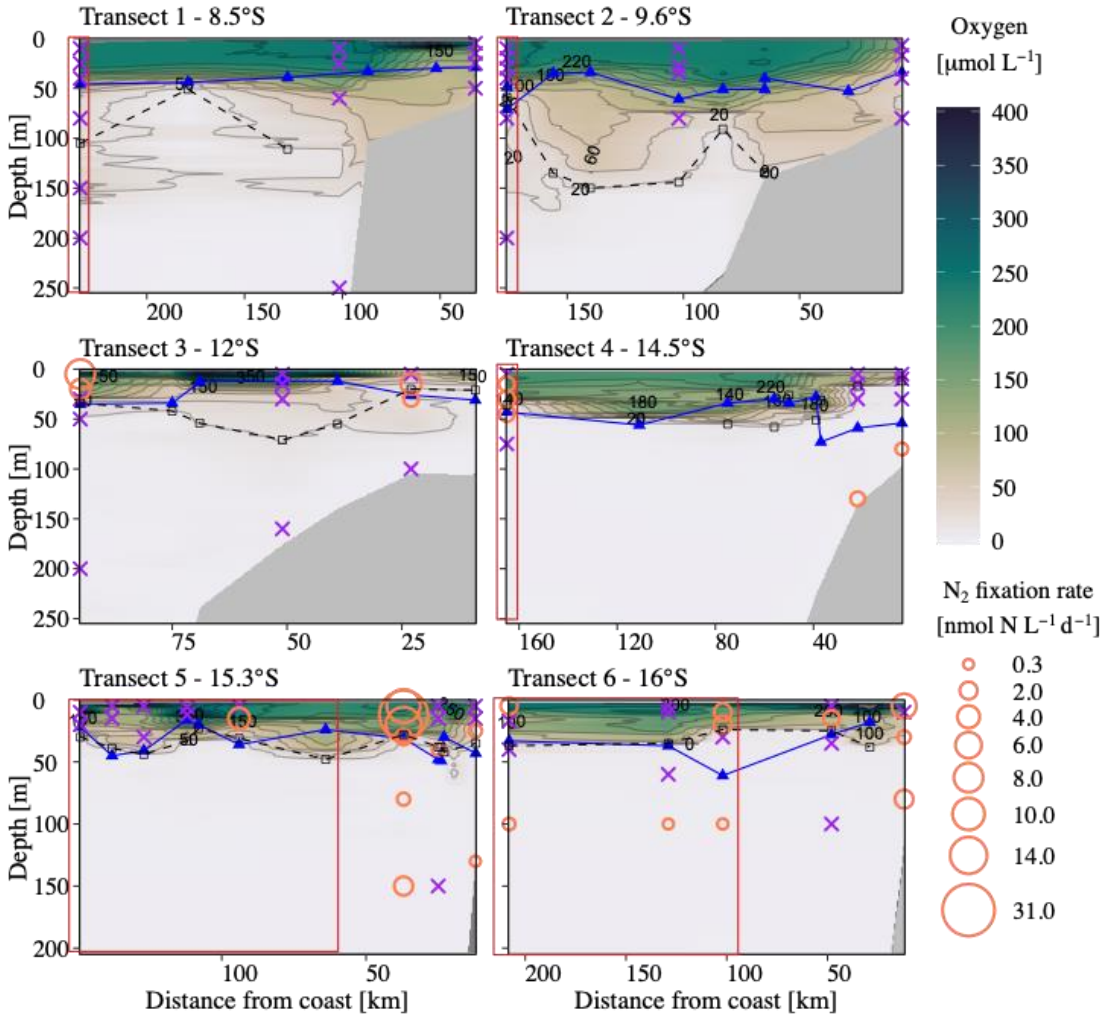

Figure 2: Measured N_2 fixation rates (empty orange circles) overlayed on the vertical distribution of O_2 concentrations (µmol L^{-1}) along the six transects. The black dotted lines and blue full line with triangles indicate the upper boundary of the OMZ waters (O_2 <20 µmol L^{-1}) and the depth of the euphotic zone (PAR = 1%) respectively. Purple crosses indicate depths where N_2 fixation rates were below detection. The red box indicates offshore stations defined as those in which the lower boundary of the OMZ was >600 m.

N_2 fixation rates were significantly positively correlated with POC, turbidity, and Chl *a,* all factors that were used as proxies for phytoplankton-associated organic matter availability (Figure 3b). In addition, temperature and oxygen were also positively correlated with N_2 fixation. Despite the co-occurrence of high N_2 fixation in surface waters with high DOP concentrations (Supplementary Info. Table 3), a weak positive relationship observed between N_2 fixation and DOP was not significant. DIN and DIN:P were both negatively correlated with

N_2 fixation rates across the whole dataset, with the lowest values observed in southern transects (Transects 4-6, Supplementary Info. Table 2).

Depth-integrated N_2 fixation rates (areal, 0 – 250 m) ranged from 18.20 to 582.11 µmol N m^{-2} d^{-1} (average ± sd, 124.04 ± 138.94 µmol N m^{-2} d^{-1}) showing latitudinal differences from the central to the southern extent of our study (12°S and 16°S). Albeit with high variability, average areal rates were highest in Transect 5 (188.15 ± 262.80 µmol N m^{-2} d^{-1}, Supplementary Info, Figure S5).

2.3.3 Macronutrients and total dissolved iron

For all stations, PO_4^{3-} and DIN concentrations in waters above the OMZ ranged between (0.50 - 2.60 µmol L^{-1}) and (0.10 – 33.17 µmol L^{-1}) respectively (Figure 4a, Supplementary Info, Figure S6). Beyond the respective limits of the euphotic zone across all stations (12 – 73 m), DIN and PO_4^{3-} concentrations exceeded 15 and 2 µmol L^{-1}, respectively. DIN:DIP ratios ranged between 0.05 – 15.17 (average in the euphotic zone was 10.00 ± 3.73, average in oxic waters was 13.76 ± 1.46), indicating a deficit of dissolved inorganic nitrogen throughout the water column (Figure 3, Supplementary Info. Table 3). PO_4^{3-} concentrations were low in Transect 1 and 2 (1.49 ± 0.56 µmol L^{-1}) coinciding with high DIN concentrations which resulted in low P* values (<0.5) down to 200 m (Figure 4a, Supplementary Info. Table 3). For Transects 3 – 6, PO_4^{3-} concentrations were on average higher (1.94 ± 0.68 µmol L^{-1}) than in the north (Figure 4a). Coupled with slightly lower NO_3^- concentrations, high P* values were measured (0.73 ± 0.35 µmol L^{-1}) between the central and southern part of our study reflecting DIN loss in most of the water column (Figure 5b, Supplementary Info, Figure S8). Upward shoaling of waters with high P* was observed in OMZ waters throughout the study area, indicating a tendency of upward advection of denitrified waters with high PO_4^{3-} relative to DIN (Supplementary Info, Figure S8). DOP concentrations were higher in the euphotic waters (0.24 ± 0.17 µmol L^{-1}) and lower at depth (range = 0 – 0.15 µmol L^{-1}). The highest DOP concentrations were measured from the surface waters of Transect 4 (1.18 µmol L^{-1}) and at a coastal station of Transect 6 (0.54 µmol L^{-1}, (Supplementary Info, Figure S9).

Total dissolvable iron (TdFe) concentrations were high in most of the incubations with slight differences in TdFe concentrations between the northern (28.11± 50.61 nmol L^{-1}), central (82.71 ± 127.17), and southern (36.31 ± 40.47 nmol L^{-1}) transects (Supplementary Info. Table 2). The highest TdFe concentrations were measured from subsurface waters close to the coast at 12°S (461.84 nmol L^{-1}). Generally, depth distributions indicated lower concentrations in surface waters close to the coast which occasionally increased towards deeper waters (Supplementary Info. Table 3). However, uniformly high TdFe concentrations were measured in surface waters of stations closest to the coast at 14°S. Concentrations in the euphotic zone (depth range, 12 – 73 m) ranged from 1.18 to 216.53 nmol L^{-1} (mean ± SD = 22.23 ± 35.03 nmol L^{-1}). In the oxic waters below the euphotic zone, TdFe concentrations increased with depth from 8.06 to 223.49 nmol L^{-1} (mean ± SD = 55.70 ± 78.06 nmol L^{-1}) but showed high variability

due to sporadic high concentrations >200 nmol L^{-1} in subsurface waters at most coastal stations in Transect 2. Within O_2-deficient waters, average concentrations were slightly higher than those in oxic waters but similarly with high variability (68.22 ± 87.13 nmol L^{-1}). $TdFe_P{}^*$ followed a similar pattern as absolute TdFe concentrations (Supplementary Info, Figure S10).

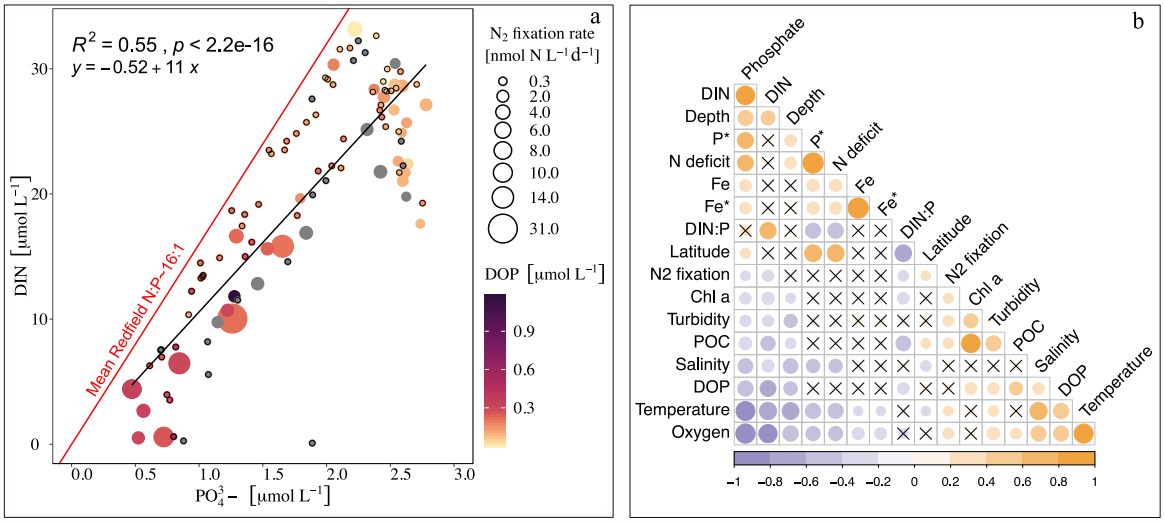

Figure 3. (a) Relationship between DIN and PO_4^{3-} concentrations for all stations during the cruise. The size of the circles corresponds to measured N_2 fixation rates and the colour corresponds to dissolved organic phosphorus concentrations (DOP). Grey points and points with black rings depict samples where DOP concentrations and N_2 fixation rates were below the detection limit respectively. (b) Spearman correlation coefficients plot including N_2 fixation rates and environmental variables (n = 103). Positive and negative correlations are displayed in orange and purple respectively. The colour intensity and size of the circles are proportional to the correlation coefficients. Non-significant correlations (adjusted *p-value >0.05*) are indicated by black crosses.

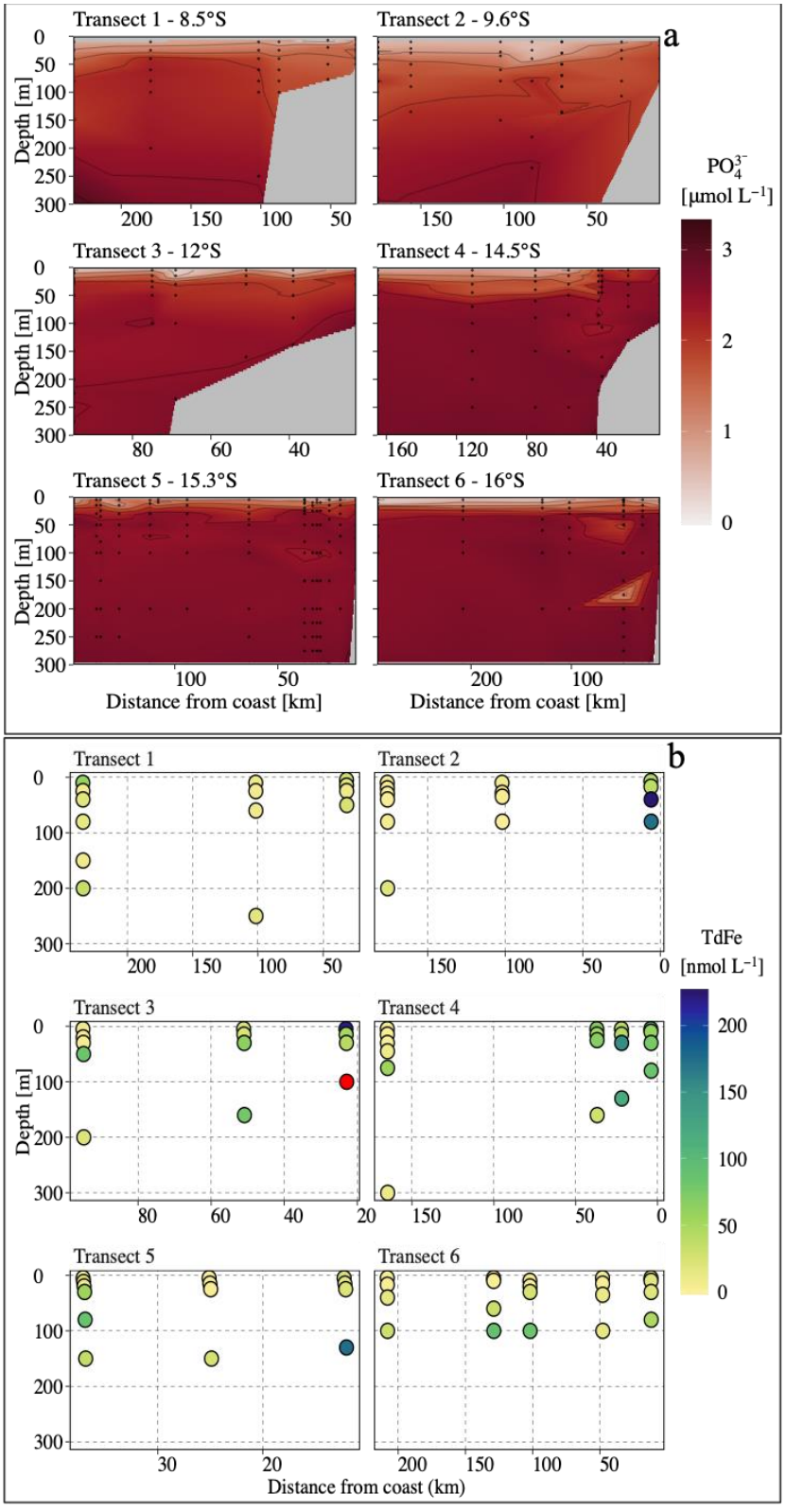

Figure 4: Profiles of (a) PO_4^{3-} concentrations and (b) total dissolvable iron (TdFe) along the 6 transects during the cruise. TdFe data corresponds to measured TdFe in each discrete incubation where N_2 fixation measurements were made. The red dot in figure b indicates the highest TdFe concentration (461.84 nmol L^{-1}).

2.3.4 Estimates of bioavailable nitrogen loss

Accumulation of NO_2^- in OMZ waters is considered a signal of active N loss since it is consumed as a substrate for anammox and is an intermediate product of denitrification (Lam et al., 2009). In this study, we use its presence to estimate N loss occurrence and its spatial association with N_2 fixation. To estimate N loss from a water parcel, we calculated the nitrate deficit (N_{def}), estimating the conversion of NO_3^- to N_2 gas. Between the northernmost transect at 8°S and the central transect at 12°S, a weak secondary NO_2^- maximum was observed where NO_2^- concentrations ranged between 0.01 – 2.14 µmol L^{-1}, except for the most coastal station at Transect 3 where subsurface NO_2^- concentrations close to the bottom reached 3.26 µmol L^{-1} (Figure 5a). A weak N_{def} signal (0 – 5 µmol L^{-1}) was only observed in subsurface waters beyond 200 m in Transects 1 – 3. Above these depths, N_{def} was mostly below 0 µmol L^{-1} (Figure 5b) indicating a reduced active N loss signal in the water mass.

At Transect 4 (14°S), stations closest to the coast had a deeper and pronounced NO_2^- maximum below 150 m. Beyond 50 km distance from the coast, the depth of the secondary NO_2^- maximum from all stations reduced to 50 m. The profile of NO_2^- in Transect 4 indicated a local NO_2^- decline between 100 and 250 m depth (Figure 5a). In Transect 5 where the highest N_2 fixation rates were measured, a much more pronounced secondary NO_2^- maximum was observed in deeper layers, extending from ~100 m, despite a shallow upper boundary of the OMZ from 50 m. Maximum NO_2^- concentrations of up to 8.3 µmol L^{-1} were measured between 250 and 300 m depth at Transect 5. At the most southern transect along 16°S, a sharp oxycline was observed in which NO_2^- was seen to accumulate in shallow OMZ waters from 30 m (Figure 5a) extending to ~300 m and reaching a maximum of 8 – 8.3 µmol L^{-1} at most stations. Consistent with the occurrence of a secondary NO_2^- maxima, our results reveal a strong N loss signal in coastal subsurface waters between 12°S and 16°S, as indicated by positive N_{def} values of up to 25 µmol L^{-1} (Figure 5b, Supplementary Info. Table 2). However, this signal was less pronounced in surface waters above the upper boundary of the OMZ (0 – <50 m).

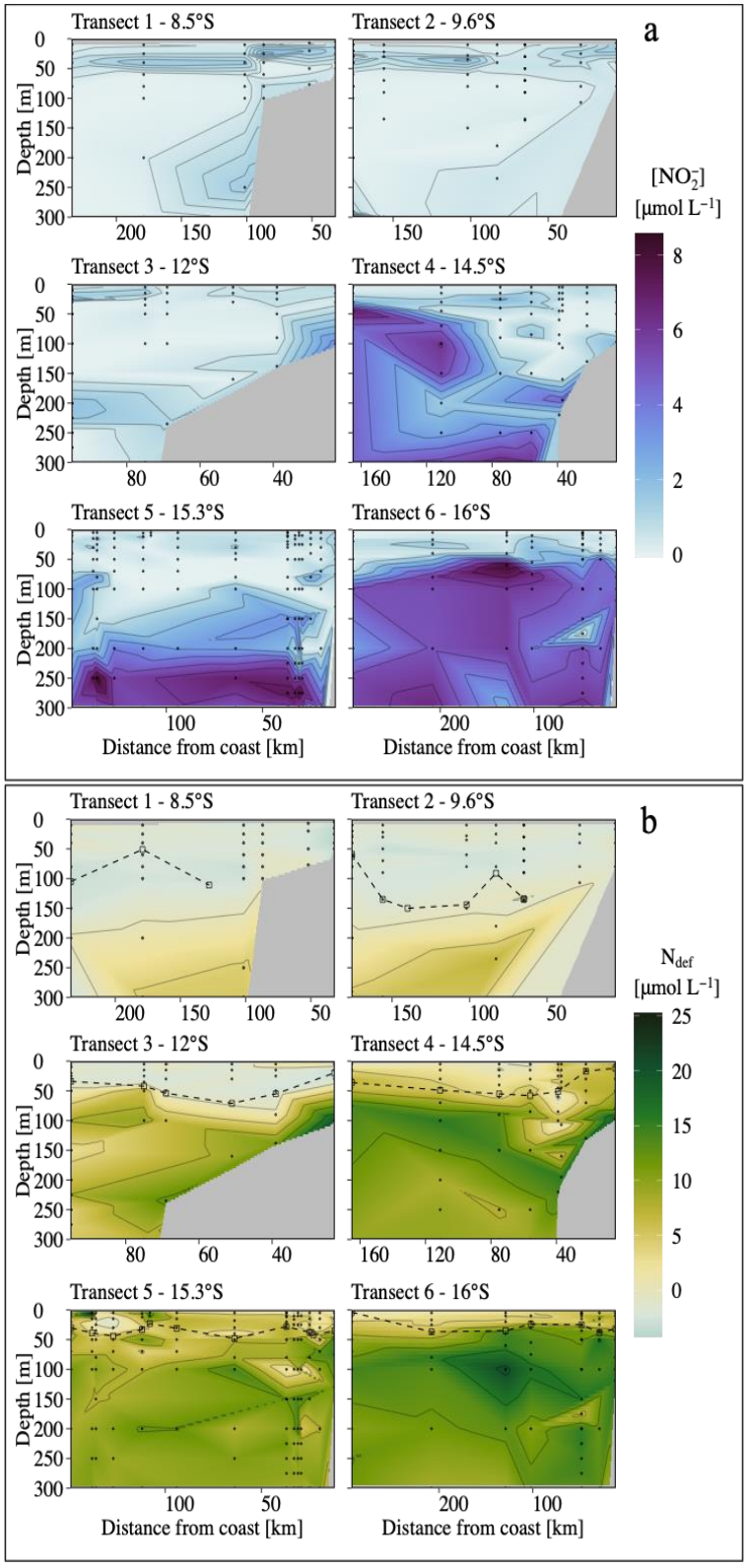

Figure 5: Distribution of (a) nitrite (NO_2^-) concentrations and (b) calculated DIN deficit (N_{def}) along the 6 transects during the cruise. The dotted line in figure b denotes the upper boundary of the OMZ layer with O_2 concentrations < 20 µmol L^{-1}.

2.4. Discussion

Within the ETSP, previous studies have shown that heterotrophic diazotrophs such as proteobacteria are dominant and contribute significantly to N_2 fixation in the region (Bonnet et al., 2008; Jayakumar & Ward, 2020; Löscher et al., 2014; Turk-Kubo et al., 2014). While unicellular cyanobacterial diazotrophs like *Crocosphaera* spp have been observed sporadically, they are not the dominant diazotrophs and their relative contribution to total N_2 fixation in the ETSP is negligible due to substantially low abundances (Bonnet et al., 2008; Löscher et al., 2014; Turk-Kubo et al., 2014). In a previous study by Chang et al. (2019), N_2 fixation rates were only detected in euphotic waters, where the abundances of nitrogenase (*nifH*) copies from proteobacteria were high with a lack of sequences from cyanobacterial diazotrophs. This demonstrates that the vertical distribution of heterotrophic diazotrophs in the ETSP is independent of light. Similarly, N_2 fixation rates in our study did not seem to be influenced by light availability as they were measured throughout the water column, from surface to aphotic waters within the OMZ without significant differences in depth horizons (Supplementary Info. Table 3). Based on this evidence, heterotrophic diazotrophy in surface waters cannot be excluded and we argue that the presence of high fixation rates in euphotic waters is not necessarily an indication of autotrophic diazotrophy. Inferring from the aforementioned studies, our observations strongly suggest that the rates we measured here can also be primarily attributed to heterotrophic diazotrophs.

2.4.1 Spatial and vertical distribution of N_2 fixation rates in relation to environmental conditions

To the best of our knowledge, this study reports the first extensive distribution of N_2 fixation rates covering a notable part (8°S - 16°S) of the coastal northern HUS (4°S – 20°S) off the Peruvian coast. It is also one of few studies to combine N_2 fixation measurements with TdFe concentrations from the incubations. At a global scale, the biogeography of diazotrophy is predicted by considering PO_4^{3-} and Fe availability (Ward et al., 2013), with diazotrophy across most of the ETSP predicted to be limited by low Fe availability (Knapp et al., 2016). Yet on the nearshore spatial scales considered herein, this does not appear to be the case as N_2 fixation rates were often lower than model predictions despite high PO_4^{3-} and TdFe availability.

One noteworthy finding of our study was a latitudinal pattern in the distribution of N_2 fixation rates. All N_2 fixation rates in the north were below detection in comparison to measurable rates in the central and southern latitudes. This could be explained by unfavourable conditions for diazotrophy in the north as conditions controlling N_2 fixation may not be uniform along the coast. Rates below detection in the north were associated with the upwelling of highly oxygenated, warm waters (>20°C, Figure 1a, 2, Supplementary Info. Table 2). Under such high O_2 conditions, diazotrophs could run into oxidative stress under which the activity of the nitrogenase enzyme is repressed or even inhibited unless O_2-avoiding mechanisms such as

organic particles are utilized (Inomura et al., 2017). However, significantly lower POC concentrations and turbidity in the north (Supplementary Info. Table 2) suggest that O_2-avoiding mechanisms through phytoplankton-associated organic particles were likely limited in this area. Lack of measurable N_2 fixation rates was also associated with the absence of a secondary NO_2^- maximum (NO_2^- <2 µmol L^{-1}, Figure 2, 5a), high availability of PO_4^{3-} and DIN concentrations and TdFe availability (Supplementary Info. Table 2). The main Fe source in the Peruvian shelf region is benthic (Chever et al., 2015), and whilst short-term redox dynamics are also clearly important for regulating the inventory of Fe in the water column (Rapp et al., 2020), the highest Fe concentrations are generally expected in the region from ~7 to 13° S where the shelf is broad and shallow (Bruland et al., 2005). Yet, despite low TdFe concentrations (<5 nmol L^{-1}) in some cases, positive $TdFe_P$* (0.27 – 222.59 nmol L^{-1}) was observed in all northern stations especially close to the coast. Hence neither phosphorus and or iron limitation seemed to be evident.

Throughout the central and southern part of our study area, detectable N_2 fixation rates between 12°S and 16°S coincided with high surface Chl *a* (Figure 1b), high POC concentrations, high turbidity, higher PO_4^{3-} concentrations and lower O_2 concentrations compared to the northern transects. Correspondingly, a Spearman correlation analysis revealed that across the entire dataset, N_2 fixation rates were significantly positively correlated with Chl *a*, POC, and turbidity (Figure 3b). This direct link between N_2 fixation and phytoplankton-associated organic matter has previously been observed in the ETSP and elsewhere in the South West Pacific (Selden, et al., 2021; Shiozaki, et al., 2014). Organic particles, consume O_2 when being remineralized, generating anoxic micro-niches that can protect heterotrophic N_2 fixation against O_2 inhibition in highly oxygenated waters (Klawonn et al., 2015). This is evident in that dissolved O_2 concentration was positively correlated with N_2 fixation rates and similarly with POC and turbidity (Fig. 3b). Therefore, while O_2 concentrations were still high in surface euphotic waters in the central and southern regions, high particulate organic matter may have increased the presence of anoxic micro-niches and thereby contributed to mitigating the negative impacts of O_2 availability on N_2 fixation. Organic matter is also a source of energy for heterotrophic N_2 fixation and has been demonstrated to enhance N_2 fixation in experiments in the ETSP (Dekaezemacker et al., 2013; Klawonn et al., 2015; Löscher et al., 2014). This would further explain the high N_2 fixation rates in surface productive waters in the southern part of the study area (Figure 1) and the lack of detectable rates in comparatively low productivity and highly oxygenated waters in the two northern transects.

Our measured rates may, however, be underestimated compared to in situ rates due to incubation artefacts, in particular, elevated incubation compared to *in-situ* temperature as well as potential O_2 contamination. Higher incubation temperatures (22.91 ± 1.36°C) relative to in-situ conditions (15.21 ± 1.46°C) may have been on the upper end of thermal tolerances for N_2 fixers associated with cool upwelled waters (3 – 18°C) such as the Gamma4 γ-proteobacteria abundantly observed from the ETSP (Cheung et al., 2021; Löscher et al., 2014; Turk-Kubo et al.,

2022; Turk-Kubo et al., 2014). Dissolved O_2 concentrations in the incubation bottles may have been higher than in situ because even though we overflowed the bottles with samples to minimize atmospheric contact with the sample, we could not exclude O_2 contamination when filling incubation bottles or during the introduction of isotope-enriched waters. This would result in slightly higher O_2 concentrations in the incubations and potentially higher diffusion of O_2 into organic particles (Chakraborty et al. 2021), which could both act to suppress N_2 fixation rates. While we cannot quantify these effects, this likely had some impact on the profiles of N_2 fixation rates because these factors would make the largest difference in rates where both in situ temperature and O_2 concentrations are lower, such as at depth and in sub-oxic waters. Nevertheless, these methodological limitations do not compromise the main finding of a latitudinal pattern of N_2 fixation rates but are rather in support of the observed low N_2 fixation rates in northern waters with significantly higher O_2 conditions (Supplementary Info Table 2).

Low magnitudes of N_2 fixation rates under phosphate availability are puzzling considering that phosphorus availability has been used to predict high N_2 fixation in this region (Deutsch et al., 2007). A significant negative relationship between N_2 fixation and PO_4^{3-} as indicated by the Spearman correlation analyses could perhaps demonstrate consumption of PO_4^{3-} by the planktonic community, including diazotrophs. However, PO_4^{3-} was not depleted and therefore much higher N_2 fixation rates would be expected for the $PO_4^{3-}$and TdFe concentrations measured herein if these were the key limiting factors. The residual PO_4^{3-} may suggest that alternative phosphorus sources or factors may play a primary role in regulating N_2 fixation rates in the study area. Diazotrophs have been known to synthesize hydrolytic enzymes to acquire P from alternative sources such as DOP (Dyhrman & Haley, 2006, Farnelid & Riemann, 2008; Meyer et al., 2016, 2017; Somes & Oschlies, 2015). However, the low to undetectable DOP concentrations and an insignificant relationship between N_2 fixation and DOP mean our data are insufficient to demonstrate any role of DOP for N_2 fixation in this study. Nevertheless, evidence that PO_4^{3-} availability did not translate to expected high N_2 fixation suggests the possibility that the diazotroph community in the ETSP may have a different response to PO_4^{3-}availability and/or requirements of alternative phosphorus compounds such as organic phosphorus.

High positive TdFe* throughout the study area (Supplementary Info, Figure S10, Table 2, 3), which is also a common feature of the coastal ETSP (Blain et al., 2008) indicates that there is enough iron, relative to phosphate, to support complete consumption of PO_4^{3-} and thus support N_2 fixation in the coastal waters of the northern HUS. The generally high TdFe availability in this study also indicates the potential for much higher N_2 fixation rates if iron were the major limiting factor for N_2 fixation in the ETSP (Dutkiewicz et al., 2012). Yet higher TdFe concentrations in coastal waters did not always translate to high N_2 fixation rates and in some cases, N_2 fixation rates were not detectable despite TdFe availability (Supplementary Info. Table 2). Therefore, the disproportionately low or undetectable N_2 fixation rates despite TdFe availability across most of the incubations from the shelf region are striking. Yet, across

the entire dataset, slight differences in TdFe concentrations by latitude and coastal-offshore dynamics appeared to be spatially concurrent to differences in N_2 fixation rates (Supplementary Info. Table 2 and 3). Despite the high variability in both N_2 fixation rates and TdFe concentrations, general trends indicated that increasing N_2 fixation rates from north to south coincided with a similar increase in TdFe concentrations (Supplementary Info. Table 2). Hence, whilst overall TdFe availability suggests that TdFe was non-limiting and therefore not a major controlling factor for N_2 fixation rates in this study, patterns in the magnitude and distribution of N_2 fixation rates versus the absolute concentrations of TdFe may point towards either further subtleties as to exactly how bioavailable TdFe is to diazotrophs, non-linearities in its regulation of N_2 fixation, or other chemical, physical and ecological constraints on N_2 fixation. Therefore, dedicated experiments are required to disentangle and understand the complex relationships between Fe availability and N_2 fixation in the ETSP.

From 27 N_2 fixation stations sampled, 11 were characterized as offshore (lower boundary of the OMZ >600 m, Figure 2) and observed to have lower TdFe concentrations (1.18 – 90.29 nmol L^{-1}) relative to coastal stations (1.15 – 461.84 nmol L^{-1}). These differences were associated with higher N_2 fixation rates at most coastal stations than at offshore stations. Our observations are consistent with previous studies reporting the lowest (maximum <1 nmol N L^{-1} d^{-1}) to non-detectable rates from open ocean low productivity waters off Peru (Chang et al., 2019; Dekaezemacker et al., 2013; Löscher et al., 2014; Selden, et al., 2021). These patterns altogether suggest that, while sedimentary iron in coastal waters is high, insufficient iron availability in open ocean waters may to some extent still limit/colimit N_2 fixation in large parts of the ETSP (Wang et al., 2019). Whilst this may occur as a direct influence of TdFe availability on N_2 fixers, it also presents the potential for an indirect effect of iron. Low TdFe availability also limits phytoplankton productivity (Browning et al., 2018, Hutchins et al., 2002), thereby resulting in low organic matter availability which is attributed to stimulating heterotrophic N_2 fixation (Bombar et al., 2016; Riemann et al., 2022).

Our study highlights that the controlling factors for N_2 fixation may be variable globally among different ocean regions. Specifically for the northern HUS, the controls on N_2 fixation may consist of non-linear correlations between multiple environmental factors. Therefore, predicting N_2 fixation rates solely on iron and PO_4^{3-} without considering other interlinking factors such as organic matter availability may have resulted in an overestimation of the role and contribution of N_2 fixation in the ETSP (Wang et al., 2019). It is worth mentioning that Chang et al. (2019) did not detect any N_2 fixation activity beyond the euphotic zone during austral winter, additionally revealing the temporal heterogeneity and patchiness of N_2 fixation activity within the northern HUS. Considering the known seasonality and climate-associated variability in physical and biogeochemical conditions such as primary productivity (Messié & Chavez, 2015), which could ultimately influence N_2 fixation in the northern HUS, we hypothesize that seasonal variability of N_2 fixation rates is likely to occur, but will be challenging to constrain due to the sporadic occurrence of high N_2 fixation rates in summer (Fernandez et

al., 2011; Löscher et al., 2014), and the period of observations required to extract seasonal variability above interannual and interdecadal dynamics.

2.4.2 Magnitudes of N_2 fixation and potential impacts on biomass production and nitrogen inventory of the ETSP

Averaged over the entire water column (0 – 300 m), our volumetric rates (1.18 ± 3.81 nmol N L^{-1} d^{-1}, n = 103 measurements) are in agreement with the global average of N_2 fixation rates (1.4 ± 4.6 nmol N L^{-1} d^{-1}) reported from coastal regions by Tang et al. (2019), and other observations from the ETSP (Bonnet et al., 2013; Chang et al., 2019; Dekaezemacker et al., 2013; Fernandez et al., 2011; Knapp et al., 2016; Löscher et al., 2014; Selden, et al., 2021). When integrated through the water column (5 – 250 m), areal N_2 fixation rates (18.12 – 582.11 µmol N m^{-2} d^{-1}, Figure 1b) are within the range but on the lower end of integrated rates (0 – 400 m, 2 – 950 µmol N m^{-2} d^{-1}) reported from the ETSP by Fernandez et al. (2011). Save for the highest areal rate (582.11 µmol N m^{-2} d^{-1}), most of our rates are lower (<200 µmol N m^{-2} d^{-1}) than the average model predictions of N_2 fixation for the region (~500 µmol N m^{-2} d^{-1}) by Deutsch et al. (2007). In line with several model results, our data confirm that predicted N_2 fixation rates may be overestimated (Moore & Doney, 2007; Wang et al., 2019), especially considering that observed N_2 fixation rates from the ETSP are comparably lower in austral winter (Chang et al., 2019).

Our sampling strategy focused on the coastal band where the highest volumetric N_2 fixation rates (up to 800 µmol N m^{-2} d^{-1}) have been measured to date (Löscher et al 2014, 2016). Episodic sulfidic events, now commonly reported from the Peruvian OMZ and eddy events (Schlosser et al., 2018; Schunck et al., 2013), were previously associated with the high coastal N_2 fixation rates and gammaproteobacterial diazotrophic activity along 12°S (Station 19, 12° 30'S 77°W) by Löscher et al. (2014, 2016). This suggests that N_2 fixation in the ETSP may be significantly enhanced under extreme episodic events such as sulfidic events (Löscher et al., 2014). These high N_2 fixation rates indicate that despite the patchiness, the dominating diazotrophic community in the ETSP given the right conditions is capable of high N_2 fixation rates comparable to those measured during *Trichodesmium* blooms in the North Atlantic (Capone et al., 2005; Fonseca-Batista et al., 2019; Mulholland et al., 2012). In contrast to Löscher et al. (2014), we measured eight times lower integrated N_2 fixation rates of 162.95 µmol m^{-2} d^{-1} along the same latitude (Station 46 at 12°S, 78°W), the closest station to Station 19 of Löscher et al. (2014), a decade later but during the same season. Furthermore, it should also be noted that for a large number of N_2 fixation rates from previous studies in the HUS and reported herein, N_2 fixation rates were consistently below detection. Hence, whilst the potential for high N_2 fixation rates may exist in the northern HUS, our study demonstrates an uncertainty of whether these high N_2 fixation rates are sustained over time. Considering that previous studies have similarly reported both detectable and low to no N_2 fixation in the northern HUS, N_2 fixation rates seem widely variable and intermittent both spatially and

temporally (Chang et al., 2019; Dekaezemacker et al., 2013; Löscher et al., 2014; Selden et al., 2021). However, while N_2 fixation may occur year-round, N_2 fixation rates in the coastal waters of the northern HUS during austral summer do not seem to be substantially high as hypothesized by Deutsch et al. (2007). These results provide further evidence to support previous conclusions that the ETSP is likely not a "hotspot" for N_2 fixation (Chang et al., 2019; Knapp et al., 2016; Selden et al., 2021; Wang et al., 2019). Nevertheless, the temporal variability of N_2 fixation needs to be considered in regional nitrogen budgets, since coastal waters may have a previously underestimated contribution to new nitrogen inputs in the HUS when N_2 fixation rates are episodically enhanced.

Net ^{13}C primary production rates measured in the same incubation bottles as N_2 fixation ranged between 0.02 – 104.09 µmol C L^{-1} d^{-1} with an average mean of 17.00 ± 28.41 µmol C L^{-1} d^{-1} from the euphotic zone (Kittu et al., 2021). Assuming the Redfield ratio (C:N~ 6.6), (Redfield, 1958), we calculated that the contribution of measured N_2 fixation to new primary production by providing new nitrogen to the euphotic zone ranged between ~0.0 and 0.50 % (average, 0.05 ± 0.11%). This demonstrates that N_2 fixation was a measurable but minor source of new nitrogen to support local new primary production during our cruise. It is therefore evident that other N sources e.g. from upwelled nitrate or regenerative nutrients (e.g ammonium) are more important for supporting the observed high primary productivity in the region (Fernández et al., 2009; Hauschildt et al., 2021).

Nevertheless, the occurrence of N_2 fixation in the coastal waters of the northern HUS might be relevant for N cycling in the highly productive Peruvian upwelling system due to the extent to which it counterbalances bioavailable N loss. Our observations do support the Deutsch et al. (2007) hypothesis for a spatial coupling of N_2 fixation and bioavailable N loss in the southern coastal productive waters off Peru, which may be important for feedback on the nitrogen inventory in the region (Landolfi et al., 2013). To assess this, we considered the distribution of N loss estimates from N_{def} calculations and secondary NO_2^- maxima measurements. Using estimates of microbial respiration and NO_3^- deficit, Codispoti and Packard (1980) established that 76% of the total N loss in the ETSP occurs from the main secondary NO_2^- maxima zone (>2 µmol L^{-1}), within a 175 km band from the coast. Based on these estimates, they demarcated a coastal area of 3.26 x 10^{11} m^{-2} between 10°S and 25°S where NO_2^- concentrations were positively correlated with denitrification rates. Our sampling area (8 to 16°S) covered approximately half of the total area demarcated with pronounced N loss. N_2 fixation rates between Transects 3 and 6 were associated with surface and subsurface waters featuring a calculated high $\mathbf{N}_{def}$ (Figure 5b, 5 – 25 µmol L^{-1}) and a pronounced secondary NO_2^- maxima in O_2 deficient coastal waters (NO_2^- range = 2 – 8 µmol L^{-1}) starting from 30 m deep (Codispoti & Packard, 1980; Kalvelage et al., 2013). Within this area, high denitrification and anammox rates of up to ~6.1 mmol N m^{-2} d^{-1} amounting to a total N loss of 12 Tg N yr^{-1} have been reported (Karthäuser et al., 2021).

To account for the potential biogeochemical significance of N_2 fixation in the ETSP, we compared reported estimates of N loss in the ETSP (range 9 – 25 Tg N yr^{-1}, Kalvelage et al., 2013; Karthäuser et al., 2021), to N_2 fixation rates measured during our study. We applied a similar approach to Karthäuser et al. (2021) and Bonnet et al. (2013) by considering the same spatial extent of N_2 fixation as for N loss to extrapolate our rates and roughly estimate annual N_2 fixation inputs over the entire area of the coastal OMZ susceptible to N loss (3.26×10^{11} m^2). Using an integrated N_2 fixation rate of 69.46 ± 120.02 µmol N m^{-2} d^{-1} averaged from 25 stations within 175 km from the coast, total N_2 fixation potentially amounts to ~0 – 0.32 Tg N yr^{-1}, replenishing ~0 to 1.3% of the N lost. Based on these estimates, N_2 fixation rates from the region would need to be 10 – 100-fold higher to balance the N loss, therefore demonstrating the low potential for austral summer N_2 fixation rates to compensate for N loss in the coastal waters of the northern HUS off Peru. While these are only rough estimates of the potential importance of N_2 fixation in the northern HUS, we note that our estimates are on the lower end of annual estimates of N_2 fixation rates for the ETSP reported by Bonnet et al. (2013) which included rates from further offshore and towards the end of austral summer (0.16 – 10%). Potential explanations for this difference could be that our samples, taken up to 300 m did not cover the extent of aphotic waters at depth (up to 2000 m) from where N_2 fixation rates were attributed to largely contribute to total areal N_2 fixation in the ETSP (Bonnet et al., 2013). Additionally, we note that while denitrification and anammox are mainly restricted to the sub-surface anoxic and sub-oxic waters within the 175 km coastal band (Kalvelage et al., 2013), N_2 fixation in the ETSP occurs over a larger spatial extent, albeit at much lower rates in the open ocean and aphotic waters beyond 300 m (Bonnet et al., 2013; Chang et al., 2019; Dekaezemacker et al., 2013; Löscher et al., 2014; Selden et al., 2021). Considering the large area of aphotic and open waters, even low but persistent N_2 fixation rates may significantly contribute to higher annual estimates. Therefore, the spatial scale and coverage of N_2 fixation over which rates are measured and extrapolated are important to consider for these comparisons. Hence our estimates from just the coastal region, within 300 m depth may be underestimated especially considering the high variability observed in N_2 fixation rates within this study and potential seasonal variability yet to be thoroughly investigated. To better understand the relationships between these two processes, we recommend that both measurements of N_2 fixation and N loss processes should be taken from the same samples in parallel.

In general, our results highlight that while the spatial coupling of N_2 fixation and N loss is evident in coastal waters of the ETSP associated with the OMZ (Dekaezemacker et al., 2013; Löscher et al., 2014), this doesn't necessarily suggest that N_2 fixation counterbalances the high N loss reported from the region. The colocation of these two processes as shown in this study supports the hypothesis that self-reinforcing feedbacks on the N cycle are likely to occur at the local scale (Landolfi et al., 2013). Considering the stoichiometric imbalance in N_2 fixation and N loss (Landolfi et al., 2013), the significance of N_2 fixation in the ETSP may be more related to the feedback that ensues concerning the N inventory rather than to its minor direct role in

nitrogen supply for primary productivity. The presence of N_2 fixation in proximity to low oxygen waters along the coast could enhance the N deficit thereby creating a self-sustaining cycle between N loss and N_2 fixation that results in net N loss locally. Hence on short (e.g., annual) time scales and considering temporal variability in N_2 fixation rates, our results suggest that the hypothesized positive feedback on the N inventory of the northern HUS (Landolfi et al., 2013) could be strengthened by enhanced N_2 fixation in the coastal waters where both phytoplankton productivity and N loss are high. If the hypothesis of a vicious cycle holds, colocation of N loss and N_2 fixation in the coastal OMZ of the northern HUS could trigger regional changes in the N inventory (Landolfi et al., 2013). These stoichiometry-driven changes in the size of the local N inventory may lead to bottom-up-regulated perturbations in food web dynamics and the efficiency of the biological pump at a local scale (Falkowski, 1997). Over longer time scales, however, the N loss in the northern HUS has been hypothesized to be counterbalanced by basin-wide N inputs through high N_2 fixation rates observed in the Western Tropical Pacific (Bonnet et al., 2017; Wang et al., 2019). However, for a local replenishment, it is still unclear whether such a large increase in annual N_2 fixation rates, 10-100 fold to be proportional to local N loss estimates, is regionally plausible in the ETSP.

2.5 Conclusion

This study provides the highest resolution of the spatial distribution of N_2 fixation so far reported from the northern HUS, with a stronger focus on coastal waters compared to previous studies. Our data revealed notable latitudinal differences in N_2 fixation in the northern HUS coinciding with a similar latitudinal pattern in N loss. N_2 fixation was below detection in the northern transects between 8 and 10°S and increased from the central to southern transects towards the region of intensified N loss and higher primary productivity. This indicates that N_2 fixation in the northern HUS may be mostly confined to the southern part of coastal waters above and within the region of intense N loss. This latitudinal pattern is likely a result of a complex interplay of multiple environmental factors which include organic matter availability, and potential factors that regulate it such as the availability of trace metals (Fe). These factors may have direct and indirect effects on the regional distribution of N_2 fixation in coastal waters of the northern HUS off Peru. Despite the observed negligible contribution of diazotrophy to supporting new primary productivity, the colocation of low N_2 fixation and high bioavailable N loss (nitrate and ammonia loss via denitrification and anammox) close to the coast provide evidence that there is potential for local self-sustaining feedback along the coast that could potentially lead to a runaway loss of N as previously hypothesized. Hence, we postulate that on short timescales, this positive feedback could be strengthened via future changes in deoxygenation, phytoplankton organic matter production, and trace metal biogeochemistry, especially in relation to sporadic occurrences of sulfidic events. Further studies are however required to quantify and determine the strength, and biogeochemical and ecological implications of this positive feedback for the coastal system as N_2 fixation rates would need to be 10 – 100 fold higher than currently measured rates to match the rates of N loss from the

same region. Additionally, temporal shifts in N_2 fixation rates associated with seasonality need to be accounted for, which is challenging due to the current patchy distribution of observed N_2 fixation rates.

Acknowledgements

This research was supported by the German Federal Ministry of Education and Research (BMBF) through the cooperative research projects Humboldt Tipping (01LC1823B) and CUSCO ("Coastal Upwelling System in a Changing Ocean", FKZ03F0). The authors are grateful to the captains, crew members, and scientists onboard the MSM80 cruise of the German R/V Maria S Merian for their support and cooperation at sea. We especially thank Joaquin Ortiz, Michael Meyerhöfer, and Rainer Kiko for assisting with onboard sampling and Kastriot Qelaj for nutrient sampling and analysis. We further thank Kerstin Nachtigall for assistance with sample analysis for mass spectrometry and Silvia Georgieva for providing help with processing and data analysis. Thanks to Carolin Löscher for her helpful comments on earlier versions of the manuscript.

Author Contributions

UR, MFM, and AJP designed the study. LRK, AJP, and MFM collected the samples onboard. LK analyzed samples for nitrogen fixation. MH designed a trace metal clean sampling procedure and analyzed trace metal samples. LRK analysed all datasets mentioned and wrote the manuscript with input from all co-authors.

Data availability

The datasets are available on PANGAEA as follows:

- N_2 fixation rates (Kittu, Paul, et al., 2021)
- Water column biogeochemistry (Kittu, Fernández-Méndez, et al., 2021)
- TdFe concentrations (Kittu, Hopwood, et al., 2021)

Supplementary Information

Supplementary Text

Text S1.Preparation of $^{15}N_2$ enriched and blank seawater and incubation conditions

$^{15}N_2$-enriched seawater was prepared by degassing prefiltered (0.2 µm) surface seawater from each station, using a peristaltic pump slowly recycling (100 mL min^{-1}) the seawater through a degassing membrane twice (Mini-Module Membrana-G542) under maximum vacuum pump pressure (960 mbar). The degassed water was directly transferred into a 2 L ($^{15}N_2$-enriched) or 1 L (blank incubation) gastight Tedlar bags (Cell Scientific Corp) fitted with a septum. Degassed water in the 2 L Tedlar bag was then amended with 1 mL $^{15}N_2$ gas (98 atom % ^{15}N, Cambridge,

Lot no: 1-18404) per 100 mL of degassed water. The bubble of $^{15}N_2$ gas was dissolved by gently slapping the enriched bubble with a ruler until the bubble disappeared. Complete dissolution of the gas bubble resulted to an average calculated $^{15}N_2$ concentration of 414.8 ± 3.0 µmol L^{-1} (mean ± S.D). 100 ml of enriched seawater was added to each incubation bottle. Bottles were gently mixed by rotating ~10 times before being incubated. For the blank incubations, degassed seawater in the 1 L Tedlar bag was amended with atmospheric air (1 mL per 100 mL) and dissolved in the same way as for the $^{15}N_2$ -enriched seawater. Depending on the depth at which samples were collected and the amount of incoming PAR measured by the PAR sensor, samples were incubated in one of the 5 incubators corresponding to the closest % of measured insitu incoming PAR (100, 40%, 30%,15%, 5% and 0%). Samples from below the euphotic zone where incoming PAR was below detection were all incubated in a 6th dark incubator covered by a black mesh.

Text S2: Limit of detection and minimum quantifiable rate calculations

N_2 fixation rates considered above the limit of detection was based on two criteria. 1.)The accuracy and precision of $^{15}N/^{14}N$ isotopic ratios scales with sample mass. For our study, we performed an instrument linearity test using standards ranging from 6 to 90 µg N to establish the lower limit of sample mass at which analytical accuracy and precision of the $^{15}N/^{14}N$ ratio could not be ascertained. The precision and accuracy of samples below 12 µg N was considered too low for rate calculation. Hence all samples with filter mass <12 µg N were considered unsuitable for rate calculation. 2.) The limit of detection (LOD) for each triplicate was calculated by substituting $A_{PON}^{t=f} - A_{PON}^{t_f=i}$ with the value of three times the standard deviation of seven 12.5 µg standards (0,001343616 atom%) as described in White et al. (2020). To account for the variability of the LOD attributed to different PON mass on each filter, a respective LOD was calculated for each triplicate filter after which a mean was determined and used to ascertain whether the average N_2 fixation was below or above LOD. Triplicates that pass both criteria were averaged to calculate the mean volumetric N_2 fixation rates per depth. In some cases, only the N_2 fixation rate from one triplicate with a mass > 12.5 µg was above LOD hence a standard deviation for that depth could not be calculated. To avoid overestimation, all average volumetric rates below the respective LOD were assigned a value of 0 nmol N L^{-1} d^{-1} before further analysis. The uncertainty of each triplicate measurement was calculated for each depth using standard methods of error propagation to derive the minimum quantifiable rate (MQR) (Gradoville et al., 2017a).

Text S3: Delimiting Euphotic zone and O_2 Minimum Zone (OMZ)

We define the euphotic zone as the depth where PAR was reduced to 1% of its surface value. In stations where PAR was not available, such as for night stations, the euphotic zone was calculated based on an empirical relationship between the diffuse attenuation coefficient and chlorophyll concentrations as described in Morel and Maritorena (2001). No agreed-upon method is used to delimit the OMZ due to a wide range of O_2 concentrations that they encompass at which an alternative electron acceptor is utilized once O_2 reaches a certain

threshold. Therefore, to define the relevant OMZ waters in the context of our study we loosely used a subjective criterion of O_2 <20 µmol L^{-1}. This threshold was specifically chosen to cover a range of subsurface O_2 levels (0 - 20 µmol kg^{-1}) at which detectable N loss activities (anammox and denitrification) have been reported from literature and O_2 sensitivity assays (Hamersley et al., 2007; Kalvelage et al., 2011, 2013; Lam et al., 2009). Based on this criterion, the upper and lower boundaries of the OMZ were calculated for each station to demarcate the water masses at which N loss is expected to be taking place. Accordingly, the demarcation of stations as offshore or coastal was based on the definition by Kalvelage et al (2013). Whereby a station was considered offshore if the lower boundary of the OMZ (O_2 < 20 µmol L^{-1}) exceeded 600 m assuming that in coastal stations the OMZ is still in contact with the sediments at water depths <600 m.

Supplementary Figures

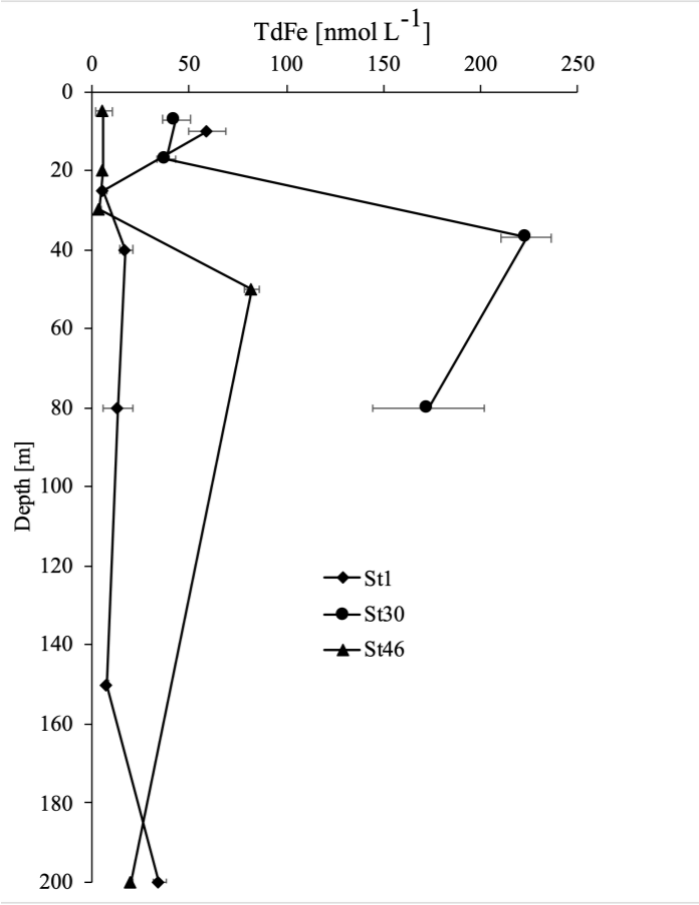

Figure S1. Mean and standard deviation of triplicate total dissolvable iron measurements performed at 3 stations

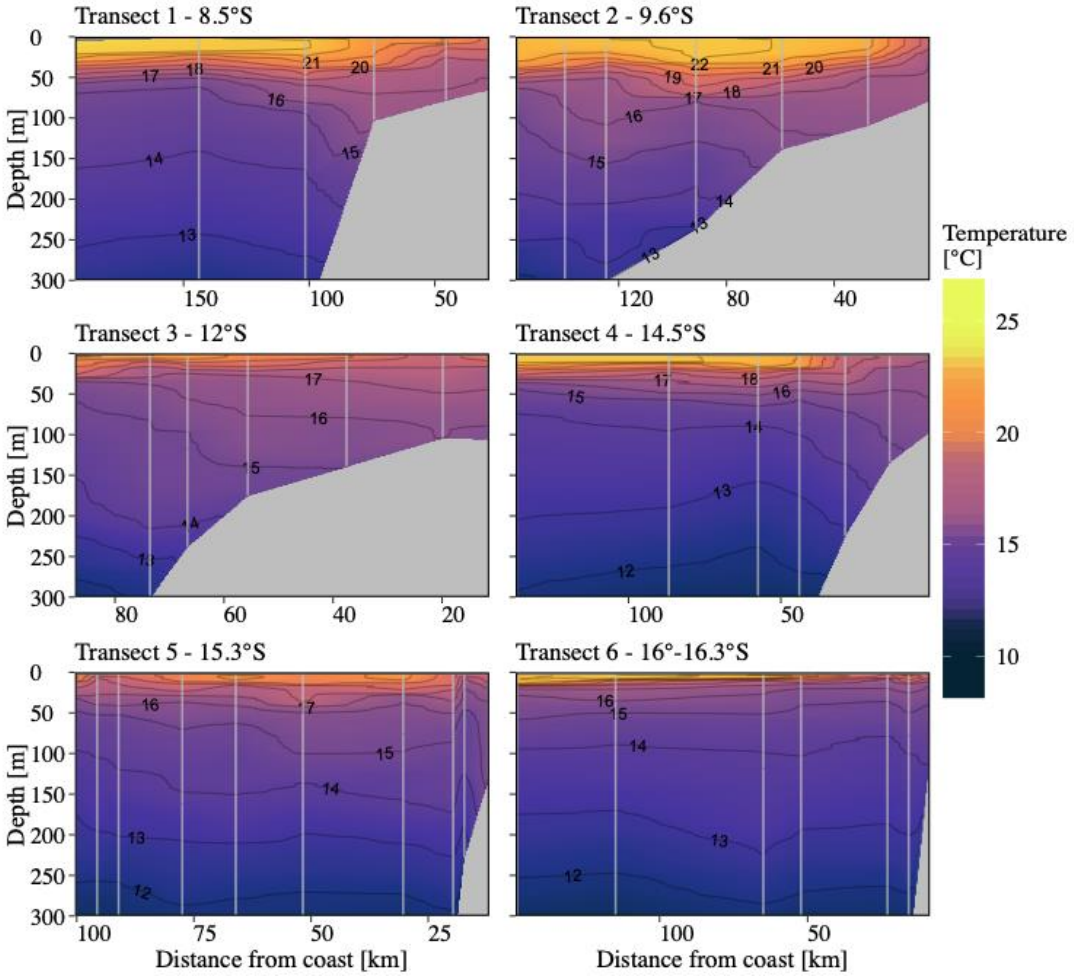

Figure S2: Interpolated vertical profiles of temperature along each transect. White vertical lines are temperature measurements from CTD profiles

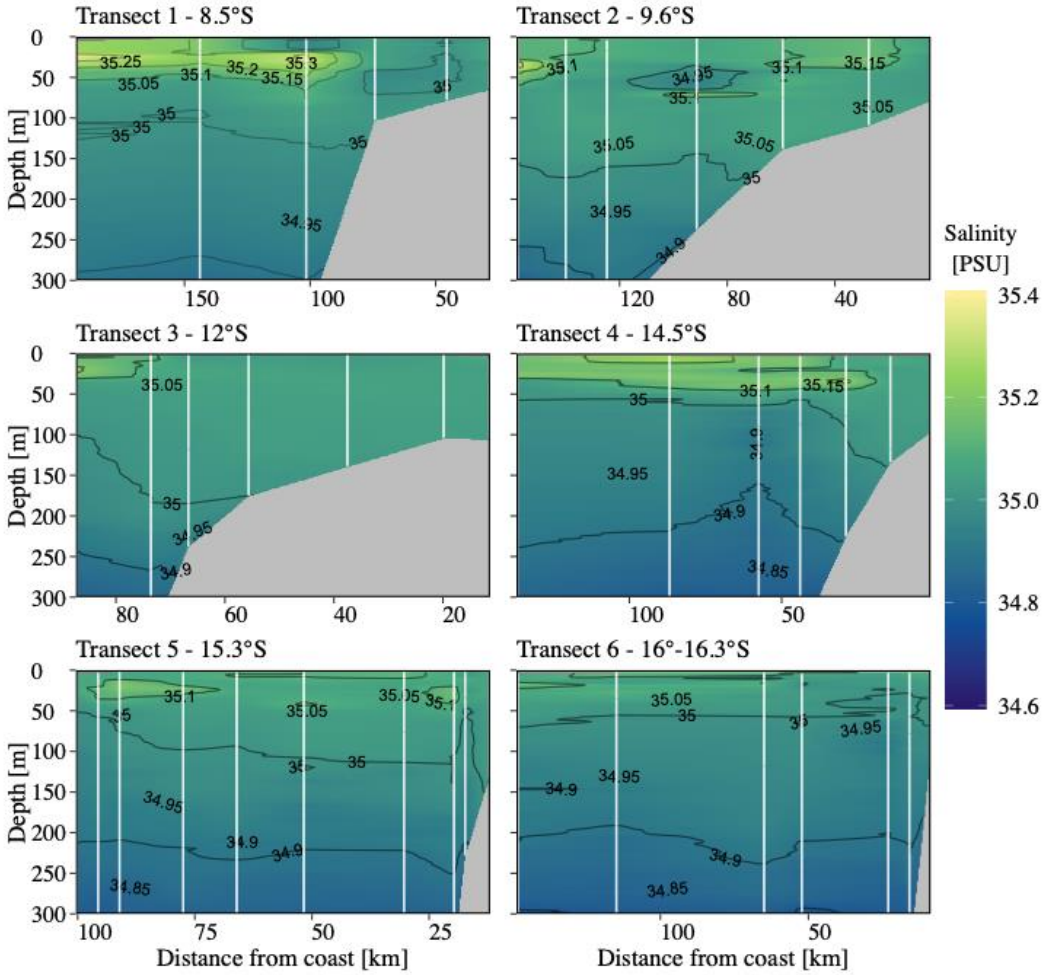

Figure S3: Interpolated vertical profiles of salinity at each transect. White vertical lines denote CTD salinity profiles

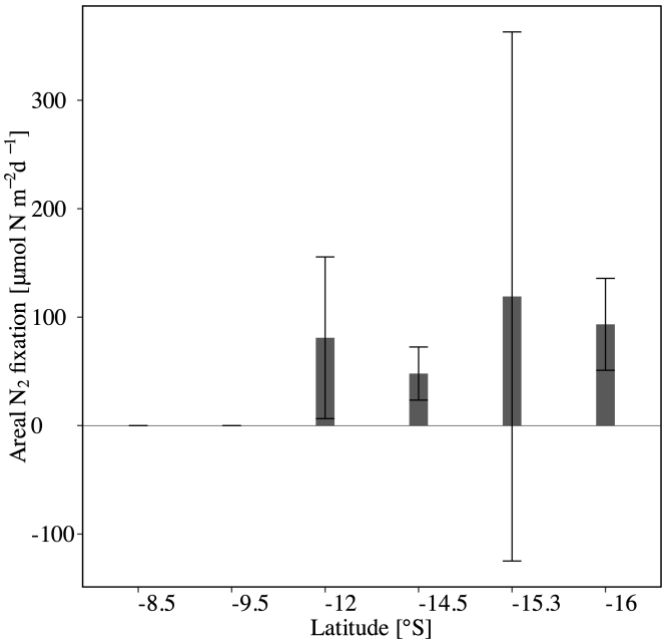

Figure S4. Averages (± SD) of areal N_2 fixation rates (µmol N m^2 d^{-1}) at each transect.

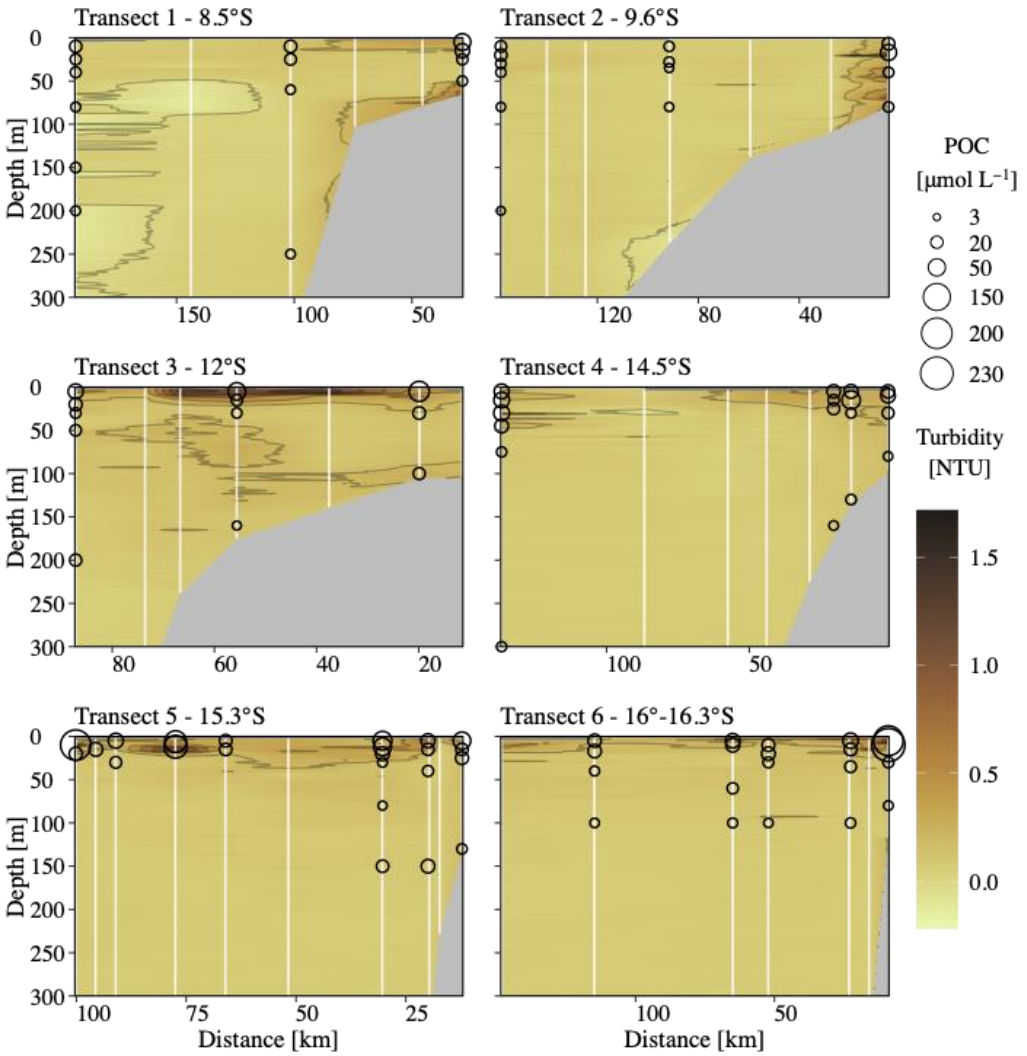

Figure S5: Concentration of particulate organic matter (POC) overlain on interpolated distribution of turbidity across the six transects. White vertical lines denote turbidity measurement points from CTD profiles.

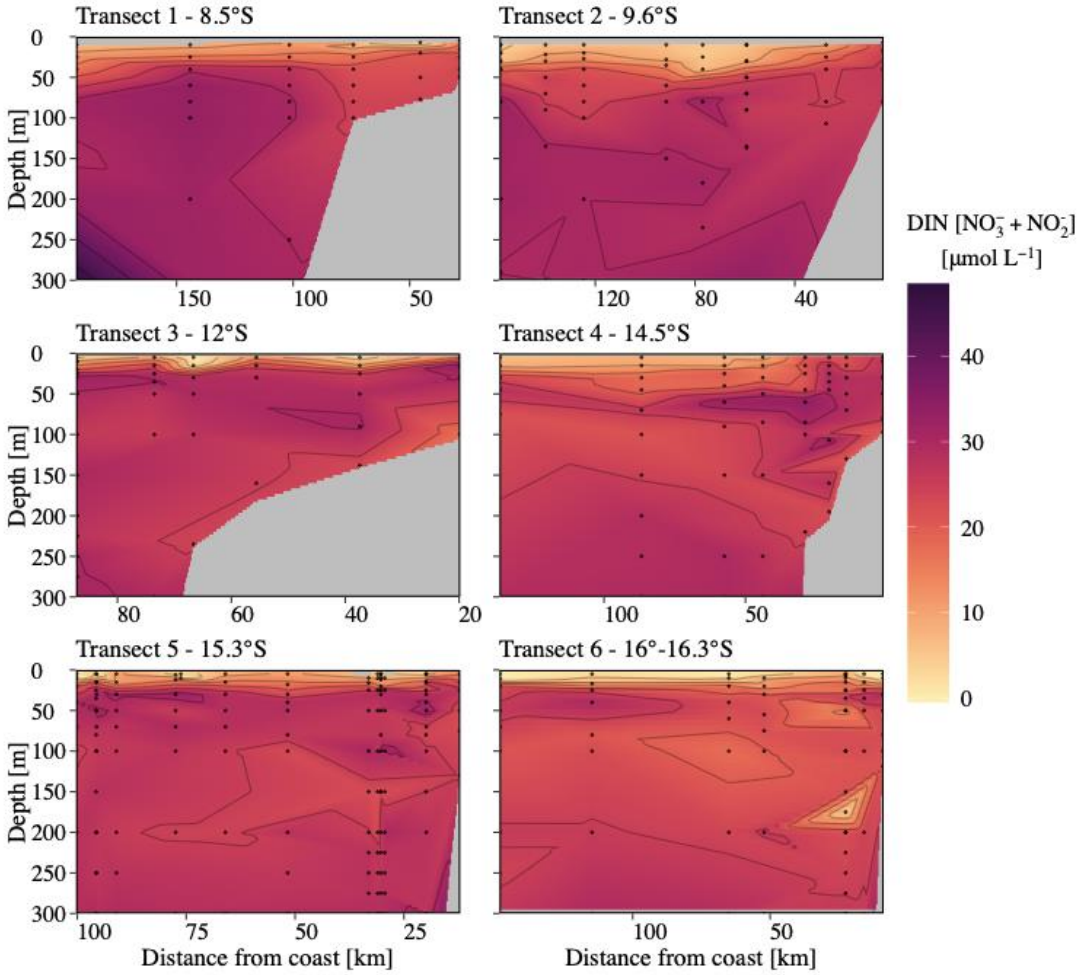

Figure S6: Interpolated vertical profiles of dissolved inorganic nutrients (nitrate + nitrite) along each transect. Black dots denote the depth of sample collection.

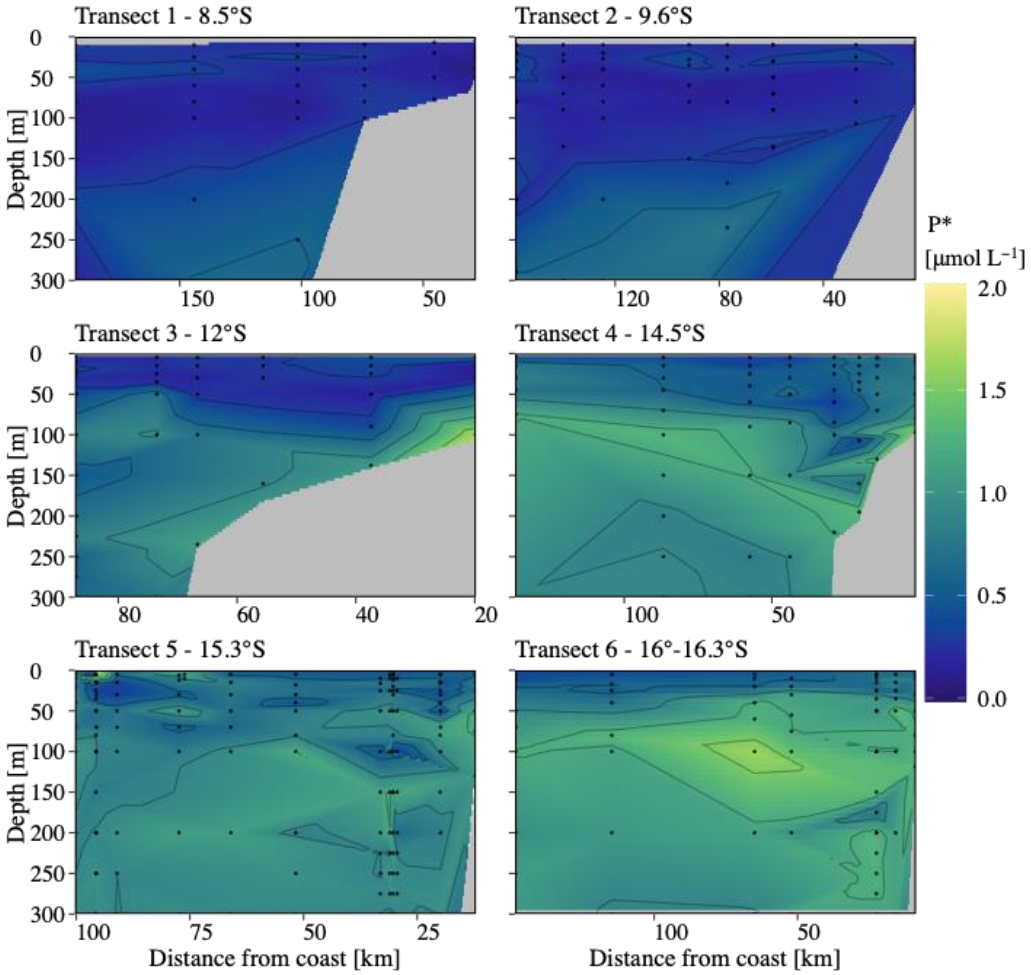

Figure S7: Interpolated vertical profiles of excess phosphate (P*) along each transect.

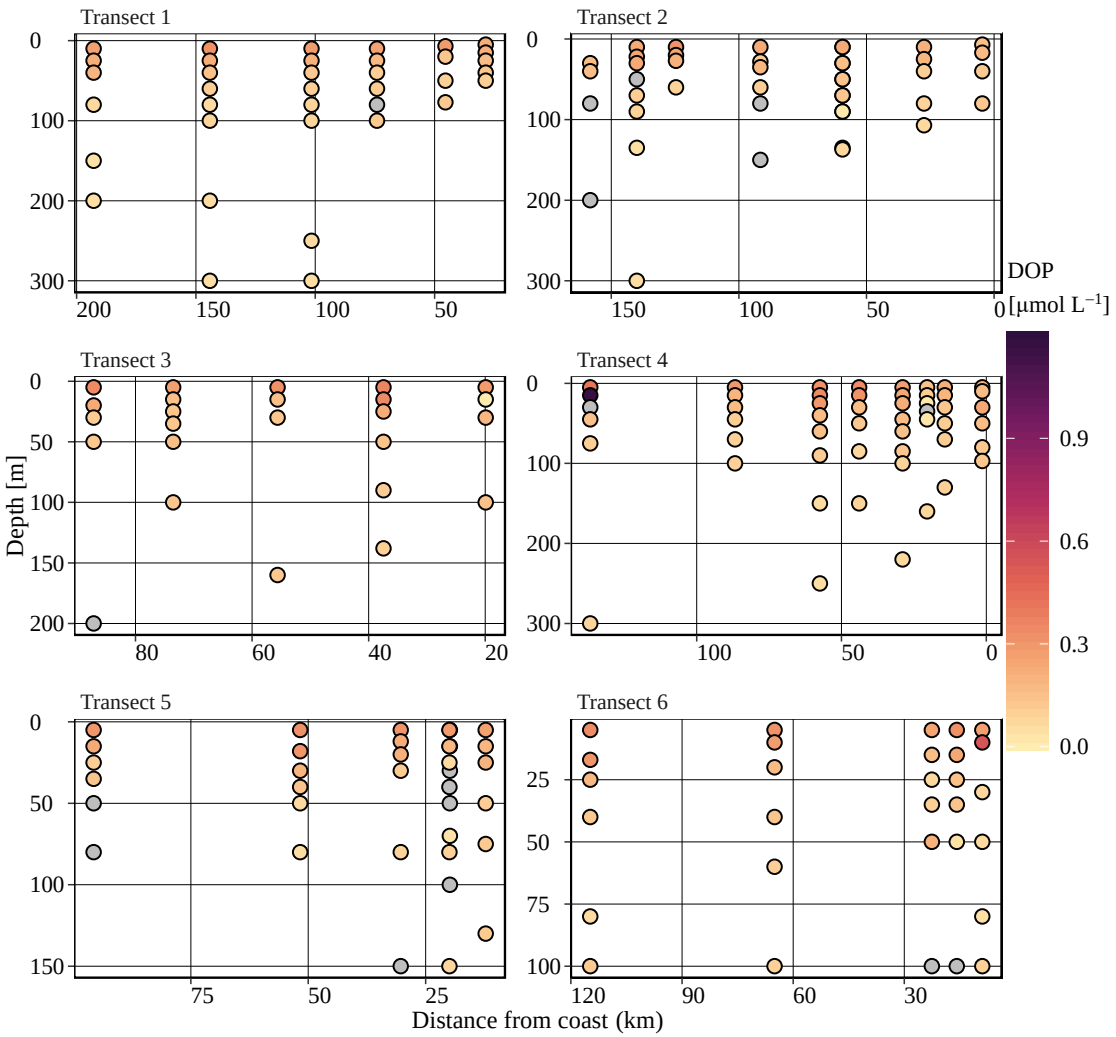

Figure S8: Concentration of dissolved organic phosphorous (DOP) in discrete samples from each transect. Grey circles indicate DOP was below the detection limit.

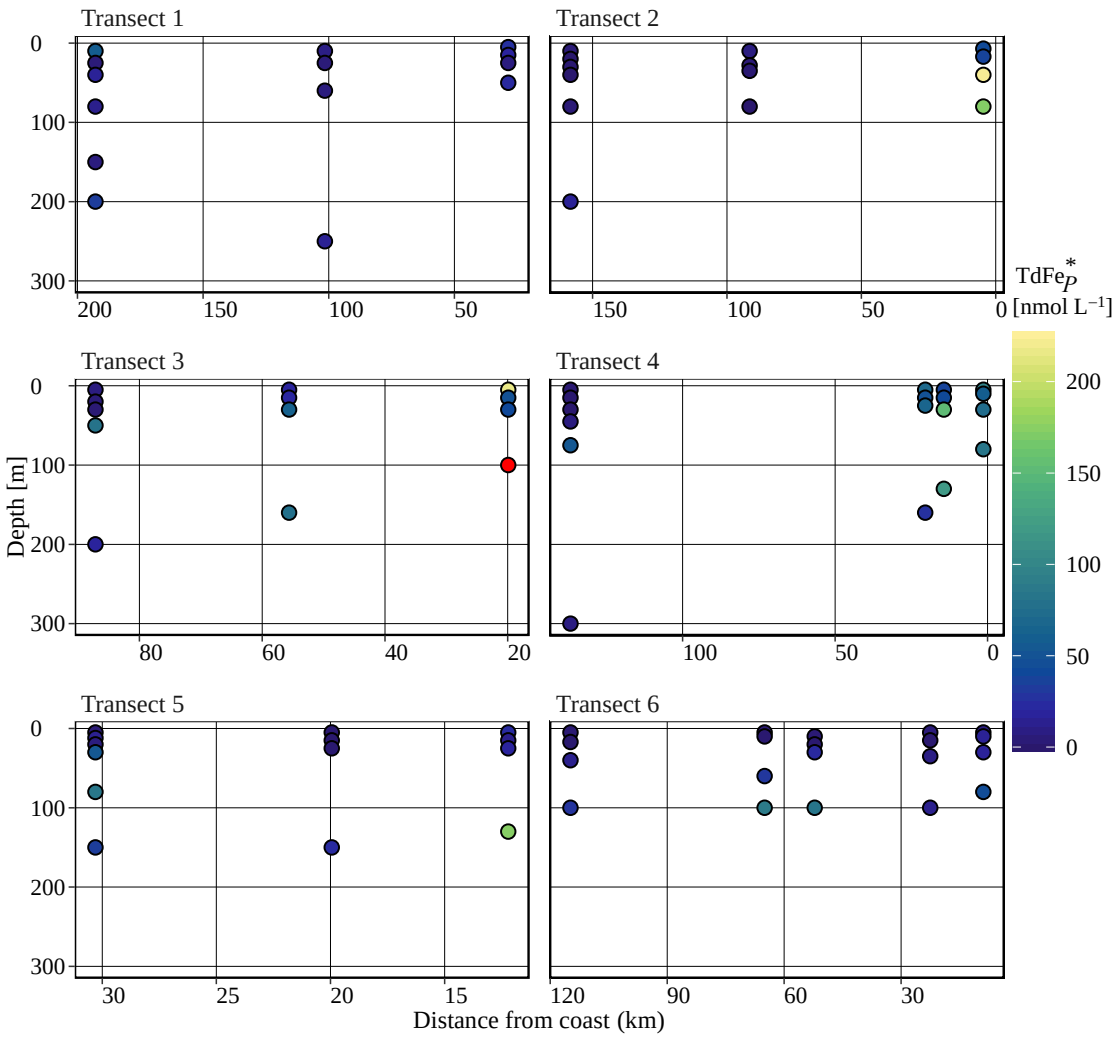

Figure S9: Concentration of excess total dissolvable iron relative to phosphate concentrations ($TdFe_P^*$) from each discrete depth where N_2 fixation samples were taken from.

Chapter 3: Manuscript II

Environmental controls for N_2 fixation in the HUS

Cobalt and nickel moderate N_2 fixation rates in the Eastern Tropical South Pacific

L. R. Kittu[1*], M. J. Hopwood[,2], A.J Paul[1], M. Fernandez-Mendez[,3], L. T. Bach[4], E.P. Achterberg[1], U. Riebesell[1]

Submitted to *Science Advances***

[1]Marine Biogeochemistry, GEOMAR Helmholtz Centre for Ocean Research Kiel, Düsternbrooker Weg 20, D-24105, Kiel, Germany.

[2] Southern University of Science and Technology, 1088 Xueyuan Avenue, 518055, Shenzhen, China.

[3]Alfred Wegner Institute for Polar and Marine Research, Am Handelshafen 12, 27570, Bremerhaven .

[4] Institute for Marine and Antarctic Studies, Ecology & Biodiversity, University of Tasmania, Hobart, TAS, Australia.

*Corresponding author: Leila Kittu (lkittu@geomar.de)

**Manuscript format in journal style

Abstract

Excess dissolved inorganic phosphorus over nitrate (P*) and dissolved iron concentrations are widely used to constrain global predictions of N_2 fixation and force biogeochemical models. There is a sound mechanistic basis for this, as P* and iron conditions theoretically create a chemically and ecologically favourable niche for diazotrophs. However, field observations indicate that neither P* nor iron distributions correlate with N_2 fixation rates in the Eastern Tropical South Pacific. Herein, using a comprehensive dataset from the ETSP, we statistically show that both cobalt and nickel explain more variability in N_2 fixation rates than iron, dissolved inorganic phosphorus, and P*. We verify that neither phosphorus nor iron addition significantly increased N_2 fixation rates using bioassay experiments. However, the supply of additional trace metals including cobalt and nickel via olivine leachate significantly enhanced N_2 fixation rates in coastal surface waters. Combined, our statistical and experimental results suggest that correlations between cobalt, nickel, and N_2 fixation rates are likely not coincidental as they better explain patterns of N_2 fixation in the ETSP than iron and phosphorus.

3.1 Introduction

Di-nitrogen fixation by diazotrophic (N_2 fixing) bacteria is responsible for almost half of the supply of bioavailable nitrogen that supports oceanic primary productivity(1). Diazotrophs are known to have higher iron (Fe) requirements than non-diazotrophs due to the biochemical role of Fe in their photosystems and as a cofactor in the enzyme nitrogenase(2). Under replete macronutrient conditions, diazotrophs face a competitive disadvantage due to the high energetic cost of N_2 fixation(3) and are outcompeted by non-diazotrophic organisms. Classically, a niche for diazotrophy is therefore characterized by high Fe, high dissolved inorganic phosphorus (P)(4), and low fixed nitrogen concentrations(5) such as in the oligotrophic equatorial Atlantic where extensive blooms of the diazotrophic cyanobacteria Trichodesmium are often observed(6). However, contrasting biogeochemical model results have so far revealed that no single factor can accurately predict marine N_2 fixation in the global ocean(7, 8).

The Eastern Tropical South Pacific (ETSP) is one of the world's most productive eastern boundary upwelling systems where the upwelling of nutrient-rich waters supports high primary production. As a result of heterotrophic decomposition of sinking organic matter combined with poor ventilation, an extensive oxygen minimum zone (OMZ) is found at depth(9). The low oxygen (O_2) conditions are considered favourable for diazotrophs because they relieve inactivation of nitrogenase by O_2(5) and are conducive to redox processes that supply benthic Fe and P to the water column(10). Therefore, studies have suggested that enhanced N_2 fixation rates should be expected in the ETSP due to an excess of P (P*) created through preferential nitrogen loss and high Fe supply(11). Whilst there is a strong mechanistic rationale for using P* and Fe distributions to define the diazotrophic niche(12), model-projected patterns of N_2 fixation in the ETSP have been difficult to reconcile with direct observations, potentially challenging the role of Fe and P* as the main drivers of N_2 fixation rates(4, 13). Irregular, sporadic high N_2 fixation rates, comparable to those associated with Trichodesmium blooms in the oligotrophic North Atlantic(14) have been reported from the ETSP off Peru

in association with sulfidic events(15), high productivity(16), and anticyclonic eddies(17). These discrete observations suggest particular conditions that may stimulate N_2 fixation. However, explicitly defining these conditions remains a challenge.

An understanding of what controls in situ N_2 fixation rates in the ETSP has been constrained by limited observations, sampling bias towards summertime in tropical and subtropical oceans, and a paucity of studies that fully resolve biogeochemical properties, particularly trace metal concentrations and N_2 fixation rates simultaneously. Using Boosted Regression Tree models (BRT) on a comprehensive dataset of N_2 fixation rates and biogeochemical variables collected across the northern Humboldt Upwelling System (HUS)(18–20) we examined the environmental factors that influence the distribution of N_2 fixation rates in the northern HUS. Additionally, in two bioassay experiments at a coastal and offshore station (Fig.1), we enhanced P and trace metal concentrations by the addition of upwelled water, iron (III) chloride ($FeCl_3$), and olivine leachate to surface waters (Supplementary methods) to probe the response of N_2 fixation rates to upwelled P and multiple trace metals. Mineral sources, such as olivine, are in many contexts a more environmentally relevant source of trace metals than spikes of individual dissolved elements. There are however numerous other effects of mineral particles on marine biogeochemistry, such as an increased surface area for bacterial growth(21), and for these reasons, we opted to use leachate rather than a direct mineral source to minimize other concurrent effects. As neither P* nor Fe appears to explain the observed variation in N_2 fixation rates across the ETSP and to some extent globally, the main goal of this study was to unravel the biogeochemical factors that explain most of the variance in N_2 fixation rates, and establish if those factors have a causative or coincidental relationship with N_2 fixation. Here we provide evidence that both cobalt (Co) and nickel (Ni), rather than Fe or P*, explain most of the variance in N_2 fixation rates across the ETSP. Considering an emerging interest in the potential use of minerals such as olivine for ocean alkalinity enhancement (OAE)(22), our results provide an unexpected and potentially beneficial link between OAE and the nitrogen cycle which warrants further investigation.

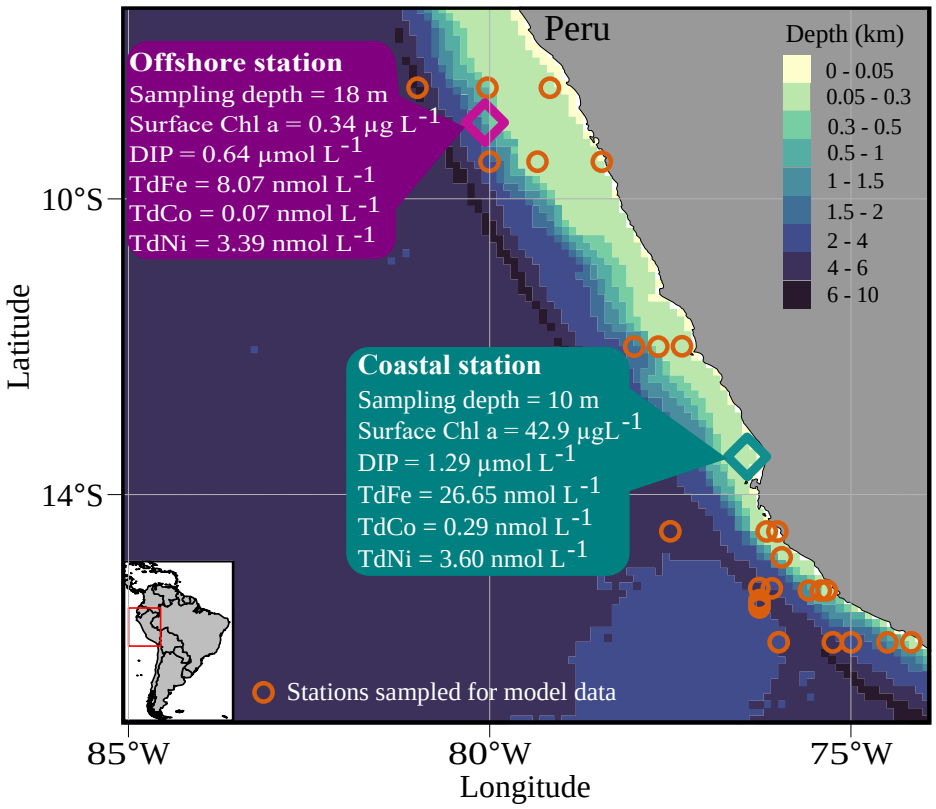

Fig. 1. Map of study area off the Peruvian coast. The map indicates the sampling sites for bioassay experiments (diamonds) and the location of stations where data was collected for the BRT statistical models (circles) overlain on bathymetry.

3.2 Results and Discussion

3.2.1 Evidence for the potential role of Co and Ni Influencing N_2 fixation in the ETSP

The influence of trace metals such as Co and Ni on marine productivity and N_2 fixation is thought to be subtle relative to Fe and has therefore received less attention. However, across the northern HUS, a statistical model based on a previous field dataset of N_2 fixation rates(19), shows that total dissolvable cobalt (TdCo), $TdCo_{Fe}$* (an index for the relative concentrations of TdFe and TdCo), and total dissolvable nickel (TdNi) explained up to 28% of the variability in N_2 fixation rates (Fig. 2B). The marginal effect plots for $TdCo_{Fe}$* (Fig. S1A) indicate a positive effect on N_2 fixation rates as $TdCo_{Fe}$* values increased towards 0. We however note that $TdCo_{Fe}$* was consistently below 0 (negative) in most of the study area due to relatively high Fe concentrations indicative of Co limitation in the region. Low $TdCo_{Fe}$* from these field observations and surface water used in bioassay experiments (all <0) are consistent with previous studies suggesting Co concentrations (range 0 – 0.4 nmol L^{-1}) in the ETSP are low relative to Fe and within the range known to proximally constrain phytoplankton growth(23–25). Additionally, all other trace metals included in the TM model had a significantly higher

influence on N_2 fixation rates than TdFe. The high model performance of the TM model (R^2 = 87%) suggests that a combination of other environmental conditions can be used to better explain N_2 fixation in the northern HUS, and likely have a larger influence than Fe alone (Fig. 2B).

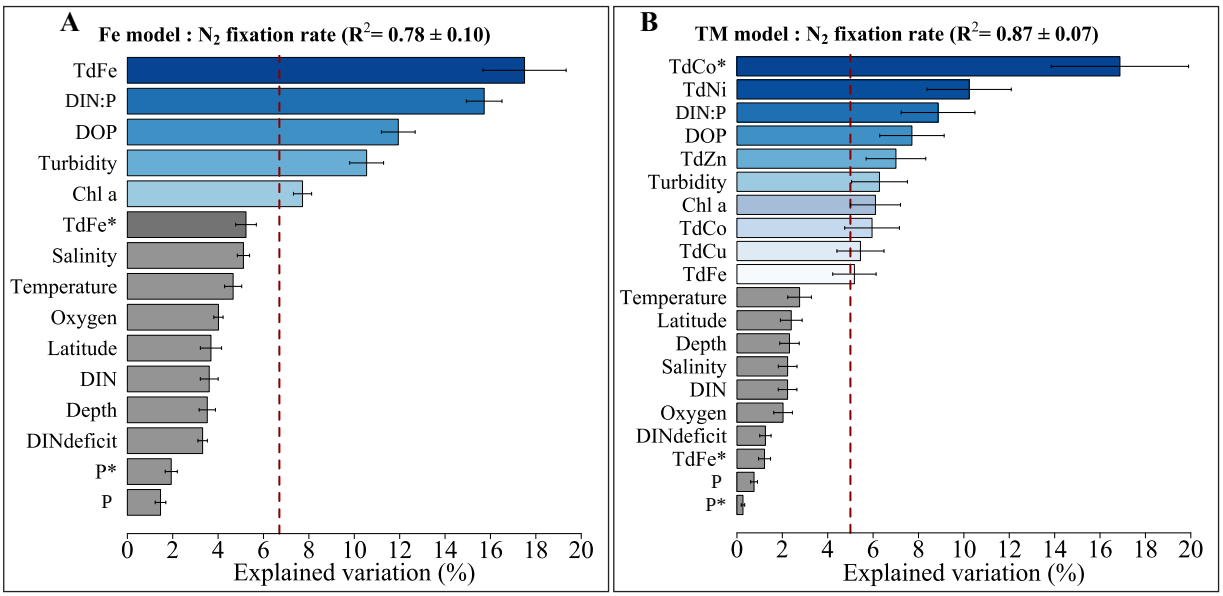

Fig. 2. BRT model results on the relative importance of environmental variables in explaining the variability of N_2 fixation rates. Two model configurations are used (A) the Fe Model looks at 15 predictor variables including TdFe as the only trace metal of interest and (B) the TM model with 20 variables, including other trace metals (TdCo, TdCo*, TdNi, TdZn, and TdCu) in addition to TdFe. The % of explained variation indicates the proportion of variability in the N_2 fixation rates explained by each variable. The error bars indicate the mean and standard deviation of the importance of each predictor variable determined from 30 BRT model runs of each respective model configuration. The blue shades indicate significant variables with an influence above what could be expected by chance (=100/no of variables), indicated by the red dotted line). Increasing blue color gradient indicates the relative importance of significant variables. R^2 in brackets represents the % of total deviance explained by the model, indicating the overall performance of the model in describing the variability of N_2 fixation rates.

3.2.2 Iron and phosphorus are not the primary drivers of N_2 fixation rates in the northern HUS

We performed bioassay experiments to assess the validity of the model outcomes, where P and TdFe concentrations in surface waters were increased through the addition of upwelled water and $FeCl_3$ (Fig. 3C, D). As a result, both P* and $TdFe_P$* (the excess of Fe relative to P) increased (Fig. S2A, C). Yet neither of these manipulations produced a significant increase in N_2 fixation rates relative to unamended incubations (Fig. 3A). The absence of a clear response

for N_2 fixation rates and ^{13}C uptake rates (as a proxy for phytoplankton productivity) to Fe and P addition even at the offshore station where TdFe concentrations were low was particularly surprising, as Fe deficiency in offshore waters is the commonly invoked reason to explain both low N_2 fixation rates(26) and low primary productivity in the high-nutrient, low-chlorophyll region of the ETSP(27). These results indicate that Fe was not the primary driver for both N_2 fixation and ^{13}C uptake rates and other factors were likely limiting N_2 fixation rates in offshore surface waters.

The addition of olivine leachate increased the concentrations of both Ni and Co, increased TdCo* in the +Oli treatment relative to the control, and significantly increased N_2 fixation rates in coastal TdFe-rich surface waters (Fig 3A, E, F, Fig. S2D). Similarly, Ni and Co addition at the coastal station significantly enhanced ^{13}C uptake rates in the +Oli treatment (Fig. 3B). Due to high variability between triplicates, enhanced N_2 fixation rates from the +Oli treatment at the offshore station were not statistically significant. Nevertheless, the slight increase in N_2 fixation rates offshore under Ni and Co addition points towards the potential for both Co, and Ni to limit N_2 fixation rates in offshore waters off Peru. Closer to the sedimentary source of Fe at the coast(10), surface water TdFe concentrations were 3-fold higher than offshore (Fig 1, 3D) and N_2 fixation rates were only significantly enhanced following Co and Ni addition. These results suggest a biochemically dependent colimitation of these trace metals (Type III limitation(28)). Therefore, whilst Fe availability in Fe-deplete areas may to some extent limit N_2 fixation, under replete Fe conditions, any addition of Co and or Ni may increase N_2 fixation rates. These bioassay results concur with the results of the statistical models positing that when additional trace metals are considered, the role of Fe in enhancing N_2 fixation rates in the coastal Fe-rich waters of the HUS appears to be relatively minor and that relative concentrations of multiple trace metals have an important role in influencing N_2 fixation rates (Fig. 4).

The minor role of TdFe, P, and P* in influencing N_2 fixation rates is broadly consistent with observations from measured N_2 fixation rates across the ETSP region, suggesting a weak or minor influence of these factors on in situ N_2 fixation rates(29). Our results provide evidence that factors other than Fe and P are likely to have a key role in influencing N_2 fixation and, unexpectedly, corroborate a role for Ni and Co in influencing both the distribution and magnitude of N_2 fixation rates in coastal waters of the ETSP.

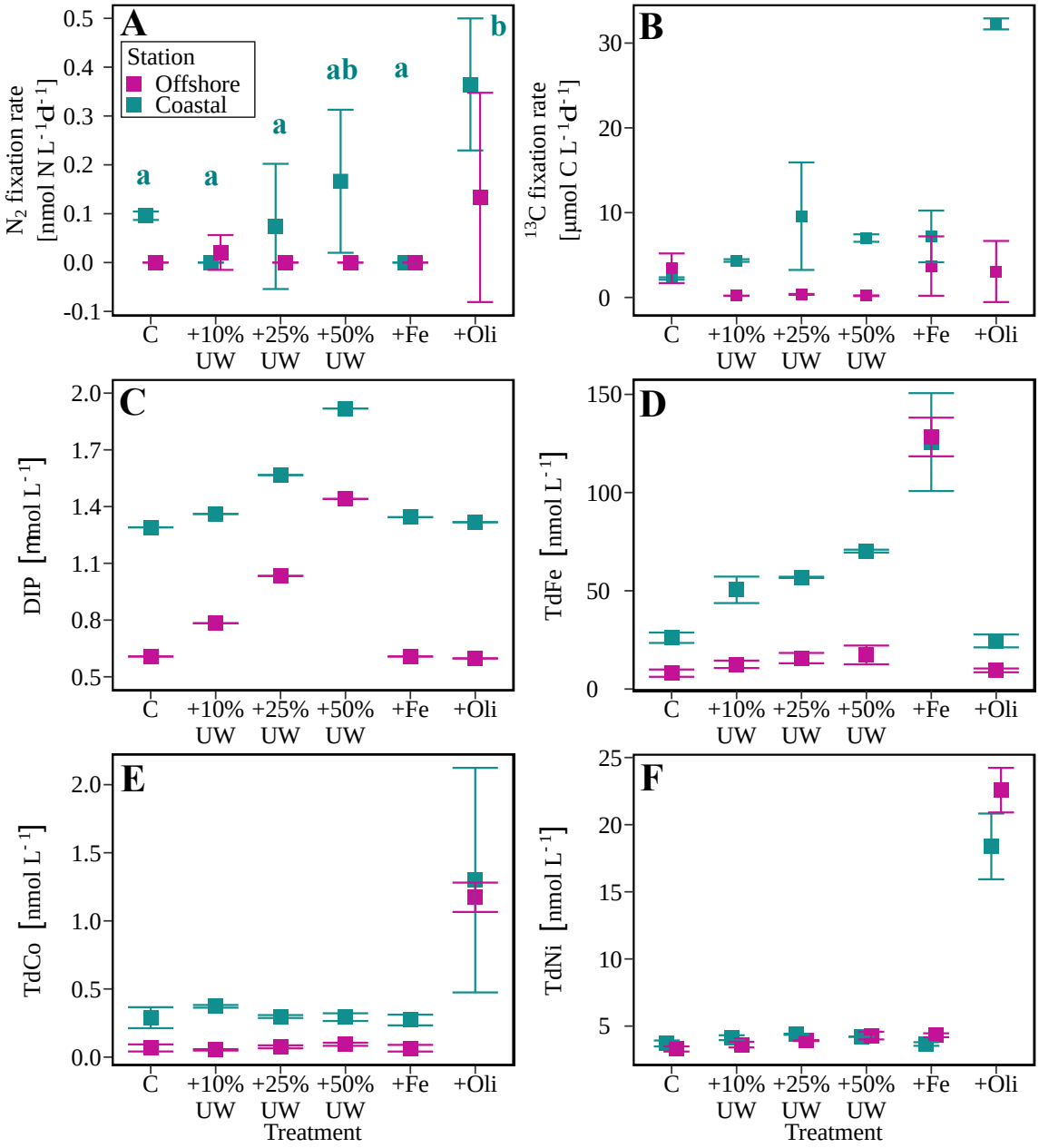

Fig. 3. N_2 fixation rates and nutrient conditions corresponding to treatment manipulations. (A, B) Mean effects of upwelling source water (UW), iron (Fe), and olivine (Oli) addition on N_2 fixation rates and ^{13}C uptake rates at a coastal and offshore station. (C-F) initial concentrations of P, TdFe, TdCo, and TdNi concentrations respectively in each treatment from the two experimental stations. Error bars indicate the standard deviation of three replicate bottles for each treatment. Alphabetical letters show the results of a test for statistically significant different means on N_2 fixation rates (one-way ANOVA, followed by a Tukey multiple comparison test). Treatments with a common letter are statistically indistinguishable at the 5% significance level ($p < 0.05$). No significant difference in N_2 fixation rates across all treatment combinations was observed from the offshore station.

3.2.3 Towards a mechanistic understanding of the role of Co and Ni for N_2 fixation

In field observations, trace metal co-limitation of N_2 fixers may be difficult to disentangle purely from biogeochemical tracers such as $TdCo_{Fe}$* and can only be confirmed through trace metal addition incubation experiments. Both our statistical model results and bioassay experiments highlight that the relative availability of Co to Fe rather than their absolute concentrations play an important role in regulating N_2 fixation. This is especially highlighted by the bioassay experiments where N_2 fixation rates were neither significantly enhanced by the availability nor additional input of Fe alone in both experiments. N_2 fixation was enhanced only under Co and Ni addition in coastal waters. Our study is the first to show from both field and experimental work that multiple trace metals may regulate N_2 fixation rates in the ETSP. When all trace metals, rather than just Fe, are included in a statistical model (Fig. 2B) the similarity of the % explained variation for all metals, turbidity, and Chlorophyll a (chl a), which each explains 5-11% of the variance, could simply reflect a close association between N_2 fixation rates and organic matter. Organic matter is a major pool of metals such that total dissolvable metals, chl a, and turbidity may change roughly proportionately. Yet the low % explained variation for TdFe does, unexpectedly, question the validity of model approaches that selectively use Fe to predict N_2 fixation.

While our model is statistical rather than mechanistic, the combination with experimental evidence provides support for the mechanistic roles of Co and Ni in regulating N_2 fixation in the ocean. An influence of Co and Ni on N_2 fixers, whilst to our knowledge a novel suggestion for the control of in situ marine N_2 fixation rates, is not a new paradigm in the global ocean. Cobalt is known to play a key biochemical role in vitamin B_{12} synthesis (cobalamin) and P acquisition by substituting zinc in the enzyme alkaline phosphatase(30). Under Fe replete conditions, evidence for a coregulatory role of Co on primary productivity has previously been observed in the ETSP off Peru(23), Costa Rican upwelling dome(25), and the Southern Ocean(31). Cobalt addition to Fe replete surface waters consistently enhanced primary productivity in bioassay experiments(23, 32, 33), providing evidence for Co (co)limitation with Fe in marine phytoplankton. Diazotrophs such as Crocosphaera spp, an obligate producer of cobalamin, and Trichodesmium spp are also known to have high Co requirements(30, 34–36).

Both of our BRT statistical models also substantiate a more important influence of dissolved organic phosphorus (DOP) in explaining the variability of N_2 fixation rates, relative to both P concentrations and P* (Fig. 2A). Previous field studies have associated high N_2 fixation rates and abundances of diazotrophs in the ETSP with elevated surface DOP concentrations(37), suggesting a role for DOP as an alternative phosphorus source for diazotrophs either exclusively or in addition to P. Alkaline phosphatase hydrolyzes DOP and enables biological utilization of P compounds in cells(38). Crocosphaera watsonii, also present in the ETSP(15), has shown a robust capacity to upregulate alkaline phosphatase activity to access bioavailable P from DOP, indicating a dual role and requirement for Co (in addition to cobalamin synthesis) in their

growth apparatus(39). Heterotrophic bacteria including gamma-proteobacteria, some of which can fix N_2, are known to utilize alkaline phosphatase and may have additional Co requirements since they are also a major microbial source of cobalamin in the ocean(40). Hence high Co availability may generally up-regulate the activity of alkaline phosphatase(41) and enhance N_2 fixation rates in diazotrophs that can utilize DOP as a phosphorus source(39, 42).

A potential role for Ni as a regulator of N_2 fixation rates is more perplexing. Ni availability is not considered a limiting factor for marine planktonic organisms mainly because surface Ni concentrations are never fully depleted, though it is not necessarily the case that residual Ni is bioavailable(43). A specific role for Ni in N_2 fixing bacteria is now well established with the determination that Ni is an essential cofactor in oxygen and hydrogen protecting enzymes Nickel-superoxide dismutase (Ni-SOD)(44) and NiFe-hydrogenase(45) respectively. Nitrogenase is extremely sensitive to permanent inactivation by O_2(46). Ni-SOD activity in N_2 fixers hence provides essential oxidative protection for nitrogenase, especially in surface oxygenated waters(44, 47). Additionally, N_2 fixation is accompanied by the production of molecular hydrogen (H_2), which has an inhibitory effect on nitrogenase. Therefore, almost all known diazotrophs contain the Ni requiring metalloenzyme NiFe-hydrogenase which oxidizes H_2 to hydrogen protons while consuming O_2 and producing energy(45) both of which benefit N_2 fixation. This demonstrates a potential link between Ni uptake, energy production, toxicity stress regulation (O_2 and H_2), and N_2 fixation rates (Fig. 4). The high Ni requirement makes N_2 fixation subject to Ni limitation(48). For example, in waters with ambient TdNi concentrations >2 nmol L^{-1}, culture experiments with Trichodesmium have demonstrated increased Ni-SOD levels(49, 50), N_2 fixation activity, and growth rates(51, 52) following Ni addition.

On a global scale, observations and model Ni data have linked heavy Ni isotopes in surface ocean waters to high N_2 fixation(53). This provides evidence that marine diazotrophs utilize isotopically light bioavailable Ni, leaving behind an isotopically heavy Ni pool. Similarly, in surface waters of the North Atlantic subtropical gyre, low Ni concentrations in surface waters have been associated with high Ni uptake by N_2 fixers stimulated by high Fe inputs(43). A potential coupling between Fe and Ni may therefore influence N_2 fixation in the ocean. Such a coupling, already observed in the subtropical North Atlantic(43), could be widespread but especially evident in coastal OMZ regions with high Fe inputs or a tendency for trace metal co-limitation(23). Whilst most direct evidence for the influence of Ni on N_2 fixation is related to Trichodesmium, it is plausible that diazotrophic heterotrophs and unicellular cyanobacteria may possess similar biochemical requirements for Ni, a topic for further exploration.

To the best of our knowledge, nitrogenase is not known to have any direct dependence on Co or Ni. However, regulatory roles for Co and Ni either through P uptake, vitamin B_{12} synthesis, energy synthesis, or H_2 and O_2 protection suggest plausible mechanistic explanations for our statistical model results and corroborating bioassay results. Our results infer that potential co-regulating factors such as Co and Ni availability require closer attention and suggest that the direct influence of Fe and P in regulating in situ N_2 fixation rates in the ETSP may have been

overstated in biogeochemical models. In light of our results, other trace metals in addition to Fe need to be considered when assessing future biogeochemical changes and feedbacks on N_2 fixation rates in the ocean.

3.2.4 Controls of N_2 fixation in the ETSP: A complex interplay of environmental drivers

The regulation of N_2 fixation by environmental conditions can take place simultaneously at a molecular level, related to transcription and translation of nitrogenase, and at a physiological level, related to growth and activity, each modulated by a different set of interacting environmental controls(54). We hypothesize that the requirements for Ni and Co are linked to the biochemical demands for N_2 fixation either directly for the nitrogenase enzyme, energy production, and growth or indirectly through organic matter availability(15) and expression of metalloenzymes responsible for O_2 and H_2 removal (Ni) and P uptake (Co), (Fig. 4). In the Peruvian OMZ, where redox conditions are partly responsible for the observed variability in trace metal distributions(55), N_2 fixers may face trade-offs related to energy allocation for these biochemical demands. Such trade-offs may additionally be tightly linked to trace metal and macronutrient gradients such as DIN:P ratios (Fig. S1A). In a scenario where low Co and Ni concentrations prevail, first, diazotrophs may allocate more energy to stress regulation than to growth and N_2 fixation activity since they may also be P-limited, and second, phytoplankton organic matter production is limited. Overall, these conditions may result in slower growth of N_2 fixers, low diazotroph abundances(56), and accumulation of H_2(57, 58) ultimately resulting in low N_2 fixation rates. Under a scenario featuring high Fe, and P, additional Ni, and Co availability may enhance the capacity of N_2 fixers to utilize these replete Fe and P conditions for rapid and optimal growth and N_2 fixation even in oxygenated waters. Additionally, phytoplankton productivity would be enhanced under additional Co and Ni availability (Fig. 3b), thereby increasing the availability of phytoplankton-associated organic matter, an important energy and potential P source for heterotrophic N_2 fixers(59) (Fig. 4).

Our results posit that the control of N_2 fixation in the northern HUS involves a complex interplay of micro, macronutrient, and organic matter availability. The variability of these drivers in space and time could explain the observed mismatch between models and observations(26), and the high variability, marked by intermittent high N_2 fixation rates so far observed from the region despite overall low rates year-round. Our results have important implications for predicting N_2 fixation rates at a regional scale in the ETSP and projecting how they will change in the face of climatic perturbations of environmental drivers. The paucity of trace metal data alongside N_2 fixation rates makes it difficult to conclude with certainty the extent to which Ni and Co and possibly other trace metals may influence N_2 fixation in the global ocean. Yet a co-regulating role of Fe, Ni, and Co for N_2 fixation rates certainly adds to a long-standing discussion on which nutrients limit marine primary production on geological timescales and points towards, as is

the case for the modern ocean, the tendency of multi-nutrient colimitations to constrain in situ productivity.

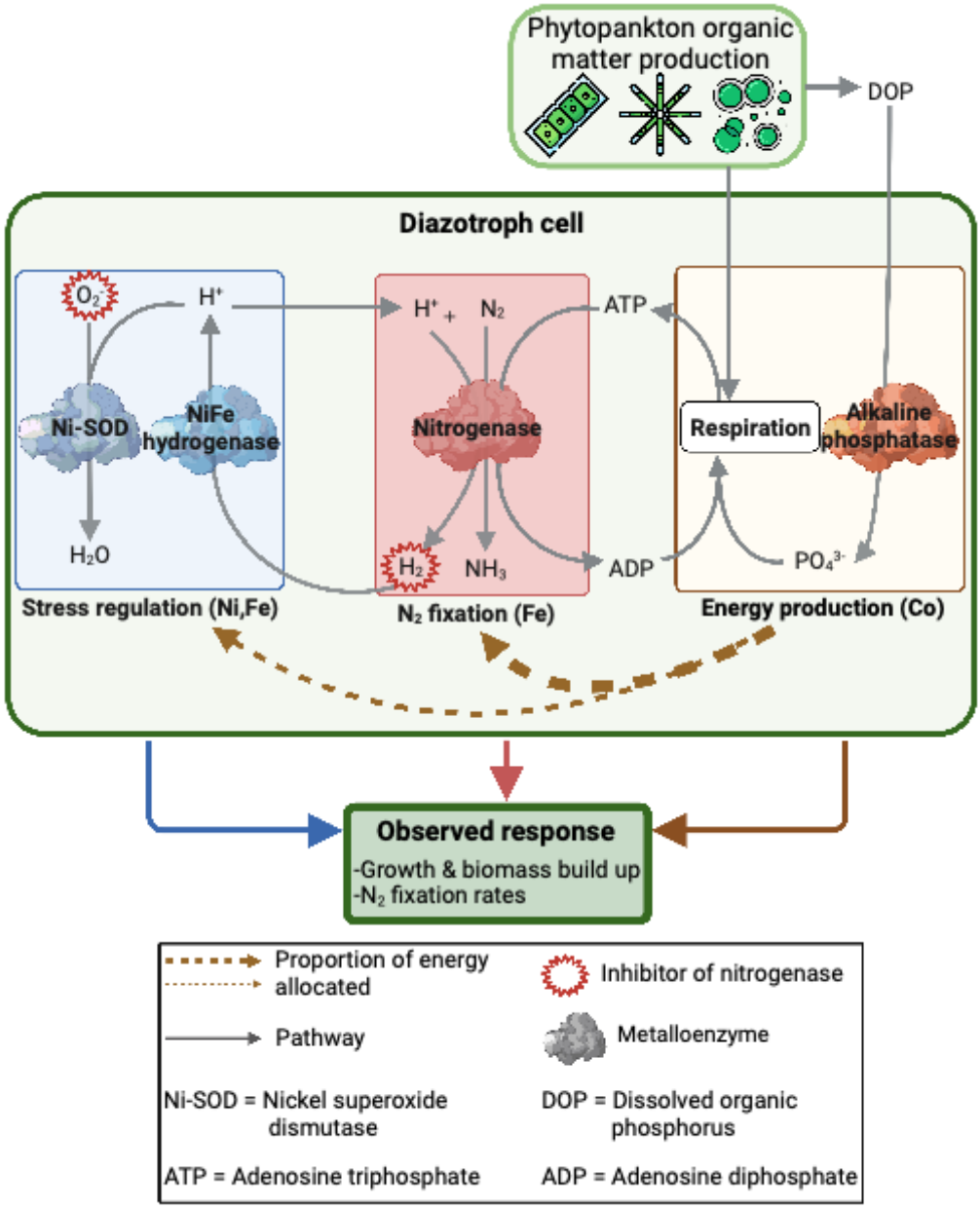

Fig. 4. Plausible mechanistic pathways for the observed role of iron (Fe), nickel (Ni), and cobalt (Co) co-regulating N_2 fixation rates. Energy production refers to the cobalt-requiring mechanism through which energy is produced. Stress regulation refers to the nickel-requiring cellular process that protects nitrogenase from permanent oxygen and/or hydrogen damage. Thin and thick brown arrows indicate relative energy allocated to N_2 fixation and stress regulation. Created with BioRender.com

3.2.5 Implications for carbon dioxide uptake

The main aim of using olivine in this study was to supply multiple trace metals in the incubations. Nevertheless, our results are of topical relevance given the emerging interest in olivine as a potential mineral alkalinity source to increase ocean carbon storage and mitigate ocean acidification ('ocean alkalinity enhancement')(22). Our bioassays show, for the first time, that the addition of olivine can stimulate both N_2 fixation and carbon fixation, thereby revealing a link between this climate intervention method to the marine nitrogen cycle. Hence this additional effect of olivine-based ocean alkalinity enhancement could affect ocean ecosystems and their capacity to sequester carbon dioxide (60) and provide other ecosystem services.

3.3 Materials and methods

3.3.1 Bioassay experiments

Sample collection

The influence of phosphorus and trace metals on N_2 fixation rates was determined using bioassay experiments conducted on the MSM80 cruise off the northern HUS in the Eastern Tropical South Pacific (austral summer, December 23, 2018, to January 30, 2019, R/V Maria S Merian). Two 4-day long bioassay experiments (Fig.1) were conducted at an offshore station and coastal station starting December 30, 2018, and January 10, 2019, respectively (denoted as offshore and coastal experiments hereafter). At each station, temperature and salinity were recorded using a Seabird 911 CTD (SBE-911 plus, Seabird-Electronics, USA). For the offshore and coastal experiments, water samples for bioassays to determine N_2 fixation rates were collected from near-surface waters at 18 and 10 m (Table. S1). During both experiments, upwelling source waters were collected from the oxygen minimum zone at a depth where the O_2 concentrations dropped below the detection limit of the O_2 sensor (1.5 µmol L^{-1}), (Table. S2).

Experimental manipulations

Bioassay experiments were conducted involving three amendments with upwelling waters (+UW), iron (+Fe), and olivine (+Oli). Additionally, four incubations for the control were performed with surface water at each station, of which 3 were incubated. Overflow of about half the bottle volume was allowed while filling all incubation bottles to minimize oxygen contamination.

For the +UW treatments, 3 acid-cleaned 10 L Nalgene polycarbonate carboys were filled with near-surface seawater from the Niskin bottles. Upwelled source waters were mixed with surface waters in each carboy at three proportions (10%, 25%, and 50%), indicating the amount

of UW added to replace surface water. 4 x 4.5 L Nalgene bottles were filled for each UW water treatment.

For the +Oli treatments, surface water was directly transferred from the Niskin bottles into 4 x 4.5 L acid-cleaned Nalgene bottles. Incubation bottles were then enriched with Co and Ni through the addition of olivine leachate prepared by dissolving olivine in prefiltered surface seawater. Briefly, in a 2.5 L acid-rinsed (3M HCl) polycarbonate bottle, 38.32 g of commercially available olivine sand $(Mg^{2+}Fe^{2+})_2\ SiO_4$) was suspended in 500 ml of pre-filtered surface seawater (0.2 µm pore size sterile filter, Whatman). Headspace was left in the bottle to allow the solution to equilibrate to avoid drastic changes in carbonate chemistry. After 10 days the solution was then filtered through 0.2 µm sterile filter (Whatman) to remove large olivine particles. 112 ml of the leachate was then added to 4 x 4.5 L incubation bottles corresponding to the +Oli treatment. Because olivine dissolves non-stoichiometrically in the short-term(22), the olivine was dissolved 10 days before each experiment (27/12/2018 – offshore experiment, 07/01/2019 – coastal experiment) and shaken each day to maximize the dissolution of olivine and release of trace metals. The main aim of adding olivine in the experiment was to simulate trace metal addition rather than to change particle load or carbonate chemistry. Considering the small mixing ratios and short dissolution time, we did not expect significant changes in carbonate chemistry (Fig. S3D, E) therefore factors such as alkalinity and pH changes were not considered in this study.

For the Fe treatment, surface water in 4.5 L incubation bottles was amended with Fe. A 5 µmol L^{-1} stock solution was prepared once on 27/12/2018 by dissolving 0.135 mg of iron (III) chloride hexahydrate ($FeCl_3$, Merck) into 45 ml of prefiltered surface water (0.2 µm nominal pore size, Whatman). 5 ml of this stock solution was added to four Fe treatment bottles.

All experimental bottles were mixed gently after amendments. For each treatment, 3 bottles were incubated to determine N_2 fixation rates. The 4^{th} bottle was used to determine initial macronutrients and trace metal concentrations in the incubation bottles after treatment amendments.

N_2 fixation measurements

N_2 fixation rates were determined according to the modified ^{15}N-N_2 gas dissolution method(61, 62) where 100 ml of seawater enriched with ^{15}N labelled N_2 gas was added to each treatment incubation bottle. For the control, filtered and degassed seawater without ^{15}N-N_2 gas was added to each bottle. All treatment bottles and the controls were capped without headspace, ensuring no bubbles then incubated for 4 days in an on-deck incubator with a continuous flow of seawater. After 4 days, subsamples from each incubation were filtered under gentle pressure (200 mbar) onto pre-combusted (450°C, 4 hours) GF75 filters (Advantec, 25 mm Ø, 0.3 µm nominal pore size) and treated with acid (1M HCl for 2 minutes) to remove particulate inorganic carbon. All filters were analyzed for particulate organic matter to determine the mass and isotopic composition (δ^{13}CPOC/δ^{15}NPON). Filters were analyzed on an elemental analyzer

(Flash EA, ThermoFisher) connected to a mass spectrometer (Delta V Advantage Isotope Ratio MS, ThermoFisher) with the ConFlo IV interface (ThermoFisher). N_2 fixation rates were then calculated according to Montoya et al.(63). The limits of detection for N_2 fixation were determined according to the method outlined in White et al.(64).

Macronutrient and trace metal analyses.

Ambient macronutrient and trace metal concentrations before treatment amendments were determined from the fourth control bottle. Samples were taken unfiltered directly from the Niskin bottles. After treatment manipulations, samples were collected from the 4^{th} incubation bottle to determine starting macronutrient and trace metal concentrations and particulate organic carbon and nitrogen isotopic composition (δ^{13}C-POC/δ^{15}N-PON) in the incubations. Samples for dissolved inorganic nitrogen (nitrate (NO_3^-), nitrite (NO_2^-) and ammonium (NH_4^+), hereafter DIN), phosphate (PO_4^{3-} here after DIP) before incubation were analyzed onboard using an autosampler (XY-2 autosampler, 199 SEAL Analytical) and a continuous flow analyzer (QUAAtro Autoanalyzer, SEAL Analytical)(65–67).

Seawater samples were taken unfiltered from each fourth treatment bottle and the control to measure total dissolvable (Td) trace metal concentrations available within our N_2 fixation incubations. Samples were retained in 125 ml low-density polyethylene sample bottles (Nalgene) which had been pre-cleaned (Mucasol®, followed by 1 week in 3M HCl and 1 week in 3M HNO_3 with 3 deionized water rinses after each stage). Plasticware for sampling was acid-cleaned similarly. Sample bottles were pre-rinsed three times with a few millilitres of the sample before filling. Sample bottles were stored double-sealed in sample bags. Total dissolved trace metal concentrations were determined via inductively coupled plasma mass spectrometry (ICP-MS) after preconcentration, per Rapp et al. (2017). Samples were acidified with ultrapure hydrochloric acid (UpA grade, Romil) to pH 1.9 and left sitting for >6 months, subjected to 4 h UV irradiation in 30 mL fluorinated ethylene propylene bottles, preconcentrated offline using a SeaFAST system (Elemental Scientific Inc), and then analyzed on an Element XR ICP-MS (Thermo Finnigan). The reference material CASS-6 was also analyzed to assess the accuracy of the analytical procedure (Table. S4).

Nutrient supply ratios

To assess trace metal and macronutrient coupling, we calculated three diagnostic tracers as measures of relative nutrient availabilities and limitations i.e DIP limitation with DIN (P*)(11), Fe limitation with PO_4^{3-} ($TdFe_P$*)(7, 68), and Co limitation with Fe ($TdCo_{Fe}$*)(23) using equations 1, 2 and 3, respectively. $R_{N:P}$, $R_{Fe:P,}$ and $R_{Fe:Co}$ represent average phytoplankton uptake requirements for respective nutrient availabilities based on the extended Redfield ratio(69) $(C_{7.75}N_1Si_1P_{0.0626})_{1000}Fe_{0.469}\ Co_{0.012}Ni_{0.0625}$.

$$P^* = \left[PO_4^{3-}\right] - \frac{[NO_3^-]+[NH_4^+]+[NO_2^-]}{R_{N:P}} \quad (1)$$

$$\mathrm{TdFe_P}^{*} = [\mathrm{TdFe}] - R_{Fe:P} \times \left[PO_4^{3-}\right] \quad (2)$$

$$\mathrm{TdCo_{Fe}}^{*} = [\mathrm{TdCo}] - R_{Co:Fe} \times [\mathrm{TdFe}] \quad (3)$$

3.3.2 Sample collection of the model dataset

N_2 fixation rates, macronutrients, and trace metal samples for the dataset used in the statistical model were collected and analyzed similarly as described above.

Statistical analysis

All statistical analyses and data visualizations were performed with R studio version 1.3.959. In the bioassay experiments, the response (N_2 fixation rates) among different treatments were compared by using a one-way ANOVA. A Tukey multiple comparison test was applied post hoc to analyze differences between each pair of treatments at the 5% significance level.

The relative influence of environmental variables on N_2 fixation using Boosted regression tree models

The underlying data used for the statistical model included 103 measurements collected from 27 stations across the northern Humboldt upwelling system. The datasets for N_2 fixation rates, dissolved organic and inorganic nutrients, and trace metals can be found under Kittu et al. (19), Kittu et al. (20), and Kittu et al. (18) respectively. Potential predictor variables were defined based on a literature review on the physiological and ecological controls of N_2 fixation both from a marine and terrestrial perspective. Using this data, two statistical model configurations were defined and run: the iron (Fe) model and the trace metal (TM) model. The Fe model was used to determine the importance of Fe as a factor influencing N_2 fixation rates in addition to other physical and biogeochemical variables. Therefore, this model included TdFe as a trace metal and the tracer $\mathrm{TdFe_P}^{*}$. The TM model builds up on the simple Fe model by including variables related to other trace metals such as TdCo, $\mathrm{TdCo_{Fe}}^{*}$and TdNi, TdZn, and TdCu as additional potential trace metal controls for N_2 fixation.

To explore the relative contributions of each predictor in explaining N_2 fixation for each respective model, we used boosted regression tree models (BRT)(70). BRTs can detect nonlinear relationships between response variables and their drivers. Furthermore, BRTs are robust to co-dependency amongst drivers which is common in ecology.

BRT analysis was carried out with the R package gbm(71) and the gbm.step function using a gaussian error structure and 10-fold cross-validation. To run the model, we chose an optimal combination of model characteristics such as tree complexity, learning rate, and bag fraction that minimizes the estimate of error (Table. S3). The bag fraction introduces randomness into the models and controls overfitting. A bootstrapping of 30 model runs was performed to ensure stable estimates of the model evaluation parameters and generate a standard deviation

of the contribution of each driver. As a measure of model performance, the percentage of deviance explained by the model, the mean residual deviance, and the mean correlation between observed and predicted values during cross-validation was used (Table. S3). To determine the environmental drivers that had a significant influence on the N_2 fixation, a threshold defined by 100/number of variables for each model was used indicating a relative influence above that expected by chance(72). Model performance measures were based on model performance parameters provided in Table S3. Before the BRT model exercise, all N_2 fixation rates were logarithm-transformed to base 10 to balance the importance of extreme values in the response variable.

Acknowledgements

We are thankful to the captains, crew members, and scientists onboard the MSM80 cruise of the German R/V Maria S Merian for their support and cooperation at sea. We thank Phil Renforth for providing the olivine sand. We especially thank Dr. Rainer Kiko, Dr. Michael Meyerhöfer, and Dr. Joaquin Ortiz for assisting with onboard sampling and Kastriot Quelaj for nutrient sampling and analysis. We further thank Kerstin Nachtigall for assistance with sample analysis for mass spectrometry and Silvia Georgieva for providing help with processing and data analysis. We thank Dr. Silvan Goldenberg and Dr. Giulia Faucher for discussions on statistical analysis and feedback on the conceptual figure.

Funding: This research was supported by the German Federal Ministry of Education and Research (BMBF) through the cooperative research projects: Humboldt Tipping (01LC1823B) and CUSCO ("Coastal Upwelling System in a Changing Ocean", FKZ03F0).

Author contributions

M.F.M., A.J.P., and L.R.K. designed experiments and collected all samples. L.R.K. and M.J.H. analyzed samples. L.R.K analyzed and visualized data and wrote the manuscript with advice and input from all co-authors.

Competing interests

The authors declare no competing interests.

Data and materials availability: The statistical model dataset on N_2 fixation rates, trace metals and water column biogeochemistry that support the findings of this study are publicly available on PANGEA[18–20]. The dataset generated in the bioassay experiments will be made available on PANGEA.

Supplementary Information

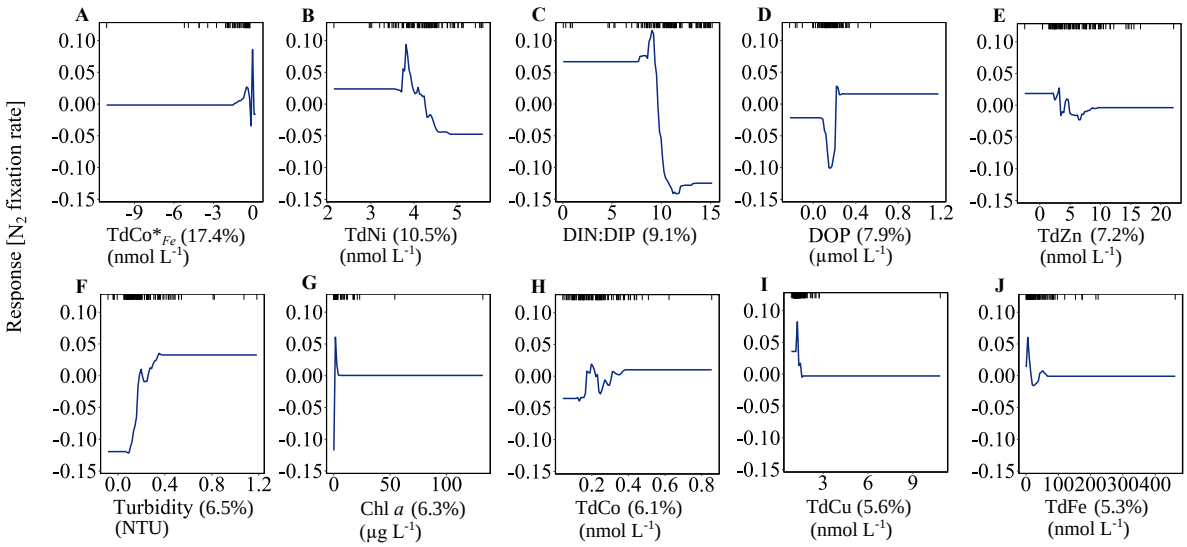

Fig. S1. Marginal effect plots for environmental variables on N_2 fixation from the TM model. The ten most influential drivers (A – J, relative importance >5%) from the TM model are shown. The plots show the mean relative effect of each variable (in parenthesis) on the variability of N_2 fixation. The y-axis indicates the response to N_2 fixation rates while changing the explanatory variable (x-axis). Black tick marks at the inside top of each plot show distribution of N_2 fixation observations across each variable.

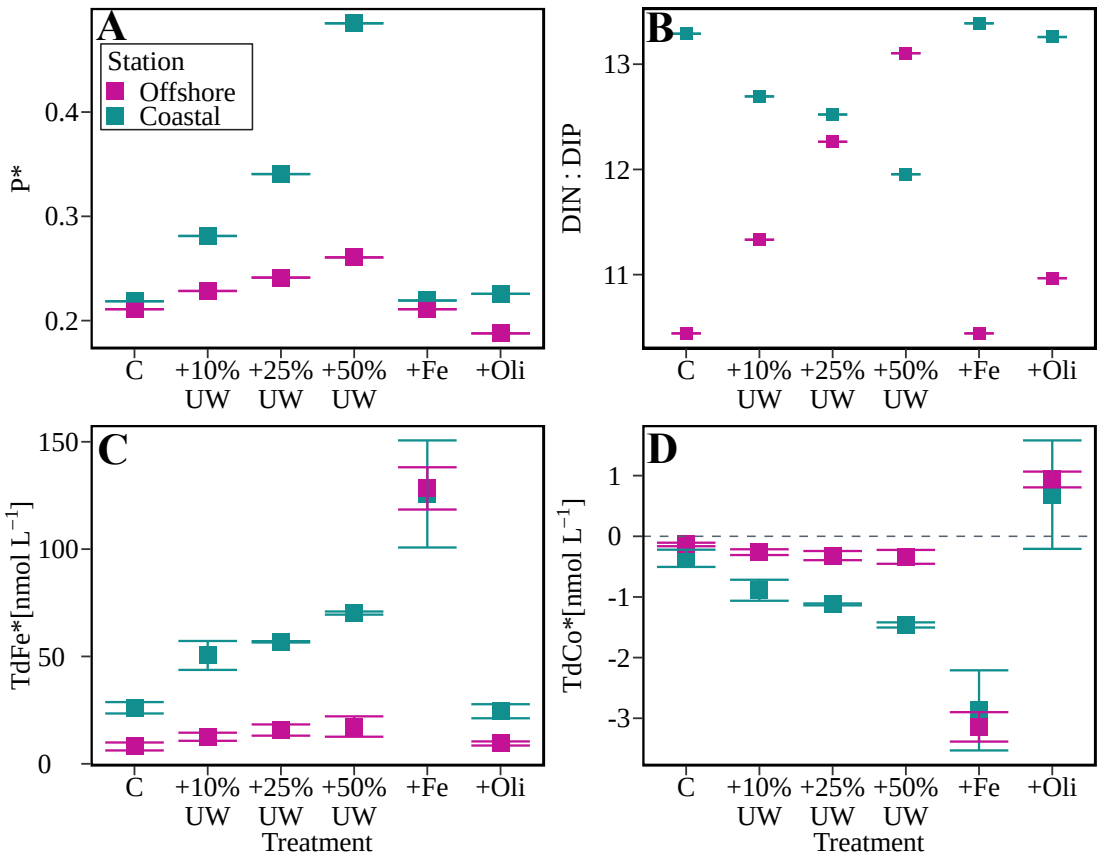

Fig. S2. Nutrient supply ratios in bioassay experiments. (A) excess phosphorus (B) DIN:DIP ratio (C) excess total dissolved iron relative to phosphorus (D) excess total dissolved cobalt relative to iron in each treatment before incubation at the two experimental stations. Error bars indicate the standard deviation of triplicate measurements.

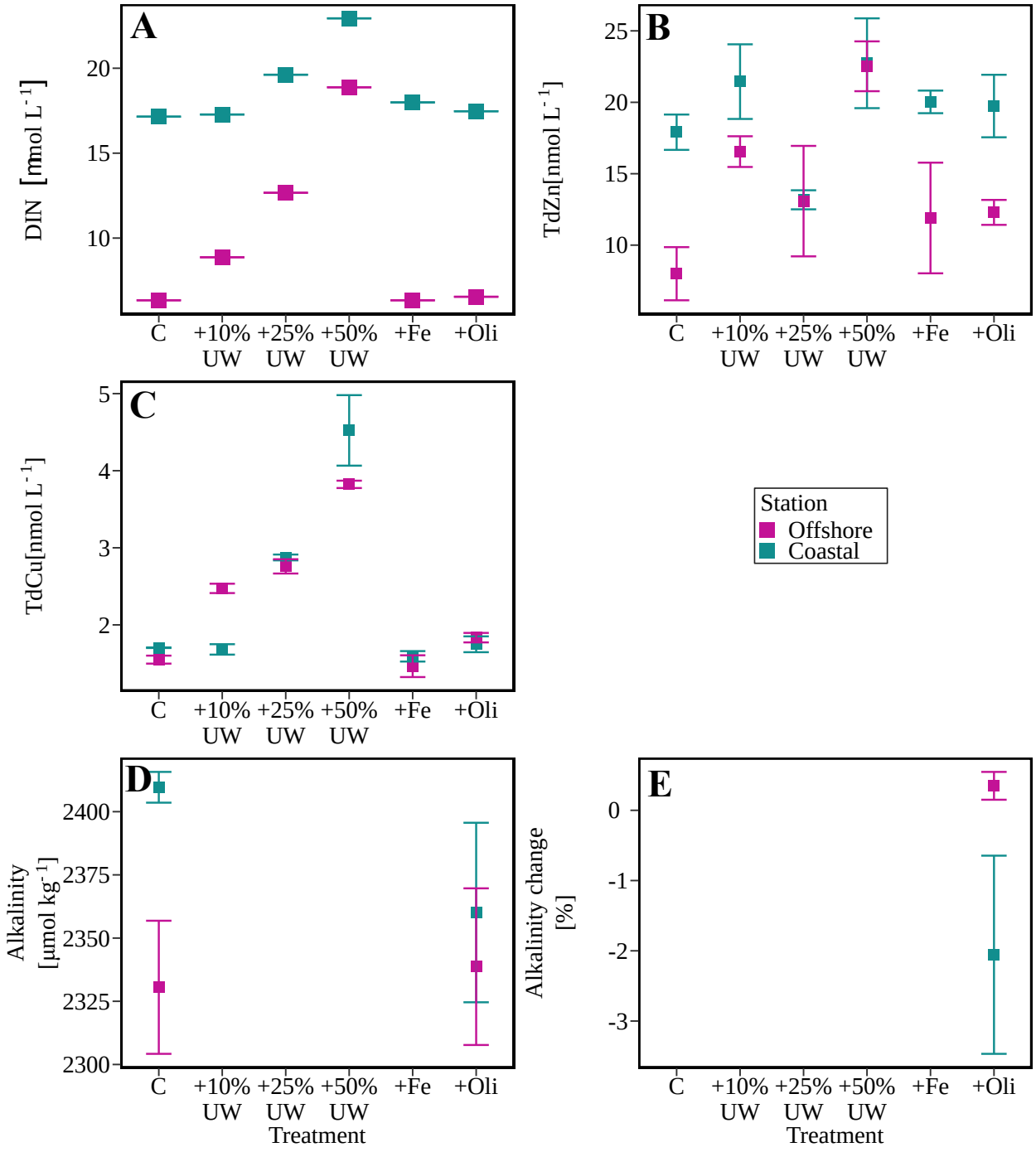

Fig. S3. ^{13}C fixation rates and biogeochemical variables measured from bioassay experiments. (A) Dissolved inorganic nitrogen (B) total dissolvable zinc, (C) total dissolvable copper (D) alkalinity measured from each treatment before incubation and (E) the change in alkalinity between the +Oli treatment and the control at the two experimental stations. Error bars indicate the standard deviation of triplicate measurements.

Table S1. Environmental conditions at bioassay stations.

Variable	Experiment 1	Experiment 2
Location	Off-shelf - Peru	Coastal - Peru
Station number (Cruise MSM80)	15	51
Latitude (°N)	-8.969	-13.389
Longitude (°W)	-80.067	-76.437
Distance from coast (km)	156	27
Bottom depth (m)	1029	101
Euphotic zone depth (m)	40	18
Average temperature in euphotic zone (°C)	22.27 ± 1.35	19.35 ± 0.95
Average oxygen in euphotic zone (µmol L^{-1})	235 ± 21	123 ± 51
Average turbidity in euphotic zone (NTU)	0.12 ± 0.03	0.50 ± 0.26
Control/surface water depth (m)	18	10
Control/surface chl *a* (µg L^{-1})	0.34	42.9

Table S2. Chemical composition of upwelling source waters (UW) at bioassay stations

Variable	Experiment 1	Experiment 2
Location	Off-shelf - Peru	Coastal - Peru
Depth of upwelling source waters (m)	150	80
DIN concentrations (µmol L^{-1})	31.61 ± 0.00	28.50 ± 0.02
Phosphate concentrations (µmol L^{-1})	0.64 ± 0.05	2.54 ± 0.01
DIN:P	49.69 ± 3.60	11.23 ± 0.04
P*	-1.33 ± 0.05	0.76 ± 0.01
TdFe concentrations (nmol L^{-1})	39.95 ± 0.61	114.03 ± 7.56
TdFe*	39.95 ± 0.61	114.03 ± 7.56
TdCo concentrations (nmol L^{-1})	0.15 ± 0.02	0.33 ± 0.06
TdCo*	-0.85 ± 0.03	-2.52 ± 0.24
TdNi concentrations (nmol L^{-1})	5.02 ± 0.49	4.67 ± 0.12
TdZn concentrations (nmol L^{-1})	14.68 ± 1.91	12.178 ± 0.59
TdCu concentrations (nmol L^{-1})	2.91 ± 0.16	8.13 ± 0.16

x ± y indicates mean ± standard deviation.

Table S3. BRT model characteristics and model performance measures of BRT models. Model performance measures were estimated from 103 observations using 30 model runs and 10-fold cross-validation and include the mean and standard deviations of the total deviance for saturated models, residual deviance, Pearson correlation coefficient (cv correlation), and the proportion of deviance. The proportion of deviance explained is comparable to an R^2 value in a regression. n indicates the number of explanatory variables in each model.

Model configuration	Fe model (n = 15)	TM model (n = 20)
	Model characteristics	
Learning rate	0.005	0.005
Tree complexity*	3	3
Bag fraction	0.5	0.5
	Model performance measures	
Total deviance	0.082	0.089
Mean residual deviance	0.068 ± 0.004	0.01 ± 0.01
CV correlation**	44.38 ± 5.32	50.09 ± 0.06
Proportion of total deviance explained (%)	77.52 ± 10.30	87.15 ± 7.15

**Tree complexity controls how many levels of interactions are fitted, learning rate determines the contribution of each new tree to the model and bag fraction specifies the proportion of data to be randomly selected while fitting each simple model i.e 0.5 means half the data was used to parametrize the model and the other half to evaluate it.*

***The CV correlation is the correlation between the testing and training data across all model runs*

Table S4. Certified and measured mean and standard deviation (std) of the standard Reference material for trace metals (CASS-6) in nmol L^{-1}. Reference material was run with pre-concentration alongside the samples.

Trace metal	Measured mean (nmol L^{-1})	Measured std (nmol L^{-1})	Certified mean (nmol L^{-1})	Certified std (nmol L^{-1})
Cadmium (Cd)	0,199	0,003	0,193	0,016
Iron (Fe)	27,988	0,151	27,934	2,149
Nickel (Ni)	6,880	0,400	7,122	0,682
Copper (Cu)	9,322	0,632	8,340	0,504
Zinc (Zn)	18,040	1,004	19,422	2,753
Cobalt (Co)	1,139	0,193	1,140	0,088

Chapter 4: Manuscript III

Major N sources in the HUS: Regulation of carbon and nitrate uptake

Assessing the influence of nitrate and light on nitrate and carbon uptake rates in the Humboldt Upwelling System off Peru

L. R. Kittu[1], M. Fernández-Méndez[1,2], A. J. Paul[1], U. Riebesell[1]

*In preparation for Limnology and Oceanography***

[1]Marine Biogeochemistry, GEOMAR Helmholtz Centre for Ocean Research Kiel, Düsternbrooker Weg 20, D-24105, Kiel, Germany
[2]Now at Alfred Wegner Institute Helmholtz Centre for Polar and Marine Research, Am Handelshafen 12, 27570, Bremerhaven

*Corresponding author: Leila Kittu (lkittu@geomar.de)

**Manuscript format in journal style

Abstract

In the Humboldt Upwelling System (HUS), where ambient nitrate concentrations are high but variable due to natural upwelling, the primary regulation of phytoplankton productivity is attributed to seasonal differences in light availability within the mixed layer depth. However, there is still limited comprehensive research from the region on the responses of phytoplankton communities to changing light and nutrient conditions. This knowledge gap makes it challenging to accurately parameterise phytoplankton responses in biogeochemical models aiming to estimate primary productivity and predict its response to climate-related changes in light and nitrate availability. To address this gap, we investigated the direct influence of varying light intensities and ambient nitrate concentrations on nitrate and carbon uptake rates at five stations in the HUS off Peru. The stations were carefully selected to represent a gradient in ambient nitrate concentrations ranging from low to high (2 – 14 μmol L^{-1}). At each station, we conducted incubations of natural phytoplankton communities from the Chlorophyll *a* (Chl *a*) maxima under a range of light conditions (0 to 750 μmol photons m^{-2} s^{-1}) for 24 hours. The incubations were supplemented with ^{15}N nitrate and ^{13}C carbon isotopes to measure nitrate uptake and corresponding carbon uptake at each light level. Across all stations, peak nitrate and carbon uptake rates across stations were observed at 30 – 40 % of incoming irradiance (228. 68 ± 25.57 μmol m^{-2} s^{-1}). At these optimal irradiances, nitrate uptake rates scaled positively with ambient nitrate concentration, while carbon uptake rates did not, indicating a decoupling of nitrate and carbon uptake in the phytoplankton community at certain stations. Notably, stations with lower nitrate concentrations and nitrate uptake rates, dominated by the mixotrophic dinoflagellate Akashiwo Sanguinea, showed higher carbon uptake rates compared to diatom-dominated stations with high nitrate concentrations and uptake rates. This finding suggests that regenerative nutrients may significantly enhance and sustain carbon uptake in a mixotrophic-dominated phytoplankton assemblage with low nitrate availability. Moreover, despite low Chl *a* concentrations at stations with low ambient nitrate concentrations, carbon uptake rates surpassed those stations with higher nitrate and Chl *a* concentrations. Correspondingly, C:N uptake ratios at these stations exceeded the Redfield ratio at these stations, pointing towards the influence of regenerated nutrients in sustaining carbon uptake at low nitrate conditions. Thus, this study demonstrates that carbon and nitrate uptake rates in the HUS cannot be simply predicted based on irradiance and chlorophyll concentrations, thereby adding complexity to the estimation and prediction of primary productivity in the region. Thus, we emphasize the need for further uptake experiments to explore the relationships between phytoplankton community structure, light and nutrient availability. This is instrumental to understanding the factors that underpin productivity in the HUS.

4.1 Introduction

Amongst the essential nutrients for primary productivity in the ocean, bioavailable nitrogen (N) is in limited supply relative to other nutrients, making it a crucial factor in regulating marine primary productivity in the global ocean (Bristow et al. 2017). Therefore, the supply of N to the surface sunlit zone, and the degree to which it is assimilated by phytoplankton determine both the primary productivity and composition of phytoplankton communities in the ocean. In the global ocean, the supply of N to phytoplankton is largely through the uptake of nitrate (NO_3^-) supplied from outside the euphotic zone by upwelling, diffusion or mixing. Thus nitrate is commonly used as an indicator of ecosystem productivity in the ocean (Dugdale and Goering 1967).

The Humboldt Upwelling System (HUS), is renowned as one of the most productive eastern boundary upwelling systems (Chavez and Messié 2009). The magnitude and spatial distribution of primary productivity and biomass in the region are strongly influenced by a combination of biological and physical processes. Seasonality in physical forcing determines the availability of nutrients and the average irradiance that phytoplankton are exposed to within the surface mixed layer (Thomas et al. 2009). These factors directly impact the physiology of phytoplankton cells, ultimately shaping the seasonality of primary production in the HUS (Pennington et al. 2006; Messié et al. 2009; Bouman et al. 2018). Consequently, the HUS exhibits a seasonal paradox. In austral summer, when upwelling intensity is weaker, nitrate concentrations are lower relative to winter months characterised by high upwelling intensity and nitrate concentrations. Yet austral summer is characterised by diatom-dominated phytoplankton blooms and higher autotrophic primary productivity relative to winter (Pennington et al. 2006; Messié and Chavez 2015). This summer productivity makes up the largest portion of the annual autotrophic production in the HUS (Chavez et al. 2008; Messié and Chavez 2015). Nevertheless, despite lower nitrate inputs from upwelling during austral summer, the concentrations remain favourable for phytoplankton growth (Barber and Chavez 1983). Hence, it is unlikely that phytoplankton productivity is primarily nitrate-limited during austral summer. This suggests that the relationship between ambient nitrate concentrations and phytoplankton productivity is not linear, and other factors may regulate primary productivity in the HUS. Thus further investigation is required to unravel the mechanisms underpinning this paradox.

The variability in mixed layer depth in the HUS is hypothesised to play a primary role in shaping phytoplankton community structure and productivity in the HUS (Echevin et al. 2008; Behrenfeld 2010; Messié and Chavez 2015). This is because the depth of the mixed layer determines the light conditions experienced by phytoplankton cells, controls the nutrient flux in and out of the euphotic zone and ultimately governs the availability of nutrients for phytoplankton growth (Echevin et al. 2008). It is hypothesized that, under stable water column conditions with reduced turbulence, an optimal mixed layer depth can provide the ideal

combination of light and nutrients for maximum phytoplankton growth and productivity (Bakun et al. 2015).

The rate of carbon uptake (photosynthesis) in phytoplankton is influenced by light irradiance and nutrient availability; with light-harvesting being a linear function of both factors. Therefore, to accurately estimate the productive potential of phytoplankton communities at any given time, it is essential to quantitatively assess the efficiency with which phytoplankton assemblages utilise light and nutrients to build biomass. Although the mechanisms for light regulation on nitrate uptake are poorly understood, the influence of irradiance on nitrate uptake by phytoplankton is assumed to be a saturation response (MacIsaac and Dugdale 1972). Yet responses of nitrate uptake to irradiance have yielded contrasting responses, confirming light dependence of nitrate uptake on one hand and a weak light dependence on another (Muggli and Smith 1993). Thus, complex interactions among environmental variables may influence non-linear responses of phytoplankton nitrogen utilisation to irradiance. The coupling of nitrate and carbon uptake in Redfield proportions has been instrumental in the use of nitrate concentrations as a proxy for primary productivity (Redfield 1958; Tyrrell 1999; Arrigo 2005). Nevertheless, the influence of regenerative nutrients and non-Redfield production poses challenges to the broad application of this coupling in predicting marine primary productivity in the HUS (Arrigo 2005; Franz et al. 2012a; b). As such deviations from the canonical Redfield production have been observed broadly in the ocean. For decades, photosynthesis (P)-irradiance (I) relationships curves (PI) have played a central role in models of phytoplankton growth and satellite-based estimates of primary productivity by describing the rate of photosynthesis (normalized to chlorophyll *a*) as a function of irradiance (Platt et al. 2017; 2018). By optimally calibrating the parameters of these curves to in-situ high-resolution observations of fluorescence and irradiance, the rate of primary productivity at a specific irradiance and chlorophyll concentration can be estimated (Jones et al. 2014). However, the limited datasets on phytoplankton responses to light and nutrients in the HUS currently restrict the application of ecological models and satellite-based tools for predicting and estimating primary productivity over large spatial scales in the region.

Although phytoplankton generally exhibit a common response pattern to light, the characteristics of this response can vary among different phytoplankton groups (Edwards et al. 2015, 2016). Thus, the parameters derived from PI relationship curves can be influenced by other environmental covariables (Platt et al. 1993), such as the composition of the phytoplankton community structure and their efficiency in nutrient uptake and utilization. The preconditioning light history of phytoplankton cells is also important in determining their maximum potential carbon uptake rate and the associated light intensity at which photosynthesis is no longer light-limited. This means that during the transitions to summer in the HUS when phytoplankton cells have been exposed to low light conditions characteristic of winter/spring, carbon uptake rates may be periodically enhanced compared to peak summer months characterized by high but stable light irradiances. Thus, differential carbon and nitrate uptake between seasons with varying light intensities can be expected to influence the overall

productivity of the system even when nitrate concentrations are optimal (Dugdale and Goering 1967; MacIsaac and Dugdale 1972).

All these factors suggest that the parameters extracted from PI curves in the HUS are dynamic and this flexibility needs to be represented in ecological and satellite-based models to accurately predict primary productivity. Currently, seasonal differences in phytoplankton carbon and nitrate uptake response to changes in light, nutrients and with respect to the phytoplankton community assemblage are largely uncharacterized in the HUS. This limits the accuracy of approaches based on PI relationships to estimate primary productivity in the region and predict its fate under climate-related changes in the environmental variables. Therefore, a detailed assessment of phytoplankton responses to variations in light, nutrients and phytoplankton community assemblage in the HUS is required to understand the flexibility of PI parameters in relation to environmental changes and optimize them for model applications (Westberry et al. 2008). To investigate these relationships, we conducted simultaneous ^{15}Nitrate and ^{13}Carbon incubations under a range of light intensities at five stations in the HUS, encompassing varying ambient nitrate concentrations and phytoplankton community assemblage from the Chlorophyll *a* maxima. Nitrate and carbon uptake rates were measured under simulated in situ light conditions in the euphotic zone to obtain a better understanding of the nitrate and carbon uptake response to light and their coupling at biogeochemically distinct stations. Photosynthetic pigment analysis allowed for an assessment of the phytoplankton functional groups constituting the photo autotrophic assemblage. Thus, our uptake rates represent maximum in situ nitrate and carbon uptake rates from the euphotic zone at each light level.

4.2 Methods

This study took place during the research cruise MSM80 on board R/V Marian S Merian from December – January 2018-2019. We collected seawater samples with natural phytoplankton communities at two central stations on 12°S (C1, C2) and three southern stations at 15°S (S1, S2, S3 along the Peruvian coast. The station selection considered the different environmental conditions between the central and the southern region covering a range of upwelling strengths, nitrate concentration and Chlorophyll a (Chl *a*) fluorescence (Table. 1). This enabled us to assess the role of these varying conditions on our response variables.

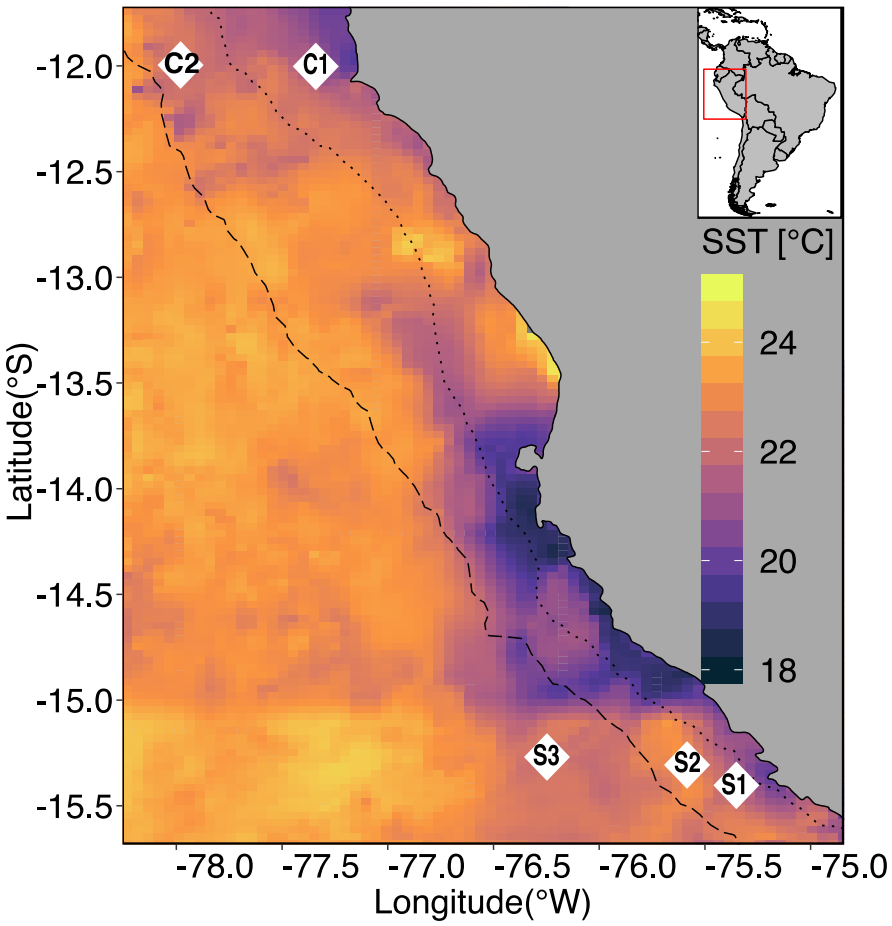

Fig. 1. Map of study area showing mean MODIS(NASA/JPL 2020) sea surface temperature (SST) in the study area overlain by sampled stations at the central (12°S) and southern transects (15°S). Black dotted and dashed lines show 200 and 2,000 m bathymetry to indicate the edge of the shelf and shelf slope, respectively.

4.2.1 Oceanographic Characterisation of sampling stations

At each station, depth profiles of temperature, salinity, dissolved oxygen (O_2), photosynthetically-active radiation (PAR) and Chl a fluorescence were taken. A Seabird (SBE-911 plus, Seabird-Electronics, USA) conductivity-temperature-depth (CTD) profiler equipped with double temperature (SBE 3) and O_2 sensors (SBE43), a LI-COR Bio spherical PAR sensor and a Wet Labs ECO-FLNTURTD chlorophyll-turbidity sensor were mounted on a 21×10 L Niskin bottle rosette water sampler from which discrete water samples were collected from desired depths for the incubations and for nutrient analyses. We selected the sampling depth for our incubations based on the depth of the respective chlorophyll *a* (Chl *a*) maxima at each station as indicated by the fluorescence profiles. Unfiltered samples for nitrate (NO_3^-), phosphate (PO_4^{3-}) and silicate ($Si(OH)_4$) were collected in triplicate and measured onboard using an autosampler (XY-2 autosampler, SEAL Analytical) and a continuous flow analyzer (QUAAtro Autoanalyzer, SEAL Analytical) according to Morris & Riley(1963).

Mixed layer depth (MLD) was determined from MSS vertical profiles. First, cross-validation between the MSS sensors and the CTD sensors was performed to derive the potential density anomaly profiles. The MLD was then defined as the depth where the potential density anomaly exceeds for the first time the average potential density anomaly of the water layer between the surface and the actual depth by 0.05 gkg^{-1}. Due to the vessel impact the stratification in the first five meters of the water column was disturbed. Thus, the minimum MLD was set to 5m even if the iterative MLD estimation revealed a shallower MLD. The euphotic zone was defined as the depth where Photosynthetic Active Radiation (PAR) was reduced to 1% of its surface value, calculated as outlined in Kittu et al. (2023).

4.2.2 ^{15}N-nitrate and ^{13}C uptake incubations

Nitrate and carbon uptake rates at each station with specific ambient nitrate concentration were obtained from samples collected at the Chl *a* max and incubated under a range of irradiances. For the incubation experiments, seawater samples from the Chl *a* max at each station were collected from the Niskin bottles into triplicate 1 L acid-cleaned (10% HCL) and Milli Q rinsed polycarbonate bottles. Nitrate and carbon uptake rate measurements were conducted using a dual stable isotope technique involving the addition of a ^{13}C and ^{15}N isotope in the same assay (Shiozaki et al. 2009). Uptake rates were determined from the incorporation of ^{13}C and ^{15}N isotopes into particulate organic matter (POM).

For nitrate uptake rates, 2.5 mg of ^{15}N potassium nitrate ($K^{15}NO_3$) was dissolved in 15 ml of Milli Q. 1 ml of this stock solution was then added to each 2 L incubation bottle to achieve isotope enrichment <12 atom % of ambient nitrate concentrations. Because nutrient concentrations were measured only after incubations were started, the enrichment of $^{15}NO_3$ at Station S3 exceeded 12 atom % (Dugdale and Wilkerson 1986) of the ambient nitrate concentrations (18.4 atom%). Such high enrichments of the available nitrate pool may artificially enhance uptake rates in tracer bioassays. However, considering the low nitrate uptake rates at station S3, there is little indication that our isotope addition stimulated substantial uptake.

For carbon uptake, a stock solution was prepared by dissolving 240 mg of ^{13}C sodium bicarbonate ($NaH^{13}CO_3$, 98 atom %, Sigma Aldrich-Merck KGAa, Darmstadt, Germany) into 10 ml of Milli Q. 500 µl of the stock solution was added to each replicate incubation bottle, roughly corresponding to 3-4 atom % enrichment.

After isotope addition to triplicate bottles, one bottle was immediately filtered for ambient particulate organic carbon/ nitrogen concentrations (POC/N) and, natural abundance isotopic composition (δ^{15}N and δ^{13}C). To obtain these measurements, seawater volumes of 0.5 – 1.5 L were gently filtered (200 mbar) through a pre-combusted (500°C for 6h), 0.3 µm pore size glass fibre filter (GF-75, Advantec, 25 mm Ø, 0.3 µm nominal pore size).

The remaining replicate bottles were incubated for 24 h under different light conditions in on-deck incubators with surface seawater continuous flow to maintain constant seawater temperature. To simulate variable incoming irradiance, incubators were shaded with neutral density screening to reproduce light conditions at 100%, 405, 30%, 15%, 5%, and 0% of incoming irradiance (Lagoon blue neutral density light screens, Lee light filters). Since the Chl a max was shallower than the euphotic zone, our samples represent maximum nitrate and carbon uptake rates from the euphotic zone at each light level (Table 1). Incubations were terminated by gently filtering samples (200 mbar, volume range 0.2 – 1 L) onto 0.3 µm pre-combusted GF/75 filters (Advantec, 25 mm Ø, 0.3 µm nominal pore size).

After filtration, all filters (natural abundance and incubation filters) were acidified with 1M HCL for 2 minutes to remove inorganic carbon before being packed in 2ml cryovials and frozen (-20°C) for storage and transported to the laboratory in Kiel, Germany. In the laboratory, filters were thawed and oven-dried overnight at 60°C, encapsulated in tin capsules, and pelleted for further mass spectrometry analysis (mass detection limit, 15 µg of N). All filters were analysed for particulate (POC/N) and isotopic N and C composition ($\delta^{13}C_{POC}/\delta^{15}N_{PON}$) on an elemental analyzer (Flash EA, ThermoFisher) connected to a mass spectrometer (Delta V Advantage Isotope Ratio MS, ThermoFisher) with the ConFlo IV interface (ThermoFisher).

4.2.3 Nitrate and Carbon uptake rate calculations

To get a precise measure of nitrate uptake related to the phytoplankton community but independent of biomass, we calculated the absolute nitrogen uptake (p_{15N}, µmol N L^{-1} d^{-1}). This depicts the total amount of nitrate taken up by a phytoplankton community without considering the biomass. As shown in Equation 1 below, p_{15N} was achieved by multiplying the PON-specific nitrate uptake rates (V_{15N}) with the average of the PON (natural abundance and final) as recommended by Dugdale and Wilkerson. (1986).

$$\text{Absolute nitrate uptake rate } (\rho_{\mathbf{15N}}) = V_{\mathbf{15N}} \times \left[\bar{x}(PON^{(t = f \,\&\, 0)})\right] \quad (1)$$

Whereby $PON^{t=f/0}$ is the PON concentration of samples after incubation (t = f) or the natural abundance samples (t=0). Δt represents the incubation period.

The specific uptake rate V_{15N} (N d^{-1}) is a biomass-dependent metric interpreted as the unit of N taken up per unit particulate N. This rate provides a measure of the efficiency of nitrate uptake relative to the biomass (PON) of the phytoplankton community. V_{15N} was calculated as the average ($\bar{x}$) of the specific uptake rate considering the initial (natural abundance) and final (after incubation) isotopic abundance (^{15}N atom %) of PON as shown in Equation 2 below

$$\text{PON-specific uptake rate } (V_{\mathbf{15N}}) = \bar{x}\frac{A_{PON(exs)}}{A_{\mathbf{tot}} - A_{PON}^{t = f/0} \times \Delta t} \quad (2)$$

Whereby $A_{PON(exs)}$ represents the ^{15}N atom % excess enrichment of the samples calculated by subtracting the natural abundance ^{15}N atom % ($A_{PON}^{t=0}$) from the final ^{15}N atom % of the filter after incubation ($A_{PON}^{t=f}$). A_{tot} is the ^{15}N atom % of the dissolved nitrate pool available in the incubation (ambient + added).

^{13}C uptake rates (hereafter carbon uptake rates, µmol C L^{-1} d^{-1}), were calculated according to Slawyk et al(1977) as shown in Equation n 3 below

$$^{13}C \text{ uptake rate } (\rho_{13C}) = \frac{A_{POC}^{t=f} - A_{POC}^{t=0}}{DIC_{\mathbf{tot}} - A_{POC}^{t=0}} \times \frac{[POC]}{\Delta t} \quad 3$$

Whereby A_{POC} represents the ^{13}C atom % of POC in the natural abundance samples ($\mathbf{t = 0}$) and enriched samples after incubation (t = f). $\mathbf{DIC_{tot}}$ represents the ^{13}C atom % of the total DIC amount in the incubation bottle taking into consideration the naturally available fraction of ^{1}DIC and the additional ^{13}C isotope added for enrichment. For this study, a constant value of 2166 µmol L^{-1} was used for all incubations as the ambient concentration of DIC, which is representative of the region based on a previous study (Fernández et al. 2009).

To account for the effects of variable Chl *a* concentration at the different stations, absolute nitrate and carbon uptake rates were normalised to Chl *a* from each sampled depth. Hence nitrate and carbon uptake rates are reported as µmol N (µg Chl a)$^{-1}$ L^{-1} d^{-1} and µmol C (µg Chl *a*)$^{-1}$ L^{-1} d^{-1}) respectively. Normalising the uptake rates to Chl *a* biomass provides a standardised way to compare the efficiency of nitrate and carbon uptake across the different stations and is relevant for use in ecological model parameterisations.

4.2.4 Pigment concentrations

For High-Performance Liquid Chromatography (HPLC) pigment analysis, samples were obtained by gently filtering 1 – 2 L of seawater through GF/75 filters (200 mbar, Advantec, 25 mm Ø, 0.3 µm nominal pore size). The filtered volume ranged from 0.5 – 1.5 L depending on the productivity of the station. Precautions were taken to minimise exposure of samples to light by using foil to cover filtration bottles. Filters were shock frozen in liquid nitrogen and stored in cryovials at -80°C until analysis.

In the laboratory, pigments were extracted in a homogenizer (Precellys, Montigny-le-Bretonneux, France) by mixing filters with glass beads and 100% HPLC grade acetone (Baker 8142, Avantor, Radnor, PA, United States). Extracted samples were then centrifuged (10 min, 4◦C, 5200 rpm), the supernatant removed with a syringe and filtered through Teflon filters (0.2 µm pore size). Photosynthetic pigments were analyzed through reverse-phase high-performance liquid chromatography on a HPLC Ultimate 3.000 analyzer with an Eclipse XDB-C8 3.5 u 4.6 × 150 column (Thermo Scientific Waltham, MA, USA). The total Chl *a* concentration was computed as the sum of Chl-a and divinyl Chl-a (dyv-Chl-*a*) as Prochlorococcus contains only dyv-Chl-*a* as its primary light-harvesting pigment.

With the CHEMTAX program v 1.95, HPLC concentrations were used to determine the phytoplankton community composition based on taxa-specific pigment ratios of phytoplankton (Mackey et al. 1998). By calculating the ratios between taxa-specific pigments and total Chl *a* [μg L^{-1}], we determined the individual contribution of 9 taxa to the total Chl *a* (diatoms, dinoflagellates, cryptophytes, pelagophytes, haptophytes (e.g., coccolithophorids and Phaeocystis), prasinophytes, chlorophytes, Synechococcus and Prochlorococcus). Pigment ratios were obtained from a previous study conducted in the ETSP (Meyer et al. 2017).

4.2.5 Statistical analysis

All results are reported as the mean of triplicate experiments ± SD. To analyze the influence of interacting irradiance and nitrate concentrations on nitrate and carbon uptake rates and C:N uptake ratios, 3D scatter plots were generated in R. A General Additive Model (GAM) with a smooth thin-plate spline interpolation was applied to the dataset to fit the 3D surface on the data points. A Spearman's rank correlation analysis was used to examine the potential relationships between nitrate uptake and carbon uptake rates and physical, biogeochemical variables. All statistical analyses were conducted using R (Version 4.0.3, packages stats, ggplot2; The R Foundation).

4.3 Results

4.3.1 Physical and biogeochemical conditions

Our study was performed at 5 stations across 2 transects in the Northern Humboldt Upwelling System (HUS) that showed a range in nutrient concentrations (Table. 1) and phytoplankton community composition (Fig. 5). Stations C1 and C2 were located in coastal waters along the 12°S transect which was considered as a transition zone for the Peruvian region with regard to physical and biogeochemical conditions present at the time of this cruise (Kittu et al. 2023). In contrast, Stations S1, S2 and S3 were located at 15°S located within coastal to offshore waters (station S3). With general SSTs ranging between 20 – 24°S, higher SSTs were observed in the northern part (22°S – 24°S) relative to the southern region of the HUS (20 -22°S). However, the lowest temperatures at sampled depths were observed at Station C1 closest to the coast at 12°S (Supplementary Fig. S1a). Within the euphotic zone where all the samples for the experiments were collected from, the water column was well-ventilated with oxygen levels >180 μmol L^{-1} (except for station C2 where oxygen concentrations were below 50 μmol L^{-1} (Supplementary Fig. S1b).

During our study, the euphotic zone depth at 12°S and 15°S was relatively similar ranging between 26 – 35 m and averaging at 30.5 ± 6.4 m and 27.00 ± 6.08 m respectively (Table 1, Supplementary Fig. S1). The mixed layer depth (MLD) was generally shallow ranging between 6.5 and 8 m and often below the depth of Chl *a* maxima for all stations (5m) except for station S2 (12m), (Table 1, Supplementary Fig. S1).

Nitrate profiles indicated lower concentrations within the euphotic zone and an increase with depth (Supplementary Fig. S1d). However, at the Chl *a* max where samples were collected (Table 1), nitrate concentrations were lower at stations that were further away from the coast (C2, S3) than closer to the coast where nitrate concentrations were highest (C1 and S3). Nitrate concentrations within the samples collected for the experiment ranged from 2.66 – 13.90 μmol L^{-1}. Taken together, low in situ temperatures and oxygen concentrations and high nitrate concentrations, observed from Station C1 (Supplementary Fig S1a, b,d), a station closest to the coast at 12°S reveal that the waters were freshly upwelled relative to old waters at station C2 where in-situ temperatures and salinity were high and nitrate concentrations were low (Supplementary Fig S1a,c).

Table 1: Environmental data for the experimental stations

Station	**C1**	**C2**	**S2**	**S1**	**S3**
Latitude	12°S		15.3°S		
Description	Coastal	Coastal	Coastal	Coastal	Offshore
Euphotic zone (m)	26	35	31	30	20
Thermocline (m)	32	30	27	14	12
Mixed Layer Depth (MLD)	8	7	6.5	7.5	7
Sampling depth (Chl *a* max) (m)	5	5	12	5	5
Chl *a* (μg/l)	22.93	2.53	20.8	3.57	17.19
Nitrate concentration (umol/l)	13.90	4.04	9.18	6.82	2.66
Phosphate concentration	1.36	0.47	1.26	1.10	1.33
Silicate concentration	7.78	1.82	3.42	2.56	3.98

4.3.2 Nitrate uptake

Across all stations, the highest nitrate uptake rates were observed at an optimum average irradiance of 228. 68 ± 25.57 μmol m^{-2} s^{-1}, corresponding to 30 – 40% of incoming irradiance. Nitrate uptake at the most coastal stations, C1 and S1 peaked at 30% of incoming irradiance corresponding to 203.34 ± 16.23 μmol m^{-2} s^{-1}, Fig. 2a). At C1, the station with the highest nitrate concentrations, significantly higher nitrate uptake rates (to 0.5 μmol N (μg Chl a)$^{-1}$ L^{-1} d^{-1}) relative to the other stations were observed at suboptimal light irradiances(~ 150 μmol m^{-2} s^{-1}). Further away from the coast but still in coastal waters, at stations C2 and S2, the nitrate uptake rates peaked at 40 and 100 % incoming irradiance respectively corresponding to 240.78 μmol m^{-2} s^{-1} and 512.60 μmol m^{-2} s^{-1} respectively. At stations, C2 and S1, nitrate uptake declined towards zero at maximum irradiances (600 μmol m^{-2} s^{-1}). Corresponding to the lowest nitrate concentrations nitrate uptake rates were lowest at the most offshore station along 15°S (station S3) and did not respond to light variability despite high Chl *a* concentrations measured from this station (Table 1).

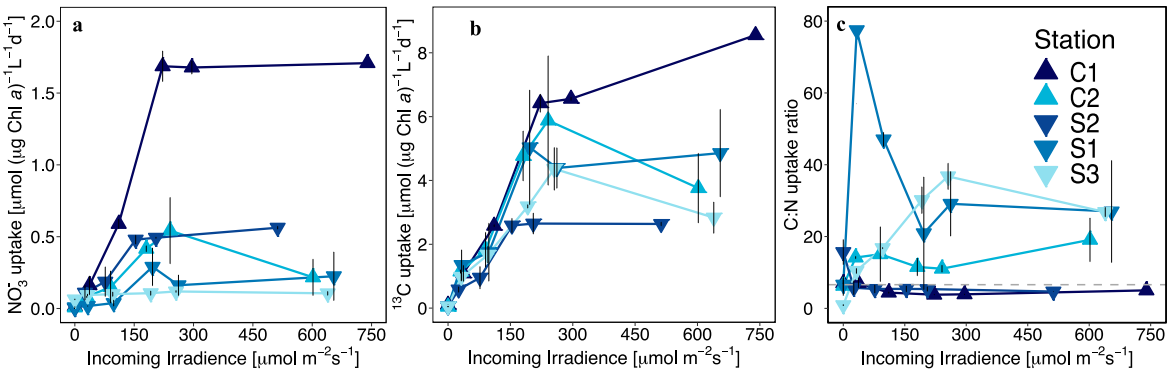

Fig. 2. Influence of light intensity on the rate of Chl *a* normalised (a) nitrate uptake, (b) carbon uptake and (c) carbon: nitrogen uptake (C:N) ratio at each station. Black vertical lines indicate positive and negative standard deviation around the mean of three triplicate measurements. The dashed horizontal line in panel (c) indicates the Redfield ratio (6.6). The gradient of blue indicates increasing ambient nitrate concentrations.

4.3.3 Carbon uptake

Carbon uptake rates generally increased exponentially with increasing incoming irradiance at all stations peaking at 30 - 40% of incoming irradiance (200 – 250 μmol m^{-2} s^{-1}, Fig. 2b). At this optimum irradiance levels, carbon uptake rates between stations did not scale with nitrate concentrations. All stations except for Station S2 (high nitrate, high chl a) had carbon uptake rates above 4 μmol C (μg Chl *a*)$^{-1}$ L^{-1} d^{-1} at the optimum irradiance levels. The lowest carbon uptake rates at these optimum irradiances were observed from Station S2 (2.60 μmol C (μg Chl *a*)$^{-1}$ L^{-1} d^{-1}). Additionally, despite this station having high ambient nitrate concentrations (Table. 1), carbon uptake remained stable at higher incoming irradiance (Fig. 2b). Similar to

nitrate uptake, the highest carbon uptake rates were at the station with the highest nitrate concentrations. observed from Station. Beyond 40% of incoming irradiance, photoinhibition, in carbon uptake rates was observed at stations C2 and S3, the stations where ambient nitrate concentrations were below 5 μmol L^{-1} (Fig. 3). However, at 100 % (600 -700 μmol m^{-2} s^{-1}), an increase in carbon uptake was observed at the most coastal stations C1 and S1 (Fig. 2c, 3).

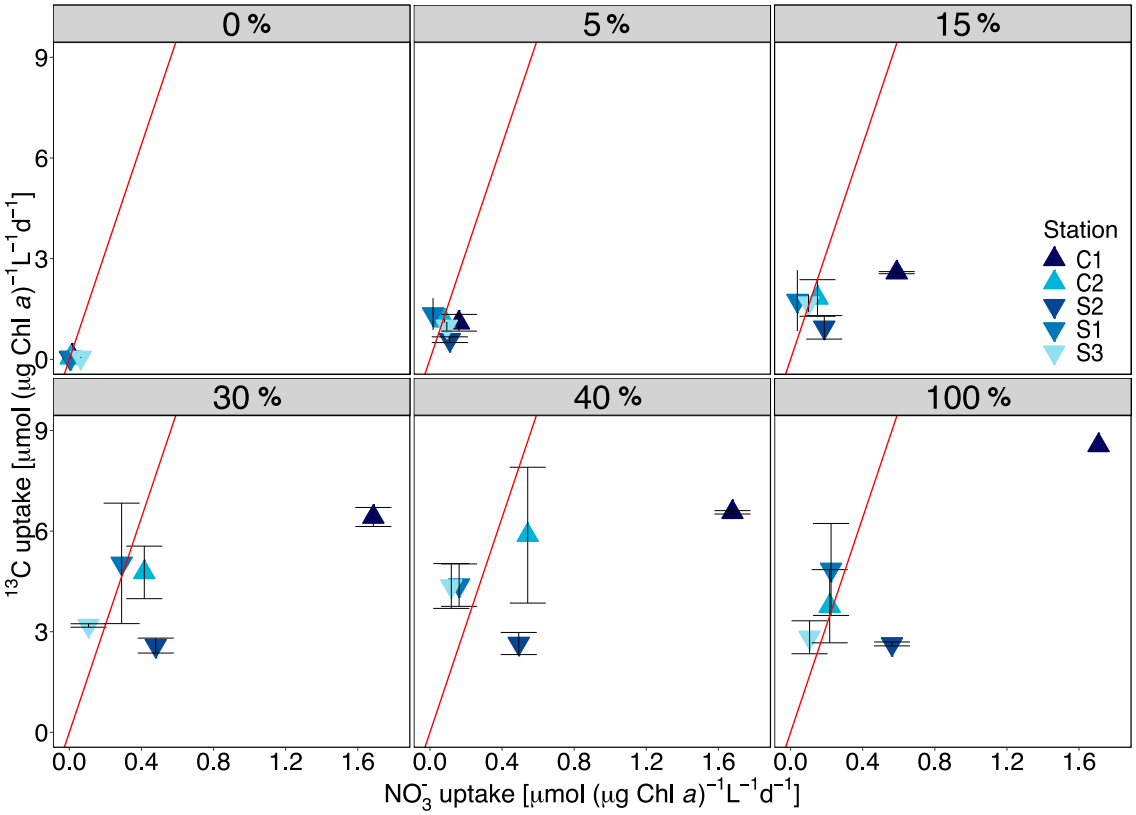

Fig. 3. Linear regression plots of Chl *a* normalised carbon uptake rates and nitrate uptake rates at each incoming irradiance (shown at the top). Black vertical lines indicate positive and negative standard deviations of the mean of triplicate carbon uptake measurements. The red line indicates the Redfield C:N ratio (6.6). Stations above and below this line at each light irradiance indicate a decoupling between carbon and nitrate uptake rates.

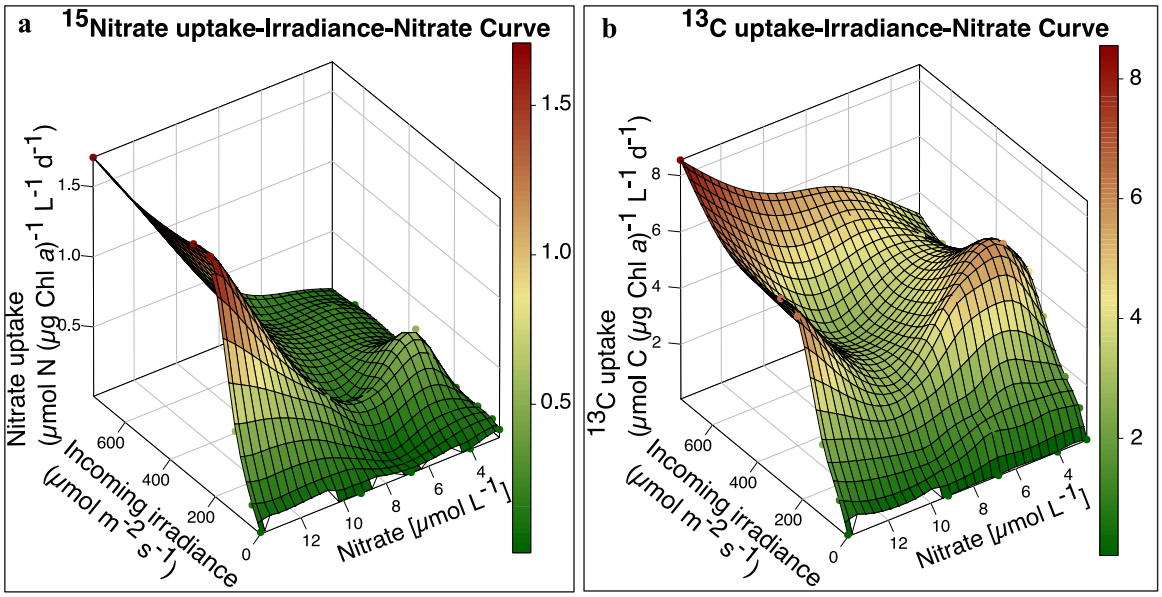

Fig. 4. 3D surface scatter plot of the relationships between nitrate and carbon uptake with light and ambient nitrate concentrations across the five sampled stations. The surface was created by applying a GAM with a smooth thin-plate spline interpolation on the data points to predict the pattern.

4.3.4 Phytoplankton community composition

In three out of the five stations sampled (stations C1, S1 and S3), diatoms had the highest contribution to the total phytoplankton assemblage, dominating > 50% of the phytoplankton community. At 12°S, the most coastal station (Station C1) was mainly dominated by diatoms, while away from the coast (Station C2), a more diverse community consisting mainly of Synechococcus and Haptophytes followed by Cryophytes was observed. Further South at 15°S, a mixed phytoplankton community dominated by diatoms, Cryophytes and some Haptophytes was present at stations S1 and S3. At both coastal stations at 15°S (stations S1 and S2), the mixotrophic dinoflagellate Akashiwo Sanguinea was observed (confirmed by microscopy), primarily dominating Station S2 (Fig. 5).

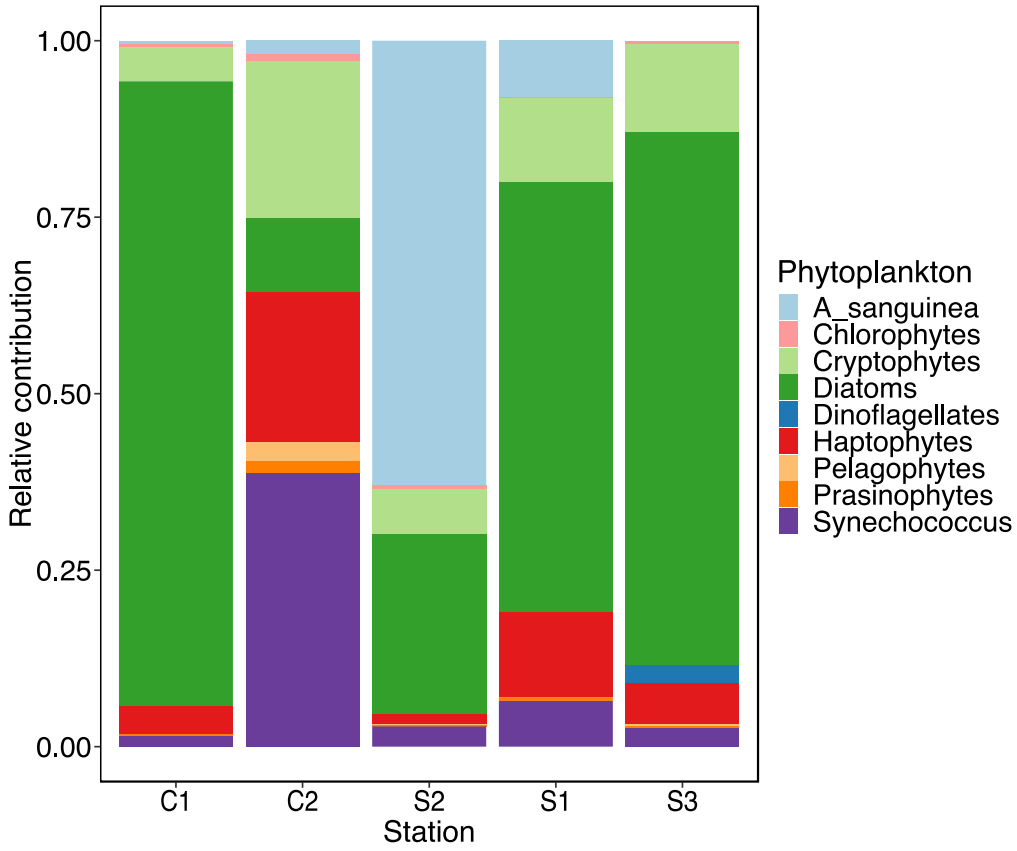

Fig. 5. Phytoplankton community assemblage. The relative contribution of different phytoplankton groups and species to total Chla concentration based on Chemtax analysis of phytoplankton pigments (HPLC).

4.4 Discussion

The primary focus of our work was to investigate the effects of light and nitrate concentrations on nitrate and carbon uptake rates from a bulk phytoplankton community in the productive HUS off Peru. With this in mind, the stations considered herein covered a wide range of phytoplankton community assemblage and productivity (Chl *a* concentrations), and nutrient concentrations (Table 1). ^{13}Carbon uptake rates are considered herein as a measurement of phytoplankton productivity but in order to distinguish the biomass-driven aerial primary productivity from the actual productivity of the individual cells, we normalized the carbon uptake rates by Chl *a* as a proxy of photosynthetic biomass. Our results show that irrespective of differences in phytoplankton community assemblage, Chl *a* and PON concentrations, nitrate uptake and corresponding carbon uptake rates resembled a Michaelis-Menten response pattern to light intensity. Notable differences in nitrate and carbon uptake rates and the potential for nitrate, light and other nutrients limiting phytoplankton productivity during our study were observed between the stations. We discuss the implications of the observed effects for estimating primary productivity in the HUS.

4.4.1 Regulation of nitrate uptake rates by light and nitrate concentrations in the HUS

In field studies, the influence of light is often masked by other factors that control phytoplankton productivity such as cell abundance and environmental preconditioning. These factors largely contribute to differences in baseline rates during experiments. Thus normalising uptake rates to Chl *a* biomass allows for comparisons across steep gradients of Chl *a* to be made. Our Chl *a* normalised nitrate and carbon uptake rates indicate that the optimum light level where maximum nitrate and carbon uptake rates were realised was similar across all stations (228. 68 ± 25.57 μmol m^{-2} s^{-1} equivalent to 30 – 40% of incoming irradiance), except for Station S2 where nitrate uptake did not respond to light irradiance. We consider this irradiance range optimal for the phytoplankton community across the study region. It is widely accepted that nitrate concentrations primarily regulate nitrate uptake rates in the ocean. We observed that maximum nitrate uptake rates at optimum irradiance across all stations scaled with nitrate concentrations (Fig 2a, 4a), thus confirming the direct role of nitrate concentrations in regulating phytoplankton nitrate uptake. This proportionality in nitrate uptake rates to nitrate concentrations probably reflects the differences in both phytoplankton species composition (Fig. 5) and the physiological state of the phytoplankton community at variable N conditions (Table. 1). Thus our results indicate that despite the differences in phytoplankton biomass and assemblage between stations (Fig. 5) the phytoplankton physiological capacity for maximum nitrate uptake at optimal irradiances was largely regulated by ambient nitrate concentrations.

The direct mechanisms by which light regulates nitrate metabolism in phytoplankton are considered species-specific. Nitrate uptake is known to be dependent on light as an energy source, either directly or indirectly through photosynthesis due to the presence of nitrate-activated ATPase in some marine phytoplankton (Cochlan et al. 1991). This provides a physiological basis for coupling light and nitrate uptake, whereby the energy (ATP) generated from photophosphorylation is required for the functioning of uptake enzymes. Previous studies have shown that under replete nutrients and treating light intensity as a substrate following Michaelis-Menten kinetics, nitrate uptake by natural phytoplankton assemblages show a rectangular hyperbola response to light intensity (MacIsaac and Dugdale 1972). Such a relationship assumes no nitrate uptake at 0 light intensity followed by an exponential increase peaking at optimum light irradiance and a plateau at high light irradiances beyond the optimum range. Based on the negligible nitrate uptake rates observed at 0 incoming irradiances (< 0.06 μmol N (μg Chl a)$^{-1}$ L^{-1}, Fig. 2a), we interpret this as the absence of dark nitrate uptake during our study, but consider the impact of suboptimal light irradiances on nitrate uptake rates.

At nitrate concentrations below 10 μmol L^{-1}, nitrate uptake rates were low and indistinguishable by stations (nitrate concentrations) when light levels were suboptimal (<100 μmol m^{-2} s^{-1}). The similarity in low Chl *a* normalised nitrate uptake rates at low irradiance across

stations with low varying nitrate concentrations suggests that a degree of light limitation influences the regulation of nitrate uptake (Fig. 4a). On the other hand, at station C1, where nitrate concentrations were highest (13.9 μmol L^{-1}), nitrate uptake was significantly and distinctly enhanced at suboptimal incoming irradiance (15% of incoming irradiance, ~100 μmol m^{-2} s^{-1}) relative to all other stations. This, suggests that under high nitrate conditions, significant nitrate uptake can still take place at light irradiance below the optimum range. Our results imply that during periods of deep vertical mixing such as in winter months when the mixed layer depth can be much deeper and nitrate concentrations are high and relatively homogeneous due to intense upwelling, phytoplankton can still take up nitrate despite lower irradiance relative to summer (Wilkerson and Dugdale 1987). Comparable studies under low irradiance such as during winter months are thus required to verify these results. This observation can also be expected when nitrate-limited phytoplankton near or below the bottom of the euphotic zone receives an upwelling pulse of nitrate as has been observed in the Central North Pacific (Kiefer et al. 1976). Nevertheless, these uptake rates are lower than the potential maximum nitrate rates that could be achieved at optimal irradiance levels, indicating the interaction of light and nutrients for maximum nitrate uptake. Additionally, it is still not certain whether the assimilated nitrate under low light irradiances can be utilised efficiently by phytoplankton to influence growth and productivity at these suboptimal irradiances. Under low-light and high nutrient conditions of surface waters in upwelling areas, nitrite excretion is linked to ~60 % of phytoplankton nitrate uptake due to incomplete nitrate assimilation thus leading to the development of a nitrite maxima (Kiefer et al. 1976; Collos 1998). Additionally, the release of dissolved organic nitrogen (DON) by phytoplankton is coupled to nitrate uptake (Hu and Smith 1998; Bronk 2002). Thus such phenomena could result in a bias of nitrate-based new production estimates using the ^{15}N tracer technique (where N is assimilated in the particulate matter) due to the loss of the ^{15}N tracer in nitrite and DON during incubation. Hence such experiments parameterising nitrate uptake to light would require nitrite and DON to be accounted for in incubations. Whilst we cannot assess these dynamics using this dataset, they should be considered especially when estimating net nitrate uptake in the HUS between seasons with varying light, and nitrate concentrations.

Following the Michaelis-Menten kinetics, it is expected that nitrate uptake would be maintained at high light intensities considering ambient nitrate concentrations are non-limiting (MacIsaac and Dugdale 1972). Contrary to this expectation, we observed that beyond the optimum range of irradiance (600 – 700 μmol m^{-2} s^{-1}, 100 % incoming irradiance), nitrate uptake rates declined at stations C2 and S1 where nitrate (< 7 μmol L^{-1}), and Chl *a* concentrations (< 4 μg L^{-1}) were low (Fig. 2a, 4a). Such as response is common in oligotrophic regions (MacIsaac and Dugdale 1972). Nonetheless, at stations C1 and S2 where nitrate (>9 μmol L^{-1}), and Chl *a* concentrations (> 20 μg L^{-1}) were high, nitrate uptake rates did not decline but demonstrated a rectangular hyperbola behaviour (Fig. 2a). These observations indicate that the capacity of phytoplankton communities to maintain high nitrate uptake rates at higher light irradiances is largely regulated by a combination of nitrate and Chl *a* concentrations. (Fig

2a, 4a). Thus we hypothesise that beyond the optimum irradiance range, either nitrate concentrations were limiting at low nitrate stations or that photoinhibition of nitrate uptake is more prevalent under low nitrate and Chl *a* conditions. Unfortunately due to the paucity of data at higher light irradiances in our study, we cannot adequately discuss photoinhibition of nitrate uptake from this study. Nevertheless, it appears that nitrate concentrations were a limiting factor at these stations and it suffices to say that nitrate uptake at lower Chl *a* and nitrate concentrations is regulated at least to a significant degree by both light and nitrate concentrations. This observed response of nitrate uptake to light resembles the well-known occurrence of light inhibition of photosynthesis. Thus nitrate uptake decline at higher light irradiances quite normally suggests itself as an explanation for the failure of nitrate uptake in the HUS to respond to increasing light under low nitrate conditions. Under oligotrophic conditions, nitrate uptake has also been suggested to be limited by other factors such as a second critical macronutrient or micronutrient such as iron (Dugdale and Goering 1967; Dugdale 1972; Hutchins et al. 2002; Bruland et al. 2005). Station C2 and S1 were observed to have the lowest silicate and phosphate concentrations suggesting as well potential colimitation of nitrate uptake rates by other macronutrients.

Our results demonstrate that the uptake of nitrate in the HUS reflects the role of light, nutrient and phytoplankton biomass conditions, indicating that profiles of uptake should be analysed in terms of the interacting influences of these variables. This highlights the importance of photosynthesis-Irradiance-nutrient (PIN) curves to identify and interpret basic patterns of uptake profiles rather than their exact prediction. Generally, predicting these responses in the HUS would require more data than available in this study.

4.4.2 Relating phytoplankton community Structure to uptake dynamics

The stations investigated herein indicate a degree of spatial heterogeneity in the phytoplankton community assemblage and give insights into its role in regulating nitrate and carbon uptake rates. At both transects, the phytoplankton community at coastal stations was typical for the coastal Peruvian region, reflecting a stronger dominance of diatoms (Fig. 5), (Franz et al. 2012b; Bach et al. 2020). Stations further away from the coast were characterised by a more diverse phytoplankton assemblage consisting of *Synechococcus* and to a lesser extent the presence of cryophytes and haptophytes (C2 and S3). Exceptions to these patterns were however observed at Station S2, where the phytoplankton assemblage was dominated by the mixotrophic dinoflagellate *Akashiwo Sanguinea*. This dinoflagellate was also present but less dominant at stations C2 and S2 (Fig. 5).

Such heterogeneity in this region can be ascribed to dynamic upwelling and relaxation events at the coast, characterised by Ekman transport of coastal waters offshore (Kämpf and Chapman 2016). The low nitrate and high Chl *a* concentration, at Station S3, is characteristic of advected coastal waters dominated by a dying bloom of diatoms, as is indicated by a lack of response in

nitrate uptake rates across all light intensities (Fig. 2a, 5). It is important to mention that station S3 was not a coastal station, suggesting a likelihood of ageing coastal post-upwelling waters, low in nitrate and high in Chl *a* concentration advected offshore. Whereas Station C2 was characterised by warmer, more saline (due to evaporation) waters advected away from the coast. At this station, the low Chl *a* and nutrient concentrations and the dominance of a post-bloom phytoplankton community dominated by *Synechococcus* and haptophytes relative to diatoms demonstrate a succession of the phytoplankton community structure typical for the Peruvian upwelling system (Fawcett and Ward 2011; Franz et al. 2012b; Paul et al. 2022). Both stations (C2 and S3) were characterised by high phytoplankton diversity but differed in the dominant phytoplankton community (Fig. 5). Nonetheless, carbon uptake rates at these stations were enhanced with increasing irradiance despite lower nitrate concentrations and relatively lower Chl *a* concentrations at Station C2 (Fig. 3, 4b). Thus despite a non-diatom dominated phytoplankton community and low Chl *a* concentrations at Station C2, high carbon uptake rates comparable to those under higher nitrate conditions were realised. While diatoms are known to contribute disproportionately to primary production in upwelling systems (Kudela and Dugdale 2000; Fawcett and Ward 2011), our results indicate that other phytoplankton groups encompassed in a diverse assemblage may perhaps contribute equally to primary productivity even when nitrate and Chl *a* concentrations are lower. Based on our results, primary productivity would likely be overestimated at station S2 characterised by high nitrate and high Chl *a* concentrations, while being underestimated at Station C2 where both Chl *a* and nitrate conditions were lower just by upscaling Chl *a* measurements to productivity. These results highlight the complexity of using fluorescence measurements and light to estimate primary productivity in the HUS.

At maximum irradiances beyond the optimum range, carbon uptake rates were photo-inhibited only at the stations with the lowest ambient nitrate, indicating the potential for photo-inhibition of carbon uptake in phytoplankton under low nitrate conditions <5 μmol L^{-1}. These results indicate that despite the important role of light, nutrient concentrations may set the limit of maximum carbon and nitrate uptake rates and hence primary productivity. This interpretation is supported by increasing nitrate and carbon uptake rates at maximum irradiance at stations where nitrate concentrations were high (> 6 μmol L^{-1}, stations C1 S1, and S3, Fig. 2, Supplementary Fig. S2). At these stations, neither photoinhibition of nitrate nor carbon uptake was observed (Fig. 2a,b), indicating that high nutrient concentrations can buffer the onset of photoinhibition for nitrate and carbon uptake rates in upwelling waters. At high nitrate conditions, saturating nitrate and carbon uptake rates are much higher relative to low nitrate conditions (Fig. 4, Supplementary Fig. S2). These differences in uptake patterns at maximum irradiance indicate that during summer months, phytoplankton can increase their productivity at high irradiances as long as nitrate is not limiting. Thus, our results emphasise the interacting role of irradiance and nitrate concentrations in enhancing phytoplankton productivity in nutrient-rich waters of the HUS.

4.4.3 Carbon uptake rates are decoupled from nitrate uptake rates evidence for the influence of other nitrogen sources.

Our results demonstrate that the capacity for primary productivity rates (carbon uptake) to reach values characteristic of coastal high-productive systems is weakly correlated with the availability of nitrate and nitrate uptake rates (Fig. 4b). We observed that despite low nitrate uptake rates at suboptimal light irradiances (S1, S2, S3), the response in carbon uptake rates scaled with light intensity at all stations. Additionally, similar carbon uptake rates at suboptimal light intensities despite very low nitrate uptake rates were observed at all stations. Thus, this reflects a basic similarity in the phytoplankton's carbon uptake capacities at suboptimal irradiances irrespective of differences in prevailing nitrate concentrations and phytoplankton community assemblage. Corresponding to these patterns, C:N uptake ratios at stations S1, S2, and S3 were above the Redfield ratio of 6.6 (10 - 77) at all light levels. Thus our results suggest a decoupling between carbon and nitrate uptake rates at low nitrate concentrations (2.66 – 6.82 μmol L^{-1}). Decoupled carbon and nitrate uptake rates were most evident at Station S3, where nitrate uptake rates at all light levels ranged from 0 to 0.1 μmol N (μg Chl a)$^{-1}$ L^{-1}, yet carbon uptake rates exhibited a strong response to light. These observations were in sharp contrast to stations with high nitrate and high Chl *a* concentrations (C1 and S2), where observed C:N uptake ratios were below or close to Redfield (Fig. 2d, 3) at all light irradiances. Notably, despite similar nitrate uptake rates at optimum irradiances between Station S2 and S1, carbon uptake rates at Station S1 were three-fold higher. Perhaps this difference may be explained by the difference in the dominant phytoplankton community at these stations. From optimum to high irradiances, all stations dominated by diatoms exhibited higher carbon uptake rates than the station dominated by *Akashiwo sanguinea.*

Our results demonstrate that the variability in maximum nitrate and carbon uptake between stations is not simply described by the interacting influences of light and nitrate concentrations. Carbon and nitrate uptake were both limited by low nitrate concentrations during our study but not in the same way across stations. It may be assumed that generally, an inadequate supply of other nutrients imposes considerable physiological variability in the phytoplankton assemblage. Additionally, the diversity of the phytoplankton community encompassing mixotrophic phytoplankton seems to have played a role in modulating the different responses in nitrate and carbon uptake between the stations.

The high carbon uptake rates corresponding to low nitrate uptake rates at Station S3 bring insight into the potential influence of regenerated nitrogen sources in supporting phytoplankton carbon uptake and productivity. Additionally, the positive response of carbon uptake rates to increasing light intensity, despite low nitrate concentrations suggests a role for irradiance in the uptake of these regenerative nitrogen sources. Conversely, it is also plausible that nitrate may have been internally stored in phytoplankton cells and not detected in nutrient measurements where samples were pre-filtered (Bode et al. 1997). Thus, the

phytoplankton community was capable of unproportionally high carbon uptake rates relative to nitrate concentrations and nitrate uptake rates.

Other nitrogen sources that might have been relevant in our study area could include dissolved inorganic nitrogen such as ammonium and DON compounds like urea which are also known to play a large role as an N source for phytoplankton (Berman and Bronk 2003). In open ocean surface waters, dissolved organic nitrogen, mostly originating from exudation by phytoplankton blooms make up 83% of the composition of nitrogen pools (Berman and Bronk 2003). At high light intensities, DON can be photochemically broken down to generate bioavailable N such as ammonium and nitrite which can be directly assimilated by phytoplankton (Bronk 2002; Berman and Bronk 2003). This may potentially explain the increasing carbon uptake at high light intensities at station S3, despite the negligible light response of nitrate uptake (Fig. 2a,c, 3). Our results highlight that future studies estimating nitrate and carbon rates in the HUS need to account for the influence of other nitrogen sources to understand the link between phytoplankton productivity and various nitrogen sources and quantify their relative importance in the HUS.

Additionally, a higher than Redfield C:N uptake ratio at the low nitrate stations despite low nitrate uptake rates suggests a range of interacting phenomena; either nitrate limitation, excess carbon uptake and/or a high rate of turnover for carbon. Such high uptake C:N ratios have previously been observed in healthy eutrophic phytoplankton populations that grow on nitrate but ambient nitrate concentrations are too low to maintain maximum specific uptake rates, hence the total nitrate taken up is too low (MacIsaac and Dugdale 1972; Sasai et al. 2022). In general, this unproportional response of carbon uptake to nitrate uptake adds another layer of complexity when estimating primary productivity and its relationship to upwelling inputs of nitrate in a seasonally variable region such as the HUS. Our results highlight that in addition to complicating our view of carbon and nitrogen coupling in the HUS, this non-Redield behaviour in carbon and nitrate uptake may compromise stoichiometric calculations of primary productivity from nitrate uptake rates (or vice versa) using the Redfield C:N ratio in the euphotic zone.

4.5 Conclusion

Our results indicate that nitrate and carbon uptake in phytoplankton communities estimated using stable isotopes are regulated by the interaction between the phytoplankton community, irradiance level and nitrogen availability. We demonstrate that Redfield productivity was only observed under high nitrate conditions, whereas at low nitrate stations, non-Redfield productivity was observed despite high Chl *a* concentrations. This suggests that carbon and nitrate uptake at low nitrate conditions are decoupled. We hypothesise the potential role of regenerated nitrogen sources and internal nutrient storage to maintain primary productivity under low nitrate concentrations and light irradiances below optimum for phytoplankton. As a result, simply predicting carbon uptake rates or phytoplankton productivity using Redfield

stoichiometric conversions with nitrate uptake may result in an underestimation of carbon uptake rates in the HUS.

Acknowledgements

We are thankful to the captains, crew members, and scientists onboard the MSM80 cruise of the German R/V Maria S Merian for their support and cooperation at sea. We especially thank Dr. Rainer Kiko, Dr. Michael Meyerhöfer, and Dr. Joaquin Ortiz for assisting with onboard sampling and Kastriot Quelaj for nutrient sampling and analysis. We further thank Kerstin Nachtigall for assistance with sample analysis for mass spectrometry.

Author Contributions

MFM, AJP and LRK designed the study. LRK, AJP, and MFM collected the samples onboard Maria S Merian. LRK analysed samples and data and wrote the manuscript with input from all co-authors.

Supplementary Information

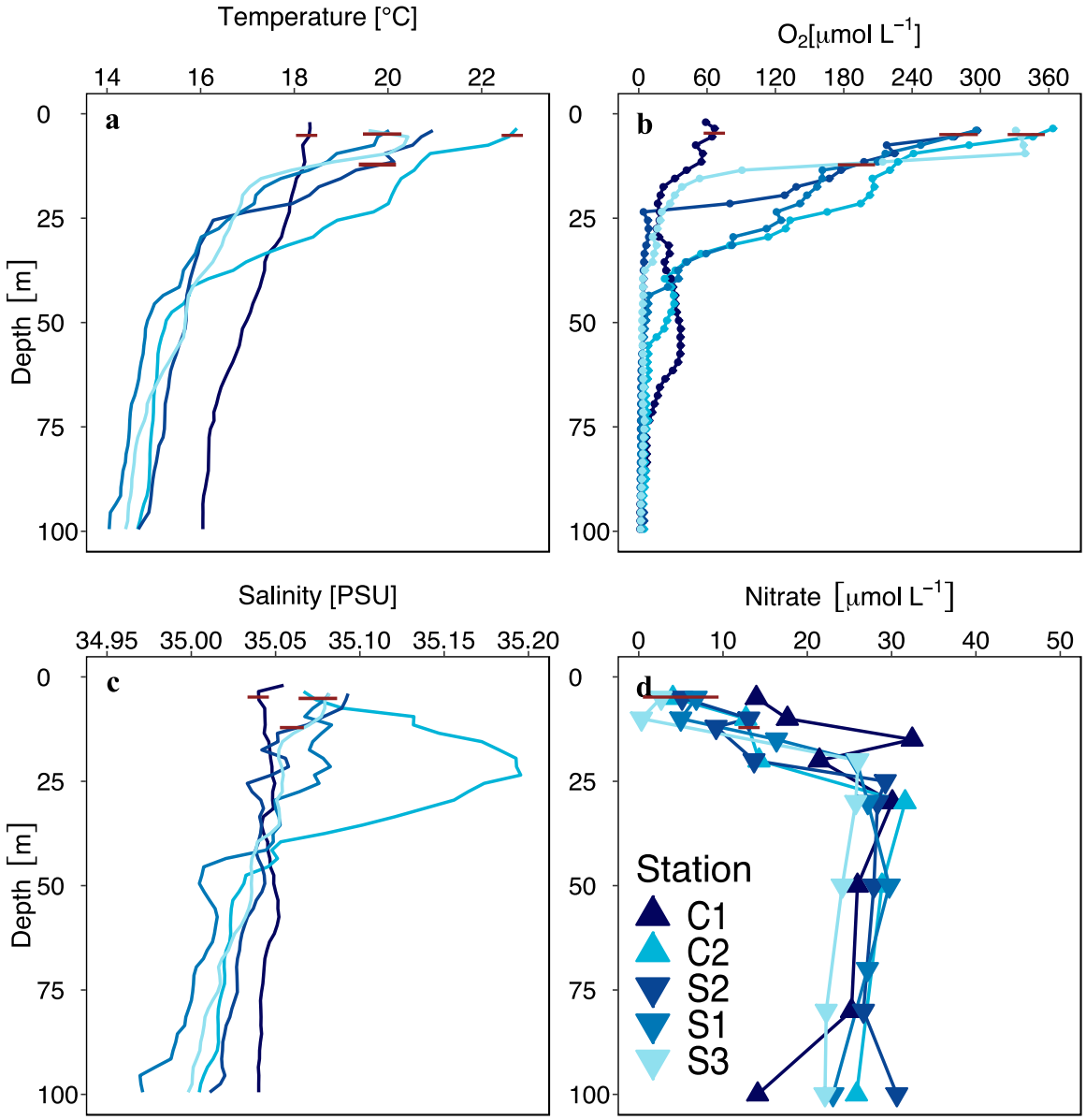

Fig. S1. Vertical profiles of (a) Temperature, (b) oxygen, (c) salinity and (d) nitrate concentrations from the five investigated stations. The red vertical line demarcates the sampling depth at each station.

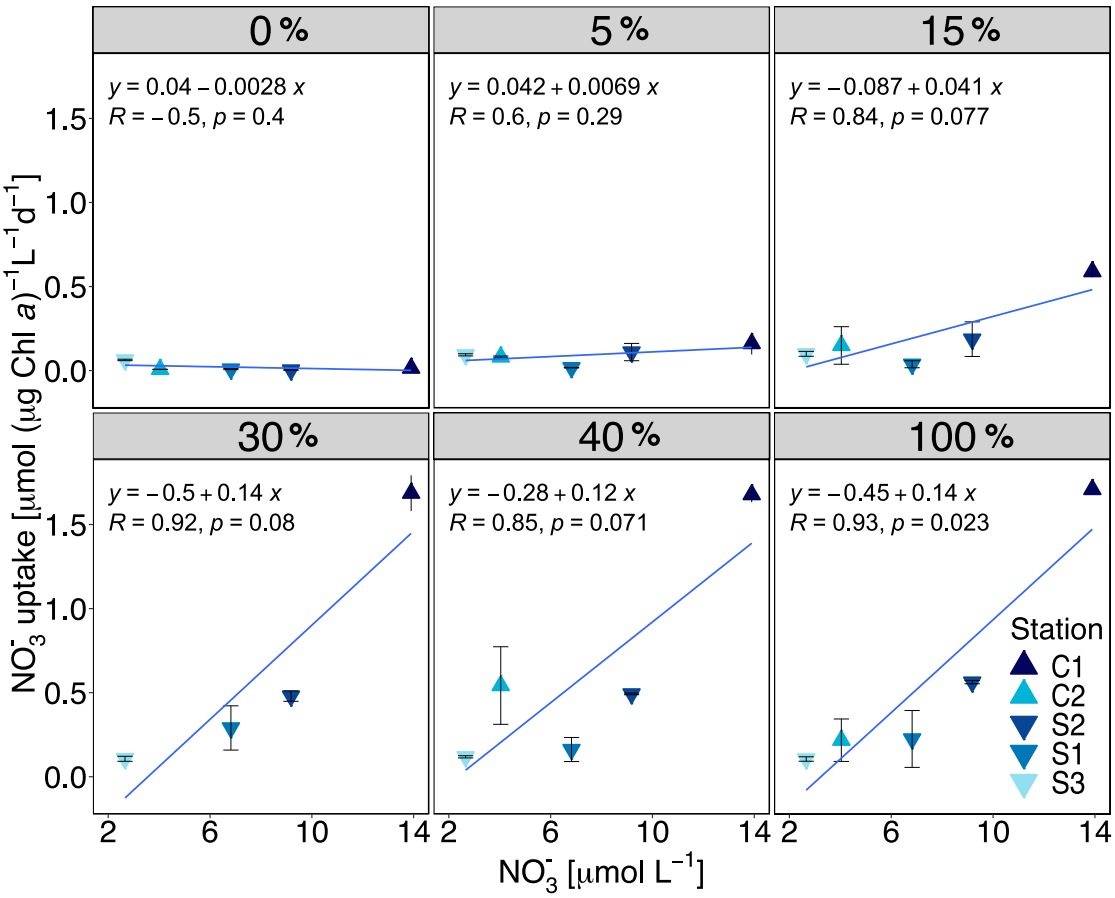

Fig. S2. Linear regression plots of Chl a normalised nitrate uptake rates and nitrate concentrations across different percentages of incoming irradiances (shown at the top). Black vertical lines indicate positive and negative standard deviation around the mean of triplicate

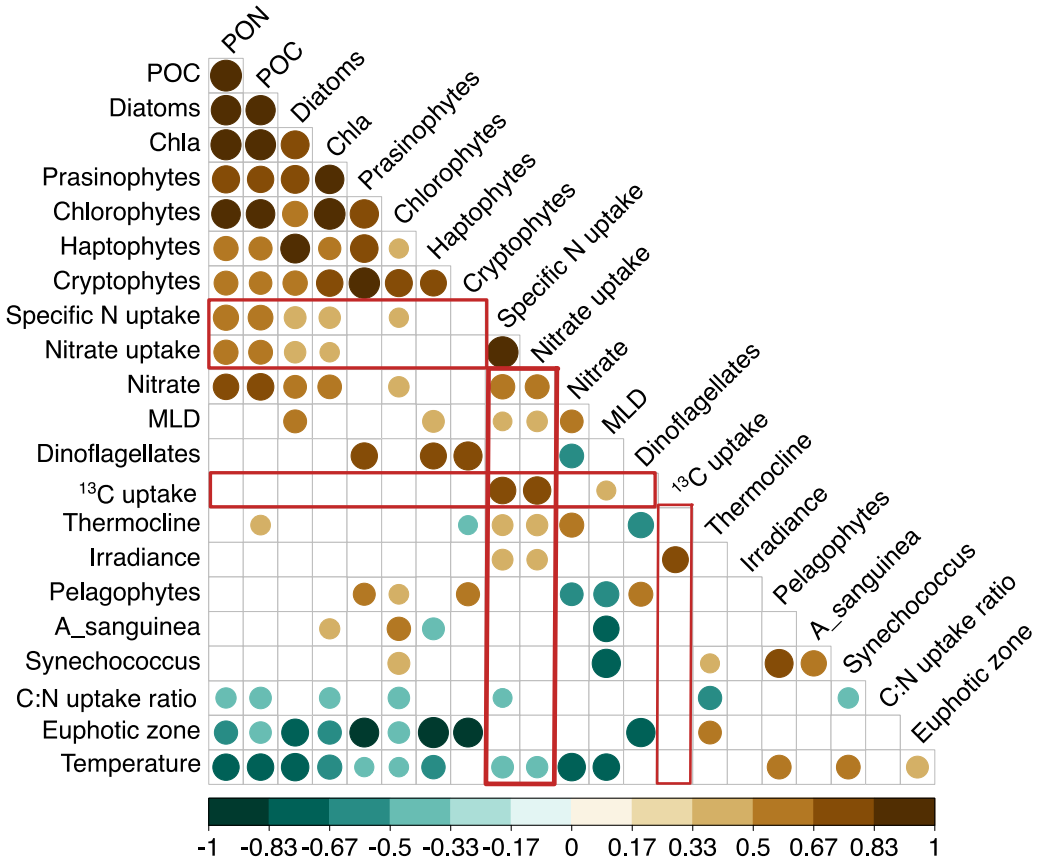

Fig. S3. Spearman correlation coefficients plot. Relationship between nitrate and carbon uptake rates with phytoplankton community and environmental parameters. Positive and negative correlations are displayed in brown and green respectively. The colour intensity and size of the circles are proportional to the correlation coefficients. Non-significant correlations (adjusted p-value >0.05) are indicated as blank boxes.

Chapter 5

Synthesis and Outlook

According to current estimates, one of the proposed reasons for the global imbalance in the marine nitrogen (N) inventory and therefore a deficit in oceanic bioavailable N is attributed to a total bioavailable N loss term exceeding the N-gain in the ocean (Codispoti, 2007). It is considered unlikely that N loss is overestimated (Codispoti, 2007), thus the apparent N deficit (100 – 250 Tg N yr^{-1}) is believed to be a result of underestimated N_2 fixation as the major source for bioavailable N (Zehr and Capone, 2021). One contributing factor to this underestimation is the limited spatiotemporal coverage of N_2 fixation rates in the global ocean (Luo et al., 2012). Furthermore, a lack of comparability in N_2 fixation measurements due to the different methods used presents another challenge (White et al., 2020). Up until the first global N_2 fixation database by Luo et al. (2012), N_2 fixation in the ETSP was singled out to be largely understudied. The ETSP houses one of the world's largest OMZs with significant N loss estimates making it crucial to understand N_2 fixation patterns in this region for a comprehensive evaluation of the regional marine N cycle.

The data presented in Chapter 2 alone are insufficient for a comprehensive assessment of the magnitude of N_2 fixation rates in the HUS across space and time. Multiple up-to-date datasets of N_2 fixation are therefore required to assess its ecological and biogeochemical significance in the ETSP. Thus, in addition to my results from Chapter 2, I compiled N_2 fixation rates from previous field campaigns conducted during the SFB754 project in the ETSP to gain a broader perspective (Löscher, 2018, 2016b, a). By analysing the combined field data set, I draw conclusions based on overarching ideas to enhance our understanding of the regulation and role of N_2 fixation for productivity and balancing the regional N cycle of the ETSP. Building upon these findings, I identify knowledge gaps that require investigation and suggest research advancements needed to improve our knowledge of marine N_2 fixation and N cycling in the ETSP.

Summary of the main findings

The findings of this dissertation show that

i. the magnitude of N_2 fixation rates in the HUS off Peru is low relative to model-predicted rates from the region. The low rates of N_2 fixation only replenish a minor fraction of the local N loss (<3%) and support a small portion of primary productivity (<0.4 %) in the coastal HUS.
ii. a southward latitudinal intensification of N_2 fixation rates during austral summer along the Peruvian coast mimics the intensity of the OMZ and N loss signal. High N_2 fixation rates were measured above and within OMZ waters associated with a pronounced secondary nitrite maximum (9 µmol L^{-1}) and a high nitrate deficit (~25 µmol N). Thus, N_2 fixation rates are reported from above and within waters undergoing N loss.
iii. Iron (Fe) and phosphorus (P) do not seem to be the primary drivers for the magnitude and distribution of N_2 fixation in the ETSP.

iv. N_2 fixation in the northern HUS is potentially regulated by a complex interplay between;
   a. phytoplankton-associated organic matter
   b. potential co-limitation between Fe and other trace metals such as nickel (Ni) and cobalt (Co)
   c. an indirect role of O_2 influencing redox conditions within the water column. While O_2 doesn't seem to directly influence N_2 fixation, the redox conditions it creates directly influence trace metal mobility and anaerobic metabolisms that may favour diazotrophy.

5.1 Characterising the patterns and magnitudes of N_2 fixation in the ETSP

5.1.1 Spatial distribution and seasonality of N_2 fixation

Over the past decade, there has been a significant accumulation of N_2 fixation data in the HUS. To make an initial estimation of the regional magnitudes of marine N_2 fixation, I compiled a list of previous datasets from the ETSP (Figure 5.1a). This compilation serves as a valuable first step in assessing the spatial distribution, and seasonality of N_2 fixation rates in the ETSP (Fig 5.3). To ensure comparability between cruises, all N_2 fixation measurements considered for this estimation were collected using the $^{15}N_2$ dissolution method in 24-hour incubations (White et al., 2020). A total of 423 volumetric N_2 fixation rates and 94 integrated profiles of N_2 fixation rates spanning from 0 and 600 m of the water column were considered for this estimation. A list of other N_2 fixation datasets which were not included in this analysis due to incomparable methods used is provided in Supplementary Info, Table. S1.

This analysis confirms the results of Chapter 2, where the distribution of N_2 fixation rates was shown to follow a latitudinal and longitudinal trend similar to the intensity of the OMZ and N loss (Fig. 5.1, 5.2). The volumetric N_2 fixation rates were binned into five depth intervals within the water column 0–5 m, 5–25 m, 25–100 m, 100–200 m and 200 – 600 m, to detect any patterns or correlations with depth and gradients associated with phytoplankton productivity and O_2 conditions. Average rates were calculated for each bin (Fig. 5.2). The highest N_2 fixation rates were observed in near-surface coastal waters (0 – 100 m) along the central and southern shelf, with a decline in rates at depth and moving away from the coast (Fig 5.1a, c, 5.2). Beyond 100 m, both within the coastal OMZ, as well as in open ocean waters, N_2 fixation rates were low and sporadic (< 1nmol L^{-1} d^{-1}).

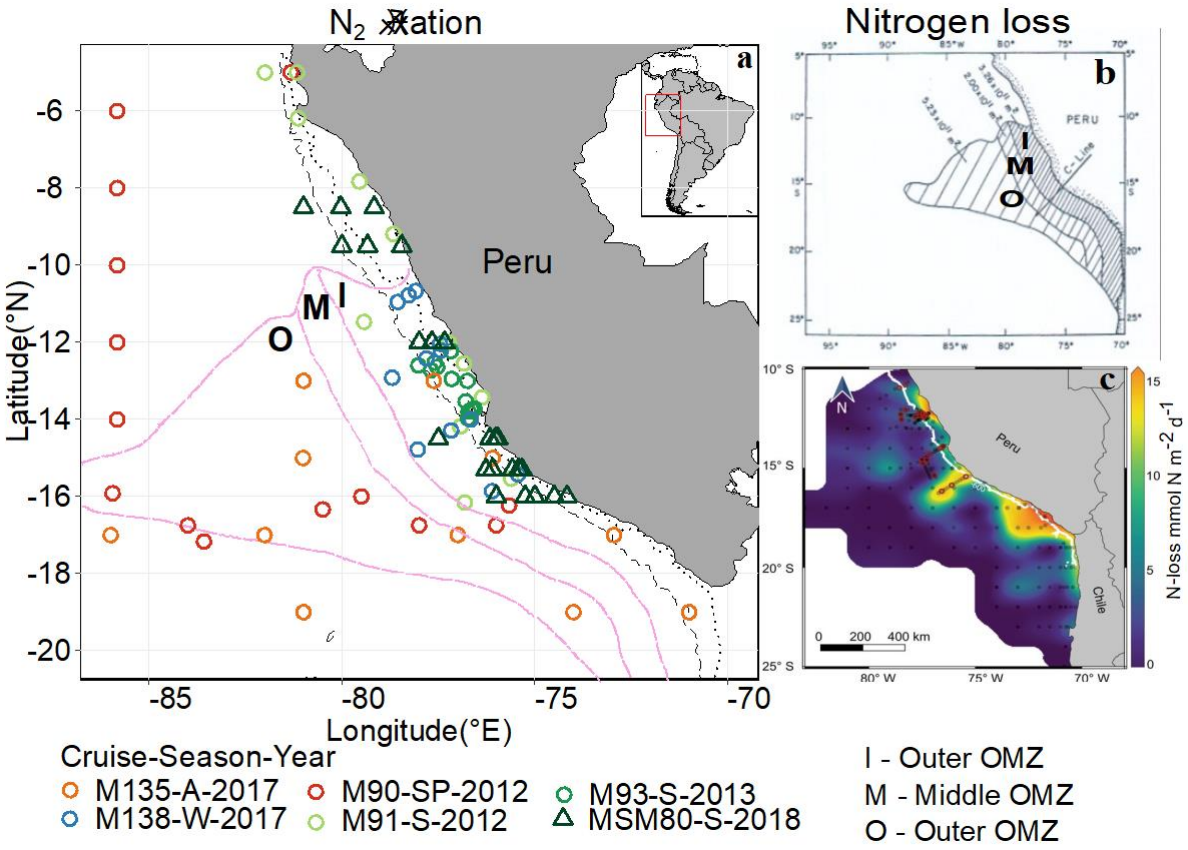

Figure 5.1: (a) Spatial distribution of N_2 fixation measurements in the HUS across 6 cruises. (b) the areal extent of the secondary nitrite maxima demarcating (c) the region of anammox-based N loss in the (I) the inner/coastal OMZ at 175 km from the coast, (M) the middle OMZ at 175 – 300km, and (iii) the outer OMZ >300 km from the shore. Black dotted and dashed lines in (a) show 200 and 2,000 m bathymetry to indicate the edge of the shelf and shelf slope, respectively. Figures b and c are adapted from Codispoti and Packard. (1980) and Karthäuser et al. (2021) respectively.

Elevated rates were predominantly observed in productive coastal waters towards the southern part of the HUS (12°s – 18°S) where the OMZ is shallowest (upper OMZ boundary ~10 m) and most intense (Chapter 2). The coastal OMZ, located at depths less than 600 m water depth, between the central and southern shelf of the Peruvian upwelling system (Fig. 5.1b,c, 10°S – 16°S) exhibits the highest N loss rates (Kalvelage et al., 2013; Karthäuser et al., 2021; Codispoti, and Packard, 1980). In Chapter 2, I documented an N deficit ranging between 10 and 25 μmol L^{-1} in the coastal OMZ between 12°S and 16°S. In contrast, in the northern region (8 – 10°S), where most N_2 fixation rates were below detection to relatively low <1 μmol $L^{-1}d^{-1}$, the OMZ is deeper and weaker and the N deficit was less pronounced (<1 μmol L^{-1}). Thus, I conclude that the N_2 fixation rates observed in the ETSP primarily occur along the coast, above and within the OMZ waters characterised by high N loss rates and a significant N deficit. Thus, a local colocation of coastal N_2 fixation and N loss processes in the northern HUS seems evident. These findings challenge traditional perspectives on N_2 fixation in the ocean since

coastal waters above and below the surface mixed layer are currently underrepresented in global N_2 fixation budgets (Tang et al., 2019; Wang et al., 2019).

Despite relatively low N_2 fixation rates (<1 nmol L^{-1} d^{-1}) in deeper (>100 m) and open ocean waters of the ETSP, previous studies suggest that low and persistent N_2 fixation rates in aphotic waters account for 90% of total water column N_2 fixation in the ETSP (Bonnet et al., 2013; Chang et al., 2019; Dekaezemacker et al., 2013; Löscher et al., 2014; Selden et al., 2021). Furthermore, the offshore OMZ has lower N loss rates but still contributes significantly to integrated water column N loss (~38%), (Fig.5.1b,c, Kalvelage et al., 2013; Wang et al., 2019; Codispoti, and Packard, 1980). This substantial contribution of N_2 fixation from aphotic and offshore waters is primarily due to integration approaches of low and patchy rates over the large volume of these waters. However, given the methodological challenges associated with low biomass and O_2 thresholds when estimating N_2 fixation rates and N loss respectively, the accuracy and precision of these rates is questionable if detection limits are not reported (White et al., 2020; Gradoville et al., 2017b; Kalvelage et al., 2011). Thus, we highlight that including these rates should be considered with caution in regional estimates of N loss and N_2 fixation.

The ETSP is characterised by its high dynamism, influenced by intense seasonality and interannual variability driven by ENSO (Pennington et al., 2006; Yang et al., 2017; Fowler et al., 2013). To assess the temporal variability of N_2 fixation rates, all studies presented in Figure 5.1a were categorized into seasons, although it should be noted that these datasets were collected over multiple years and under different ENSO conditions. Across seasons, ~60% of the rates fell within the range of 0,001 to 15 nmol L^{-1} d^{-1} while only 1.8% of the rates were between 15 and 66 nmol L^{-1} d^{-1}. A proportion of rates (31%) were below the detection limit, and there was no discernible pattern associated with the likelihood of N_2 fixation rates falling below detection in terms of season or year (Supp Info Fig. A2). This indicates the presence of small-scale patchiness in the spatiotemporal distribution of N_2 fixation in the ETSP even within the same season.

N_2 fixation rates in the HUS exhibit low median values (< 1 nmol L^{-1} d^{-1}) throughout the seasons, indicating that seasonality in rates is not pronounced (Fig 5.3). However, the observed high variability in our estimates is likely attributed to patchiness and sporadic localized occurrences of enhanced N_2 fixation rates during the productive austral summer months. In a previous study, elevated N_2 fixation rates (~20 - 66 nmol L^{-1} d^{-1}, integrated rates ~ 800 μmol m^{-2} d^{-1}) were reported during summer off the Peruvian coast at a coastal sulphidic station, suggesting that sulphidic events may sporadically enhance N_2 fixation rates (Löscher et al., 2014; Schunck et al., 2013). Although we cannot confirm the presence of a sulphidic event during the MSM80 cruise (Chapter 2), these events are known to be frequent, persistent, and typically observed during austral summer. Additionally, they are known to be restricted to neutral or La Niña phases when primary productivity and organic matter production are high (Callbeck et al., 2021; Schunck et al., 2013). Based on the Southern Oscillation Index (SOI) used to describe ENSO, our sampling months (Dec 2018 - Jan 2019, Chapter 2) corresponded to an SOI index

between 1 and 0, indicating La Niña to neutral phase (https://www.ncei.noaa.gov/access/monitoring/enso/soi). Despite their frequency, sulphidic events in the ETSP often go unnoticed due to the activity of sulphide oxidizing nitrate-reducing bacteria that detoxify sulphide to sulphate (Lavik et al., 2009). Therefore, we cannot entirely rule out the possibility of a sulphidic event during the cruise period. Nonetheless, nearly a decade after Löscher et al. (2014) reported sporadic high rates, we also observe a few rates but of similar magnitude during austral summer (10 – 30 nmol N L^{-1} d^{-1}, Fig 5.3, Chapter 2). Thus, it can be inferred from this compiled dataset that sporadic high N_2 fixation rates appear to be a common feature of the HUS during the summer months.

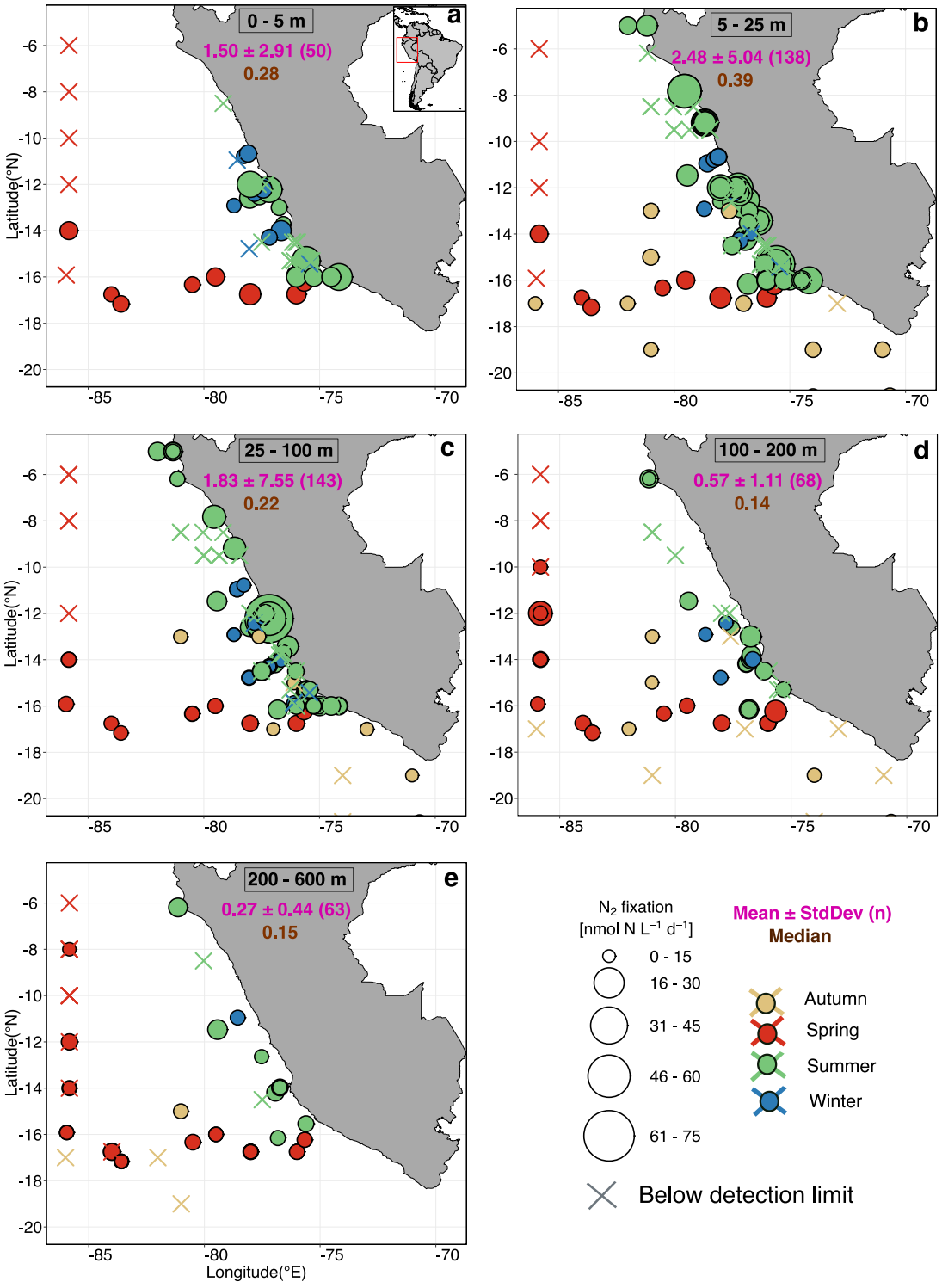

Fig 5.2: Mean and median volumetric N_2 fixation rates in (**a**) 0–5 m, (**b**) 5–25 m, (**c**) 25–100 m, (**d**) 100-200 m, and (**e**) 200 - 600 m depths.

An interesting observation about these sporadic rates is that they are comparable in magnitude to those observed during *Trichodesmium* spp and UCYN-A blooms in the North Atlantic and the Western Tropical South Pacific (Fonseca-Batista et al., 2019; Mulholland et al., 2012; Bonnet

et al., 2017; Messer et al., 2016). While these ocean regions differ substantially in terms of nutrients, these sporadic rates in the ETSP highlight the potential for ecologically and biogeochemically relevant N_2 fixation inputs in localized pockets of the water column if conditions are episodically favourable. However, the high variability and sporadic nature associated with these estimates present a challenge in establishing patterns of N_2 fixation in the ETSP and identifying the key environmental controls. If these sporadic N_2 fixation rates during austral summer or La ñina phases dominate the collected datasets characterised by a large number of low N_2 fixation rates, they could lead to an overestimation of local N_2 fixation in the ETSP. Additionally, significant uncertainties remain regarding whether these high rates are sustained on annual to interannual time scales, which would be crucial for their relevance in primary productivity and N cycling. Thus, conducting regular sampling programs at finer temporal and spatial scales (vertical and horizontal) throughout all seasons will aid in accounting for this high variability.

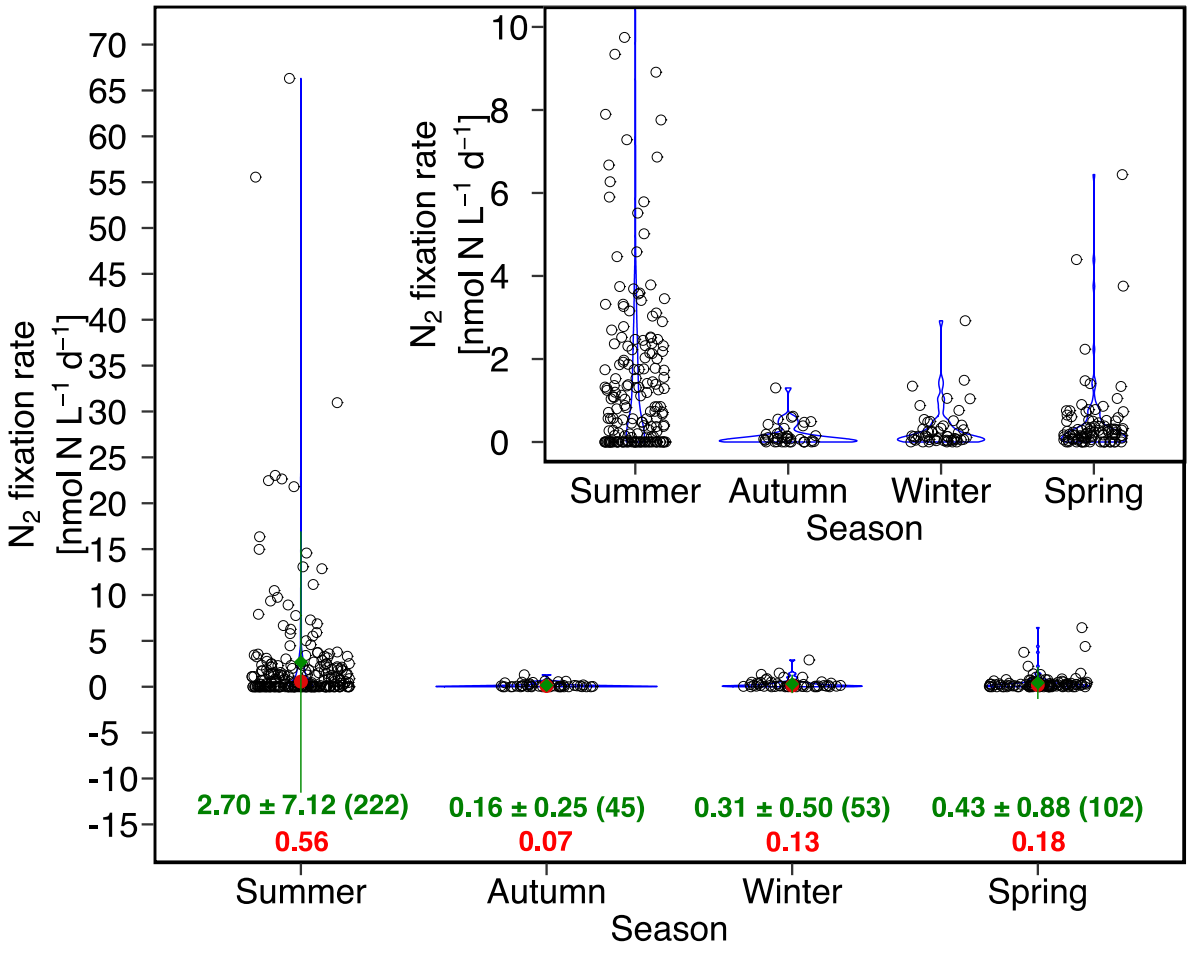

Figure 5.3: Violin plots indicating the (green) mean and stdDev and (red) median of volumetric N_2 fixation rates from the northern HUS off Peru across seasons. Data represented include SFB754 (Fig. 5.1) and MSM80 (presented in Chapter 2) cruises. The Inset figure is a close-up of the distribution on the lower values (0 -10 nmol N L^{-1} d^{-1}) of the main chart.

5.1.2 Assessing the regional versus basin-wide coupling of N_2 fixation and N loss: Implications for the marine N inventory

The most direct diagnostic of the biogeochemical role of N_2 fixation is its ability to compensate for N losses at a regional, basin, and global scale. Globally, heterotrophic denitrification serves as the primary sink for oceanic fixed nitrogen. However, studies focusing on the Peruvian OMZ have failed to detect significant denitrifying activity within this region. Instead, anammox has been identified as the dominant process responsible for the high N loss. Annamox accounts for 73% (19 Tg N yr^{-1}, volumetric rates ~5 - 225 nmol N L^{-1} d^{-1}) of the estimated N loss rates (9 - 26 Tg N yr-1) for the entire ETSP (Codispoti, and Packard, 1980; Karthäuser et al., 2021; Kalvelage et al., 2013; Callbeck et al., 2017). Denitrification is detectable only during summer months in southern coastal waters associated with sulphidic events, occurring at rates comparable to N_2 fixation rates (~2-5 nmol N L^{-1} d^{-1}), (Kalvelage et al., 2013). Therefore, it seems that on an annual scale, the average high N_2 fixation rates during summer coincide with THE occurrence of denitrification. However, this coupling does not appear to be sustained all year round. N_2 fixation rates are lowest in winter and autumn (Fig. 5.3), and to date, no denitrification has been reported during these seasons. Thus, whilst a balance in magnitudes between N_2 fixation and denitrification is apparent, I infer that a net loss of nitrogen is highly likely if these two processes are indeed spatially and temporally coupled, considering the positive feedback hypothesised by Landolfi et al. (2013). For this synthesis, I will use the collective term "N loss" from here on which encompasses mainly anammox but also includes denitrification.

In this dissertation, I capitalise on the extensive N_2 fixation dataset collected in the ETSP to evaluate its biogeochemical role. By calculating average integrated N_2 fixation estimates that are more representative of the coastal Peruvian OMZ, we find that N_2 fixation accounts for less than 5% of the coastal N loss from the inner OMZ off Peru (Fig. 5.1b,c, Table 1). Additionally, fixed N estimates of 0.22 ± 0.32 Tg N yr^{-1} for the coastal Peruvian system where rates are highest would only replenish a small proportion of global N loss (0.12 ± 0.16%). Extrapolating these rates to the entire Peruvian OMZ, our estimates only account for up to 13% of the N loss at the highest end (Fig. 5.1c, Table 1). To achieve a local balance within the Peruvian OMZ, N_2 fixation rates would need to be 2-3 times higher. However, there is currently limited evidence for consistently high N_2 fixation rates throughout the year in the ETSP (Supplementary Info, Table S1), and the variability in our estimates is high. Therefore, it is highly uncertain whether these conservative N_2 fixation rates when extrapolated to the entire ETSP would sufficiently compensate for the regional N loss. While it is apparent that N_2 fixation and denitrification can co-occur spatially and temporally in the Peruvian OMZ (Fig 5.1) as suggested by Deutsch et al. (2007), a closer examination of the magnitudes in this dissertation presents contrasting views of the spatial coupling hypothesis from a biogeochemical perspective. Based on these estimates extrapolated to the ETSP, the low magnitudes of N_2 fixation rates and high variability suggest that the ETSP does not play a significant role in locally compensating for N loss. Thus, at least on timescales of up to a year, the greater loss of fixed nitrogen relative to inputs in the

ETSP implies a sustained net N loss in the regional N inventory, as N_2 fixation appears to only partially compensate for N loss. Therefore, if the local N inventory is to be balanced, the deficit would need to be compensated for through higher N_2 fixation rates elsewhere.

Maintaining a balance between N_2 fixation with N losses is crucial for sustaining ocean productivity both regionally and globally over long time scales. However, accurately obtaining estimates of basin-scale rates by extrapolating from limited observations remains a persistent challenge given the relatively low density and limited geographical range of such observations in the ocean. The recently updated database of N_2 fixation rates compiled by Shao et al. (2023) serves as a valuable reference, offering a larger number of global N_2 fixation measurements compared to a decade ago (Luo et al., 2012). According to this database, the South Pacific basin is responsible for ~49% of global N_2 fixation (~180 Tg N yr^{-1}), confirming its status as a basin-wide "hotspot" for diazotrophy (Bonnet et al., 2017, 2023; Messer et al., 2016). In comparison, the ETSP contributes ~13% of N_2 fixation rates within the South Pacific, representing a significant but minor fraction relative to the rest of the South Pacific basin.

Previously, conservative basin-wide estimates of N_2 fixation using N deficits (N*) have hypothesized that N_2 fixation in the Pacific Ocean is not uniformly distributed but primarily concentrated in the western (from ~140°W) of the subtropical gyres (Deutsch et al., 2001). The newly updated database of N_2 fixation rates supports this hypothesis, revealing an increased number of high in-situ N_2 fixation rates in the South Pacific, particularly in the western part of the basin. Currently, average measured rates from the Western Tropical South Pacific (WTSP) are 5 - 10 times higher than those observed in the ETSP and are temporally sustained (Bonnet et al., 2017, 2018; Messer et al., 2016; Berthelot et al., 2017; Knapp et al., 2018). These high in-situ rates reinforce the significance of large-scale intra- and inter-basin N transport in maintaining a balanced fixed-N budget at both local and global scales (Wang et al., 2019). Therefore, I propose that the elevated N deficits resulting from intensified N loss rates (anammox and denitrification) in the ETSP are transported through shallow circulation pathways and compensated by N_2 fixation occurring in the WTSP. Based on the current estimates (Table 1), it appears that a basin-wide coupling of N inputs and losses is sufficient to generate robust basin-wide stabilizing feedback at least on annual scales (Bonnet et al., 2018, 2017; Berthelot et al., 2017; Messer et al., 2016; Knapp et al., 2018).

Table 1: N_2 fixation rates from synthesised conservative estimates and model predictions in comparison to current N loss estimates (denitrification and anammox) in the Peruvian OMZ and extrapolated to the ETSP. For comparison basin-wide and global estimates of N_2 fixation and N loss rates are also reported. Proportion of nitrogen loss refers to the amount of N loss compensated by N_2 fixation.

Region	Ocean area ($\times 10^{12}$ m^2)	Mean N_2 fixation rate (µmol N m^{-2} d^{-1})	Areal N_2 fixation (Tg N yr^{-1})	Areal nitrogen loss[f] (Tg N yr^{-1})	Latitudinal range	Proportion of nitrogen loss (%)
Model predicted						
ETSP (Deutsch et al., 2007)	21	547.95[e]	58.83[e]	26 ± 4.1[d]	0° - 20°S	100
First order estimates from this dissertation (measurement based)						
Coastal/Inner Peruvian OMZ	0.32	132.92 ± 192.92[a]	0.22 ± 0.32[a]	12[b(anammox)]	6°S – 17.5°S	1.83 ± 2.67
Total Peruvian OMZ (coastal + offshore)	1.53	132.92 ± 192.92[c]	1.04 ± 1.51[c]	19[d(anammox)] 10[d(denitrification)]	5°S – 20°S	5.47 ± 7.95
ETSP (This dissertation)	21	132.92 ± 192.92[c]	14.27 ± 20.71[c]	26 ± 4.1[d]	0° - 20°S	58.87 ± 68.80
Version 2 global database of N_2 (measurement based)						
South Pacific	69	250 ± 66	88 ± 23[g]		0°- 45°S	
Global Ocean			181 ± 20[g]	201[h]		90 – 100

[a]This dissertation, [b](Karthäuser et al., 2021), [c] Extrapolated from average N_2 fixation in inner OMZ where N_2 fixation is highest, [d](Kalvelage et al., 2013; Hamersley et al., 2007; Codispoti, and Packard, 1980; Deutsch et al., 2001; DeVries et al., 2012), [e] (Deutsch et al., 2007), [f]combined anammox and denitrification rates, [g](Shao et al., 2023), [h] (Wang et al., 2019).

N_2 fixation is a common process in the marine environment and even low background rates in the ETSP may have considerable implications for primary productivity if the colocation with N

loss supports the accumulation of N deficits, as hypothesised by Landolfi et al. (2013). Considering the tight coupling between nitrogen and carbon cycles, a sustained decrease in fixed N in the ETSP could have profound effects on short-term primary productivity. A key question arising from this dissertation is whether the stoichiometric constraints highlighted by the vicious cycle hypothesis are also valid for anammox, the dominant N loss pathway in the ETSP and whether its prevalence year-round may mitigate the negative consequences of a positive feedback (net N loss) in the ETSP.

Given the substantial increase in global N input and output terms over the years (Table 1), even small imbalances, positive or negative could have significant local and regional implications. Therefore, it is important not to overlook the mismatch between measured and model-predicted N_2 fixation rates in the ETSP. While future global model projections of N_2 fixation show similarities, regional projections from different models differ considerably (Yao et al., 2022). It is worth noting that models with similar structures can exhibit significant discrepancies in N_2 fixation and other nitrogen cycle processes without differing in their net primary productivity (Davies-Barnard et al., 2022; Oschlies et al., 2019). Thus, caution needs to be exercised when using global trends in N_2 fixation rates to predict regional patterns of primary productivity, as certain regions may be influenced by local environmental factors that are not necessarily reflected in global N_2 fixation patterns, which are assumed to be primarily driven by Fe and P* (Chapter 3).

Our findings raise concerns regarding the specific factors within different N_2 fixation parameterizations in biogeochemical models that contribute to regional variations in N_2 fixation. It is thus crucial that the accuracy of these model projections of N_2 fixation be assessed closely. Moreover, the influence of combined N sources from anthropogenically fixed atmospheric deposition and terrestrial runoff is rapidly increasing due to intensified fertiliser use in coastal agriculture. This increase can have contrasting effects, either boosting coastal primary productivity and suppressing N_2 fixation serving as negative feedback or contributing to the expansion of OMZ due to high organic matter load, thereby creating favourable conditions for heterotrophic N_2 fixation (Duce et al., 2008; Gruber, 2004; Kim et al., 2014). Consequently, accurately predicting how primary productivity in the ETSP may be altered by changes in regional and basin-scale N inputs and losses requires precise local parameterisations and simulations of N inputs (N_2 fixation, terrestrial runoff and atmospheric deposition) as well as N losses, and the elemental cycling of redox-dependent biochemical micronutrients in the ETSP. Currently, this remains a knowledge gap that needs to be addressed in future research.

5.1.3 Conservative estimates of N_2 fixation rates in the ETSP support a minor ecological role of N_2 fixation

While the temporal resolution of N_2 fixation rates in the ETSP is still limited, the combined cruise work shown in Figure 5.1a provides a good overview of the magnitudes of coastal N_2

fixation rates across seasons (Fig. 5.3), which can aid in understanding and assessing the role of coastal N_2 fixation in the ETSP. In Chapter 2, we report average volumetric N_2 fixation rates of 1.19 ± 3.81 nmol N L^{-1} d^{-1}, (mean ± stdDev) which fall within the same range as or conservative estimates from the synthesised datasets herein (1.58 ± 5.32 nmol N L^{-1} d^{-1}, mean ± stdDev) and align with average N_2 fixation rates reported from coastal waters globally (1.40 ± 4.61 nmol N L^{-1} d^{-1}, Tang et al., 2019a). Hence, the N_2 fixation rates reported in Chapter 2 are considered to be representative of average coastal N_2 fixation rates in the ETSP region.

When integrating these conservative estimates throughout the water column, N_2 fixation amounts to 132.92 ± 192.92 μmol m^{-2} d^{-1}, which is two to five times lower than the average N_2 fixation rates predicted by Deutsch et al. (2007) for the ETSP (545.945 μmol m^{-2} d^{-1}). Our estimates are in relatively good agreement with other incubation-based (bubble and bubble-free methods) and isotope-based estimates of N_2 fixation from the ETSP (38 ± 74 μmol m^{-2} d^{-1}, Selden et al., 2021; Chang et al., 2019; Dekaezemacker et al., 2013; Meyer et al., 2017; Knapp et al., 2016) and comparable to estimates from the South Pacific Gyre (94 ± 61 μmol m^{-2} d^{-1}, Halm et al., 2012). This indicates that there is an agreement across several studies that when N_2 fixation rates are integrated to depth, the ETSP does not exhibit elevated N_2 fixation rates as predicted by Deutsch et al. (2007).

In Chapter 2, the estimated N_2 fixation in the coastal HUS off Peru was found to support < 0.3% of daily primary productivity. To assess its ecological significance, we compared the average daily and yearly N_2 fixation inputs against respective primary productivity estimates (16.40 μmol C L^{-1} d^{-1}, ~900 Tg C yr^{-1}) from the coastal Peruvian system (Pennington et al., 2006; Fernández et al., 2009). We determine that N_2 fixation contributes to ~0.4% of primary productivity in the coastal Peruvian upwelling system. Thus, I demonstrate the minor role of N_2 fixation as a source of N for new productivity in the ETSP, where an estimated 50% of new N is contributed by upwelled nitrate and regenerative N sources from the region (Fernández et al., 2009). However, despite its minor ecological impact on primary productivity, low but persistent coastal N_2 fixation above and within the OMZ may remain biogeochemically relevant locally due to its spatial and perhaps temporal coupling with N loss processes.

In well-characterised "hotspots" of N_2 fixation, such as the tropical and subtropical oligotrophic waters of the North Pacific and the Western South Pacific, volumetric rates are 1 - 2 orders of magnitude higher than the ETSP (500 and 1200 μmol m^{-2} d^{-1}), (Berthelot et al., 2017; Bonnet et al., 2017; Mulholland et al., 2019; Capone et al., 2005; Carpenter and Capone, 2008). If we consider these magnitudes to be representative of hotspots, it can be concluded that these conservative first-order estimates of N_2 fixation rates in the ETSP, across seasons and years, align with previous findings indicating that this region is unlikely to be a "hotspot" for N_2 fixation (Chang et al., 2019; Knapp et al., 2016; Selden et al., 2021; Wang et al., 2019; Shao et al., 2023).

My analysis confirms that model estimates of N_2 fixation rates in the ETSP may indeed be overestimated. These findings highlight a significant mismatch and discrepancy between direct measurements of N_2 fixation and model predictions in the ETSP, which has been previously acknowledged in other biogeochemical models (Deutsch et al., 2007; Wang et al., 2019; Shao et al., 2023; Deutsch et al., 2001; Moore and Doney, 2007). It is important to note that these estimations are based on an average of a limited number of highly resolved studies focused on the coastal HUS and should therefore be considered first-order estimates for the ETSP. This discrepancy is likely associated with model parameterizations governing the regulation of N_2 fixation. Therefore, we suggest that this mismatch is taken into account in the development of biogeochemical models aiming to predict N_2 fixation in the ETSP.

5.2 Developing perspectives on the ecological and biogeochemical controls for N_2 fixation in the ETSP

5.2.1 Weak response of coastal N_2 fixation rates to Fe and P suggests model biases

To achieve the average integrated N_2 fixation rates reported in this synthesis, (132.92 ± 192.92 μmol N m^{-2} d^{-1}), estimated P uptake rates would average 8.31 ± 12.06 μmol P m^2 d^{-1} under Redfield conditions. Sedimentary P fluxes to the water column in the Peruvian region are 10 - 100 times higher (1040 ± 730 μmol P m^{-2} d^{-1}) than the estimated P utilization for these N_2 fixation rates (Lomnitz et al., 2016). Additionally, high P concentrations and positive P* values were observed in the study area in relation to low N_2 fixation (Chapter 2). A small uptake term from N_2 fixation in addition to phytoplankton uptake may be masked by the high sedimentary P fluxes entering the water column, making it challenging to assess based on standing stocks of P often measured during research cruises. Nonetheless, these simple estimations indicate that the conditions for P availability and concentrations necessary to support N_2 fixation are met in the HUS. This conclusion is further supported by the bioassay experiments in Chapter 3, where the addition of upwelled waters to N_2 fixation incubations resulted in increased P concentrations. However, even the highest increase in P concentrations did not correspond to a significant enhancement of N_2 fixation rates compared to the control. Our results align with a previous study that indicated a minor role of N_2 fixation as a mechanism for P reduction in the ETSP (Meyer et al., 2017). Additionally, we demonstrate that both P and P* explain < 4% of the variability in N_2 fixation rates in the region (Chapter 3). The correlation between N_2 fixation rates and N:P ratios did not show a significant relationship and indicated that most rates were measured at N:P ratios > 5, with an upper threshold of 11 beyond which N_2 fixation rates were below detection (Chapter 2, Fig 5.4b, c). Therefore, while P concentrations were non-limiting in the study area, their contribution to enhancing N_2 fixation was minor, and the relative availability of N to some degree did not appear to restrict N_2 fixation activity (Fig. 5.4b).

Fe concentrations in the Peruvian shelf often exceeded 1 nmol L^{-1} at the surface and increase with depth, reaching concentrations of up to 100 nmol L^{-1}. Such elevated concentrations are not unique to the ETSP and are attributed to redox processes associated with the OMZ, leading to increased sedimentary Fe (II) release from anoxic coastal sediments (Noffke et al., 2012; Rapp et al., 2020; Scholz, 2018). Under anoxic conditions, the high Fe supply, along with the preferential release of phosphorus (P) during N loss, creates a Fe:P:N ratio conducive to N_2 fixation (Lomnitz et al., 2016; Noffke et al., 2012). Therefore, it is not entirely surprising that N_2 fixation rates, as reported in Chapter 2 and observed across multiple studies to date (Supplementary Info, Table. S1), are highest in shelf Fe-rich waters above and within the OMZ, where conditions may favour diazotrophic growth relative to the open ocean. It is important to note that our results do not discount the possibility of iron limitation for N_2 fixation in open ocean waters, which were not the focus of this dissertation work. Fe availability in the open ocean of the ETSP is limited due to weak lateral transport and scavenging processes (Bruland et al., 2005; Rapp et al., 2020). Therefore, previous reports of relatively low to undetected N_2 fixation rates from open ocean waters within the ETSP have suggested that low Fe concentrations are a major limiting factor for N_2 fixation in this region (Knapp et al., 2016). Nonetheless, contrary to the expected strong influence of Fe, low magnitudes of N_2 fixation close to the coast indicate a minor role of Fe in enhancing coastal N_2 fixation rates in the ETSP (Fig. 5.4a).

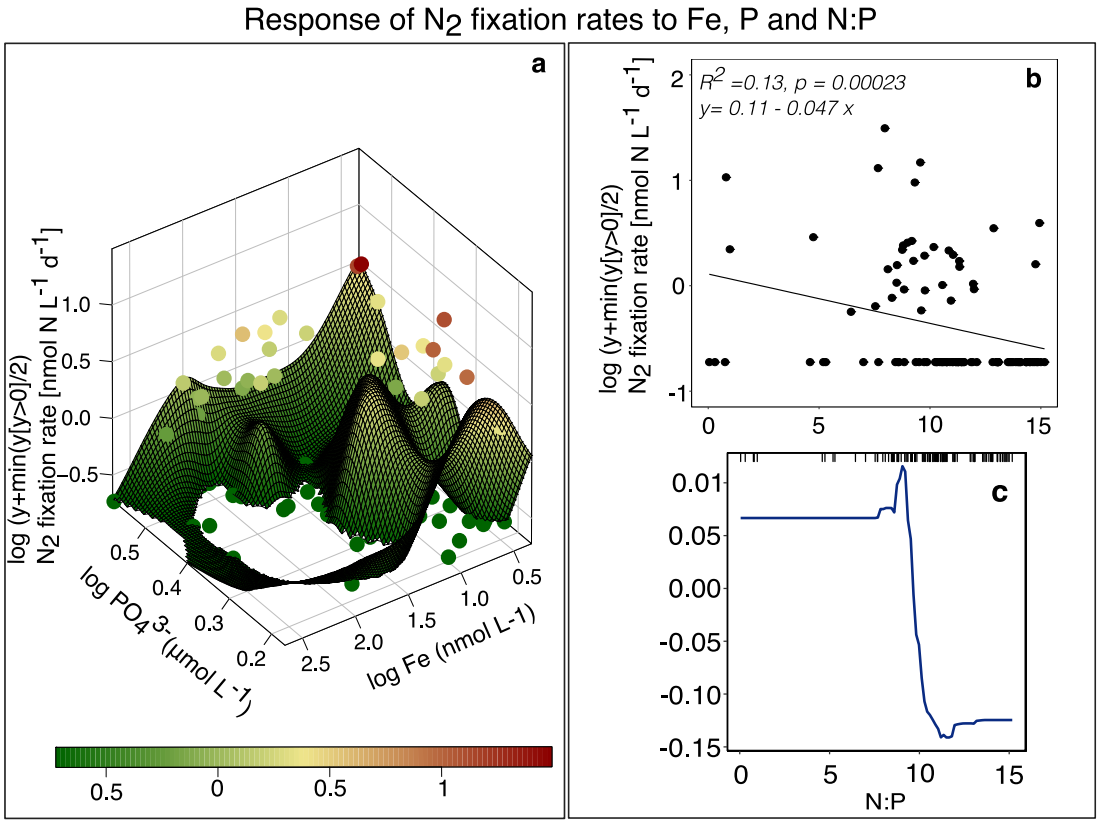

Figure 5.4: (a) 3D surface scatter response plot showing the relationship between N_2 fixation, Phosphate and total dissolved iron concentrations. The graph is a 3D projection of all measured

values from Chapter 2. Circles indicate the data points. Surface interpolations are model predictions of the observed relationship performed using a General Additive Model (GAM) fit. The blank surface represents no data in the range of concentrations of either or one of the response variables. **(b)** linear regression of N_2 fixation rates and N:P and **(c)** non-linear mean response of N_2 fixation to the range of N:P ratios. Black tick marks at the inside top of Figure (c) show the location of N_2 fixation observations along the X-axis. Due to considerable non-detectable rates (converted to zero), a and few high rates, the N_2 fixation rates were log transformed to balance the importance of extreme values in the analysis (log of the sum of rate value and half of the smallest non-zero value).

In Chapter 3, the statistical model that included Fe as the only trace metal demonstrates a lower model fit compared to when other trace metals were included, suggesting that other trace metals may also play a significant role in N_2 fixation regulation. This finding was further supported by bioassays experiments in which N_2 fixation did not significantly respond to the addition of Fe (as $FeCl_3$) addition. These observations confirm the minor influence of Fe in regulating N_2 fixation rates in Fe and P-rich coastal waters of the HUS. These findings raise questions on the role of Fe and P in regulating coastal N_2 fixation in the ETSP, as has been widely referenced in field studies and biogeochemical models. Thus, I propose that parameterizing N_2 fixation rates based on the availability and concentrations of P and Fe has likely led to an overestimation of model-based estimates of N_2 fixation rates in the ETSP (Table. 1, Section 5.1.2, 5.1.3).

The high Fe requirement in N_2 fixing organisms is primarily associated with the photosynthesis process, in addition to nitrogenase requirements, in autotrophic cyanobacterial diazotrophs such as *Trichodesmium* spp (Berman-Frank et al., 2001a). However, for non-cyanobacterial diazotrophs (NCDs) that are reported to dominate the ETSP, the absence of a photosystem may result in reduced Fe requirements. Furthermore, some diazotrophs such as *Crocosphaera spp* which have also been reported in the ETSP (Kittu et al. *in prep*) have demonstrated efficient adaptation mechanisms for Fe utilisation. These involve allocating Fe to the photosynthesis reaction during the day and reusing it at night for nitrogen fixation, thereby decreasing the overall Fe requirements (Saito et al., 2011). Taken together, these explanations suggest that Fe requirements for the dominant diazotrophic groups along the Peruvian coast are likely adequately met. Therefore, the low rates of coastal N_2 fixation (Fig. 5.4a) point towards additional parameters that may regulate N_2 fixation rates locally.

For decades, marine biogeochemists have sought to generalise stoichiometric controls on N_2 fixation, primarily focusing on geochemical tracers of N, P and Fe (Ward et al., 2013). Consequently, regional rates in the ETSP have been derived by combining spatial deviations in the N:P ratio from the canonical Redfield ratio, (often defined as N*) with the measures of the rate of ocean circulation (Deutsch and Weber, 2012). While this approach may have some validity at global scales, our findings indicate that the application of these tracers in biogeochemical models may have limitations at regional spatial scales. The discrepancy

between model-predicted N_2 fixation rates from Deutsch et al. (2007) and our conservative estimates from the synthesised datasets, coupled with the low explanatory power of N:P and P (Fig. 5.4), indicate that a fundamental assumption in diagnostic models (based on spatial variations in P* and N* and N:P restoration) namely the assumption of constant N:P stoichiometry at Redfield stoichiometry partially invalidates model-based estimates of N_2 fixation in the ETSP.

Deviation from Redfield N:P (16:1) relationship may not always be attributed solely to N inputs or losses but could arise from variations in the stoichiometry of nitrate uptake and remineralisation (Martiny et al., 2013; Mills and Arrigo, 2010). In Chapter 4, we demonstrate that upwelled nitrate and other regenerative nitrogen sources, such as ammonium play a major role in driving primary productivity in the ETSP and to a large extent regulate N:P ratios (Franz et al., 2012). Furthermore, N:P ratio signals resulting from N loss and N_2 fixation can offset each other if they occur in the same region or if host waters are mixed in a way that prevents their construction (Marconi et al., 2017). These limitations suggest that the systemic bias in estimates of N_2 fixation rates due to the assumption of constant phytoplankton N:P in biogeochemical models is likely high in the ETSP. There is in principle a range of elements that could limit N_2 fixation in the ETSP, particularly considering the dominance of physiologically unexplored NCDs and an absence of *Trichodesmium* spp. Our study highlights that the assumption of a fixed Redfield N:P ratio for these elements seems to be a considerable oversimplification of N_2 fixation controls in the ETSP. Therefore, we conclude that other elements besides N, P or Fe may serve as a stoichiometric or functional bottleneck to N_2 fixation activity (Löscher et al., 2014; Turk-Kubo et al., 2014). Expanding our knowledge to explore other unknown controls that control N_2 fixation could provide valuable insights into the environments where N_2 fixation is significant or negligible, as well as its global biogeography in the ocean.

5.2.2 Emerging controls of N_2 fixation in the ETSP

An influence of cobalt (Co) and nickel (Ni) on N_2 fixation, whilst to our knowledge a novel suggestion for the control of marine N_2 fixation rates, is not a new paradigm in other environmental realms such as terrestrial systems. In the marine environment, Co and Ni are considered to have a more subtle impact compared to iron (Fe) and thus have received limited attention. In Chapter 3**,** I used statistical models and bioassay experiments to examine the response of N_2 fixation to various environmental factors including trace metals such as cobalt (Co) and nickel (Ni). As a novel part of this dissertation work, my findings demonstrate that Co and Ni have the potential to regulate N_2 fixation rates in the ETSP because they appear to limit N_2 fixation activity at ambient concentrations (Chapter 3). While the absolute concentrations of total dissolvable Fe (TdFe) and Co (TdCo) did exert a significant influence on N_2 fixation, their relative availability, specifically the excess Co relative to Fe (TdCo*), played a more prominent role in explaining the highest variability of N_2 fixation rates in the ETSP. Through bioassay experiments involving the enhancement of both Fe, Ni and Co, we verify that, in the presence

of non-limiting Fe concentrations, additional Co and Ni enhanced N_2 fixation rates compared to when Fe alone is replete. Thus, it appears that other elemental requirements can coexist in diazotrophs in addition to Fe and P.

The elevated Fe concentrations observed along the coast can create co-limiting conditions for other biochemically relevant trace metals such as Co and Ni, thus limiting the response of N_2 fixation to the local availability of Fe (Chapters 2 and 3). In Chapter 3, we propose a hypothesis elucidating the mechanistic pathways through which Ni and Co may enhance N_2 fixation rates in the ETSP, owing to their crucial role as biochemical cofactors in metalloenzymes that support the N_2 fixation process. Recent studies have indicated that *Crocosphaera* spp and *Trichodesmium* spp have an obligate Co requirement and exhibit enhanced growth rates when Ni is added in incubations, suggesting a link between these trace elements and diazotrophs (Bonnet et al., 2010; Rodriguez & Ho, 2014, 2015). In line with our findings, recent research has emphasised the emerging role of Co in regulating marine N_2 fixation, given its function as a cofactor in various biochemical enzymes that influence the growth and activity of diazotrophs. Co serves a dual central role as a cofactor in vitamin B_{12} synthesis and alkaline phosphatase, which is crucial for phosphate acquisition in cyanobacterial and heterotrophic diazotrophs that utilize organic P sources (Bertrand et al., 2011; Dyhrman and Haley, 2006). Furthermore, Co has been proposed to limit primary productivity in the ETSP, potentially establishing an indirect link to N_2 fixation by supporting organic matter inputs (Browning et al., 2018). While Co plumes have frequently been observed in the ETSP, Co scarcity in parts of the ETSP may be associated with its sensitivity to redox conditions (Saito et al., 2017, 2004; Hawco et al., 2016). This implies that during ventilation episodes or in surface oxygenated waters, a significant amount of Co is biologically inert and thus limits the activity of phytoplankton and diazotrophs (Browning et al., 2018; Rapp et al., 2017; Saito et al., 2004).

A potential role for Ni in regulating N_2 fixation is somewhat perplexing, considering that total dissolvable Ni concentrations in surface waters are rarely depleted below 2 nmol L^{-1} in surface waters (John et al., 2022). In the Peruvian region, Ni concentrations typically range between 2 – 10 nmol L^{-1}, which should theoretically be sufficient to support biological activity (Rapp et al., 2020). However, recent studies suggest that not all residual Ni is bioavailable, indicating that Ni can still be limiting biological processes that depend on its bioavailability (Middag et al., 2020). While concentrations of redox trace metals such as Co and Fe increase under anoxic conditions, redox-insensitive trace metals like Ni, do not display such patterns. Thus, Ni concentrations throughout the water column are relatively consistent regardless of O_2 conditions (Hopwood et al. *pers. Comm*, Biller & Bruland, 2013). Ni is deposited in shelf sediments as a component of organic matter and is prone to strong ligand formation, rendering it biologically inert (Dupont et al., 2010). Thus, in highly productive coastal regions such as the ETSP, the high organic matter load in OMZ waters, particularly during summer, coupled with burial in shelf sediments may act as a net sink for Ni (Saito et al., 2004). Consequently, despite a strong Fe source from shelf sediments under anoxic conditions, low Ni bioavailability may co-limit biological processes such as N_2 fixation.

Our findings provide support for an emerging perspective that Ni and Co play a significant regulatory role in N_2 fixation within the Fe-rich coastal waters of the ETSP, challenging previous assumptions for the primary role of P and Fe especially close to the coast. However, the extent of Ni and Co's influence remains unclear. While it is known that both Co and Ni can regulate the growth and activity of autotrophic diazotrophic and non-diazotrophic cyanobacteria, their potential to modulate N_2 fixation in NCDs is still poorly understood (Huertas et al., 2014; Saito et al., 2003). The precise threshold concentrations of Co and Ni for diazotrophs in the ETSP and the global ocean have not been well characterised. Nevertheless, based on my findings, it remains plausible that low concentrations of Ni and Co (Chapter 3), particularly relative to high Fe and P may limit N_2 fixation, at least locally in the ETSP. Currently, resolving the role and strength of overlooked environmental factors such as Co and Ni is complicated by the limited available evidence, which so far reflects local rather than global processes. Therefore, future studies will serve as valuable opportunities to test the proposed role of Ni and Co derived from this dissertation work and determine the extent to which they regulate N_2 fixation in the ETSP and on a global scale.

The advantages offered to diazotrophs' by their presence in proximity to the coast depend on the physicochemical properties of the water column, the metabolic requirements and the genetic capabilities of diazotrophs. In Chapter 2, we observed a significant positive correlation between N_2 fixation rates and proxies for phytoplankton-associated organic matter availability, including POC, turbidity, and chlorophyll *a*, particularly in the southern region where the highest N_2 fixation rates were observed. Our results support previous findings that indicate a direct link between N_2 fixation and phytoplankton-associated organic matter in the ETSP (Löscher et al., 2014; Selden et al., 2021). The enhanced availability of carbon-rich organic particles in productive coastal waters during summer may serve as an energy source for heterotrophic N_2 fixers (Bombar et al., 2016; Pedersen et al., 2018). Moreover, micro-anaerobic environments within particles could provide suitable niches for diazotrophs, protecting nitrogenase from O_2 damage (Severin et al., 2015; Gallon, 1981; Berman-Frank et al., 2005). Thus, a dominance of heterotrophic diazotrophs associated with organic matter or particles may explain the observation of the highest N_2 fixation rates in surface oxic waters during summer (Chapter 2). The sporadic high rates perhaps reflect the heterogeneity of particles, where O_2 and organic carbon are optimal for diazotrophs. During other seasons characterised by low primary productivity, such as autumn and winter (Pennington et al., 2006; Echevin et al., 2008), lower organic matter availability would primarily limit heterotrophic diazotrophs associated with organic particles in the ETSP as was previously demonstrated by Chang et al. (2019). Indeed, sinking particles have been identified as loci for high diazotrophic activity in various oceanic regions (Chakraborty et al., 2021; Pedersen et al., 2018). On the other hand, a high organic matter load may also act as a net sink for Ni (John et al., 2022). Thus, this may reduce bioavailable Ni concentrations to levels that can limit physiological processes supporting growth and N_2 fixation activity such as protection from molecular hydrogen produced during N_2 fixation (Chapter 2, Fig 5.5b,c). These contrasting effects of organic matter

highlight the complexity of understanding its role in regulating N_2 fixation rates. Therefore, a focused assessment is required to unravel the mechanisms by which N_2 fixation rates can be enhanced within particles and quantify the response of N_2 fixation to sinking organic particles in the ETSP.

Despite the co-occurrence of N_2 fixation rates with an intense OMZ, our results did not reveal a significant relationship between N_2 fixation and O_2 concentrations. Instead, we propose an indirect role of O_2 in regulating N_2 fixation in the ETSP. Our findings suggest that the feedback associated with redox changes in environmental variables under sub-oxic to anoxic conditions may have a role in modulating N_2 fixation rates (Fig. 5.5). Anoxic waters often underlie highly productive surface waters with elevated organic particle export (Lam and Kuypers, 2011) whose implications have been discussed above. Additionally, the oxidation state of seawater in the water column primarily influences the distribution of redox-sensitive trace metals such as Fe and Co (Zerkle et al., 2006). Consequently, short to long term fluctuations in O_2 levels can result in significant changes in the concentration of these trace metals, generally exhibiting enhanced concentrations under anoxic conditions (Fig. 5.5). Overall, the regulation of N_2 fixation in the ETSP appears to involve a complex interplay between the seawater redox state, organic matter and trace metal availability (Chapter 2 and 3). It seems that there is a narrow optimal window where these factors align to support significant N_2 fixation rates, but this window is likely not sustained in time due to the dynamic nature of the ETSP. This window may correspond to periods or localised pockets within the water column that result in the sporadic episodes of enhanced rates so far reported despite consistently low rates (Kittu et al., 2023; Löscher et al., 2014).

5.3 Potential mechanisms underpinning spatiotemporal patterns of N_2 fixation and N loss in the ETSP.

Anaerobic microbes exhibit varying sensitivities to O_2 depending on the specific metabolic pathways involved. Exploring this redox sensitivity may provide insights into the observed patterns of N_2 fixation in the ETSP. Within the OMZ of the ETSP, *nif*H genes and transcripts are predominantly associated with proteobacterial sequences, particularly methylotrophic and heterotrophic bacteria including known sulfate-reducers and oxidisers and denitrifiers. This demonstrates the potential for metabolic plasticity in the microbial assemblage of OMZs (Bonnet et al., 2013; Chang et al., 2019; Jayakumar and Ward, 2020; Kalvelage et al., 2013; Turk-Kubo et al., 2014; Löscher et al., 2014; Reeder and Löscher, 2022). Based on these previous studies and the synthesis presented herein, we propose three scenarios that could explain the spatial and temporal patterns and magnitudes of N_2 fixation rates, including the latitudinal pattern, consistently low rates throughout the year and sporadic high rates in summer.

Low N_2 fixation rates approaching the detection limit are consistently observed during austral winter, autumn, and spring, as well as in the northern, less productive part of the HUS during

summer (Fig. 5.3, Chapter 2). Within these spatial-temporal scales, common features such as reduced stratification, higher dilution and a deep mixed layer contribute to the light limitation of primary productivity (Chapter 4), resulting in lower organic matter production (Fig. 5.5a). This limited organic matter availability has been proposed as a major constraint on both complete denitrification and N_2 fixation in the Peruvian OMZ especially in autumn and winter (Dalsgaard et al., 2012; Ward et al., 2008; Chang et al., 2019).

Autonomous continuous profiling floats deployed off Peru have revealed episodic intrusions of O_2 into the OMZ core, predominantly occurring in winter and spring (Whitmire et al., 2009). These events maintain O_2 conditions above the threshold required for complete denitrification and sulphate oxidation or reduction (Ulloa et al., 2012). Although the frequency of these intrusions is not yet well understood, such O_2 dynamics likely play a crucial role in regulating the biogeochemical cycling of redox-dependent elements and processes like N_2 fixation and denitrification. In the sequential process of denitrification, the second and third steps are more sensitive to O_2 sensitive than the first step (Eqn. 2a), thus complete denitrification would be inhibited under periodic reoxygenation events or suboxic conditions. This may explain the low to undetectable rates of complete denitrification reported during the winter-autumn season in the ETSP (Kalvelage et al., 2011, 2013). However, anammox which can tolerate wider O_2 fluctuations would still dominate due to the availability of nitrite from incomplete denitrification (Dalsgaard et al., 2012; Kalvelage et al., 2013). Under these conditions, N_2 fixation could still be dominated by particle-associated NCDs, and some cyanobacteria such as *Crocosphaera* may also be present (Turk-Kubo et al., 2014, Kittu et al., *in prep*). However, anoxic conditions created in organic particles may be temporary. Depending on particle size and carbon-to-nitrogen composition in particles, diazotrophic activity could be carbon limited. Additionally, O_2 diffusion into particles during reoxygenation events may exceed microbial respiration and thus limit N_2 fixation (Chakraborty et al., 2021). Furthermore, concentrations of redox-associated essential trace metals like Fe and Co may also be redox-influenced (Fig. 5.5a). Thus under, periodic anoxic conditions, the duration of time particles harbour low O_2 micro niches and therefore support N_2 fixation may be short-lived. Molecular studies conducted in the ETSP revealed that the presence and expression of *nifH* genes do not necessarily correspond to N_2 fixation activity. Meaning that even though *nifH* transcripts may be present, post-transcription of *nifH* genes and metabolic strategies to actively fix N_2 may still be limited by environmental conditions within, and surrounding diazotrophic cells. This would provide a possible explanation for the low baseline rates in the first spatiotemporal scenario, especially in the euphotic zone (Turk-Kubo et al., 2014).

In the second scenario, when the ETSP experiences enhanced stratification and light availability coupled with nitrate availability such as during summer, a shallower mixed layer and a thin but highly productive euphotic zone develop (Fig. 5.5b). This configuration would result in higher fluxes of organic matter and a shallower upper OMZ (Fig. 5.5b). First, the high organic matter would provide carbon energy sources for particle-associated diazotrophs, such as NCDs. Furthermore, the high organic matter inputs supply organic phosphorus, which has been

shown to support the growth of diazotrophs such as *Crocosphaera* spp and gamma-proteobacteria that are known to thrive mainly on dissolved organic over inorganic phosphorus sources and have also been reported from the ETSP (Dyhrman and Haley, 2006; Ruttenberg and Dyhrman, 2012). Second, the remineralisation of this organic matter consumes O_2, resulting in persistent anoxic conditions where O_2 levels are low enough to support organisms with a denitrification pathway (Kalvelage et al., 2011). Denitrification has been shown to occur mainly during episodes of high organic matter inputs along the Peruvian coast (Dalsgaard et al., 2012; Thamdrup et al., 2006; Ward et al., 2008). Thus, this may partly explain the similarity in the range of magnitudes (0 – 5 nmol N L^{-1} d^{-1}) and the spatiotemporal coupling between N_2 fixation and denitrification during the austral summer season (Chapter 2, Fig. 5.5b), (Kalvelage et al., 2013; Löscher et al., 2014, 2016b; Kittu et al., 2023). Similar patterns can be expected during periods of restratification, such as in spring when light limitation on phytoplankton is relaxed relative to winter and primary production increases.

I propose that the apparent enigma of high *nifH* abundances but low N_2 fixation rates in the ETSP may be attributed to the metabolic plasticity of diazotrophs. For instance, *Dechloromonas* and *Pseudomonadales* clades (*Pseudomonas stutzeri*) found in the Peruvian OMZ exhibit versatile metabolic capabilities, involving coupled denitrification and N_2 fixation within the same cell (Reeder and Löscher, 2022). This suggests the existence of a cryptic N_2 fixation process (Kalvelage et al., 2013; Reeder and Löscher, 2022). In such a case, the N_2 fixation process is utilised to produce H_2 which can then be converted to electrons by a hydrogenase (Li et al., 2022; Robson and Postgate, 1980). These electrons can be subsequently used in the reduction of nitrate during denitrification (Fig. 5.5b). Furthermore, the assimilation of NH_4^+ generated from N_2 fixation may enable these organisms to circumvent the energetically costly process of assimilating nitrate in an anoxic environment . In this case, N_2 is derived internally from nitrate reduction.

The periodicity and seasonality of denitrification, characterised by low to no detectable rates during ventilation events and low organic matter periods, suggest the presence of a natural feedback mechanism that may help maintain nitrate/nitrite within the OMZ. This feedback mechanism could arrest the positive feedback loop between N loss and N_2 fixation at a temporal scale (Su et al., 2015) and allow for anammox, an autotrophic process to prevail. This means, in summer when denitrification is coupled with N_2 fixation rates, the N loss is only partially replenished (section 5.1.2). Thus, at the end of summer, primary productivity in overlying waters becomes N limited. Towards autumn and winter, strong top-down control and a deeper mixed layer result in light limitation on phytoplankton activity, which decreases primary productivity further (Landolfi et al., 2021; Echevin et al., 2008). Thus, a combination of reduced phytoplankton-associated organic matter and intermittent ventilation events limits denitrification rates and the coupling with N_2 fixation during these seasons, thus maintaining nitrate within the OMZ (Canfield, 2006).

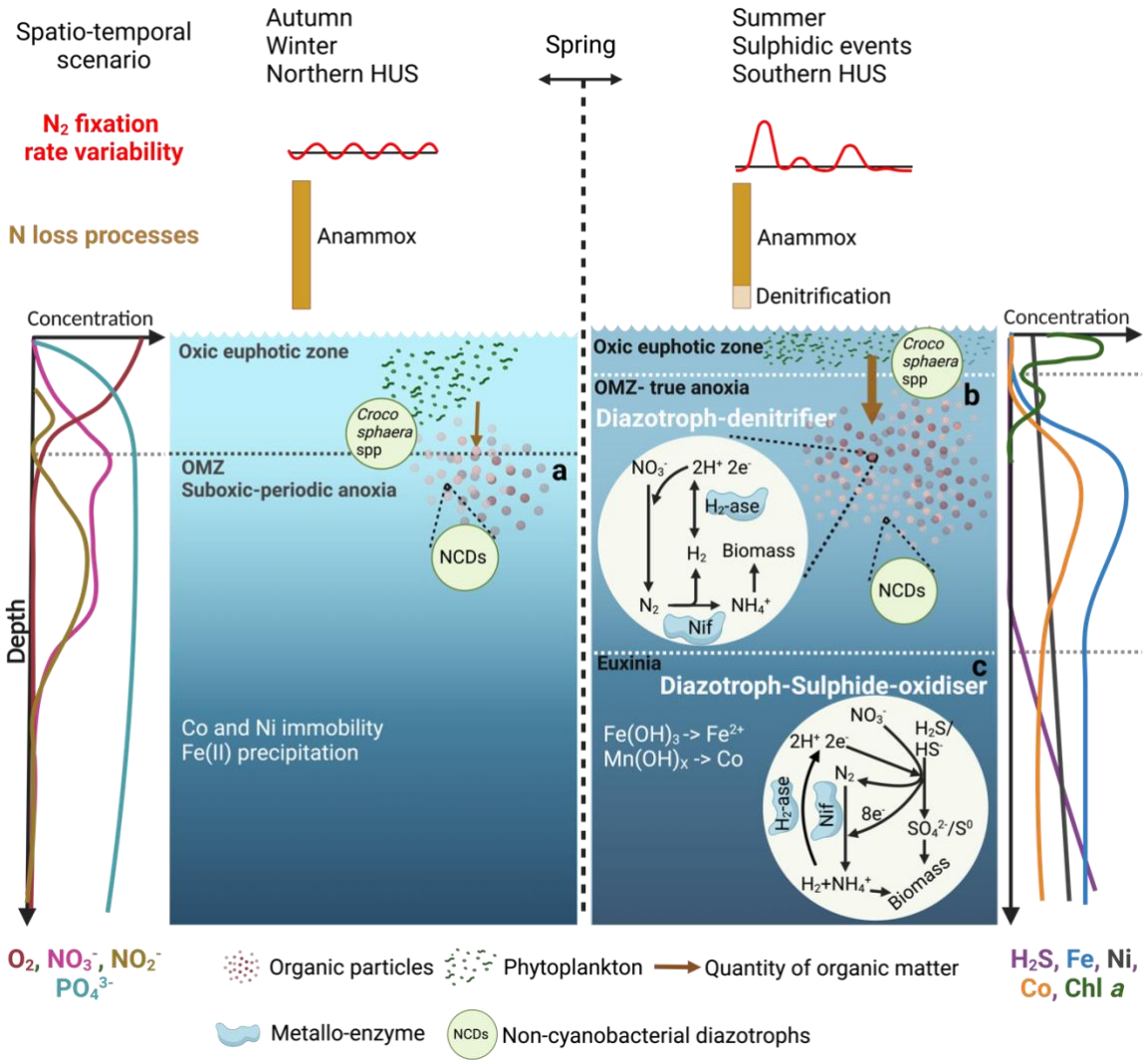

Figure 5.5: Schematic illustration of the response of N_2 fixation and nitrogen loss under various spatial and temporal scenarios. To the far left are simplistic profiles of oxygen (O_2) and macronutrient (nitrate, nitrite, phosphate) distributions in the water column. On the far right are simplistic profiles of trace metals (iron, nickel and cobalt), hydrogen sulphide (H_2S) and Chlorophyll *a*. On (b) and (c) is a schematic overview of proposed metabolic pathways of diazotrophs in fully anoxic and euxinic conditions respectively. *Figure created with BioRender.com.*

In the third scenario, we propose that sulphidic events may play a substantial role in enhancing N_2 fixation rates in the ETSP (Fig 5.5c). Currently, sulphidic events have been reported to be frequent in the ETSP, and their occurrence is predicted to increase in the future due to the expansion of coastal deoxygenation (Callbeck et al., 2018, 2021; Schunck et al., 2013). Marine sulphidic events are extreme cases of anoxia that occur after periods of intense upwelling and high primary productivity, resulting in significant organic matter fluxes and remineralisation. The organic carbon fuels microbial sulphate reduction and sulphide production in shelf sediments. During summer, when ventilation is sluggish, dissolved hydrogen sulphide (H_2S)

diffuses out of the sediments and accumulates in nitrate-free anoxic shelf waters, reaching concentrations exceeding 20 µmol L^{-1}(Callbeck et al., 2021; Schunck et al., 2013). In the ETSP, sulphidic events have been frequently observed and have been shown to alter both N_2 fixation and N loss patterns (Callbeck et al., 2017, 2021; Kalvelage et al., 2013; Löscher et al., 2014).

For instance, two studies have reported sporadic observations of N_2 fixation rates above the average range(> 10 nmol L^{-1} d^{-1}, Supplementary Info, Fig. S1) at coastal sulphidic stations in the ETSP (Schunck et al., 2013). Moreover, denitrification during the austral summer has been linked to high H_2S concentrations and the presence of denitrifier-sulphide-oxidising organisms (Kalvelage et al., 2013). These findings establish a connection between sporadic N_2 fixation rates, denitrification and sulphidic events (Löscher, 2018; Löscher et al., 2014). One possible explanation for the association between N_2 fixation and sulphidic events is that H_2S regulates the bioavailability of bio-essential elements like Fe and Co. Sulphidic events in the Peruvian OMZ coincide with exceptionally high dissolved (Fe^{2+}) concentrations in the water column (Schlosser et al., 2018). Furthermore, the dissolution of manganese oxides, Fe and Co sulphides in localised organic particles or environments during sulphidic conditions may enhance the bioavailability of Co (Dyrssen and Kremling, 1990; Hawco et al., 2016). Consequently, increased concentrations of bio-essential trace metals such as Co and Fe and their utilisation in the metalloenzyme active sites of diazotrophs could periodically enhance N_2 fixation rates during austral summer months (Fig. 5.5c). In this scenario similar to diazotrophs-denitrifiers, enhanced N_2 fixation may be relevant at a cellular level. However, more studies are required to assess the fate of fixed N_2 and its relevance in the environment.

Metabolic plasticity is also common in sulfur-reducing and oxidizing bacteria. Metagenomic studies have provided evidence that a significant proportion of sulphur-reducing and oxidizing bacteria found in organic carbon-rich waters and sediments of the ETSP are also microbes involved in facultative N_2 fixation depending on the level of anoxia (Fernandez et al., 2011; Gier et al., 2016; Löscher et al., 2014; Reeder and Löscher, 2022; Turk-Kubo et al., 2022). For instance, the diazotroph-sulfide-oxidiser *Thiosirochaeta* has been shown to actively fix N_2 in eutrophic OMZs with euxinic conditions (Farnelid et al., 2013; Jayakumar and Ward, 2020; Lavik et al., 2009; Reeder and Löscher, 2022). In a small window where nitrate and H_2S exist, the oxidation of H_2S with nitrate can serve as an electron source for the energetically expensive N_2 fixation activity of diazotrophs sulphur/sulphide-oxidisers (Fig. 5.5c).

It is the case that sulphidic events and true anoxia can coexist within the water column of the ETSP at least temporarily at different depths (Canfield & Kraft, 2022). The intermittency of denitrification, sulphide oxidation and reduction and high N_2 fixation rates suggest that there is a dynamic regime of seawater oxidation state from oxic to anoxic to euxinic waters which could have considerable implications on N cycling locally at fine spatiotemporal scales. Sulphidic events can be seen as analogues for past oceanic states in Earth's history when persistent anoxic events, were characterised by ferruginous waters interspersed with euxinic conditions (Boyle et al., 2013). Thus, these events reveal sequences of biogeochemical

processes in response to intensifying ocean deoxygenation and high organic matter inputs and should therefore be considered a framework to assess N cycling under sustained anoxic conditions in the ETSP. Here the evolutionary history of diazotrophs and requirements may bring insights into what may control N_2 fixation in this scenario.

The coupling of N_2 fixation with other metabolic pathways such as denitrification, sulphide oxidation and reduction suggests that local cellular-level N_2 fixation may be occurring, but may not be detectable using currently employed methods. In both cases of diazotroph-denitrifiers and diazotrophs sulphur-oxidisers, these metabolic pathways would circumvent the high energy required for nitrate assimilation. However, the $^{15}N_2$ incubation method commonly used to estimate N_2 fixation rates may miss the signal of N_2 fixation as N_2 is primarily derived from nitrate reduction rather than from atmospheric N_2. The kinetic isotope effect of consuming N_2 generated from nitrate reduction versus atmospheric N_2 may differ substantially due to stronger isotope fractionation during nitrate reduction (Ryabenko, 2013). Hence this could provide an additional methodical underestimation of N_2 fixation in the ETSP, which would partially explain the generally low measured N_2 fixation rates.

My hypotheses are largely speculative, and considering the high energetic cost of N_2 fixation, one might question why proposed organisms with metabolic plasticity would engage in such an energetically demanding process of N_2 fixation to support other metabolic functions. In addition to the presence of obligate N_2 fixers, a facultative anaerobic lifestyle of diazotrophs in the ETSP could also be inferred from these hypotheses and has previously been suggested to be prevalent in most NCDs (Turk-Kubo et al., 2022; Chakraborty et al., 2021). Thus, to further investigate the pathways proposed, bioassay experiments under the hypothesised scenarios with ^{15}nitrate addition and tracking the release of $^{15}N_2$ and incorporation of $^{15}NH_4^+$ produced via N_2 fixation in biomass could be conducted. Alongside this, metagenome and metatranscriptomic analyses need to be applied to explore the ecophysiology of diazotrophs in the ETSP.

The complexity of interacting physical, and biogeochemical conditions within OMZs, suggests that extrapolations of N_2 fixation controls from other well-studied regions and organisms may not be applicable in the HUS. With these hypotheses, I highlight a largely unexplored niche for organic matter and micronutrient controls extending beyond Fe in both field measurements and biogeochemical models of N_2 fixation. I propose that the next generation of models should be able to couple biogeochemical cycles (macro and micronutrient and including sulphur cycling) in a stoichiometric-explicit and flexible way to enhance our understanding and predictive capabilities of N_2 fixation at a regional scale in the ETSP. The need for such coupled approaches is particularly crucial in the realm of marine biogeochemistry, which has traditionally relied on the Redfield N:P ratio as a primary framework to define the biogeography of biological processes such as N_2 fixation (Ward et al., 2013; Mills and Arrigo, 2010).

5.4 Outlook

5.4.1 Predicted Dynamics of the ETSP

The ETSP faces severe threats of climate change as a result of anthropogenic activity since the beginning of industrialization. These changes have direct and indirect impacts on the systems productivity (Chavez et al., 2011). Rising temperatures in the atmosphere are predicted to contribute to warming which in turn intensifies water column stratification (Schmidtko et al., 2017). Under increased stratification, the fluxes of nitrate to the euphotic zone of the ETSP are predicted to weaken, thus impacting nutrient availability for primary production (Cross-chapter box on net primary production in the ocean, 2023). Additionally, stratification results in an expansion of the thermocline which impedes the ventilation of subsurface waters and reduces the resupply of O_2 into the OMZ (Keeling and Garcia, 2002). Increasing water temperatures also lower the solubility of O_2 in the water column further promoting deoxygenation. With an exponential increase in the coastal human population and need for food, a predicted increase in domestic waste and the use of agricultural fertilizers will likely increase anthropogenic eutrophication of coastal waters further amplifying the imbalance of O_2 demands and resupply (Breitburg et al., 2018).

On the other hand, the predicted intensification of upwelling related to climate change, bringing nitrate to surface waters while good for productivity (Gutiérrez et al., 2011) could expand the OMZ through increased organic matter inputs to subsurface waters. Hence it appears that changes in temperature, upwelling intensity and O_2 concentrations in the HUS suggest an expansion and intensification of the OMZ with direct impacts on N loss (anammox and denitrification) and associated feedbacks (Karstensen et al., 2008). This predicted expansion of the OMZ in the HUS is currently confirmed by model results and observational data (Stramma et al., 2008; Oschlies et al., 2008; Bopp et al., 2013). Hence the O_2-sensitive marine N cycle could be significantly impacted by these climate-related changes as the volume of anoxic and hypoxic waters with O_2 concentrations below the threshold for microbial N loss processes is likely to increase. The occurrence of sulphidic events associated with increased organic matter demonstrates that such events can act as temporally limited hotspots of N turn-over reflected by high N_2 fixation and N loss. Thus, these dynamics suggest a strengthening of the positive feedback loop in the ETSP under the hypothesized scenarios (Fig. 5.5b, c).

How the marine N cycle responds to deoxygenation will determine long-term trends in nutrient retention and marine primary production in the HUS. However, assessing these changes is constrained by uncertainty in how the N source-sink balance will evolve (Buchanan et al., 2019). Nevertheless, a reduction in bioavailable N from the system will have significant implications for primary production that could shift the system from high to low productivity if N loss persists under future expansion in the OMZ and is not compensated by enhanced N_2 fixation at similar magnitudes (Landolfi et al., 2013; Weber and Deutsch, 2014). Small variations in the ratio of N_2 fixation to N loss can significantly impact global atmospheric CO_2

concentrations and marine primary productivity at regional and global scales on short to long timescales (Falkowski, 1997). These characteristics of the OMZ make the ETSP a key environment for controlling the oceans' nitrogen balance (Yang et al., 2017) and therefore a strategic region to keep understanding the potential feedback between the dominant processes of N_2 fixation and N loss.

5.4.2 N_2 fixation in a modern changing ocean

The modern ocean is emerging as neither a direct extension of its earlier forms nor a simple precursor to its future state. Today, we know just enough about the present conditions to develop intriguing hypotheses about the future state and conditions of the ocean and its associated life forms. The arguments presented in this dissertation offer explanations for the observed spatiotemporal patterns and magnitude of N_2 fixation in the HUS, as well as its potential implications in a dynamically changing ocean. These hypotheses should be primarily viewed as fertile ground and a fresh perspective to guide future research endeavors.

The increasing availability of measurements in the global database of N_2 fixation rates over the past decade has shown promise in unravelling the spatial and temporal patterns of N_2 fixation (Luo et al., 2012; Shao et al., 2023). Nonetheless, these measurements have also given rise to more questions, particularly when model predictions deviate from robust field observations (Marconi et al., 2017; Wang et al., 2019). N_2 fixation is known to be energetically expensive and highly sensitive to O_2 inactivation unless cellular mechanisms or diazotroph behaviour mitigate the influence of O_2. In addition, I demonstrate the potential for redox-related environmental conditions such as trace metals to modulate N_2 fixation in reduced environments. Considering the proposed expansion of oxygen minimum zones and the consequent alterations in nitrogen inventories within oxygen-deficient water masses, this dissertation provides insights for future research questions that may help advance our understanding of N_2 fixation in OMZs (Lam and Kuypers, 2011; Canfield and Kraft, 2022; Kalvelage et al., 2011; Stramma et al., 2008).

Considering the evidence for basin-wide coupling of N_2 fixation and N loss in the South Pacific, gaps still remain in assessing the mechanisms governing this intra-basin coupling. Additionally, the timescales at which this basin-wide coupling is relevant are currently not so well understood. On the other hand, the biogeochemical implications of a local coupling of N_2 fixation and N loss on short temporal scales in the ETSP are not clear in the context of an intra-basin coupling. Thus, I propose that a dedicated study on the N cycle in the South Pacific is needed to assess these knowledge gaps. The study would cover the east-to-west extent of the basin on multiple transects. Concurrent N_2 fixation and N loss measurements should be conducted at fine spatiotemporal scales to accurately assess the implications of locally variable biogeochemical N cycle feedbacks in the ETSP for basin-wide N inventories or vice-versa.

The roles and quantitative importance of different groups of N_2-fixing microorganisms are a function of physiological adaptations and ecological controls on growth and activity. These factors, in turn, influence the geographic distribution, ecological competitiveness, and activities of individual species and groups. Molecular-level studies have highlighted the dominance of non-cyanobacterial diazotrophs (NCDs) such as Gamma-proteobacteria and UCYN-A over the bloom-forming cyanobacteria *Trichodesmium* spp in the ETSP (Chang et al., 2019; Löscher et al., 2014; Turk-Kubo et al., 2014). However, a major challenge lies in the fact that many NCDs are to date unculturable, necessitating the development of novel cultivation-independent approaches using natural populations. Nevertheless, Identifying and understanding the physiological functioning of the dominating diazotrophs is important due to the significant variations in size and activity exhibited by different species. Thus, progress in culturing NCDs is crucial for understanding their growth, activity and physiological requirements. This is not only essential for predicting N_2 fixation rates but also the fate of fixed N in the ETSP i.e., what role does it play in the ecosystem?

N_2 fixation is a highly regulated process both due to the high energy demand (high ATP and reductant requirement), sensitivity to O_2 and associated trace metal availability. Thus, multiple pathways are involved before rates can be measured. Unfortunately, the use of *nifH* gene sequences is limited in predicting the metabolic strategies of diazotrophs (Turk-Kubo et al., 2022). Whilst there is some agreement between *nifH* gene sequences and 16S rRNA gene-based phylogeny, this agreement is more robust for cyanobacterial than for NCDs, which are spread across multiple *nifH* clusters (Turk-Kubo et al., 2022; Zehr et al., 2003).

As has been discussed in this dissertation, the involvement of supporting proteins, and enzymes beyond nitrogenase suggests that the complexity of N_2 fixation is influenced by the interactions between the oxidative state of seawater, trace metal cofactors, energy and alternative N sources. Therefore, although the detection of *nifH* gene abundances and expression has been used to infer N_2 fixation activity in NCDs, it is not entirely accurate as N_2 fixation activity can be subject to transcriptional and post-transcriptional control (Turk-Kubo et al., 2022). This means that the recovery of *nifH* sequences and transcripts does not guarantee the presence of organisms that are obligately capable and actively fixing N_2. Some diazotrophic taxa may lack the genes for a functional nitrogenase or dependent enzymes may be limited by environmental conditions (Mise et al., 2021). Thus, the transient nature of N_2 fixation activity associated with NCDs and facultative diazotrophs with diverse metabolic pathways, such as in *P. stutzeri* presents a challenge in validating environmental rates with experimental data. Therefore, inferring N_2 fixation activity and metabolic strategies in diazotrophic species with a high degree of metabolic diversity and flexibility using *nifH* gene abundances and expression as in PCR-based approaches is unsatisfactory. This limitation hinders our understanding of the activity and role of metabolically diverse diazotrophs residing in reduced environments such as coastal OMZs and may explain the observed discrepancy between *nifH* sequence and abundances and N_2 fixation rates in the ETSP (Turk-Kubo et al., 2014).

With ongoing global climate change, the physiological responses of diazotrophic groups to environmental conditions may vary. Thus, it is crucial to mechanistically characterise the metabolic strategies and lifestyles of NCDs to establish links between metabolic diversity, active N_2 fixation and environmental factors that promote their activity. In this regard, I propose that *in situ* measurements should be coupled with bioassay experiments, that aim to disentangle the drivers of N_2 fixation rates. Moreover, techniques exploring the genomic potential and linking N_2 fixers to active N_2 fixation need to be applied in both *in situ* measurements and bioassay experiments to assess the link between metabolic status and activity of NCDs with environmental conditions. These techniques could include whole-genome transcription analysis using pyrosequencing that can detect genes of unknown functions. More broadly, efforts such as the TARA oceans expedition should also be conducted and used to construct metagenome-assembled genomes to evaluate the full range of metabolic potential for uncultured NCDs (Delmont et al., 2021). These large-scale investigations have demonstrated the wealth of diversity in marine microbial communities and functional genes in the ocean. Generally, understanding the ecophysiology of NCDs will pave the way for novel models that are adaptive to the expanding diversity of diazotrophs beyond *Trichodesmium* spp. This advancement will enable the mapping of species-specific growth patterns, elucidating the factors governing their distribution, and evaluating their impact on N cycling (Zehr and Capone, 2020). Such models are instrumental in accurately predicting N_2 fixation rates over longer time scales and forecasting the potential effects of climate change.

One limiting factor to predicting N_2 fixation rates is the paucity of studies reporting trace metal data in parallel with N_2 fixation rates in the ETSP. Among the five datasets presented in this synthesis, only three include accompanying Fe data, and only one encompasses a wide range of trace metals beyond Fe (Kittu et al., 2021). Considering the potential role of trace metals demonstrated in this dissertation work (Chapter 3), and their importance throughout the evolutionary history of diazotrophs, it should become common practice to comprehensively sample trace metal distributions alongside N_2 fixation measurements. Sustaining efforts such as the GEOTRACES Program is crucial for obtaining a better understanding of how trace metal distributions impact biological processes such as diazotrophy in various oceanic regions. The stoichiometry of macro and micronutrient utilization can vary under different nutrient and O_2 regimes (Ho et al 2003). Hence, a fundamental question arising from this doctoral dissertation is whether environmental changes associated with water column redox chemistry, such as the predicted decline in O_2 concentrations (Bopp et al., 2013), trigger evolutionary innovation in marine diazotrophs or enable the emergence of metabolic pathways that existed but remained suppressed over time. Therefore, integrated studies examining diverse gene expressions of metalloenzymes and trace metal requirements for diazotrophs should be adopted in bioassay experiments and field studies to unravel the extent to which trace metals regulate N_2 fixation in reduced environments like OMZs.

When examining the distribution of N_2 fixation in the global ocean, it becomes apparent that marine N_2 fixation exhibits variations across various temporal and spatial scales both regionally

and globally. The concept of space, as utilised in most studies, encompasses N_2 fixation across different geographical locations in the ocean, from water column to sediments, and from coastal to open ocean. Moreover, it can also include processes and interactions at the cellular-to-molecular level. At a temporal scale, the dynamics of geological timescales and changes that occur within that timescale are often investigated after changes have occurred, making it challenging to detect tipping points in processes like N_2 fixation within a system. Thus, on shorter timescales and local geographic scales, it is crucial to identify and develop reliable proxies for N_2 fixation to gain insights into the impacts and sensitivities of the nitrogen cycle to immediate environmental changes. Currently, each component of these complex spatiotemporal scales is studied independently by different disciplines such as genetics, organic chemistry, geobiology, and physical and biological oceanography among others. However, progress can be expedited through research approaches that integrate multiple disciplines to bridge the existing gaps. Considering the sporadic behaviour and high variability of N_2 fixation rates associated with NCDs in the ETSP, single-cell N_2 fixation rates both from *in situ* measurements and bioassay experiments are critically needed to validate the role of NCDs in marine N_2 fixation and better understand their activity. In this regard, coupling isotopic incubations and nanoSIMS (nanoscale secondary ion mass spectrometry) in both *in situ* and bioassay experiments may enable measurements of targeted NCDs single-cell N_2 fixation rates. Additionally, in the case of particle-associated NCDs, the use of nitrogenase immunolabelling approaches can be useful in understanding the mechanisms involved in organic matter-associated N_2 fixation (Geisler et al., 2019).

Although discoveries have resulted in major changes in perspectives, numerous questions remain to be resolved before a comprehensive understanding and accurate predictions of N_2 fixation can be achieved. Certainly, studies on quantifying N_2 fixation in various environments are essential to enhance the resolution upon which large-scale extrapolations are based. In parallel, bioassay experiments under in situ conditions as we have shown are beneficial for disentangling the drivers of N_2 fixation rates. As we look into the next decade of more N_2 fixation measurements that will increase its predictive capacity, promises of exciting new insights and yet more paradigm shifts in our understanding of marine N_2 fixation are evident.

Supplementry information

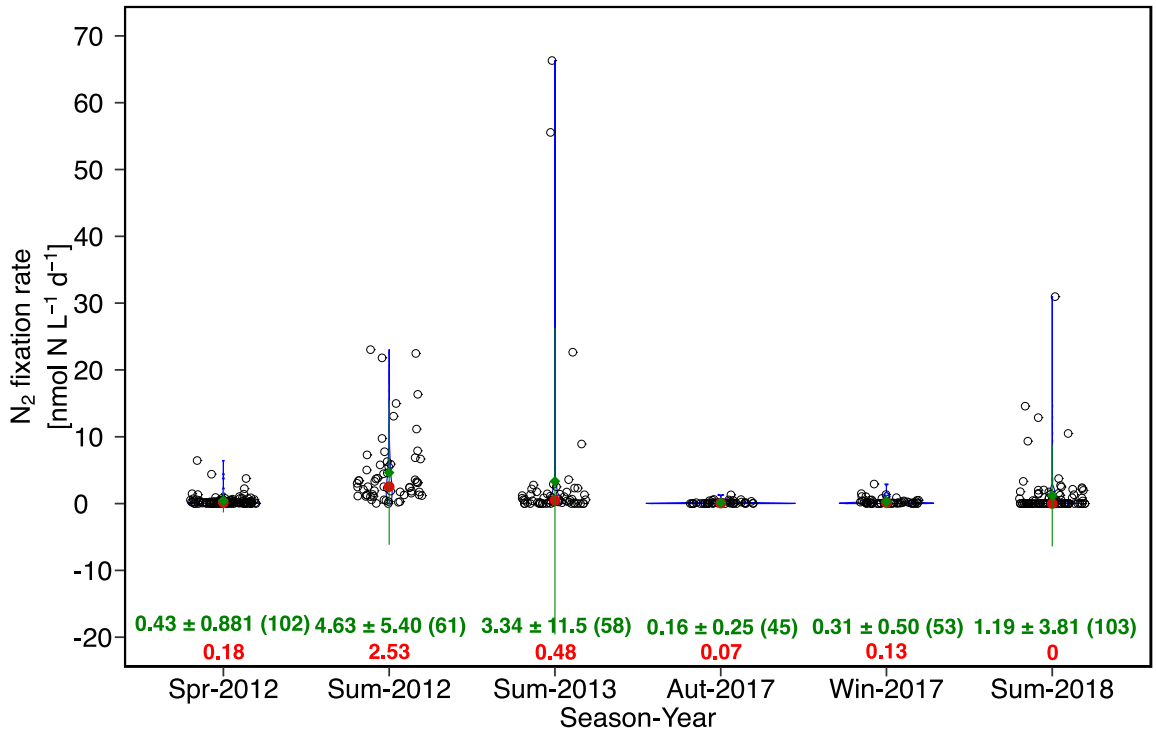

Figure S1: Violin plots indicating the mean and standard deviation and median of volumetric N_2 fixation rates from the northern HUS off Peru across years. N_2 fixation rates from Sum 2018 are the focus of this dissertation work. All other rates were collected during SFB754 cruises (Kittu et al., 2021a). Numbers in parenthesis indicate number of observations per study.

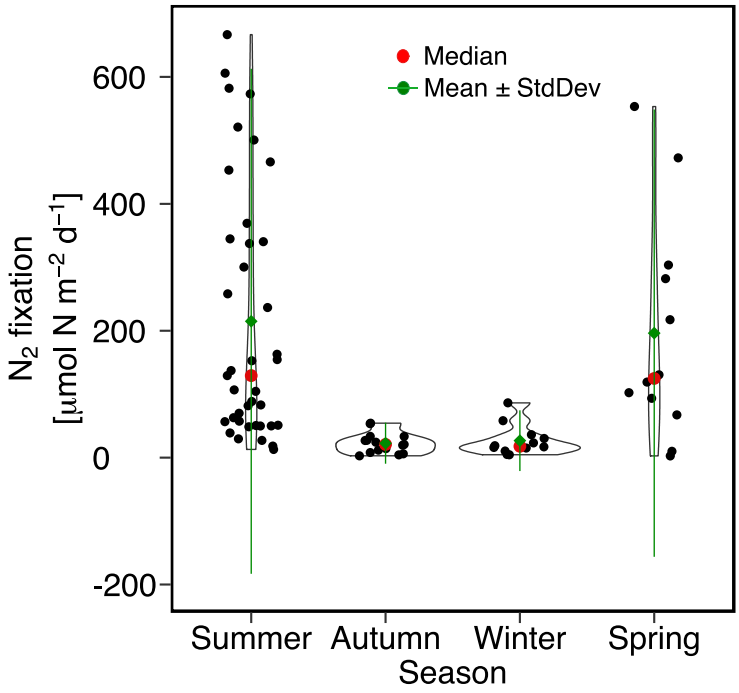

Figure S2: Violin plots indicating the mean and standard deviation and median of integrated N_2 fixation rates from the northern HUS off Peru across seasons. N_2 fixation rates from this dissertation work are included in summer rates (Kittu et al., 2021a). All other rates were collected during SFB754 cruises (Löscher, 2016b, a, 2018)

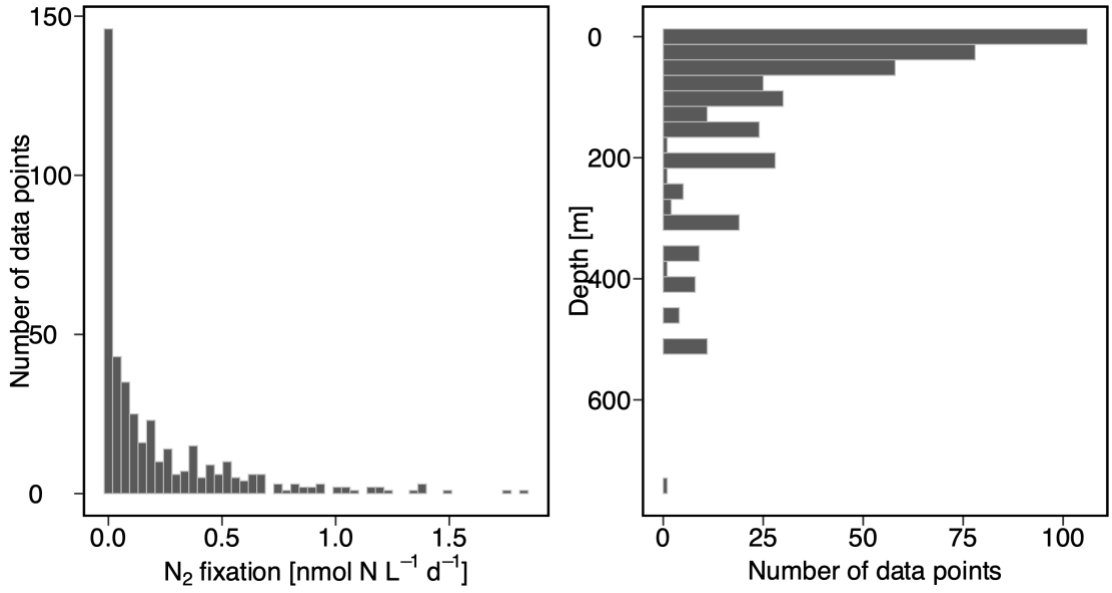

Figure S3: Linear scale distribution of N_2 fixation rates and (b) based on vertical (depth) distribution of data (note the different y-axis).

Table S1: Range of all volumetric N_2 fixation rates reported from the ETSP OMZ between 2006 and 2019

Region	Depth (m)	Location	Austral Season, year	Volumetric N_2 fixation rate (nmol N L^{-1} d^{-1})	Reference
ETSP- Chile	0 - 50	35 – 38.5°S	Summe-Spring 2006, 2009, 2011	0 – 2.5 (2006, 2011) 0 – 120(2011)	(Fernandez et al., 2015)
ETSP - Peru	0 - 400	0° - 20°S	Spring 2005 & Summer 2007	0 - 4	(Fernandez et al., 2011)
ETSP - Peru	0 - 100	Transects at 10°S and 15°S	Summer 2008/2009	BDL – 30	(Löscher et al., 2014)
ETSP - Peru	0 – 2000	Transects at 10°S and 20°S	Summer – Autumn 2010/2011	BDL – 0.80	(Bonnet et al., 2013)
ETSP - Peru	0 - 400	Transect at 20°S	Autumn 2010 & 2011	0 – 1.26	(Knapp et al., 2016)
ETSP - Peru	0 - 200	Transects at 10°S and 20°S	Summer – Autumn 2010/2011	0.01 – 0.88	(Dekaezemacker et al., 2013)
ETSP - Peru	0 - 500	16°S – 17°S	Spring – summer 2012	0 - 5	(Löscher et al., 2016a)
ETSP - Peru	0 - 700	12°S – 20°S	Summer 2015	0 – 0.77	(Selden et al., 2021)
ETSP - Peru	0 - 200	12°S – 13.5°S	Summer-Autumn 2013	0 - 5	(Meyer et al., 2017)
ETSP - Peru	0 - 400	12°S – 20°s	Winter 2013	0 - 5	(Chang et al., 2019)
ETSP - Peru	0 - 300	8°S – 16°S	Summer 2018 - 2019	BDL - 31	(Kittu et al., 2023)*

Bibliography

Chapter 1 & 5.

Altabet, M. A.: Constraints on oceanic N balance/imbalance from sedimentary ^{15}N records, Biogeosciences, 4, 75–86, https://doi.org/10.5194/bg-4-75-2007, 2007.

Anbar, A. D. and Knoll, A. H.: Proterozoic Ocean Chemistry and Evolution: A Bioinorganic Bridge? Science, 297, 1137–1142, https://doi.org/10.1126/science.1069651, 2002.

Arrigo, K. R.: Marine microorganisms and global nutrient cycles, Nature, 437, 349–355, https://doi.org/10.1038/nature04159, 2005.

Barber, R. T. and Chavez, F. P.: Biological Consequences of El Niño, Science, 222, 1203–1210, https://doi.org/10.1126/science.222.4629.1203, 1983.

Behrenfeld, M. J., Randerson, J. T., McClain, C. R., Feldman, G. C., Los, S. O., Tucker, C. J., Falkowski, P. G., Field, C. B., Frouin, R., Esaias, W. E., Kolber, D. D., and Pollack, N. H.: Biospheric Primary Production During an ENSO Transition, Science, 291, 2594–2597, https://doi.org/10.1126/science.1055071, 2001.

Benavides, M. and Voss, M.: Five decades of N_2 fixation research in the North Atlantic Ocean, Front. Mar. Sci., 2, 40, https://doi.org/10.3389/fmars.2015.00040, 2015.

Bentzon-Tilia, M., Severin, I., Hansen, L. H., and Riemann, L.: Genomics and ecophysiology of heterotrophic nitrogen-fixing bacteria isolated from estuarine surface water, mBio, 6, e00929-15, https://doi.org/10.1128/mBio.00929-15, 2015.

Berman-Frank, I., Cullen, J. T., Shaked, Y., Sherrell, R. M., and Falkowski, P. G.: Iron availability, cellular iron quotas, and nitrogen fixation in *Trichodesmium*, Limnol. Oceanogr., 46, 1249–1260, https://doi.org/10.4319/lo.2001.46.6.1249, 2001a.

Berman-Frank, I., Lundgren, P., Chen, Y.-B., Küpper, H., Kolber, Z., Bergman, B., and Falkowski, P.: Segregation of nitrogen fixation and oxygenic photosynthesis in the marine cyanobacterium *Trichodesmium*, Science, 294, 1534–1537, https://doi.org/10.1126/science.1064082, 2001b.

Berman-Frank, I., Chen, Y.-B., Gerchman, Y., Dismukes, G. C., and Falkowski, P. G.: Inhibition of nitrogenase by oxygen in marine cyanobacteria controls the global nitrogen and oxygen cycles, Biogeosci. Discuss., 2, 261–273, https://doi.org/10.5194/bgd-2-261, 2005.

Berthelot, H., Benavides, M., Moisander, P. H., Grosso, O., and Bonnet, S.: High-nitrogen fixation rates in the particulate and dissolved pools in the Western Tropical Pacific (Solomon and Bismarck Seas), Geophys. Res. Lett, 44, 8414–8423, https://doi.org/10.1002/2017GL073856, 2017.

Bertrand, E. M., Saito, M. A., Jeon, Y. J., and Neilan, B. A.: Vitamin B_{12} biosynthesis gene diversity in the Ross Sea: the identification of a new group of putative polar B_{12} biosynthesizers, Environ. Microbiol., 13, 1285–1298, https://doi.org/10.1111/j.1462-2920.2011.02428.x, 2011.

Bettencourt, J. H., López, C., Hernández-García, E., Montes, I., Sudre, J., Dewitte, B., Paulmier, A., and Garçon, V.: Boundaries of the Peruvian oxygen minimum zone shaped by coherent mesoscale dynamics, Nat. Geosci., 8, 937–940, https://doi.org/10.1038/ngeo2570, 2015.

Bianchi, D., Dunne, J. P., Sarmiento, J. L., and Galbraith, E. D.: Data-based estimates of suboxia, denitrification, and N_2O production in the ocean and their sensitivities to dissolved O_2, Global Biogeochem. Cycles, 26, https://doi.org/10.1029/2011GB004209, 2012.

Biller, D. V. and Bruland, K. W.: Sources and distributions of Mn, Fe, Co, Ni, Cu, Zn, and Cd relative to macronutrients along the central California coast during the spring and summer upwelling season, Marine Chemistry, 155, 50–70, https://doi.org/10.1016/j.marchem.2013.06.003, 2013.

Bombar, D., Paerl, R. W., and Riemann, L.: Marine non-cyanobacterial diazotrophs: Moving beyond molecular detection, Trends. Microbiol, 24, 916–927, https://doi.org/10.1016/j.tim.2016.07.002, 2016.

Bonnet, S., Webb, E., Panzeca, C., Karl, D., Capone, D., and Wilhelmy, S. A. S.: Vitamin B_{12} excretion by cultures of the marine cyanobacteria *Crocosphaera* and *Synechococcus*, https://doi.org/10.4319/LO.2010.55.5.1959, 2010.

Bonnet, S., Dekaezemacker, J., Turk-Kubo, K. A., Moutin, T., Hamersley, R. M., Grosso, O., Zehr, J. P., and Capone, D. G.: Aphotic N_2 fixation in the eastern tropical South Pacific Ocean, PLoS ONE, 8, e81265, https://doi.org/10.1371/journal.pone.0081265, 2013.

Bonnet, S., Caffin, M., Berthelot, H., and Moutin, T.: Hot spot of N_2 fixation in the western tropical South Pacific pleads for a spatial decoupling between N_2 fixation and denitrification, PNAS, 114, E2800–E2801, https://doi.org/10.1073/pnas.1619514114, 2017.

Bonnet, S., Caffin, M., Berthelot, H., Grosso, O., Benavides, M., Helias-Nunige, S., Guieu, C., Stenegren, M., and Foster, R. A.: In-depth characterization of diazotroph activity across the western tropical South Pacific hotspot of N_2 fixation (OUTPACE cruise), Biogeosciences, 15, 4215–4232, https://doi.org/10.5194/bg-15-4215-2018, 2018.

Bonnet, S., Guieu, C., Taillandier, V., Boulart, C., Bouruet-Aubertot, P., Gazeau, F., Scalabrin, C., Bressac, M., Knapp, A. N., Cuypers, Y., González-Santana, D., Forrer, H. J., Grisoni, J.-M., Grosso, O., Habasque, J., Jardin-Camps, M., Leblond, N., Le Moigne, F. A. C., Lebourges-Dhaussy, A., Lory, C., Nunige, S., Pulido-Villena, E., Rizzo, A. L., Sarthou, G., and Tilliette, C.: Natural iron fertilization by shallow hydrothermal sources fuels diazotroph blooms in the ocean, Science, 380, 812–817, https://doi.org/10.1126/science.abq4654, 2023.

Bopp, L., Resplandy, L., Orr, J. C., Doney, S. C., Dunne, J. P., Gehlen, M., Halloran, P., Heinze, C., Ilyina, T., Séférian, R., Tjiputra, J., and Vichi, M.: Multiple stressors of ocean ecosystems in the 21st century: projections with CMIP5 models, Biogeosciences, 10, 6225–6245, https://doi.org/10.5194/bg-10-6225-2013, 2013.

Boyd, E., Hamilton, T., and Peters, J.: An Alternative Path for the Evolution of Biological Nitrogen Fixation, Front. Microbiol., 2, 2011.

Boyd, E. S. and Peters, J. W.: New insights into the evolutionary history of biological nitrogen fixation, Front. Microbiol., 4, 201, https://doi.org/10.3389/fmicb.2013.00201, 2013.

Cross-chapter box on net primary production in the ocean: https://epic.awi.de/id/eprint/37516/, last access: 26 June 2023.

Boyer, T. P., Antonov, J. I., Baranova, O. K., Coleman, C., Garcia, H. E., Grodsky, A., Johnson, D. R., Locarnini, R. A., Mishonov, A. V., O'Brien, T. D., Paver, C. R., Reagan, J. R., Seidov, D., Smolyar, I. V., and Zweng, M. M.: World Ocean Database 2013., NOAA Printing Office, https://doi.org/10.25607/OBP-1454, 2013.

Boyle, R. A., Clark, J. R., Poulton, S. W., Shields-Zhou, G., Canfield, D. E., and Lenton, T. M.: Nitrogen cycle feedbacks as a control on euxinia in the mid-Proterozoic Ocean, Nat Commun, 4, 1533, https://doi.org/10.1038/ncomms2511, 2013.

Brandes, J. A. and Devol, A. H.: A global marine-fixed nitrogen isotopic budget: Implications for Holocene nitrogen cycling, Global Biogeochem. Cycles, 16, 67-1-67–14, https://doi.org/10.1029/2001GB001856, 2002.

Breitbarth, E., Oschlies, A., and LaRoche, J.: Physiological constraints on the global distribution of *Trichodesmium* – effect of temperature on diazotrophy, Biogeosciences, 4, 53–61, https://doi.org/10.5194/bg-4-53-2007, 2007.

Breitburg, D., Levin, L., Oschlies, A., Grégoire, M., Chavez, F., Conley, D., Garçon, V., Gilbert, D., Gutiérrez, D., Isensee, K., Jacinto, G., Limburg, K., Montes, I., Naqvi, S., Pitcher, G., Rabalais, N., Roman, M., Rose, K., Seibel, B., Telszewski, M., Yasuhara, M., and Zhang, J.: Declining oxygen in the global ocean and coastal waters, Science, 359, https://doi.org/10.1126/science.aam7240, 2018.

Brink, K. H., Halpern, D., Huyer, A., and Smith, R. L.: The physical environment of the Peruvian upwelling system, Prog. Oceanogr., 12, 285–305, https://doi.org/10.1016/0079-6611(83)90011-3, 1983.

Browning, T. J., Rapp, I., Schlosser, C., Gledhill, M., Achterberg, E. P., Bracher, A., and Moigne, F. A. C. L.: Influence of Iron, Cobalt, and Vitamin B_{12} Supply on Phytoplankton Growth in the

Tropical East Pacific During the 2015 El Niño, Geophys. Res. Lett., 45, 6150–6159, https://doi.org/10.1029/2018GL077972, 2018.

Bruland, K. W., Rue, E. L., Smith, G. J., and DiTullio, G. R.: Iron, macronutrients and diatom blooms in the Peru upwelling regime: brown and blue waters of Peru, Mar. Chem., 93, 81–103, https://doi.org/10.1016/j.marchem.2004.06.011, 2005.

Buchanan, P. J., Chase, Z., Matear, R. J., Phipps, S. J., and Bindoff, N. L.: Marine nitrogen fixers mediate a low latitude pathway for atmospheric CO_2 drawdown, Nat. Commun., 10, 4611, https://doi.org/10.1038/s41467-019-12549-z, 2019.

Callbeck, C. M., Lavik, G., Stramma, L., Kuypers, M. M. M., and Bristow, L. A.: Enhanced Nitrogen Loss by Eddy-Induced Vertical Transport in the Offshore Peruvian Oxygen Minimum Zone, PLOS ONE, 12, e0170059, https://doi.org/10.1371/journal.pone.0170059, 2017.

Callbeck, C. M., Lavik, G., Ferdelman, T. G., Fuchs, B., Gruber-Vodicka, H. R., Hach, P. F., Littmann, S., Schoffelen, N. J., Kalvelage, T., Thomsen, S., Schunck, H., Löscher, C. R., Schmitz, R. A., and Kuypers, M. M. M.: Oxygen minimum zone cryptic sulfur cycling sustained by offshore transport of key sulfur-oxidizing bacteria, Nat. Commun., 9, 1729, https://doi.org/10.1038/s41467-018-04041-x, 2018.

Callbeck, C. M., Canfield, D. E., Kuypers, M. M. M., Yilmaz, P., Lavik, G., Thamdrup, B., Schubert, C. J., and Bristow, L. A.: Sulfur cycling in oceanic oxygen minimum zones, Limnol. Oceanogr., 66, 2360–2392, https://doi.org/10.1002/lno.11759, 2021.

Canfield, D. E.: Models of oxic respiration, denitrification and sulfate reduction in zones of coastal upwelling, Geochim. Cosmochim. Acta., 70, 5753–5765, https://doi.org/10.1016/j.gca.2006.07.023, 2006.

Canfield, D. E. and Kraft, B.: The 'oxygen' in oxygen minimum zones, Environ. Microb., 24, 5332–5344, https://doi.org/10.1111/1462-2920.16192, 2022.

Canfield, D. E., Erik Kristensen, and Bo Thamdrup: The Nitrogen Cycle, in: Advances in Marine Biology, vol. 48, edited by: Canfield, D. E., Kristensen, E., and Thamdrup, B., Academic Press, 205–267, https://doi.org/10.1016/S0065-2881(05)48007-4, 2005.

Canfield, D. E., Glazer, A. N., and Falkowski, P. G.: The evolution and future of Earth's nitrogen cycle, Science, 330, 192–196, https://doi.org/10.1126/science.1186120, 2010.

Capone, D. G. and Carpenter, E. J.: Nitrogen fixation in the marine environment, Science, 217, 1140–1142, https://doi.org/10.1126/science.217.4565.1140, 1982.

Capone, D. G., Zehr, J. P., Paerl, H. W., Bergman, B., and Carpenter, E. J.: *Trichodesmium*, a globally significant marine cyanobacterium, Science, 276, 1221–1229, https://doi.org/10.1126/science.276.5316.1221, 1997.

Capone, D. G., Burns, J. A., Montoya, J. P., Subramaniam, A., Mahaffey, C., Gunderson, T., Michaels, A. F., and Carpenter, E. J.: Nitrogen fixation by *Trichodesmium* spp.: An important source of new nitrogen to the tropical and subtropical North Atlantic Ocean, Global Biogeochem. Cycles, 19, GB2024, https://doi.org/10.1029/2004GB002331, 2005.

Carpenter, E. J. and Capone, D. G.: Chapter 4 - Nitrogen Fixation in the Marine Environment, in: Nitrogen in the Marine Environment (2nd Edition), Academic Press, San Diego, 141–198, https://doi.org/10.1016/B978-0-12-372522-6.00004-9, 2008.

Chaigneau, A., Dominguez, N., Eldin, G., Vasquez, L., Flores, R., Grados, C., and Echevin, V.: Near-coastal circulation in the Northern Humboldt Current System from shipboard ADCP data, Journal of Geophysical Research: Oceans, 118, 5251–5266, https://doi.org/10.1002/jgrc.20328, 2013.

Chakraborty, S., Andersen, K. H., Visser, A. W., Inomura, K., Follows, M. J., and Riemann, L.: Quantifying nitrogen fixation by heterotrophic bacteria in sinking marine particles, Nat. Commun., 12, 4085, https://doi.org/10.1038/s41467-021-23875-6, 2021.

Chang, B. X., Devol, A. H., and Emerson, S. R.: Denitrification and the nitrogen gas excess in the eastern tropical South Pacific oxygen-deficient zone, Deep Sea Research Part I: Oceanographic Research Papers, 57, 1092–1101, https://doi.org/10.1016/j.dsr.2010.05.009, 2010.

Chang, B. X., Jayakumar, A., Widner, B., Bernhardt, P., Mordy, C. W., Mulholland, M. R., and Ward, B. B.: Low rates of dinitrogen fixation in the eastern tropical South Pacific, Limnol. Oceanogr., 64, 1913–1923, https://doi.org/10.1002/lno.11159, 2019.

Chavez, F., Bertrand, A., Guevara-Carrasco, R., Soler, P., and Csirke, J.: The northern Humboldt Current System: Brief history, present status and a view towards the future, Prog. Oceanogr., 79, 95–105, https://doi.org/10.1016/j.pocean.2008.10.012, 2008.

Chavez, F. P., Messié, M., and Pennington, J. T.: Marine primary production in relation to climate variability and change, Ann. Rev. Mar. Sci, 3, 227–260, https://doi.org/10.1146/annurev.marine.010908.163917, 2011.

Chisnell, J. R., Premakumar, R., and Bishop, P. E.: Purification of a second alternative nitrogenase from a *nifHDK* deletion strain of *Azotobacter vinelandii*, Journal of Bacteriology, 170, 27–33, https://doi.org/10.1128/jb.170.1.27-33.1988, 1988.

Christensen, V., de la Puente, S., Sueiro, J. C., Steenbeek, J., and Majluf, P.: Valuing seafood: The Peruvian fisheries sector, Marine Policy, 44, 302–311, https://doi.org/10.1016/j.marpol.2013.09.022, 2014.

Codispoti, L. A.: An oceanic fixed nitrogen sink exceeding 400 Tg N a^{-1} vs the concept of homeostasis in the fixed-nitrogen inventory, Biogeosciences, 4, 233–253, https://doi.org/10.5194/bg-4-233-2007, 2007.

Codispoti, L. A. and Packard, T. T.: Denitrification rates in the eastern tropical South Pacific, J. Mar. Res., 38, 1980.

Codispoti, L. A., Brandes, J. A., Christensen, J. P., Devol, A. H., Naqvi, S. W. A., Paerl, H. W., and Yoshinari, T.: The oceanic fixed nitrogen and nitrous oxide budgets: Moving targets as we enter the Anthropocene? Sci. mar., 65, 85–105, https://doi.org/10.3989/scimar.2001.65s285, 2001.

Cornejo-Castillo, F. M. and Zehr, J. P.: Intriguing size distribution of the uncultured and globally widespread marine non-cyanobacterial diazotroph Gamma-A, ISME J, 15, 124–128, https://doi.org/10.1038/s41396-020-00765-1, 2021.

Dalsgaard, T., Thamdrup, B., Farías, L., and Revsbech, N. P.: Anammox and denitrification in the oxygen minimum zone of the eastern South Pacific, Limnol. Oceanogr., 57, 1331–1346, https://doi.org/10.4319/lo.2012.57.5.1331, 2012.

Davies-Barnard, T., Zaehle, S., and Friedlingstein, P.: Assessment of the impacts of biological nitrogen fixation structural uncertainty in CMIP6 earth system models, Biogeosciences, 19, 3491–3503, https://doi.org/10.5194/bg-19-3491-2022, 2022.

Dekaezemacker, J. and Bonnet, S.: Sensitivity of N_2 fixation to combined nitrogen forms (NO_3^- and NH_4^+) in two strains of the marine diazotroph *Crocosphaera watsonii* (Cyanobacteria), Mar. Ecol. Prog. Ser, 438, 33–46, https://doi.org/10.3354/meps09297, 2011.

Dekaezemacker, J., Bonnet, S., Grosso, O., Moutin, T., Bressac, M., and Capone, D. G.: Evidence of active dinitrogen fixation in surface waters of the eastern tropical South Pacific during El Niño and La Niña events and evaluation of its potential nutrient controls, Global Biogeochem. Cycles, 27, 768–779, https://doi.org/10.1002/gbc.20063, 2013.

Delmont, T. O., Pierella Karlusich, J. J., Veseli, I., Fuessel, J., Eren, A. M., Foster, R. A., Bowler, C., Wincker, P., and Pelletier, E.: Heterotrophic bacterial diazotrophs are more abundant than their cyanobacterial counterparts in metagenomes covering most of the sunlit ocean, ISME J, 1–10, https://doi.org/10.1038/s41396-021-01135-1, 2021.

Deutsch, C. and Weber, T.: Nutrient ratios as a tracer and driver of ocean biogeochemistry, Ann, 4, 113–141, https://doi.org/10.1146/annurev-marine-120709-142821, 2012.

Deutsch, C., Gruber, N., Key, R. M., Sarmiento, J. L., and Ganachaud, A.: Denitrification and N_2 fixation in the Pacific Ocean, Global Biogeochem. Cycles, 15, 483–506, https://doi.org/10.1029/2000GB001291, 2001.

Deutsch, C., Sarmiento, J. L., Sigman, D. M., Gruber, N., and Dunne, J. P.: Spatial coupling of nitrogen inputs and losses in the ocean, Nature, 445, 163, https://doi.org/10.1038/nature05392, 2007.

DeVries, T., Deutsch, C., Primeau, F., Chang, B., and Devol, A.: Global rates of water-column denitrification derived from nitrogen gas measurements, Nat. Geosci., 5, 547–550, https://doi.org/10.1038/ngeo1515, 2012.

Dore, J. E., Letelier, R. M., Church, M. J., Lukas, R., and Karl, D. M.: Summer phytoplankton blooms in the oligotrophic North Pacific Subtropical Gyre: Historical perspective and recent observations, Prog. Oceanogr., 76, 2–38, https://doi.org/10.1016/j.pocean.2007.10.002, 2008.

Duce, R. A., LaRoche, J., Altieri, K., Arrigo, K. R., Baker, A. R., Capone, D. G., Cornell, S., Dentener, F., Galloway, J., Ganeshram, R. S., Geider, R. J., Jickells, T., Kuypers, M. M., Langlois, R., Liss, P. S., Liu, S. M., Middelburg, J. J., Moore, C. M., Nickovic, S., Oschlies, A., Pedersen, T., Prospero, J., Schlitzer, R., Seitzinger, S., Sorensen, L. L., Uematsu, M., Ulloa, O., Voss, M., Ward, B., and Zamora, L.: Impacts of atmospheric anthropogenic nitrogen on the open ocean, Science, 320, 893–897, https://doi.org/10.1126/science.1150369, 2008.

Dugdale, R. C. and Goering, J. J.: Uptake of new and regenerated forms of nitrogen in primary productivity, Limnol. Oceanogr., 12, 196–206, https://doi.org/10.4319/lo.1967.12.2.0196, 1967.

Dupont, C. L., Yang, S., Palenik, B., and Bourne, P. E.: Modern proteomes contain putative imprints of ancient shifts in trace metal geochemistry, Proc. Natl. Acad. Sci., 103, 17822–17827, https://doi.org/10.1073/pnas.0605798103, 2006.

Dupont, C. L., Buck, K. N., Palenik, B., and Barbeau, K.: Nickel utilization in phytoplankton assemblages from contrasting oceanic regimes, Deep Sea Research Part I: Oceanographic Research Papers, 57, 553–566, https://doi.org/10.1016/j.dsr.2009.12.014, 2010.

Duteil, O. and Oschlies, A.: Sensitivity of simulated extent and future evolution of marine suboxia to mixing intensity, Geophysical Research Letters, 38, https://doi.org/10.1029/2011GL046877, 2011.

Dyhrman, S. T. and Haley, S. T.: Phosphorus Scavenging in the Unicellular Marine Diazotroph *Crocosphaera watsonii*, Appl. Environ. Microbiol., 72, 1452–1458, https://doi.org/10.1128/AEM.72.2.1452-1458.2006, 2006.

Dyhrman, S. T., Chappell, P. D., Haley, S. T., Moffett, J. W., Orchard, E. D., Waterbury, J. B., and Webb, E. A.: Phosphonate utilization by the globally important marine diazotroph *Trichodesmium*, Nature, 439, 68–71, https://doi.org/10.1038/nature04203, 2006.

Dyrssen, D. and Kremling, K.: Increasing hydrogen sulfide concentration and trace metal behaviour in the anoxic Baltic waters, Marine Chemistry, 30, 193–204, https://doi.org/10.1016/0304-4203(90)90070-S, 1990.

Echevin, V., Aumont, O., Ledesma, J., and Flores, G.: The seasonal cycle of surface chlorophyll in the Peruvian upwelling system: A modelling study, Prog. Oceanogr., 79, 167–176, 2008.

Falkowski, P. G.: Evolution of the nitrogen cycle and its influence on the biological sequestration of CO_2 in the ocean, Nature, 387, 272–275, https://doi.org/10.1038/387272a0, 1997.

Farnelid, H., Bentzon-Tilia, M., Andersson, A. F., Bertilsson, S., Jost, G., Labrenz, M., Jürgens, K., and Riemann, L.: Active nitrogen-fixing heterotrophic bacteria at and below the chemocline of the central Baltic Sea, ISME J, 7, 1413–1423, https://doi.org/10.1038/ismej.2013.26, 2013.

Fernández, C., Farías, L., and Alcaman, M. E.: Primary production and nitrogen regeneration processes in surface waters of the Peruvian upwelling system, Prog. Oceanogr., 83, 159–168, https://doi.org/10.1016/j.pocean.2009.07.010, 2009.

Fernandez, C., Farías, L., and Ulloa, O.: Nitrogen fixation in denitrified marine waters, PLoS ONE, 6, e20539, https://doi.org/10.1371/journal.pone.0020539, 2011.

Fernandez, C., González, M. L., Muñoz, C., Molina, V., and Farias, L.: Temporal and spatial variability of biological nitrogen fixation off the upwelling system of central Chile (35–38.5°S), J. Geophys. Res. Oceans, 120, 3330–3349, https://doi.org/10.1002/2014JC010410, 2015.

Fernández-Méndez, M., Turk-Kubo, K. A., Buttigieg, P. L., Rapp, J. Z., Krumpen, T., Zehr, J. P., and Boetius, A.: Diazotroph Diversity in the Sea Ice, Melt Ponds, and Surface Waters of the Eurasian Basin of the Central Arctic Ocean, Front. in Microbiol., 7, 1884, https://doi.org/10.3389/fmicb.2016.01884, 2016.

Fiedler, P. C. and Talley, L. D.: Hydrography of the eastern tropical Pacific: A review, Prog. Oceanogr., 69, 143–180, https://doi.org/10.1016/j.pocean.2006.03.008, 2006.

Field, C. B., Behrenfeld, M. J., Randerson, J. T., and Falkowski, P.: Primary production of the biosphere: integrating terrestrial and oceanic components, Science, 281, 237–240, https://doi.org/10.1126/science.281.5374.237, 1998.

Filella, A., Riemann, L., Van Wambeke, F., Pulido-Villena, E., Vogts, A., Bonnet, S., Grosso, O., Diaz, J. M., Duhamel, S., and Benavides, M.: Contrasting Roles of DOP as a Source of Phosphorus and Energy for Marine Diazotrophs, Frontiers in Marine Science, 9, 2022.

Fonseca-Batista, D., Li, X., Riou, V., Michotey, V., Deman, F., Fripiat, F., Guasco, S., Brion, N., Lemaitre, N., Tonnard, M., Gallinari, M., Planquette, H., Planchon, F., Sarthou, G., Elskens, M., LaRoche, J., Chou, L., and Dehairs, F.: Evidence of high N_2 fixation rates in the temperate northeast Atlantic, Biogeosciences, 16, 999–1017, https://doi.org/10.5194/bg-16-999-2019, 2019.

Fowler, D., Coyle, M., Skiba, U., Sutton, M. A., Cape, J. N., Reis, S., Sheppard, L. J., Jenkins, A., Grizzetti, B., Galloway, J. N., Vitousek, P., Leach, A., Bouwman, A. F., Butterbach-Bahl, K., Dentener, F., Stevenson, D., Amann, M., and Voss, M.: The global nitrogen cycle in the twenty-first century, Philosophical Transactions of the Royal Society B: Biological Sciences, 368, 20130164, https://doi.org/10.1098/rstb.2013.0164, 2013.

Franz, J., Krahmann, G., Lavik, G., Grasse, P., Dittmar, T., and Riebesell, U.: Dynamics and stoichiometry of nutrients and phytoplankton in waters influenced by the oxygen minimum zone in the eastern tropical Pacific, Deep Sea Res. Part I Oceanogr. Res. Pap, 62, 20–31, https://doi.org/10.1016/j.dsr.2011.12.004, 2012.

von Friesen, L. W. and Riemann, L.: Nitrogen Fixation in a Changing Arctic Ocean: An Overlooked Source of Nitrogen? Front. in Microbiol., 11, 2020.

Fu, F.-X., Zhang, Y., Bell, P. R. F., and Hutchins, D. A.: Phosphate Uptake and Growth Kinetics of *Trichodesmium* (cyanobacteria) Isolates from the North Atlantic Ocean and the Great Barrier Reef, Australia1, Journal of Phycology, 41, 62–73, https://doi.org/10.1111/j.1529-8817.2005.04063.x, 2005.

Fuenzalida, R., Schneider, W., Garcés-Vargas, J., Bravo, L., and Lange, C.: Vertical and horizontal extension of the oxygen minimum zone in the eastern South Pacific Ocean, Deep Sea Research Part II: Topical Studies in Oceanography, 56, 992–1003, https://doi.org/10.1016/j.dsr2.2008.11.001, 2009.

Gallon, J. R.: The oxygen sensitivity of nitrogenase: a problem for biochemists and micro-organisms, Trends in Biochemical Sciences, 6, 19–23, https://doi.org/10.1016/0968-0004(81)90008-6, 1981.

Galloway, J. N., Dentener, F. J., Capone, D. G., Boyer, E. W., Howarth, R. W., Seitzinger, S. P., Asner, G. P., Cleveland, C. C., Green, P. A., Holland, E. A., Karl, D. M., Michaels, A. F., Porter, J. H., Townsend, A. R., and Vöosmarty, C. J.: Nitrogen cycles: Past, present, and future, Biogeochemistry, 70, 153–226, https://doi.org/10.1007/s10533-004-0370-0, 2004.

Ganeshram, R. S., Pedersen, T. F., Calvert, S. E., and Murray, J. W.: Large changes in oceanic nutrient inventories from glacial to interglacial periods, Nature, 376, 755–758, https://doi.org/10.1038/376755a0, 1995.

Geisler, E., Bogler, A., Rahav, E., and Bar-Zeev, E.: Direct Detection of Heterotrophic Diazotrophs Associated with Planktonic Aggregates, Sci Rep, 9, 9288, https://doi.org/10.1038/s41598-019-45505-4, 2019.

Gier, J., Sommer, S., Löscher, C. R., Dale, A. W., Schmitz, R. A., and Treude, T.: Nitrogen fixation in sediments along a depth transect through the Peruvian oxygen minimum zone, Biogeosciences, 13, 4065–4080, https://doi.org/10.5194/bg-13-4065-2016, 2016.

van de Graaf, A. A., Mulder, A., de Bruijn, P., Jetten, M. S., Robertson, L. A., and Kuenen, J. G.: Anaerobic oxidation of ammonium is a biologically mediated process, Appl. Environ. Microbiol., 61, 1246–1251, https://doi.org/10.1128/aem.61.4.1246-1251.1995, 1995.

Gradoville, Bombar Deniz, Crump Byron C., Letelier Ricardo M., Zehr Jonathan P., and White Angelicque E.: Diversity and activity of nitrogen-fixing communities across ocean basins, Limnol. Oceanogr., 62, 1895–1909, https://doi.org/10.1002/lno.10542, 2017a.

Gradoville, M. R., Bombar, D., Crump, B. C., Letelier, R. M., Zehr, J. P., and White, A. E.: Diversity and activity of nitrogen-fixing communities across ocean basins, Limnol. Oceanogr., 62, 1895–1909, https://doi.org/10.1002/lno.10542, 2017b.

Großkopf, T. and LaRoche, J.: Direct and indirect costs of dinitrogen fixation in *Crocosphaera watsonii* WH8501 and possible implications for the nitrogen cycle, Front. Microbiol., 3, https://doi.org/10.3389/fmicb.2012.00236, 2012.

Großkopf, T., Mohr, W., Baustian, T., Schunck, H., Gill, D., Kuypers, M. M. M., Lavik, G., Schmitz, R. A., Wallace, D. W. R., and LaRoche, J.: Doubling of marine dinitrogen-fixation rates based on direct measurements, Nature, 488, 361–364, https://doi.org/10.1038/nature11338, 2012.

Gruber, N.: The Dynamics of the Marine Nitrogen Cycle and its Influence on Atmospheric CO_2 Variations, in: The Ocean Carbon Cycle and Climate, Dordrecht, 97–148, https://doi.org/10.1007/978-1-4020-2087-2_4, 2004.

Gruber, N.: Chapter 1 - The Marine nitrogen cycle: Overview and Challenges, in: Nitrogen in the marine environment (Second edition), edited by: Capone, D. G., Bronk, D. A., Mulholland, M. R., and Carpenter, E. J., Academic Press, San Diego, 1–50, https://doi.org/10.1016/B978-0-12-372522-6.00001-3, 2008.

Gruber, N. and Galloway, J. N.: An Earth-system perspective of the global nitrogen cycle, Nature, 451, 293–296, https://doi.org/10.1038/nature06592, 2008.

Gruber, N. and Sarmiento, J. L.: Global patterns of marine nitrogen fixation and denitrification, Global Biogeochem. Cycles, 11, 235–266, https://doi.org/10.1029/97GB00077, 1997.

Gutiérrez, D., Bouloubassi, I., Sifeddine, A., Purca, S., Goubanova, K., Graco, M., Field, D., Méjanelle, L., Velazco, F., Lorre, A., Salvatteci, R., Quispe, D., Vargas, G., Dewitte, B., and Ortlieb, L.: Coastal cooling and increased productivity in the main upwelling zone off Peru since the mid-twentieth century, Geophys. Res. Lett., 38, https://doi.org/10.1029/2010GL046324, 2011.

Hales, B. J., Case, E. E., Morningstar, J. E., Dzeda, M. F., and Mauterer, L. A.: Isolation of a new vanadium-containing nitrogenase from *Azotobacter vinelandii*, Biochemistry, 25, 7251–7255, https://doi.org/10.1021/bi00371a001, 1986.

Halm, H., Lam, P., Ferdelman, T. G., Lavik, G., Dittmar, T., LaRoche, J., D'Hondt, S., and Kuypers, M. M. M.: Heterotrophic organisms dominate nitrogen fixation in the South Pacific Gyre, ISME J, 6, 1238–1249, https://doi.org/10.1038/ismej.2011.182, 2012.

Hamersley, M. R., Lavik, G., Woebken, D., Rattray, J. E., Lam, P., Hopmans, E. C., Damsté, J. S. S., Krüger, S., Graco, M., Gutiérrez, D., and Kuypers, M. M. M.: Anaerobic ammonium oxidation in the Peruvian oxygen minimum zone, Limnol. Oceanogr., 52, 923–933, https://doi.org/10.4319/lo.2007.52.3.0923, 2007.

Hawco, N. J., Ohnemus, D. C., Resing, J. A., Twining, B. S., and Saito, M. A.: A dissolved cobalt plume in the oxygen minimum zone of the eastern tropical South Pacific, Biogeosciences, 13, 5697–5717, https://doi.org/10.5194/bg-13-5697-2016, 2016.

Helly, J. J. and Levin, L. A.: Global distribution of naturally occurring marine hypoxia on continental margins, Deep Sea Res. Part I Oceanogr. Res. Pap, 51, 1159–1168, https://doi.org/10.1016/j.dsr.2004.03.009, 2004.

Ho, T.-Y.: Nickel limitation of nitrogen fixation in *Trichodesmium*, Limnol. Oceanogr., 58, 112–120, https://doi.org/10.4319/lo.2013.58.1.0112, 2013.

Hood, R. R., Michaels, A. F., and Capone, D. G.: Answers sought to the enigma of marine nitrogen fixation, Eos, Transactions American Geophysical Union, 81, 133–139, https://doi.org/10.1029/00EO00086, 2000.

Howarth, R. W., Marino, R., and Cole, J. J.: Nitrogen fixation in freshwater, estuarine, and marine ecosystems. 2. Biogeochemical controls, Limnol. Oceanogr., 33, 688–701, https://doi.org/10.4319/lo.1988.33.4part2.0688, 1988.

Huertas, M. J., López-Maury, L., Giner-Lamia, J., Sánchez-Riego, A. M., and Florencio, F. J.: Metals in Cyanobacteria: Analysis of the Copper, Nickel, Cobalt and Arsenic Homeostasis Mechanisms, Life (Basel), 4, 865–886, https://doi.org/10.3390/life4040865, 2014.

Hutchins, D. A. and Boyd, P. W.: Marine phytoplankton and the changing ocean iron cycle, Nature Clim Change, 6, 1072–1079, https://doi.org/10.1038/nclimate3147, 2016.

Huyer, A., Knoll, M., Paluszkiewicz, T., and Smith, R. L.: The Peru Undercurrent: a study in variability, Deep Sea Research Part A. Oceanographic Research Papers, 38, S247–S271, https://doi.org/10.1016/S0198-0149(12)80012-4, 1991.

Ingall, E. and Jahnke, R.: Evidence for enhanced phosphorus regeneration from marine sediments overlain by oxygen-depleted waters, Geochim Cosmochim Acta, 58, 2571–2575, https://doi.org/10.1016/0016-7037(94)90033-7, 1994.

Inomura, K., Bragg, J., Riemann, L., and Follows, M. J.: A quantitative model of nitrogen fixation in the presence of ammonium, PLOS ONE, 13, e0208282, https://doi.org/10.1371/journal.pone.0208282, 2018.

Inomura, K., Deutsch, C., Wilson, S. T., Masuda, T., Lawrenz, E., Bučinská, L., Sobotka, R., Gauglitz, J. M., Saito, M. A., Prášil, O., and Follows, M. J.: Quantifying Oxygen Management and Temperature and Light Dependencies of Nitrogen Fixation by *Crocosphaera watsonii*, mSphere, 4, https://doi.org/10.1128/mSphere.00531-19, 2019.

Jayakumar, A. and Ward, B. B.: Diversity and distribution of Nitrogen Fixation Genes in the Oxygen Minimum Zones of the World Oceans, Biogeosci. Discuss., 1–28, https://doi.org/10.5194/bg-2019-445, 2020.

Jayakumar, A., Al-Rshaidat, M. M. D., Ward, B. B., and Mulholland, M. R.: Diversity, distribution, and expression of diazotroph *nifH* genes in oxygen-deficient waters of the Arabian Sea, FEMS Microbiol. Ecol., 82, 597–606, https://doi.org/10.1111/j.1574-6941.2012.01430.x, 2012.

Jensen, M. M., Lam, P., Revsbech, N. P., Nagel, B., Gaye, B., Jetten, M. S., and Kuypers, M. M.: Intensive nitrogen loss over the Omani Shelf due to anammox coupled with dissimilatory nitrite reduction to ammonium, ISME J, 5, 1660–1670, https://doi.org/10.1038/ismej.2011.44, 2011.

Jickells, T. D., Buitenhuis, E., Altieri, K., Baker, A. R., Capone, D., Duce, R. A., Dentener, F., Fennel, K., Kanakidou, M., LaRoche, J., Lee, K., Liss, P., Middelburg, J. J., Moore, J. K., Okin, G., Oschlies, A., Sarin, M., Seitzinger, S., Sharples, J., Singh, A., Suntharalingam, P., Uematsu, M., and Zamora, L. M.: A reevaluation of the magnitude and impacts of anthropogenic atmospheric nitrogen inputs on the ocean, Global Biogeochem. Cycles, 31, 289–305, https://doi.org/10.1002/2016GB005586, 2017.

John, S. G., Kelly, R. L., Bian, X., Fu, F., Smith, M. I., Lanning, N. T., Liang, H., Pasquier, B., Seelen, E. A., Holzer, M., Wasylenki, L., Conway, T. M., Fitzsimmons, J. N., Hutchins, D. A., and Yang, S.-C.: The biogeochemical balance of oceanic nickel cycling, Nat. Geosci., 1–7, https://doi.org/10.1038/s41561-022-01045-7, 2022.

Kalvelage, T., Jensen, M. M., Contreras, S., Revsbech, N. P., Lam, P., Günter, M., LaRoche, J., Lavik, G., and Kuypers, M. M. M.: Oxygen sensitivity of anammox and coupled N-cycle processes in oxygen minimum zones, PLoS ONE, 6, e29299, https://doi.org/10.1371/journal.pone.0029299, 2011.

Kalvelage, T., Lavik, G., Lam, P., Contreras, S., Arteaga, L., Löscher, C. R., Oschlies, A., Paulmier, A., Stramma, L., and Kuypers, M. M. M.: Nitrogen cycling driven by organic matter export in the South Pacific oxygen minimum zone, Nat. Geosci., 6, 228–234, https://doi.org/10.1038/ngeo1739, 2013.

Kämpf, J. and Chapman, P.: The Functioning of Coastal Upwelling Systems, in: Upwelling Systems of the World: A Scientific Journey to the Most Productive Marine Ecosystems, edited by: Kämpf, J. and Chapman, P., Springer International Publishing, Cham, 31–65, https://doi.org/10.1007/978-3-319-42524-5_2, 2016.

Karl, D., Michaels, A., Bergman, B., Capone, D., Carpenter, E., Letelier, R., Lipschultz, F., Paerl, H., Sigman, D., and Stal, L.: Dinitrogen fixation in the world's oceans, Biogeochemistry, 57–58, 47–98, https://doi.org/10.1023/A:1015798105851, 2002.

Karl, D. M. and Björkman, K. M.: Chapter 5 - Dynamics of dissolved organic phosphorus, in: Biogeochemistry of Marine Dissolved Organic Matter (Second Edition), edited by: Hansell, D. A. and Carlson, C. A., Academic Press, Boston, 233–334, https://doi.org/10.1016/B978-0-12-405940-5.00005-4, 2015.

Karl, D. M. and Letelier, R. M.: Nitrogen fixation-enhanced carbon sequestration in low nitrate, low chlorophyll seascapes, Mar Ecol Prog Ser, 364, 257–268, https://doi.org/10.3354/meps07547, 2008.

Karl, D. M., Church, M. J., Dore, J. E., Letelier, R. M., and Mahaffey, C.: Predictable and efficient carbon sequestration in the North Pacific Ocean supported by symbiotic nitrogen fixation, Proc. Natl. Acad. Sci., 109, 1842–1849, https://doi.org/10.1073/pnas.1120312109, 2012.

Karlusich, J. J. P., Pelletier, E., Lombard, F., Carsique, M., Dvorak, E., Colin, S., Picheral, M., Cornejo-Castillo, F. M., Acinas, S. G., Pepperkok, R., Karsenti, E., de Vargas, C., Wincker, P., Bowler, C., and Foster, R. A.: Global distribution patterns of marine nitrogen-fixers by imaging and molecular methods, Nat. Commun., 12, 1–18, https://doi.org/10.1038/s41467-021-24299-y, 2021.

Karstensen, J. and Ulloa, O.: Peru–Chile Current System, in: Encyclopedia of Ocean Sciences (Second Edition), edited by: Steele, J. H., Academic Press, Oxford, 385–392, https://doi.org/10.1016/B978-012374473-9.00599-3, 2009.

Karstensen, J., Stramma, L., and Visbeck, M.: Oxygen minimum zones in the eastern tropical Atlantic and Pacific Oceans, Prog. Oceanogr., 77, 331–350, https://doi.org/10.1016/j.pocean.2007.05.009, 2008.

Karthäuser, C., Ahmerkamp, S., Marchant, H. K., Bristow, L. A., Hauss, H., Iversen, M. H., Kiko, R., Maerz, J., Lavik, G., and Kuypers, M. M. M.: Small sinking particles control anammox rates in the Peruvian oxygen minimum zone, Nat. Commun., 12, 3235, https://doi.org/10.1038/s41467-021-23340-4, 2021.

Kasting, J. F. and Siefert, J. L.: Biogeochemistry. The nitrogen fix, Nature, 412, 26–27, https://doi.org/10.1038/35083660, 2001.

Keeling, R. F. and Garcia, H. E.: The change in oceanic O_2 inventory associated with recent global warming, Proc. Natl. Acad. Sci., 99, 7848–7853, https://doi.org/10.1073/pnas.122154899, 2002.

Kim, T.-W., Lee, K., Duce, R., and Liss, P.: Impact of atmospheric nitrogen deposition on phytoplankton productivity in the South China Sea, Geophysical Research Letters, 41, 3156–3162, https://doi.org/10.1002/2014GL059665, 2014.

Kittu, L., Paul, A. J., Fernández-Méndez, M., and Riebesell, U.: Nitrogen and carbon fixation rates and organic matter concentrations from water column samples during RV Maria S. Merian cruise MSM80 off the northern Humboldt Upwelling System, https://doi.org/10.1594/PANGAEA.939726, 2021a.

Kittu, L., Hopwood, M. J., Paul, A. J., Fernández-Méndez, M., Achterberg, E. P., and Riebesell, U.: Trace metal data from water column samples during RV Maria S. Merian cruise MSM80 off the northern Humboldt Upwelling System, https://doi.org/10.1594/PANGAEA.939670, 2021b.

Kittu, L. R., Paul, A. J., Fernández-Méndez, M., Hopwood, M. J., and Riebesell, U.: Coastal N_2 Fixation Rates Coincide Spatially with Nitrogen Loss in the Humboldt Upwelling System off Peru, Global Biogeochem. Cycles, 37, e2022GB007578, https://doi.org/10.1029/2022GB007578, 2023.

Knapp, A. N.: The sensitivity of marine N_2 fixation to dissolved inorganic nitrogen, Front. Microbiol., 3, 374, https://doi.org/10.3389/fmicb.2012.00374, 2012.

Knapp, A. N., Casciotti, K. L., Berelson, W. M., Prokopenko, M. G., and Capone, D. G.: Low rates of nitrogen fixation in eastern tropical South Pacific surface waters, Proc. Natl. Acad. Sci., 113, 4398, https://doi.org/10.1073/pnas.1515641113, 2016.

Knapp, A. N., McCabe, K. M., Grosso, O., Leblond, N., Moutin, T., and Bonnet, S.: Distribution and rates of nitrogen fixation in the western tropical South Pacific Ocean constrained by

nitrogen isotope budgets, Biogeosciences, 15, 2619–2628, https://doi.org/10.5194/bg-15-2619-2018, 2018.

Kustka, A., Carpenter, E. J., and Sañudo-Wilhelmy, S. A.: Iron and marine nitrogen fixation: progress and future directions, Research in Microbiology, 153, 255–262, https://doi.org/10.1016/S0923-2508(02)01325-6, 2002.

Kustka, A. B., Sañudo-Wilhelmy, S. A., Carpenter, E. J., Capone, D., Burns, J., and Sunda, W. G.: Iron requirements for dinitrogen- and ammonium-supported growth in cultures of *Trichodesmium* (IMS 101): Comparison with nitrogen fixation rates and iron: carbon ratios of field populations, Limnol. Oceanogr., 49, 1869–1884, https://doi.org/10.4319/lo.2003.48.5.1869, 2003.

Kuypers, M. M. M., Sliekers, A. O., Lavik, G., Schmid, M., Jørgensen, B. B., Kuenen, J. G., Sinninghe Damsté, J. S., Strous, M., and Jetten, M. S. M.: Anaerobic ammonium oxidation by anammox bacteria in the Black Sea, Nature, 422, 608–611, https://doi.org/10.1038/nature01472, 2003.

Kuypers, M. M. M., Lavik, G., Woebken, D., Schmid, M., Fuchs, B. M., Amann, R., Jørgensen, B. B., and Jetten, M. S. M.: Massive nitrogen loss from the Benguela upwelling system through anaerobic ammonium oxidation, Proc. Natl. Acad. Sci., 102, 6478–6483, 2005.

Lam, P. and Kuypers, M. M. M.: Microbial nitrogen cycling processes in oxygen minimum zones, Ann Rev Mar Sci, 3, 317–345, https://doi.org/10.1146/annurev-marine-120709-142814, 2011.

Lam, P., Lavik, G., Jensen, M. M., van de Vossenberg, J., Schmid, M., Woebken, D., Gutiérrez, D., Amann, R., Jetten, M. S. M., and Kuypers, M. M. M.: Revising the nitrogen cycle in the Peruvian oxygen minimum zone, Proc. Natl. Acad. Sci., 106, 4752–4757, https://doi.org/10.1073/pnas.0812444106, 2009.

Landolfi, A., Dietze, H., Koeve, W., and Oschlies, A.: Overlooked runaway feedback in the marine nitrogen cycle: the vicious cycle, Biogeosciences, 10, 1351–1363, https://doi.org/10.5194/bg-10-1351-2013, 2013.

Landolfi, A., Prowe, A. E. F., Pahlow, M., Somes, C. J., Chien, C.-T., Schartau, M., Koeve, W., and Oschlies, A.: Can Top-Down Controls Expand the Ecological Niche of Marine N_2 Fixers? Front. in Microbiol., 12, 2021.

Langlois, R. J., Hümmer, D., and LaRoche, J.: Abundances and Distributions of the Dominant *nifH* Phylotypes in the Northern Atlantic Ocean, Appl. Environ. Microbiol., 74, 1922–1931, https://doi.org/10.1128/AEM.01720-07, 2008.

Lavik, G., Stührmann, T., Brüchert, V., Van der Plas, A., Mohrholz, V., Lam, P., Mußmann, M., Fuchs, B. M., Amann, R., Lass, U., and Kuypers, M. M. M.: Detoxification of sulphidic African

shelf waters by blooming chemolithotrophs, Nature, 457, 581–584, https://doi.org/10.1038/nature07588, 2009.

Li, H.-T., Tuo, S.-H., Lu, M.-C., and Ho, T.-Y.: The effects of Ni availability on H_2 production and N_2 fixation in a model unicellular diazotroph: The expression of hydrogenase and nitrogenase, Limnol. Oceanogr., 67, 1566–1576, https://doi.org/10.1002/lno.12151, 2022.

Liebig, J. F. von: Principles of Agricultural Chemistry: With Special Reference to the Late Researches Made in England, John Wiley, 132 pp., 1855.

Lomnitz, U., Sommer, S., Dale, A. W., Löscher, C. R., Noffke, A., Wallmann, K., and Hensen, C.: Benthic phosphorus cycling in the Peruvian oxygen minimum zone, Biogeosciences, 13, 1367–1386, https://doi.org/10.5194/bg-13-1367-2016, 2016.

Löscher, C. R.: Nitrogen and carbon fixation rates during METEOR cruise M90, https://doi.org/10.1594/PANGAEA.860731, 2016a.

Löscher, C. R.: Nitrogen and carbon fixation rates during METEOR cruise M91, https://doi.org/10.1594/PANGAEA.860732, 2016b.

Löscher, C. R.: Nitrogen and carbon fixation rates during METEOR cruise M93, https://doi.org/10.1594/PANGAEA.884928, 2018.

Löscher, C. R., Großkopf, T., Desai, F. D., Gill, D., Schunck, H., Croot, P. L., Schlosser, C., Neulinger, S. C., Pinnow, N., Lavik, G., Kuypers, M. M. M., LaRoche, J., and Schmitz, R. A.: Facets of diazotrophy in the oxygen minimum zone waters off Peru, ISME J, 8, 2180–2192, https://doi.org/10.1038/ismej.2014.71, 2014.

Löscher, C. R., Bourbonnais, A., Dekaezemacker, J., Charoenpong, C. N., Altabet, M. A., Bange, H. W., Czeschel, R., Hoffmann, C., and Schmitz, R.: N_2 fixation in eddies of the eastern tropical South Pacific Ocean, Biogeosciences, 13, 2889–2899, https://doi.org/10.5194/bg-13-2889-2016, 2016a.

Löscher, C. R., Bange, H. W., Schmitz, R. A., Callbeck, C. M., Engel, A., Hauss, H., Kanzow, T., Kiko, R., Lavik, G., Loginova, A., Melzner, F., Meyer, J., Neulinger, S. C., Pahlow, M., Riebesell, U., Schunck, H., Thomsen, S., and Wagner, H.: Water column biogeochemistry of oxygen minimum zones in the eastern tropical North Atlantic and eastern tropical South Pacific oceans, Biogeosciences, 13, 3585–3606, https://doi.org/10.5194/bg-13-3585-2016, 2016b.

Luo, Y.-W., Doney, S. C., Anderson, L. A., Benavides, M., Berman-Frank, I., Bode, A., Bonnet, S., Boström, K. H., Böttjer, D., Capone, D. G., Carpenter, E. J., Chen, Y. L., Church, M. J., Dore, J. E., Falcón, L. I., Fernández, A., Foster, R. A., Furuya, K., Gómez, F., Gundersen, K., Hynes, A. M., Karl, D. M., Kitajima, S., Langlois, R. J., LaRoche, J., Letelier, R. M., Marañón, E., Jr, M., J, D., Moisander, P. H., Moore, C. M., Mouriño-Carballido, B., Mulholland, M. R., Needoba, J. A.,

Orcutt, K. M., Poulton, A. J., Rahav, E., Raimbault, P., Rees, A. P., Riemann, L., Shiozaki, T., Subramaniam, A., Tyrrell, T., Turk-Kubo, K. A., Varela, M., Villareal, T. A., Webb, E. A., White, A. E., Wu, J., and Zehr, J. P.: Database of diazotrophs in global ocean: abundance, biomass and nitrogen fixation rates, ESSD, 4, 47–73, https://doi.org/10.5194/essd-4-47-2012, 2012.

Luo, Y.-W., Lima, I. D., Karl, D. M., Deutsch, C. A., and Doney, S. C.: Data-based assessment of environmental controls on global marine nitrogen fixation, Biogeosciences, 11, 691–708, https://doi.org/10.5194/bg-11-691-2014, 2014.

Mahaffey, C., Michaels, A. F., and Capone, D. G.: The conundrum of marine N_2 fixation, Am. J. Sci., 305, 546–595, https://doi.org/10.2475/ajs.305.6-8.546, 2005.

Marconi, D., Sigman, D. M., Casciotti, K. L., Campbell, E. C., Alexandra Weigand, M., Fawcett, S. E., Knapp, A. N., Rafter, P. A., Ward, B. B., and Haug, G. H.: Tropical Dominance of N_2 Fixation in the North Atlantic Ocean, Global Biogeochem. Cycles, 31, 1608–1623, https://doi.org/10.1002/2016GB005613, 2017.

Martiny, A. C., Vrugt, J. A., Primeau, F. W., and Lomas, M. W.: Regional variation in the particulate organic carbon to nitrogen ratio in the surface ocean, Global Biogeochem. Cycles, 27, 723–731, https://doi.org/10.1002/gbc.20061, 2013.

Messer, L. F., Mahaffey, C., M Robinson, C., Jeffries, T. C., Baker, K. G., Bibiloni Isaksson, J., Ostrowski, M., Doblin, M. A., Brown, M. V., and Seymour, J. R.: High levels of heterogeneity in diazotroph diversity and activity within a putative hotspot for marine nitrogen fixation, ISME J, 10, 1499–1513, https://doi.org/10.1038/ismej.2015.205, 2016.

Messié, M. and Chavez, F. P.: Seasonal regulation of primary production in eastern boundary upwelling systems, Prog. Oceanogr., 134, 1–18, https://doi.org/10.1016/j.pocean.2014.10.011, 2015.

Messié, M., Ledesma, J., Kolber, D. D., Michisaki, R. P., Foley, D. G., and Chavez, F. P.: Potential new production estimates in four eastern boundary upwelling ecosystems, Prog. Oceanogr., 83, 151–158, https://doi.org/10.1016/j.pocean.2009.07.018, 2009.

Meyer, J., Löscher, C. R., Lavik, G., and Riebesell, U.: Mechanisms of P* Reduction in the Eastern Tropical South Pacific, Front. Mar. Sci., 4, https://doi.org/10.3389/fmars.2017.00001, 2017.

Middag, R., de Baar, H. J. W., Bruland, K. W., and van Heuven, S. M. A. C.: The Distribution of Nickel in the West-Atlantic Ocean, Its Relationship with Phosphate and a Comparison to Cadmium and Zinc, Front. Mar. Sci., 7, 2020.

Mills, M. M. and Arrigo, K. R.: Magnitude of oceanic nitrogen fixation influenced by the nutrient uptake ratio of phytoplankton, Nat. Geosci., 3, 412–416, https://doi.org/10.1038/ngeo856, 2010.

Mise, K., Masuda, Y., Senoo, K., and Itoh, H.: Undervalued Pseudo-*nifH* Sequences in Public Databases Distort Metagenomic Insights into Biological Nitrogen Fixers, mSphere, 6, e00785-21, https://doi.org/10.1128/msphere.00785-21, 2021.

Mohr, W., Großkopf, T., Wallace, D. W. R., and LaRoche, J.: Methodological Underestimation of Oceanic Nitrogen Fixation Rates, PLoS ONE, 5, e12583, https://doi.org/10.1371/journal.pone.0012583, 2010.

Moisander, P., Benavides, M., Bonnet, S., Berman-Frank, I., E White, A., and Riemann, L.: Chasing after non-cyanobacterial nitrogen fixation in marine pelagic environments, Front. Microbiol., 8, https://doi.org/10.3389/fmicb.2017.01736, 2017.

Monteiro, F., Dutkiewicz, S., and J. Follows, M.: Biogeographical controls on the marine nitrogen fixers, Global Biogeochem. Cycles, 25, https://doi.org/10.1029/2010GB003902, 2011.

Montoya, J. P., Holl, C. M., Zehr, J. P., Hansen, A., Villareal, T. A., and Capone, D. G.: High rates of N_2 fixation by unicellular diazotrophs in the oligotrophic Pacific Ocean, Nature, 430, 1027, https://doi.org/10.1038/nature02824, 2004.

Moore, C. M., Mills, M. M., Achterberg, E. P., Geider, R. J., LaRoche, J., Lucas, M. I., McDonagh, E. L., Pan, X., Poulton, A. J., Rijkenberg, M. J. A., Suggett, D. J., Ussher, S. J., and Woodward, E. M. S.: Large-scale distribution of Atlantic nitrogen fixation controlled by iron availability, Nat. Geosci., 2, 867–871, https://doi.org/10.1038/ngeo667, 2009.

Moore, C. M., Mills, M. M., Arrigo, K. R., Berman-Frank, I., Bopp, L., Boyd, P. W., Galbraith, E. D., Geider, R. J., Guieu, C., Jaccard, S. L., Jickells, T. D., La Roche, J., Lenton, T. M., Mahowald, N. M., Marañón, E., Marinov, I., Moore, J. K., Nakatsuka, T., Oschlies, A., Saito, M. A., Thingstad, T. F., Tsuda, A., and Ulloa, O.: Processes and patterns of oceanic nutrient limitation, Nat. Geosci, 6, 701–710, https://doi.org/10.1038/ngeo1765, 2013.

Moore, J. K. and Doney, S. C.: Iron availability limits the ocean nitrogen inventory stabilizing feedbacks between marine denitrification and nitrogen fixation, Global Biogeochem. Cycles, 21, n/a-n/a, https://doi.org/10.1029/2006GB002762, 2007.

Morel, A. and Maritorena, S.: Bio-optical properties of oceanic waters: A reappraisal, Journal of Geophysical Research: Oceans, 106, 7163–7180, https://doi.org/10.1029/2000JC000319, 2001.

Morel, F. M. M. and Price, N. M.: The biogeochemical cycles of trace metals in the oceans, Science, 300, 944–947, https://doi.org/10.1126/science.1083545, 2003.

Moutin, T., Karl, D. M., Duhamel, S., Rimmelin, P., Raimbault, P., Van Mooy, B. A. S., and Claustre, H.: Phosphate availability and the ultimate control of new nitrogen input by nitrogen

fixation in the tropical Pacific Ocean, Biogeosciences, 5, 95–109, https://doi.org/10.5194/bg-5-95-2008, 2008.

Mulholland, M. R., Floge, S., Carpenter, E. J., and Capone, D. G.: Phosphorus dynamics in cultures and natural populations of *Trichodesmium* spp., MEPS, 239, 45–55, https://doi.org/10.3354/meps239045, 2002.

Mulholland, M. R., Bernhardt, P. W., Blanco-Garcia, J. L., Mannino, A., Hyde, K., Mondragon, E., Turk, K., Moisander, P. H., and Zehr, J. P.: Rates of dinitrogen fixation and the abundance of diazotrophs in North American coastal waters between Cape Hatteras and Georges Bank, Limnol. Oceanogr., 57, 1067–1083, https://doi.org/10.4319/lo.2012.57.4.1067, 2012.

Mulholland, M. R., Bernhardt, P. W., Widner, B. N., Selden, C. R., Chappell, P. D., Clayton, S., Mannino, A., and Hyde, K.: High Rates of N_2 Fixation in Temperate, Western North Atlantic Coastal Waters Expand the Realm of Marine Diazotrophy, Global Biogeochem. Cycles, 33, 826–840, https://doi.org/10.1029/2018GB006130, 2019.

Noffke, A., Hensen, C., Sommer, S., Scholz, F., Bohlen, L., Mosch, T., Graco, M., and Wallmann, K.: Benthic iron and phosphorus fluxes across the Peruvian oxygen minimum zone, Limnol. Oceanogr., 57, 851–867, https://doi.org/10.4319/lo.2012.57.3.0851, 2012.

Oschlies, A., Schulz, K. G., Riebesell, U., and Schmittner, A.: Simulated 21st century's increase in oceanic suboxia by CO_2-enhanced biotic carbon export, Global Biogeochem. Cycles, 22, https://doi.org/10.1029/2007GB003147, 2008.

Oschlies, A., Koeve, W., Landolfi, A., and Kähler, P.: Loss of fixed nitrogen causes net oxygen gain in a warmer future ocean, Nat. Commun., 10, 2805, https://doi.org/10.1038/s41467-019-10813-w, 2019.

Paulmier, A., Kriest, I., and Oschlies, A.: Stoichiometries of remineralisation and denitrification in global biogeochemical ocean models, Biogeosciences, 6, 923–935, https://doi.org/10.5194/bg-6-923-2009, 2009.

Pauly, D. and Christensen, V.: Primary production required to sustain global fisheries, Nature, 374, 255–257, https://doi.org/10.1038/374255a0, 1995.

Pedersen, J. N., Bombar, D., Paerl, R. W., and Riemann, L.: Diazotrophs and N_2-Fixation Associated With Particles in Coastal Estuarine Waters, Front. Microbiol., 9, 2759, https://doi.org/10.3389/fmicb.2018.02759, 2018.

Pennington, J. T., Mahoney, K. L., Kuwahara, V. S., Kolber, D. D., Calienes, R., and Chavez, F. P.: Primary production in the eastern tropical Pacific: A review, Prog. Oceanogr., 69, 285–317, https://doi.org/10.1016/j.pocean.2006.03.012, 2006.

Penven, P., Echevin, V., Pasapera, J., Colas, F., and Tam, J.: Average circulation, seasonal cycle, and mesoscale dynamics of the Peru Current System: A modelling approach, Journal of Geophysical Research: Oceans, 110, https://doi.org/10.1029/2005JC002945, 2005.

Rahav, E., Bar-Zeev, E., Ohayion, S., Elifantz, H., Belkin, N., Herut, B., Mulholland, M. R., and Berman-Frank, I. R.: Dinitrogen fixation in aphotic oxygenated marine environments, Front. Microbiol., 4, https://doi.org/10.3389/fmicb.2013.00227, 2013.

Raimbault, P. and Garcia, N.: Evidence for efficient regenerated production and dinitrogen fixation in nitrogen-deficient waters of the South Pacific Ocean: impact on new and export production estimates, Biogeosciences, 5, 323–338, https://doi.org/10.5194/bg-5-323-2008, 2008.

Rapp, I., Schlosser, C., Rusiecka, D., Gledhill, M., and Achterberg, E. P.: Automated preconcentration of Fe, Zn, Cu, Ni, Cd, Pb, Co, and Mn in seawater with analysis using high-resolution sector field inductively-coupled plasma mass spectrometry, Anal Chim Acta, 976, 1–13, https://doi.org/10.1016/j.aca.2017.05.008, 2017.

Rapp, I., Schlosser, C., Browning, T. J., Wolf, F., Le Moigne, F. A. C., Gledhill, M., and Achterberg, E. P.: El Niño-Driven Oxygenation Impacts Peruvian Shelf Iron Supply to the South Pacific Ocean, Geophysical Research Letters, 47, e2019GL086631, https://doi.org/10.1029/2019GL086631, 2020.

Raymond, J., Siefert, J. L., Staples, C. R., and Blankenship, R. E.: The Natural History of Nitrogen Fixation, Molecular Biology and Evolution, 21, 541–554, https://doi.org/10.1093/molbev/msh047, 2004.

Redfield, A. C.: The biological control of chemical factors in the environment, Am. Sci, 46, 205–221, 1958.

Reeder, C. F. and Löscher, C. R.: Nitrogenases in Oxygen Minimum Zone Waters, Front. Mar. Sci., 9, 2022.

Richards, F. A., Cline, J. D., Broenkow, W. W., and Atkinson, L. P.: Some Consequences of the Decomposition of Organic Matter in Lake Nitinat, an Anoxic Fjord, Limnol. Oceanogr., 10, R185–R201, https://doi.org/10.4319/lo.1965.10.suppl2.r185, 1965.

Riemann, L., Farnelid, H., and Steward, G. F.: Nitrogenase genes in non-cyanobacterial plankton: prevalence, diversity and regulation in marine waters, Aquat. Microb. Ecol., 61, 235–247, https://doi.org/10.3354/ame01431, 2010.

Riemann, L., Eyal Rahav, Uta Passow, Hans-Peter Grossart, Dirk de Beer, Isabell Klawonn, Meri Eichner, Mar Benavides, and Edo Bar-Zeev: Planktonic Aggregates as Hotspots for

Heterotrophic Diazotrophy: The Plot Thickens, Front. in Microbiol., https://doi.org/10.3389/fmicb.2022.875050, 2022.

Robson, R. L. and Postgate, J. R.: Oxygen and hydrogen in biological nitrogen fixation, Annu Rev Microbiol, 34, 183–207, https://doi.org/10.1146/annurev.mi.34.100180.001151, 1980.

Rodriguez, I. B. and Ho, T.-Y.: Diel nitrogen fixation pattern of *Trichodesmium*: the interactive control of light and Ni, Sci Rep, 4, 4445, https://doi.org/10.1038/srep04445, 2014.

Rodriguez, I. B. and Ho, T.-Y.: Influence of Co and B_{12} on the growth and nitrogen fixation of *Trichodesmium*, Front. in Microbiol., 6, 623, https://doi.org/10.3389/fmicb.2015.00623, 2015.

Romero, I., Klein, N., Sanudo-Wilhelmy, S., and Capone, D.: Potential Trace Metal Co-Limitation Controls on N_2 Fixation and NO_3^- Uptake in Lakes with Varying Trophic Status, Front. in Microbiol., 4, 2013.

Ruttenberg, K. C. and Dyhrman, S. T.: Dissolved organic phosphorus production during simulated phytoplankton blooms in a coastal upwelling system, Front. Microbiol., 3, https://doi.org/10.3389/fmicb.2012.00274, 2012.

Ryabenko, E.: Stable isotope methods for the study of the nitrogen cycle, in: Topics in Oceanography, IntechOpen, Rijeka, Ch. 3, https://doi.org/10.5772/56105, 2013.

Saito, M. A., Sigman, D. M., and Morel, F. M. M.: The bioinorganic chemistry of the ancient ocean: The co-evolution of cyanobacterial metal requirements and biogeochemical cycles at the Archean-Proterozoic boundary? INORG. CHIM. ACTA, 356, 308–318, https://doi.org/10.1016/S0020-1693(03)00442-0, 2003.

Saito, M. A., Moffett, J. W., and DiTullio, G. R.: Cobalt and nickel in the Peru upwelling region: A major flux of labile cobalt utilized as a micronutrient, Global Biogeochem. Cycles, 18, https://doi.org/10.1029/2003GB002216, 2004.

Saito, M. A., Bertrand, E. M., Dutkiewicz, S., Bulygin, V. V., Moran, D. M., Monteiro, F. M., Follows, M. J., Valois, F. W., and Waterbury, J. B.: Iron conservation by reduction of metalloenzyme inventories in the marine diazotroph *Crocosphaera watsonii*, Proc. Natl. Acad. Sci., 108, 2184–2189, https://doi.org/10.1073/pnas.1006943108, 2011.

Saito, M. A., Noble, A. E., Hawco, N., Twining, B. S., Ohnemus, D. C., John, S. G., Lam, P., Conway, T. M., Johnson, R., Moran, D., and McIlvin, M.: The acceleration of dissolved cobalt's ecological stoichiometry due to biological uptake, remineralization, and scavenging in the Atlantic Ocean, Biogeosciences, 14, 4637–4662, https://doi.org/10.5194/bg-14-4637-2017, 2017.

Schlosser, C., Streu, P., Frank, M., Lavik, G., Croot, P. L., Dengler, M., and Achterberg, E. P.: H_2S events in the Peruvian oxygen minimum zone facilitate enhanced dissolved Fe concentrations, Sci Rep, 8, 12642, https://doi.org/10.1038/s41598-018-30580-w, 2018.

Schmidtko, S., Stramma, L., and Visbeck, M.: Decline in global oceanic oxygen content during the past five decades, Nature, 542, 335–339, https://doi.org/10.1038/nature21399, 2017.

Scholz, F.: Identifying oxygen minimum zone-type biogeochemical cycling in Earth history using inorganic geochemical proxies, Earth-Science Reviews, 184, 29–45, https://doi.org/10.1016/j.earscirev.2018.08.002, 2018.

Schunck, H., Lavik, G., Desai, D. K., Großkopf, T., Kalvelage, T., Löscher, C. R., Paulmier, A., Contreras, S., Siegel, H., Holtappels, M., Rosenstiel, P., Schilhabel, M. B., Graco, M., Schmitz, R. A., Kuypers, M. M. M., and LaRoche, J.: Giant Hydrogen Sulfide Plume in the Oxygen Minimum Zone off Peru Supports Chemolithoautotrophy, PLOS ONE, 8, e68661, https://doi.org/10.1371/journal.pone.0068661, 2013.

Selden, C. R., Mulholland, M. R., Widner, B., Bernhardt, P., and Jayakumar, A.: Toward resolving disparate accounts of the extent and magnitude of nitrogen fixation in the Eastern Tropical South Pacific oxygen-deficient zone, Limnol. Oceanogr., 66, 1950–1960, https://doi.org/10.1002/lno.11735, 2021.

Severin, I., Bentzon-Tilia, M., Moisander, P. H., and Riemann, L.: Nitrogenase expression in estuarine bacterioplankton influenced by organic carbon and availability of oxygen, FEMS Microbiology Letters, 362, https://doi.org/10.1093/femsle/fnv105, 2015.

Shao, Z., Xu, Y., Wang, H., Luo, W., Wang, L., Huang, Y., and Luo, Y.-W.: Version 2 of the global oceanic diazotroph database, Earth System Science Data Discussions, 1–44, https://doi.org/10.5194/essd-2023-13, 2023.

Shiozaki, T., Fujiwara, A., Ijichi, M., Harada, N., Nishino, S., Nishi, S., Nagata, T., and Hamasaki, K.: Diazotroph community structure and the role of nitrogen fixation in the nitrogen cycle in the Chukchi Sea (western Arctic Ocean), Limnol. Oceanogr., 63, 2191–2205, https://doi.org/10.1002/lno.10933, 2018.

Silva, J. J. R. F. da, Williams, R. J. P., Silva, J. J. R. F. da, and Williams, R. J. P.: The Biological Chemistry of the Elements: The Inorganic Chemistry of Life, Second Edition., Oxford University Press, Oxford, New York, 600 pp., 2001.

Sipler, R. E., Gong, D., Baer, S. E., Sanderson, M. P., Roberts, Q. N., Mulholland, M. R., and Bronk, D. A.: Preliminary estimates of the contribution of Arctic nitrogen fixation to the global nitrogen budget, Limnol. Oceanogr. Lett., 2, 159–166, https://doi.org/10.1002/lol2.10046, 2017.

Sohm, J. A. and Capone, D. G.: Phosphorus dynamics of the tropical and subtropical north Atlantic: *Trichodesmium* spp. versus bulk plankton, Mar. Ecol. Prog. Ser, 317, 21–28, https://doi.org/10.3354/meps317021, 2006.

Sohm, J. A., Webb, E. A., and Capone, D. G.: Emerging patterns of marine nitrogen fixation, Nat Rev Microbiol, 9, 499–508, https://doi.org/10.1038/nrmicro2594, 2011.

Stramma, L., Johnson, G. C., Sprintall, J., and Mohrholz, V.: Expanding oxygen-minimum zones in the tropical oceans, Science, 320, 655–658, https://doi.org/10.1126/science.1153847, 2008.

Stramma, L., Schmidtko, S., Bograd, S. J., Ono, T., Ross, T., Sasano, D., and Whitney, F. A.: Trends and decadal oscillations of oxygen and nutrients at 50 to 300 m depth in the equatorial and North Pacific, Biogeosciences, 17, 813–831, https://doi.org/10.5194/bg-17-813-2020, 2020.

Su, B., Pahlow, M., Wagner, H., and Oschlies, A.: What prevents nitrogen depletion in the oxygen minimum zone of the eastern tropical South Pacific? Biogeosciences, 12, 1113–1130, https://doi.org/10.5194/bg-12-1113-2015, 2015.

Tang, W. and Cassar, N.: Data-Driven Modeling of the Distribution of Diazotrophs in the Global Ocean, Geophysical Research Letters, 46, 12258–12269, https://doi.org/10.1029/2019GL084376, 2019.

Tang, W., Li, Z., and Cassar, N.: Machine Learning Estimates of Global Marine Nitrogen Fixation, Journal of Geophysical Research: Biogeosciences, 124, 717–730, https://doi.org/10.1029/2018JG004828, 2019a.

Tang, W., Wang, S., Fonseca-Batista, D., Dehairs, F., Gifford, S., Gonzalez, A. G., Gallinari, M., Planquette, H., Sarthou, G., and Cassar, N.: Revisiting the distribution of oceanic N_2 fixation and estimating diazotrophic contribution to marine production, Nat. Commun., 10, 831, https://doi.org/10.1038/s41467-019-08640-0, 2019b.

Thamdrup, B. and Dalsgaard, T.: Production of N_2 through anaerobic ammonium oxidation coupled to nitrate reduction in marine sediments, Appl. Environ. Microbiol., 68, 1312–1318, https://doi.org/10.1128/AEM.68.3.1312-1318.2002, 2002.

Thamdrup, B., Dalsgaard, T., Jensen, M. M., Ulloa, O., Farías, L., and Escribano, R.: Anaerobic ammonium oxidation in the oxygen-deficient waters off northern Chile, Limnol. Oceanogr., 51, 2145–2156, https://doi.org/10.4319/lo.2006.51.5.2145, 2006.

Tsuchiya, M. and Talley, L. D.: A Pacific hydrographic section at 88°W: Water-property distribution, Journal of Geophysical Research: Oceans, 103, 12899–12918, https://doi.org/10.1029/97JC03415, 1998.

Tuo, S., Rodriguez, I. B., and Ho, T.-Y.: H_2 accumulation and N_2 fixation variation by Ni limitation in Cyanothece, Limnol. Oceanogr., 65, 377–386, https://doi.org/10.1002/lno.11305, 2020.

Turk-Kubo, K., Achilles, K., Serros, T., Ochiai, M., Montoya, J., and Zehr, J.: Nitrogenase (*nifH*) gene expression in diazotrophic cyanobacteria in the Tropical North Atlantic in response to nutrient amendments, Front. in Microbiol., 3, 386, https://doi.org/10.3389/fmicb.2012.00386, 2012.

Turk-Kubo, K. A., Karamchandani, M., Capone, D. G., and Zehr, J. P.: The paradox of marine heterotrophic nitrogen fixation: abundances of heterotrophic diazotrophs do not account for nitrogen fixation rates in the Eastern Tropical South Pacific, Environ. Microbiol., 16, 3095–3114, https://doi.org/10.1111/1462-2920.12346, 2014.

Turk-Kubo, K. A., Connell, P., Caron, D., Hogan, M. E., Farnelid, H. M., and Zehr, J. P.: In Situ Diazotroph Population Dynamics Under Different Resource Ratios in the North Pacific Subtropical Gyre, Front. Microbiol., 9, https://doi.org/10.3389/fmicb.2018.01616, 2018.

Turk-Kubo, K. A., Gradoville, M. R., Cheung, S., Cornejo-Castillo, F. M., Harding, K. J., Morando, M., Mills, M., and Zehr, J. P.: Non-cyanobacterial diazotrophs: global diversity, distribution, ecophysiology, and activity in marine waters, FEMS Microbiology Reviews, fuac046, https://doi.org/10.1093/femsre/fuac046, 2022.

Tyrrell, T.: The relative influences of nitrogen and phosphorus on oceanic primary production, Nature, 400, 525, https://doi.org/10.1038/22941, 1999.

Ulloa, O., Canfield, D. E., DeLong, E. F., Letelier, R. M., and Stewart, F. J.: Microbial oceanography of anoxic oxygen minimum zones, Proc. Natl. Acad. Sci., 109, 15996–16003, https://doi.org/10.1073/pnas.1205009109, 2012.

Voss, M., Bange, H. W., Dippner, J. W., Middelburg, J. J., Montoya, J. P., and Ward, B.: The marine nitrogen cycle: recent discoveries, uncertainties and the potential relevance of climate change, Philos Trans R Soc Lond B Biol Sci, 368, https://doi.org/10.1098/rstb.2013.0121, 2013.

Wang, W.-L., Moore, J. K., Martiny, A. C., and Primeau, F. W.: Convergent estimates of marine nitrogen fixation, Nature, 566, 205–211, https://doi.org/10.1038/s41586-019-0911-2, 2019.

Ward, B. A., Dutkiewicz, S., Moore, C. M., and Follows, M. J.: Iron, phosphorus, and nitrogen supply ratios define the biogeography of nitrogen fixation, Limnol. Oceanogr., 58, 2059–2075, https://doi.org/10.4319/lo.2013.58.6.2059, 2013.

Ward, B. B., Tuit, C. B., Jayakumar, A., Rich, J. J., Moffett, J., and Naqvi, S. W. A.: Organic carbon, and not copper, controls denitrification in oxygen minimum zones of the ocean, Deep Sea Research Part I: Oceanographic Research Papers, 55, 1672–1683, https://doi.org/10.1016/j.dsr.2008.07.005, 2008.

Weber, T. and Deutsch, C.: Local versus basin-scale limitation of marine nitrogen fixation, Proc. Natl. Acad. Sci., 201317193, https://doi.org/10.1073/pnas.1317193111, 2014.

White, A. E., Foster, R. A., Benitez-Nelson, C. R., Masqué, P., Verdeny, E., Popp, B. N., Arthur, K. E., and Prahl, F. G.: Nitrogen fixation in the Gulf of California and the Eastern Tropical North Pacific, Prog. Oceanogr., 109, 1–17, https://doi.org/10.1016/j.pocean.2012.09.002, 2013.

White, A. E., Granger, J., Selden, C., Gradoville, M. R., Potts, L., Bourbonnais, A., Fulweiler, R. W., Knapp, A. N., Mohr, W., Moisander, P. H., Tobias, C. R., Caffin, M., Wilson, S. T., Benavides, M., Bonnet, S., Mulholland, M. R., and Chang, B. X.: A critical review of the $^{15}N_2$ tracer method to measure diazotrophic production in pelagic ecosystems, Limnol. Oceanogr-Meth., 18, 129–147, https://doi.org/10.1002/lom3.10353, 2020.

Whitmire, A. L., Letelier, R. M., Villagrán, V., and Ulloa, O.: Autonomous observations of in vivo fluorescence and particle backscattering in an oceanic oxygen minimum zone, Opt. Express., 17, 21992–22004, https://doi.org/10.1364/OE.17.021992, 2009.

Yang, S., Gruber, N., Long, M. C., and Vogt, M.: ENSO-Driven Variability of Denitrification and Suboxia in the Eastern Tropical Pacific Ocean, Global Biogeochem. Cycles, 31, 1470–1487, https://doi.org/10.1002/2016GB005596, 2017.

Yao, W., Kvale, K. F., Koeve, W., Landolfi, A., Achterberg, E., Bertrand, E. M., and Oschlies, A.: Simulated Future Trends in Marine Nitrogen Fixation Are Sensitive to Model Iron Implementation, Global Biogeochem. Cycles, 36, e2020GB006851, https://doi.org/10.1029/2020GB006851, 2022.

Zehr, J. P. and Capone, D. G.: Changing perspectives in marine nitrogen fixation, Science, 368, eaay9514, https://doi.org/10.1126/science.aay9514, 2020.

Zehr, J. P. and Capone, D. G.: N_2 Fixation in Ocean Basins, in: Marine Nitrogen Fixation, edited by: Zehr, J. P. and Capone, D. G., Springer International Publishing, Cham, 143–156, https://doi.org/10.1007/978-3-030-67746-6_8, 2021.

Zehr, J. P., Mellon, M. T., and Zani, S.: New nitrogen-fixing microorganisms detected in oligotrophic oceans by amplification of Nitrogenase (*nifH*) genes, Appl. Environ. Microbiol., 64, 3444–3450, 1998.

Zehr, J. P., Jenkins, B. D., Short, S. M., and Steward, G. F.: Nitrogenase gene diversity and microbial community structure: a cross-system comparison, Environ. Microbiol., 5, 539–554, https://doi.org/10.1046/j.1462-2920.2003.00451.x, 2003.

Zerkle, A. L., House, C. H., and Brantley, S. L.: Biogeochemical signatures through time as inferred from whole microbial genomes, Am. J. Sci., 305, 467–502, https://doi.org/10.2475/ajs.305.6-8.467, 2005.

Zerkle, A. L., House, C. H., Cox, R. P., and Canfield, D. E.: Metal limitation of cyanobacterial N_2 fixation and implications for the Precambrian nitrogen cycle, Geobiology, 4, 285–297, https://doi.org/10.1111/j.1472-4669.2006.00082.x, 2006.

Chapter 2

Formatted in Global Biogeochemical Cycles Style

Bevington, P., & Robinson, D. K. (2002). *Data reduction and error analysis for the physical sciences* (Revised edition). Boston: Mcgraw Hill Book Co.

Blain, S., Bonnet, S., & Guieu, C. (2008). Dissolved iron distribution in the tropical and sub-tropical South Eastern Pacific. *Biogeosciences*, *5*(1), 269–280. https://doi.org/10.5194/bg-5-269-2008

Bombar, D., Paerl, R. W., & Riemann, L. (2016). Marine non-cyanobacterial diazotrophs: Moving beyond molecular detection. *Trends in Microbiology*, *24*(11), 916–927. https://doi.org/10.1016/j.tim.2016.07.002

Bonnet, S., Guieu, C., Bruyant, F., Prášil, O., Van Wambeke, F., Raimbault, P., et al. (2008). Nutrient limitation of primary productivity in the Southeast Pacific (BIOSOPE cruise). *Biogeosciences*, *5*(1), 215–225. https://doi.org/10.5194/bg-5-215-2008

Bonnet, Sophie, Dekaezemacker, J., Turk-Kubo, K. A., Moutin, T., Hamersley, R. M., Grosso, O., et al. (2013). Aphotic N_2 fixation in the eastern tropical South Pacific Ocean. *PLOS ONE*, *8*(12), e81265. https://doi.org/10.1371/journal.pone.0081265

Bonnet, Sophie, Caffin, M., Berthelot, H., & Moutin, T. (2017). Hot spot of N_2 fixation in the western tropical South Pacific pleads for a spatial decoupling between N_2 fixation and denitrification. *Proceedings of the National Academy of Sciences*, *114*(14), E2800–E2801. https://doi.org/10.1073/pnas.1619514114

Browning, T. J., Rapp, I., Schlosser, C., Gledhill, M., Achterberg, E. P., Bracher, A., & Moigne, F. A. C. L. (2018). Influence of Iron, Cobalt, and Vitamin B12 Supply on Phytoplankton Growth in the Tropical East Pacific During the 2015 El Niño. *Geophysical Research Letters*, *45*(12), 6150–6159. https://doi.org/10.1029/2018GL077972

Bruland, K. W., Rue, E. L., Smith, G. J., & DiTullio, G. R. (2005). Iron, macronutrients and diatom blooms in the Peru upwelling regime: brown and blue waters of Peru. *Marine Chemistry*, *93*(2), 81–103. https://doi.org/10.1016/j.marchem.2004.06.011

Capone, D. G., Burns, J. A., Montoya, J. P., Subramaniam, A., Mahaffey, C., Gunderson, T., et al. (2005). Nitrogen fixation by *Trichodesmium spp.*: An important source of new nitrogen

to the tropical and subtropical North Atlantic Ocean. *Global Biogeochemical Cycles*, *19*(2), GB2024. https://doi.org/10.1029/2004GB002331

Chang, B. X., Devol, A. H., & Emerson, S. R. (2010). Denitrification and the nitrogen gas excess in the eastern tropical South Pacific oxygen-deficient zone. *Deep Sea Research Part I: Oceanographic Research Papers*, *57*(9), 1092–1101. https://doi.org/10.1016/j.dsr.2010.05.009

Chang, B. X., Jayakumar, A., Widner, B., Bernhardt, P., Mordy, C. W., Mulholland, M. R., & Ward, B. B. (2019). Low rates of dinitrogen fixation in the eastern tropical South Pacific. *Limnology and Oceanography*, *64*(5), 1913–1923. https://doi.org/10.1002/lno.11159

Cheung, S., Zehr, J. P., Xia, X., Tsurumoto, C., Endo, H., Nakaoka, S., et al. (2021). Gamma4: a genetically versatile Gammaproteobacterial *nifH* phylotype that is widely distributed in the North Pacific Ocean. *Environmental Microbiology*, *23*(8), 4246–4259. https://doi.org/10.1111/1462-2920.15604.

Chever, F., Rouxel, O. J., Croot, P. L., Ponzevera, E., Wuttig, K., & Auro, M. (2015). Total dissolvable and dissolved iron isotopes in the water column of the Peru upwelling regime. *Geochimica et Cosmochimica Acta*, *162*, 66–82. https://doi.org/10.1016/j.gca.2015.04.031

Codispoti, L. A., & Packard, T. T. (1980). Denitrification rates in the eastern tropical South Pacific, *38*(3).

Codispoti, L. A., Brandes, J. A., Christensen, J. P., Devol, A. H., Naqvi, S. W. A., Paerl, H. W., & Yoshinari, T. (2001). The oceanic fixed nitrogen and nitrous oxide budgets: Moving targets as we enter the Anthropocene? *Scientia Marina*, *65*(S2), 85–105. https://doi.org/10.3989/scimar.2001.65s285

Dekaezemacker, J., Bonnet, S., Grosso, O., Moutin, T., Bressac, M., & Capone, D. G. (2013). Evidence of active dinitrogen fixation in surface waters of the eastern tropical South Pacific during El Niño and La Niña events and evaluation of its potential nutrient controls. *Global Biogeochemical Cycles*, *27*(3), 768–779. https://doi.org/10.1002/gbc.20063

Deutsch, C., Sarmiento, J. L., Sigman, D. M., Gruber, N., & Dunne, J. P. (2007). Spatial coupling of nitrogen inputs and losses in the ocean. *Nature*, *445*(7124), 163. https://doi.org/10.1038/nature05392

DeVries, T., Deutsch, C., Primeau, F., Chang, B., & Devol, A. (2012). Global rates of water-column denitrification derived from nitrogen gas measurements. *Nature Geoscience*, *5*(8), 547–550. https://doi.org/10.1038/ngeo1515

Dutkiewicz, S., Ward, B. A., Monteiro, F., & Follows, M. J. (2012). Interconnection of nitrogen fixers and iron in the Pacific Ocean: Theory and numerical simulations. *Global Biogeochemical Cycles*, *26*(1), GB1012. https://doi.org/10.1029/2011GB004039

Dyhrman, S. T., & Haley, S. T. (2006). Phosphorus Scavenging in the Unicellular Marine Diazotroph *Crocosphaera watsonii*. *Applied and Environmental Microbiology*, *72*(2), 1452–1458. https://doi.org/10.1128/AEM.72.2.1452-1458.2006

Falkowski, P. G. (1997). Evolution of the nitrogen cycle and its influence on the biological sequestration of CO_2 in the ocean. *Nature*, *387*(6630), 272–275. https://doi.org/10.1038/387272a0

Farnelid, H., & Riemann, L. (2008). Heterotrophic N_2 -fixing Bacteria: Overlooked in the Marine Nitrogen Cycle? In *Nitrogen Fixation Research Progress* (pp. 409–423).

Fernández, C., Farías, L., & Alcaman, M. E. (2009). Primary production and nitrogen regeneration processes in surface waters of the Peruvian upwelling system. *Progress in Oceanography*, *83*(1), 159–168. https://doi.org/10.1016/j.pocean.2009.07.010

Fernandez, C., Farías, L., & Ulloa, O. (2011). Nitrogen fixation in denitrified marine waters. *PLOS ONE*, *6*(6), e20539. https://doi.org/10.1371/journal.pone.0020539

Fernandez, C., González, M. L., Muñoz, C., Molina, V., & Farias, L. (2015). Temporal and spatial variability of biological nitrogen fixation off the upwelling system of central Chile (35–38.5°S). *Journal of Geophysical Research: Oceans*, *120*(5), 3330–3349. https://doi.org/10.1002/2014JC010410

Fonseca-Batista, D., Li, X., Riou, V., Michotey, V., Deman, F., Fripiat, F., et al. (2019). Evidence of high N_2 fixation rates in the temperate northeast Atlantic. *Biogeosciences*, *16*(5), 999–1017. https://doi.org/10.5194/bg-16-999-2019

Gradoville, Bombar Deniz, Crump Byron C., Letelier Ricardo M., Zehr Jonathan P., & White Angelicque E. (2017). Diversity and activity of nitrogen-fixing communities across ocean basins. *Limnology and Oceanography*, *62*(5), 1895–1909. https://doi.org/10.1002/lno.10542

Großkopf, T., Mohr, W., Baustian, T., Schunck, H., Gill, D., Kuypers, M. M. M., et al. (2012). Doubling of marine dinitrogen-fixation rates based on direct measurements. *Nature*, *488*(7411), 361–364. https://doi.org/10.1038/nature11338

Gruber, N. (2004). The Dynamics of the Marine Nitrogen Cycle and its Influence on Atmospheric CO_2 Variations. In M. Follows & T. Oguz (Eds.), *The Ocean Carbon Cycle and Climate* (pp. 97–148). Dordrecht: Springer Netherlands. https://doi.org/10.1007/978-1-4020-2087-2_4

Gruber, N., & Galloway, J. N. (2008). An Earth-system perspective of the global nitrogen cycle. *Nature*, *451*(7176), 293–296. https://doi.org/10.1038/nature06592

Hamersley, M. R., Lavik, G., Woebken, D., Rattray, J. E., Lam, P., Hopmans, E. C., et al. (2007). Anaerobic ammonium oxidation in the Peruvian oxygen minimum zone. *Limnology and Oceanography*, *52*(3), 923–933. https://doi.org/10.4319/lo.2007.52.3.0923

Hansen, H. P., & Koroleff, F. (1999). Determination of nutrients. In *Methods of Seawater Analysis* (pp. 159–228). John Wiley & Sons, Ltd. https://doi.org/10.1002/9783527613984.ch10

Hauschildt, J., Thomsen, S., Echevin, V., Oschlies, A., José, Y. S., Krahmann, G., et al. (2021). The fate of upwelled nitrate off Peru shaped by sub-mesoscale filaments and fronts. *Biogeosciences*, *18*(12), 3605–3629. https://doi.org/10.5194/bg-18-3605-2021

Holmes, R. M., Aminot, A., Kérouel, R., Hooker, B. A., & Peterson, B. J. (2011). A simple and precise method for measuring ammonium in marine and freshwater ecosystems. *Canadian Journal of Fisheries and Aquatic Sciences*. https://doi.org/10.1139/f99-128

Hopwood, M. J., Meyer, J., Achterberg, E. P., Gledhill, M., Mutzberg, A., & Nehir, M. (2021). Trace metal data from water samples during METEOR cruise M135 [Data set]. PANGAEA. https://doi.org/10.1594/PANGAEA.928117

Hutchins, D. A., Hare, C. E., Weaver, R. S., Zhang, Y., Firme, G. F., Ditullio, G. R., et al. (2002). Phytoplankton iron limitation in the Humboldt Current and Peru Upwelling. *Limnology and Oceanography*, *47*(4), 997–1011. https://doi.org/10.4319/lo.2002.47.4.0997

Inomura, K., Bragg, J., & Follows, M. J. (2017). A quantitative analysis of the direct and indirect costs of nitrogen fixation: a model based on *Azotobacter vinelandii*. *The ISME Journal*, *11*(1), 166–175. https://doi.org/10.1038/ismej.2016.97

Jayakumar, A., & Ward, B. B. (2020). Diversity and distribution of Nitrogen Fixation Genes in the Oxygen Minimum Zones of the World Oceans. *Biogeosciences*, 1–28. https://doi.org/10.5194/bg-2019-445

Kalvelage, T., Lavik, G., Lam, P., Contreras, S., Arteaga, L., Löscher, C. R., et al. (2013). Nitrogen cycling driven by organic matter export in the South Pacific oxygen minimum zone. *Nature Geoscience*, *6*(3), 228–234. https://doi.org/10.1038/ngeo1739

Karl, D. M., Church, M. J., Dore, J. E., Letelier, R. M., & Mahaffey, C. (2012). Predictable and efficient carbon sequestration in the North Pacific Ocean supported by symbiotic nitrogen fixation. *Proceedings of the National Academy of Sciences*, *109*(6), 1842–1849. https://doi.org/10.1073/pnas.1120312109

Karstensen, J., Stramma, L., & Visbeck, M. (2008). Oxygen minimum zones in the eastern tropical Atlantic and Pacific Oceans. *Progress in Oceanography*, *77*, 331–350. https://doi.org/10.1016/j.pocean.2007.05.009

Karthäuser, C., Ahmerkamp, S., Marchant, H. K., Bristow, L. A., Hauss, H., Iversen, M. H., et al. (2021). Small sinking particles control anammox rates in the Peruvian oxygen minimum zone. *Nature Communications*, *12*(1), 3235. https://doi.org/10.1038/s41467-021-23340-4

Kittu, L., Fernández-Méndez, M., Paul, A. J., Kiko, R., & Riebesell, U. (2021). Dissolved inorganic and organic nutrients from water column samples during RV Maria S. Merian cruise MSM80 off the northern Humboldt Upwelling System [Data set]. PANGAEA. https://doi.org/10.1594/PANGAEA.939667

Kittu, L., Paul, A. J., Fernández-Méndez, M., & Riebesell, U. (2021). Nitrogen and carbon fixation rates and organic matter concentrations from water column samples during RV Maria S. Merian cruise MSM80 off the northern Humboldt Upwelling System [Data set]. PANGAEA. https://doi.org/10.1594/PANGAEA.939726

Kittu, L., Hopwood, M. J., Paul, A. J., Fernández-Méndez, M., Achterberg, E. P., & Riebesell, U. (2021). Trace metal data from water column samples during RV Maria S. Merian cruise MSM80 off the northern Humboldt Upwelling System [Data set]. PANGAEA. https://doi.org/10.1594/PANGAEA.939670

Klawonn, I., Bonaglia, S., Brüchert, V., & Ploug, H. (2015). Aerobic and anaerobic nitrogen transformation processes in N_2-fixing cyanobacterial aggregates. *The ISME Journal*, *9*(6), 1456–1466. https://doi.org/10.1038/ismej.2014.232

Knapp, A. N., Casciotti, K. L., Berelson, W. M., Prokopenko, M. G., & Capone, D. G. (2016). Low rates of nitrogen fixation in eastern tropical South Pacific surface waters. *Proceedings of the National Academy of Sciences*, *113*(16), 4398. https://doi.org/10.1073/pnas.1515641113

Kustka, A., Carpenter, E. J., & Sañudo-Wilhelmy, S. A. (2002). Iron and marine nitrogen fixation: progress and future directions. *Research in Microbiology*, *153*(5), 255–262. https://doi.org/10.1016/S0923-2508(02)01325-6

Kustka, A. B., Sañudo-Wilhelmy, S. A., Carpenter, E. J., Capone, D., Burns, J., & Sunda, W. G. (2003). Iron requirements for dinitrogen- and ammonium-supported growth in cultures of *Trichodesmium* (IMS 101): Comparison with nitrogen fixation rates and iron: carbon ratios of field populations. *Limnology and Oceanography*, *49*(4), 1869–1884. https://doi.org/10.4319/lo.2003.48.5.1869

Lam, P., Lavik, G., Jensen, M. M., van de Vossenberg, J., Schmid, M., Woebken, D., et al. (2009). Revising the nitrogen cycle in the Peruvian oxygen minimum zone. *Proceedings of the National Academy of Sciences of the United States of America*, *106*(12), 4752–4757. https://doi.org/10.1073/pnas.0812444106

Landolfi, A., Dietze, H., Koeve, W., & Oschlies, A. (2013). Overlooked runaway feedback in the marine nitrogen cycle: the vicious cycle. *Biogeosciences*, *10*(3), 1351–1363. https://doi.org/10.5194/bg-10-1351-2013

Riemann, L., Eyal Rahav, Uta Passow, Hans-Peter Grossart, Dirk de Beer, Isabell Klawonn, et al. (2022). Planktonic Aggregates as Hotspots for Heterotrophic Diazotrophy: The Plot Thickens. *Frontiers in Microbiology*. https://doi.org/10.3389/fmicb.2022.875050

Löscher, C. R., Großkopf, T., Desai, F. D., Gill, D., Schunck, H., Croot, P. L., et al. (2014). Facets of diazotrophy in the oxygen minimum zone waters off Peru. *The ISME Journal*, *8*(11), 2180–2192. https://doi.org/10.1038/ismej.2014.71

Luo, Y.-W., Lima, I. D., Karl, D. M., Deutsch, C. A., & Doney, S. C. (2014). Data-based assessment of environmental controls on global marine nitrogen fixation. *Biogeosciences*, *11*(3), 691–708. https://doi.org/10.5194/bg-11-691-2014

Messié, M., & Chavez, F. P. (2015). Seasonal regulation of primary production in eastern boundary upwelling systems. *Progress in Oceanography*, *134*, 1–18. https://doi.org/10.1016/j.pocean.2014.10.011

Meyer, J., Löscher, C. R., Neulinger, S. C., Reichel, A. F., Loginova, A., Borchard, C., et al. (2016). Changing nutrient stoichiometry affects phytoplankton production, DOP accumulation, and dinitrogen fixation – a mesocosm experiment in the eastern tropical North Atlantic. *Biogeosciences*, *13*(3), 781–794. https://doi.org/10.5194/bg-13-781-2016

Meyer, J., Löscher, C. R., Lavik, G., & Riebesell, U. (2017). Mechanisms of P* Reduction in the Eastern Tropical South Pacific. *Frontiers in Marine Science*, *4*. https://doi.org/10.3389/fmars.2017.00001

Mohr, W., Großkopf, T., Wallace, D. W. R., & LaRoche, J. (2010). Methodological Underestimation of Oceanic Nitrogen Fixation Rates. *PLOS ONE*, *5*(9), e12583. https://doi.org/10.1371/journal.pone.0012583

Montoya, J. P., Voss, M., Kahler, P., & Capone, D. G. (1996). A simple, high-precision, high-sensitivity tracer assay for N_2 fixation. *Applied and Environmental Microbiology*, *62*(3), 986–993. https://doi: 10.1128/aem.62.3.986-993.1996.

Moore, C. M. (2016). Diagnosing oceanic nutrient deficiency. *Philosophical Transactions of the Royal Society A: Mathematical, Physical and Engineering Sciences*, *374*(2081), 20150290. https://doi.org/10.1098/rsta.2015.0290

Moore, C. M., Mills, M. M., Arrigo, K. R., Berman-Frank, I., Bopp, L., Boyd, P. W., et al. (2013). Processes and patterns of oceanic nutrient limitation. *Nature Geoscience*, *6*(9), 701–710. https://doi.org/10.1038/ngeo1765.

Moore, J. K., & Doney, S. C. (2007). Iron availability limits the ocean nitrogen inventory stabilizing feedback between marine denitrification and nitrogen fixation. *Global Biogeochemical Cycles*, *21*(2), n/a-n/a. https://doi.org/10.1029/2006GB002762

Morris, A. W., & Riley, J. P. (1963). The determination of nitrate in seawater. *Analytica Chimica Acta*, *29*, 272–279. https://doi.org/10.1016/S0003-2670(00)88614-6

Mulholland, M. R., Bernhardt, P. W., Blanco-Garcia, J. L., Mannino, A., Hyde, K., Mondragon, E., et al. (2012). Rates of dinitrogen fixation and the abundance of diazotrophs in North American coastal waters between Cape Hatteras and Georges Bank. *Limnology and Oceanography*, *57*, 1067–1083. https://doi.org/10.4319/lo.2012.57.4.1067

Murphy, J., & Riley, J. P. (1962). A modified single solution method for the determination of phosphate in natural waters. *Analytica Chimica Acta*, *27*, 31–36. https://doi.org/10.1016/S0003-2670(00)88444-5

NASA Ocean Biology Processing Group. (2017). MODIS-Aqua Level 3 Mapped Chlorophyll Data Version R2018.0 [Data set]. NASA Ocean Biology DAAC. https://doi.org/10.5067/AQUA/MODIS/L3M/CHL/2018

NASA/JPL. (2020). MODIS Aqua Level 3 SST Thermal IR Annual 4km Daytime V2019.0 [Data set]. NASA Physical Oceanography DAAC. https://doi.org/10.5067/MODSA-AN4D9

Noffke, A., Hensen, C., Sommer, S., Scholz, F., Bohlen, L., Mosch, T., et al. (2012). Benthic iron and phosphorus fluxes across the Peruvian oxygen minimum zone. *Limnology and Oceanography*, *57*(3), 851–867. https://doi.org/10.4319/lo.2012.57.3.0851

Parekh, P., Follows, M. J., & Boyle, E. A. (2005). Decoupling of iron and phosphate in the global ocean. *Global Biogeochemical Cycles*, *19*(2). https://doi.org/10.1029/2004GB002280

Paulmier, A., Kriest, I., & Oschlies, A. (2009). Stoichiometries of remineralisation and denitrification in global biogeochemical ocean models. *Biogeosciences*, *6*(5), 923–935. https://doi.org/10.5194/bg-6-923-2009

Rapp, I., Schlosser, C., Rusiecka, D., Gledhill, M., & Achterberg, E. P. (2017). Automated preconcentration of Fe, Zn, Cu, Ni, Cd, Pb, Co, and Mn in seawater with analysis using

high-resolution sector field inductively-coupled plasma mass spectrometry. *Analytica Chimica Acta*, *976*, 1–13. https://doi.org/10.1016/j.aca.2017.05.008

Rapp, I., Schlosser, C., Browning, T. J., Wolf, F., Moigne, F. A. C. L., Gledhill, M., & Achterberg, E. P. (2020). El Niño-Driven Oxygenation Impacts Peruvian Shelf Iron Supply to the South Pacific Ocean. *Geophysical Research Letters*, *47*(7), e2019GL086631. https://doi.org/10.1029/2019GL086631

Redfield, A. C. (1958). The biological control of chemical factors in the environment. *American Scientist*, *46*(3), 205–221.

Schlosser, C., Streu, P., Frank, M., Lavik, G., Croot, P. L., Dengler, M., & Achterberg, E. P. (2018). H_2S events in the Peruvian oxygen minimum zone facilitate enhanced dissolved Fe concentrations. *Scientific Reports*, *8*(1), 12642. https://doi.org/10.1038/s41598-018-30580-w

Schunck, H., Lavik, G., Desai, D. K., Großkopf, T., Kalvelage, T., Löscher, C. R., et al. (2013). Giant Hydrogen Sulfide Plume in the Oxygen Minimum Zone off Peru Supports Chemolithoautotrophy. *PLOS ONE*, *8*(8), e68661. https://doi.org/10.1371/journal.pone.0068661

Selden, C. R., Mulholland, M. R., Widner, B., Bernhardt, P., & Jayakumar, A. (2021). Toward resolving disparate accounts of the extent and magnitude of nitrogen fixation in the Eastern Tropical South Pacific oxygen-deficient zone. *Limnology and Oceanography*, *66*(5), 1950–1960. https://doi.org/10.1002/lno.11735

Shiozaki, T., Kodama, T., & Furuya, K. (2014). Large-scale impact of the island mass effect through nitrogen fixation in the western South Pacific Ocean. *Geophysical Research Letters*, *41*(8), 2907–2913. https://doi.org/10.1002/2014GL059835

Somes, C. J., & Oschlies, A. (2015). On the influence of "non-Redfield" dissolved organic nutrient dynamics on the spatial distribution of N_2 fixation and the size of the marine fixed nitrogen inventory. *Global Biogeochemical Cycles*, *29*(7), 973–993. https://doi.org/10.1002/2014GB005050

Tang, W., Li, Z., & Cassar, N. (2019). Machine Learning Estimates of Global Marine Nitrogen Fixation. *Journal of Geophysical Research: Biogeosciences*, *124*(3), 717–730. https://doi.org/10.1029/2018JG004828

Tang, W., Wang, S., Fonseca-Batista, D., Dehairs, F., Gifford, S., Gonzalez, A. G., et al. (2019). Revisiting the distribution of oceanic N_2 fixation and estimating diazotrophic contribution to marine production. *Nature Communications*, *10*(1), 831. https://doi.org/10.1038/s41467-019-08640-0

code (TOMS 760, H. A. (Fortran, 761, and 433)), 697, functions), A. G. (R port (interp*, functions), bicubic*, function), T. P. (aspline, et al. (2021, November 2). Akima: Interpolation of Irregularly and Regularly Spaced Data (Version 0.6-2.3). Retrieved from https://CRAN.R-project.org/package=akima

Turk-Kubo, K. A., Karamchandani, M., Capone, D. G., & Zehr, J. P. (2014). The paradox of marine heterotrophic nitrogen fixation: abundances of heterotrophic diazotrophs do not account for nitrogen fixation rates in the Eastern Tropical South Pacific. *Environmental Microbiology*, *16*(10), 3095–3114. https://doi.org/10.1111/1462-2920.12346.

Turk-Kubo, K. A., Gradoville, M. R., Cheung, S., Cornejo-Castillo, F. M., Harding, K. J., Morando, M., et al. (2022). Non-cyanobacterial diazotrophs: global diversity, distribution, ecophysiology, and activity in marine waters. *FEMS Microbiology Reviews*, fuac046. https://doi.org/10.1093/femsre/fuac046

Vedamati, J., Goepfert, T., & Moffett, J. W. (2014). Iron speciation in the eastern tropical South Pacific oxygen minimum zone off Peru. *Limnology and Oceanography*, *59*(6), 1945–1957. https://doi.org/10.4319/lo.2014.59.6.1945

Wang, W.-L., Moore, J. K., Martiny, A. C., & Primeau, F. W. (2019). Convergent estimates of marine nitrogen fixation. *Nature*, *566*(7743), 205–211. https://doi.org/10.1038/s41586-019-0911-2

Ward, B. A., Dutkiewicz, S., Moore, C. M., & Follows, M. J. (2013). Iron, phosphorus, and nitrogen supply ratios define the biogeography of nitrogen fixation. *Limnology and Oceanography*, *58*(6), 2059–2075. https://doi.org/10.4319/lo.2013.58.6.2059

Weiss, R. F. (1970). The solubility of nitrogen, oxygen, and argon in water and seawater. *Deep Sea Research and Oceanographic Abstracts*, *17*(4), 721–735. https://doi.org/10.1016/0011-7471(70)90037-9

White, A. E., Granger, J., Selden, C., Gradoville, M. R., Potts, L., Bourbonnais, A., et al. (2020). A critical review of the 15N2 tracer method to measure diazotrophic production in pelagic ecosystems. *Limnology and Oceanography: Methods*, *18*(4), 129–147. https://doi.org/10.1002/lom3.10353

Yang, S., Gruber, N., Long, M. C., & Vogt, M. (2017). ENSO-Driven Variability of Denitrification and Sub-oxia in the Eastern Tropical Pacific Ocean. *Global Biogeochemical Cycles*, *31*(10), 1470–1487. https://doi.org/10.1002/2016GB005596

Chapter 3

Formatted in Science Advances style

1. N. Gruber, J. N. Galloway, An Earth-system perspective of the global nitrogen cycle. Nature. 451, 293–296 (2008).

2. I. Berman-Frank, J. T. Cullen, Y. Shaked, R. M. Sherrell, P. G. Falkowski, Iron availability, cellular iron quotas, and nitrogen fixation in Trichodesmium. Limnol. Oceanogr. 46, 1249–1260 (2001).

3. F. Monteiro, S. Dutkiewicz, M. J. Follows, Biogeographical controls on the marine nitrogen fixers. Global Biogeochem Cycles. 25 (2011).

4. T. Moutin, D. M. Karl, S. Duhamel, P. Rimmelin, P. Raimbault, B. A. S. Van Mooy, H. Claustre, Phosphate availability and the ultimate control of new nitrogen input by nitrogen fixation in the tropical Pacific Ocean. Biogeosciences. 5, 95–109 (2008).

5. Y.-W. Luo, I. D. Lima, D. M. Karl, C. A. Deutsch, S. C. Doney, Data-based assessment of environmental controls on global marine nitrogen fixation. Biogeosciences. 11, 691–708 (2014).

6. D. G. Capone, J. P. Zehr, H. W. Paerl, B. Bergman, E. J. Carpenter, Trichodesmium, a globally significant marine cyanobacterium. Science. 276, 1221–1229 (1997).

7. W. Tang, S. Wang, D. Fonseca-Batista, F. Dehairs, S. Gifford, A. G. Gonzalez, M. Gallinari, H. Planquette, G. Sarthou, N. Cassar, Revisiting the distribution of oceanic N_2 fixation and estimating diazotrophic contribution to marine production. Nat Commun. 10, 831 (2019).

8. W. Tang, Z. Li, N. Cassar, Machine Learning Estimates of Global Marine Nitrogen Fixation. Journal of Geophysical Research: Biogeosciences. 124, 717–730 (2019).

9. J. Karstensen, L. Stramma, M. Visbeck, Oxygen minimum zones in the eastern tropical Atlantic and Pacific Oceans. Prog. Oceanogr. 77, 331–350 (2008).

10. A. Noffke, C. Hensen, S. Sommer, F. Scholz, L. Bohlen, T. Mosch, M. Graco, K. Wallmann, Benthic iron and phosphorus fluxes across the Peruvian oxygen minimum zone. Limnol. Oceanogr. 57, 851–867 (2012).

11. C. Deutsch, J. L. Sarmiento, D. M. Sigman, N. Gruber, J. P. Dunne, Spatial coupling of nitrogen inputs and losses in the ocean. Nature. 445, 163 (2007).

12. B. A. Ward, S. Dutkiewicz, C. M. Moore, M. J. Follows, Iron, phosphorus, and nitrogen supply ratios define the biogeography of nitrogen fixation. Limnol. Oceanogr. 58, 2059–2075 (2013).

13. M. N. W. Grabowski, M. J. Church, D. M. Karl, Nitrogen fixation rates and controls at Stn ALOHA. Aquatic Microbial Ecology. 52, 175–183 (2008).

14. D. Fonseca-Batista, X. Li, V. Riou, V. Michotey, F. Deman, F. Fripiat, S. Guasco, N. Brion, N. Lemaitre, M. Tonnard, M. Gallinari, H. Planquette, F. Planchon, G. Sarthou, M. Elskens, J. LaRoche, L. Chou, F. Dehairs, Evidence of high N_2 fixation rates in the temperate northeast Atlantic. Biogeosciences. 16, 999–1017 (2019).

15. C. R. Löscher, T. Großkopf, F. D. Desai, D. Gill, H. Schunck, P. L. Croot, C. Schlosser, S. C. Neulinger, N. Pinnow, G. Lavik, M. M. M. Kuypers, J. LaRoche, R. A. Schmitz, Facets of diazotrophy in the oxygen minimum zone waters off Peru. ISME J. 8, 2180–2192 (2014).

16. C. R. Selden, M. R. Mulholland, B. Widner, P. Bernhardt, A. Jayakumar, Toward resolving disparate accounts of the extent and magnitude of nitrogen fixation in the Eastern Tropical South Pacific oxygen deficient zone. Limnology and Oceanography. 66, 1950–1960 (2021).

17. C. R. Löscher, A. Bourbonnais, J. Dekaezemacker, C. N. Charoenpong, M. A. Altabet, H. W. Bange, R. Czeschel, C. Hoffmann, R. Schmitz, N_2 fixation in eddies of the eastern tropical South Pacific Ocean. Biogeosciences. 13, 2889–2899 (2016).

18. L. Kittu, M. J. Hopwood, A. J. Paul, M. Fernández-Méndez, E. P. Achterberg, U. Riebesell, Trace metal data from water column samples during RV Maria S. Merian cruise MSM80 off the northern Humboldt Upwelling System (2021).

19. L. Kittu, A. J. Paul, M. Fernández-Méndez, U. Riebesell, Nitrogen and carbon fixation rates and organic matter concentrations from water column samples during RV Maria S. Merian cruise MSM80 off the northern Humboldt Upwelling System (2021).

20. L. Kittu, M. Fernández-Méndez, A. J. Paul, R. Kiko, U. Riebesell, Dissolved inorganic and organic nutrients from water column samples during RV Maria S. Merian cruise MSM80 off the northern Humboldt Upwelling System (2021).

21. G. T. Taylor, J. D. Gulnick, Enhancement of marine bacterial growth by mineral surfaces. Can. J. Microbiol. 42, 911–918 (1996).

22. F. Montserrat, P. Renforth, J. Hartmann, M. Leermakers, P. Knops, F. J. R. Meysman, Olivine Dissolution in Seawater: Implications for CO2 Sequestration through Enhanced Weathering in Coastal Environments. Environ. Sci. Technol. 51, 3960–3972 (2017).

23. T. J. Browning, I. Rapp, C. Schlosser, M. Gledhill, E. P. Achterberg, A. Bracher, F. A. C. L. Moigne, Influence of Iron, Cobalt, and Vitamin B12 Supply on Phytoplankton Growth in the Tropical East Pacific During the 2015 El Niño. Geophys. Res. Lett. 45, 6150–6159 (2018).

24. M. A. Saito, J. W. Moffett, G. R. DiTullio, Cobalt and nickel in the Peru upwelling region: A major flux of labile cobalt utilized as a micronutrient. Global Biogeochemical Cycles. 18 (2004).

25. N. J. Hawco, D. C. Ohnemus, J. A. Resing, B. S. Twining, M. A. Saito, A dissolved cobalt plume in the oxygen minimum zone of the eastern tropical South Pacific. Biogeosciences. 13, 5697–5717 (2016).

26. A. N. Knapp, K. L. Casciotti, W. M. Berelson, M. G. Prokopenko, D. G. Capone, Low rates of nitrogen fixation in eastern tropical South Pacific surface waters. Proc. Natl. Acad. Sci. USA. 113, 4398 (2016).

27. D. A. Hutchins, C. E. Hare, R. S. Weaver, Y. Zhang, G. F. Firme, G. R. Ditullio, M. B. Alm, S. F. Riseman, J. M. Maucher, M. E. Geesey, C. G. Trick, G. J. Smith, E. L. Rue, J. Conn, K. W. Brul, Phytoplankton iron limitation in the Humboldt Current and Peru Upwelling. Limnol. Oceanogr. 47, 997–1011 (2002).

28. M. A. Saito, T. J. Goepfert, J. T. Ritt, Some thoughts on the concept of colimitation: Three definitions and the importance of bioavailability. Limnology and Oceanography. 53, 276–290 (2008).

29. B. X. Chang, A. Jayakumar, B. Widner, P. Bernhardt, C. W. Mordy, M. R. Mulholland, B. B. Ward, Low rates of dinitrogen fixation in the eastern tropical South Pacific. Limnol. Oceanogr. 64, 1913–1923 (2019).

30. W. G. Sunda, S. A. Huntsman, Cobalt and zinc interreplacement in marine phytoplankton: Biological and geochemical implications. Limnology and Oceanography. 40, 1404–1417 (1995).

31. E. M. Bertrand, J. P. McCrow, A. Moustafa, H. Zheng, J. B. McQuaid, T. O. Delmont, A. F. Post, R. E. Sipler, J. L. Spackeen, K. Xu, D. A. Bronk, D. A. Hutchins, A. E. Allen, Phytoplankton–bacterial interactions mediate micronutrient colimitation at the coastal Antarctic sea ice edge. PNAS. 112, 9938–9943 (2015).

32. E. M. Bertrand, M. A. Saito, J. M. Rose, C. R. Riesselman, M. C. Lohan, A. E. Noble, P. A. Lee, G. R. DiTullio, Vitamin B12 and iron colimitation of phytoplankton growth in the Ross Sea. Limnology and Oceanography. 52, 1079–1093 (2007).

33. M. A. Saito, G. Rocap, J. W. Moffett, Production of cobalt binding ligands in a Synechococcus feature at the Costa Rica upwelling dome (2005).

34. C. Panzeca, A. J. Beck, K. Leblanc, G. T. Taylor, D. A. Hutchins, S. A. Sañudo-Wilhelmy, Potential cobalt limitation of vitamin B_{12} synthesis in the North Atlantic Ocean. Global Biogeochemical Cycles. 22 (2008).

35. I. B. Rodriguez, T.-Y. Ho, Influence of Co and B_{12} on the growth and nitrogen fixation of Trichodesmium. Frontiers in Microbiology. 6, 623 (2015).

36. S. Bonnet, E. Webb, C. Panzeca, D. Karl, D. Capone, S. A. S. Wilhelmy, Vitamin B_{12} excretion by cultures of the marine cyanobacteria Crocosphaera and Synechococcus (2010).

37. J. Meyer, C. R. Löscher, G. Lavik, U. Riebesell, Mechanisms of P* Reduction in the Eastern Tropical South Pacific. Front. Mar. Sci. 4 (2017).

38. K. C. Ruttenberg, S. T. Dyhrman, Dissolved organic phosphorus production during simulated phytoplankton blooms in a coastal upwelling system. Front. Microbiol. 3 (2012).

39. S. T. Dyhrman, S. T. Haley, Phosphorus Scavenging in the Unicellular Marine Diazotroph Crocosphaera watsonii. Applied and Environmental Microbiology. 72, 1452–1458 (2006).

40. E. M. Bertrand, M. A. Saito, Y. J. Jeon, B. A. Neilan, Vitamin B_{12} biosynthesis gene diversity in the Ross Sea: the identification of a new group of putative polar B_{12} biosynthesizers. Environ Microbiol. 13, 1285–1298 (2011).

41. M. A. Saito, A. E. Noble, N. Hawco, B. S. Twining, D. C. Ohnemus, S. G. John, P. Lam, T. M. Conway, R. Johnson, D. Moran, M. McIlvin, The acceleration of dissolved cobalt's ecological stoichiometry due to biological uptake, remineralization, and scavenging in the Atlantic Ocean. Biogeosciences. 14, 4637–4662 (2017).

42. S. T. Dyhrman, P. D. Chappell, S. T. Haley, J. W. Moffett, E. D. Orchard, J. B. Waterbury, E. A. Webb, Phosphonate utilization by the globally important marine diazotroph Trichodesmium. Nature. 439, 68–71 (2006).

43. R. Middag, H. J. W. de Baar, K. W. Bruland, S. M. A. C. van Heuven, The Distribution of Nickel in the West-Atlantic Ocean, Its Relationship With Phosphate and a Comparison to Cadmium and Zinc. Frontiers in Marine Science. 7 (2020).

44. C. L. Dupont, K. Neupane, J. Shearer, B. Palenik, Diversity, function and evolution of genes coding for putative Ni-containing superoxide dismutases. Environ Microbiol. 10, 1831–1843 (2008).

45. P. Tamagnini, E. Leitão, P. Oliveira, D. Ferreira, F. Pinto, D. J. Harris, T. Heidorn, P. Lindblad, Cyanobacterial hydrogenases: diversity, regulation and applications. FEMS Microbiology Reviews. 31, 692–720 (2007).

46. J. R. Gallon, The oxygen sensitivity of nitrogenase: a problem for biochemists and micro-organisms. Trends in Biochemical Sciences. 6, 19–23 (1981).

47. C.-C. Chen, I. B. Rodriguez, Y. L. Chen, J. P. Zehr, Y.-R. Chen, S.-T. D. Hsu, S.-C. Yang, T.-Y. Ho, Nickel superoxide dismutase protects nitrogen fixation in Trichodesmium. Limnology and Oceanography Letters. 7, 363–371 (2022).

48. S. G. John, R. L. Kelly, X. Bian, F. Fu, M. I. Smith, N. T. Lanning, H. Liang, B. Pasquier, E. A. Seelen, M. Holzer, L. Wasylenki, T. M. Conway, J. N. Fitzsimmons, D. A. Hutchins, S.-C. Yang, The biogeochemical balance of oceanic nickel cycling. Nat. Geosci., 1–7 (2022).

49. A. Kustka, E. J. Carpenter, S. A. Sañudo-Wilhelmy, Iron and marine nitrogen fixation: progress and future directions. Research in Microbiology. 153, 255–262 (2002).

50. A. Puppo, J. Rigaud, Superoxide dismutase: an essential role in the protection of the nitrogen fixation process? FEBS Letters. 201, 187–189 (1986).

51. T.-Y. Ho, Nickel limitation of nitrogen fixation in Trichodesmium. Limnology and Oceanography. 58, 112–120 (2013).

52. I. B. Rodriguez, T.-Y. Ho, Diel nitrogen fixation pattern of Trichodesmium: the interactive control of light and Ni. Sci Rep. 4, 4445 (2014).

53. N. Lemaitre, C. Archer, G. de Souza, J. (JD) Du, D. Vance, "The oceanic biogeochemistry of nickel and its isotopes" in (GOLDSCHMIDT, 2021; https://2021.goldschmidt.info/goldschmidt/2021/meetingapp.cgi/Paper/5232).

54. J. A. Coyer, A. Cabello-Pasini, H. Swift, R. S. Alberte, N_2 fixation in marine heterotrophic bacteria: dynamics of environmental and molecular regulation. Proceedings of the National Academy of Sciences. 93, 3575–3580 (1996).

55. I. Rapp, C. Schlosser, T. J. Browning, F. Wolf, F. A. C. L. Moigne, M. Gledhill, E. P. Achterberg, El Nino-driven oxygenation impacts Peruvian shelf iron supply to the South Pacific Ocean. Geophysical Research Letters. 47, (2020).

56. K. A. Turk-Kubo, M. Karamchandani, D. G. Capone, J. P. Zehr, The paradox of marine heterotrophic nitrogen fixation: abundances of heterotrophic diazotrophs do not account for nitrogen fixation rates in the Eastern Tropical South Pacific. Environ. Microbiol. 16, 3095–3114 (2014).

57. H.-T. Li, S.-H. Tuo, M.-C. Lu, T.-Y. Ho, The effects of Ni availability on H_2 production and N_2 fixation in a model unicellular diazotroph: The expression of hydrogenase and nitrogenase. Limnology and Oceanography. 67, 1566–1576 (2022).

58. S. Tuo, I. B. Rodriguez, T.-Y. Ho, H_2 accumulation and N_2 fixation variation by Ni limitation in Cyanothece. Limnology and Oceanography. 65, 377–386 (2020).

59. L. Riemann, Eyal Rahav, Uta Passow, Hans-Peter Grossart, Dirk de Beer, Isabell Klawonn, Meri Eichner, Mar Benavides, Edo Bar-Zeev, Planktonic Aggregates as Hotspots for Heterotrophic Diazotrophy: The Plot Thickens. Frontiers in Microbiology (2022).

60. L. T. Bach, S. J. Gill, R. E. M. Rickaby, S. Gore, P. Renforth, CO_2 Removal With Enhanced Weathering and Ocean Alkalinity Enhancement: Potential Risks and Co-benefits for Marine Pelagic Ecosystems. Frontiers in Climate. 1 (2019).

61. T. Großkopf, W. Mohr, T. Baustian, H. Schunck, D. Gill, M. M. M. Kuypers, G. Lavik, R. A. Schmitz, D. W. R. Wallace, J. LaRoche, Doubling of marine dinitrogen-fixation rates based on direct measurements. Nature. 488, 361–364 (2012).

62. W. Mohr, T. Großkopf, D. W. R. Wallace, J. LaRoche, Methodological Underestimation of Oceanic Nitrogen Fixation Rates. PLoS ONE. 5, e12583 (2010).

63. J. P. Montoya, M. Voss, P. Kahler, D. G. Capone, A simple, high-precision, high-sensitivity tracer assay for N_2 fixation. Appl. Environ. Microbiol. 62, 986–993 (1996).

64. A. E. White, J. Granger, C. Selden, M. R. Gradoville, L. Potts, A. Bourbonnais, R. W. Fulweiler, A. N. Knapp, W. Mohr, P. H. Moisander, C. R. Tobias, M. Caffin, S. T. Wilson, M. Benavides, S. Bonnet, M. R. Mulholland, B. X. Chang, A critical review of the $^{15}N_2$ tracer method to measure diazotrophic production in pelagic ecosystems. Limnol Oceanogr-Meth. 18, 129–147 (2020).

65. R. M. Holmes, A. Aminot, R. Kérouel, B. A. Hooker, B. J. Peterson, A simple and precise method for measuring ammonium in marine and freshwater ecosystems. Can. J. Fish. Aquat. Sci. (2011).

66. A. W. Morris, J. P. Riley, The determination of nitrate in sea water. Anal. Chim. Acta. 29, 272–279 (1963).

67. J. Murphy, J. P. Riley, A modified single solution method for the determination of phosphate in natural waters. Anal. Chim. Acta. 27, 31–36 (1962).

68. P. Parekh, M. J. Follows, E. A. Boyle, Decoupling of iron and phosphate in the global ocean. Global Biogeochemical Cycles. 19 (2005).

69. C. M. Moore, Diagnosing oceanic nutrient deficiency. Philosophical Transactions of the Royal Society A: Mathematical, Physical and Engineering Sciences. 374, 20150290 (2016).

70. J. Elith, J. R. Leathwick, T. Hastie, A working guide to boosted regression trees. J Anim Ecol. 77, 802–813 (2008).

71. B. Greenwell, B. Boehmke, J. Cunningham, G. B. M. Developers (https://github.com/gbm-developers), gbm: Generalized Boosted Regression Models (2020).

72. D. Müller, P. J. Leitão, T. Sikor, Comparing the determinants of cropland abandonment in Albania and Romania using boosted regression trees. Agricultural Systems. 117, 66–77 (2013).

Chapter 4

Formatted in Limnology and Oceanography Style

Arrigo, K. R. 2005. Marine microorganisms and global nutrient cycles. Nature **437**: 349–355. doi:10.1038/nature04159

Bach, L. T., A. J. Paul, T. Boxhammer, and others. 2020. Factors controlling plankton community production, export flux, and particulate matter stoichiometry in the coastal upwelling system off Peru. Biogeosciences **17**: 4831–4852. doi:https://doi.org/10.5194/bg-17-4831-2020

Bakun, A., B. A. Black, S. J. Bograd, M. García-Reyes, A. J. Miller, R. R. Rykaczewski, and W. J. Sydeman. 2015. Anticipated Effects of Climate Change on Coastal Upwelling Ecosystems. Curr. Clim. Change. **Rep 1:** 85–93. doi:10.1007/s40641-015-0008-4

Barber, R. T., and F. P. Chavez. 1983. Biological Consequences of El Niño. Science **222**: 1203–1210. doi:10.1126/science.222.4629.1203

Behrenfeld, M. J. 2010. Abandoning Sverdrup's Critical Depth Hypothesis on phytoplankton blooms. Ecology **91**: 977–989. doi:10.1890/09-1207.1

Berman, T., and D. A. Bronk. 2003. Dissolved organic nitrogen: a dynamic participant in aquatic ecosystems. Aquat. Microb. Ecol. **31:** 279–305. doi:10.3354/ame031279

Bouman, H. A., T. Platt, M. Doblin, and others. 2018. Photosynthesis–irradiance parameters of marine phytoplankton: synthesis of a global data set. Earth System Science Data **10**: 251–266. doi:10.5194/essd-10-251-2018

Bristow, L. A., W. Mohr, S. Ahmerkamp, and M. M. M. Kuypers. 2017. Nutrients that limit growth in the ocean. Curr. Biol. **27**: R474–R478. doi:10.1016/j.cub.2017.03.030

Bronk, D. A. 2002. Chapter 5 - Dynamics of DON, p. 153–247. In D.A. Hansell and C.A. Carlson [eds.], Biogeochemistry of Marine Dissolved Organic Matter. Academic Press.

Bruland, K. W., E. L. Rue, G. J. Smith, and G. R. DiTullio. 2005. Iron, macronutrients and diatom blooms in the Peru upwelling regime: brown and blue waters of Peru. Mar. Chem. **93**: 81–103. doi:10.1016/j.marchem.2004.06.011

Chavez, F., A. Bertrand, R. Guevara-Carrasco, P. Soler, and J. Csirke. 2008. The northern Humboldt Current System: Brief history, present status and a view towards the future. Prog. Oceanogr. 79: 95–105. doi:10.1016/j.pocean.2008.10.012

Chavez, F. P., and M. Messié. 2009. A comparison of Eastern Boundary Upwelling Ecosystems. Progr. Oceanogr. 83: 80–96. doi:10.1016/j.pocean.2009.07.032

Cochlan, W. P., N. M. Price, and P. J. Harrison. 1991. Effects of irradiance on nitrogen uptake by phytoplankton: comparison of frontal and stratified communities. Mar. Ecol. Progr. Ser. 69: 103.

Collos, Y. 1998. Nitrate uptake, nitrite release and uptake, and new production estimates. Mar. Ecol. Prog. Ser. 171: 293–301. doi:10.3354/meps171293

Dugdale, R. C. 1972. Chemical oceanography and primary productivity in upwelling regions. Geoforum 3: 47–61. doi:10.1016/0016-7185(72)90085-1

Dugdale, R. C., and J. J. Goering. 1967. Uptake of new and regenerated forms of nitrogen in primary productivity. Limnol. Oceanogr. 12: 196–206. doi:10.4319/lo.1967.12.2.0196

Dugdale, R. C., and F. P. Wilkerson. 1986. The use of ^{15}N to measure nitrogen uptake in eutrophic oceans; experimental considerations. Limnol. Oceanogr. 31: 673–689. doi:10.4319/lo.1986.31.4.0673

Echevin, V., O. Aumont, J. Ledesma, and G. Flores. 2008. The seasonal cycle of surface chlorophyll in the Peruvian upwelling system: A modelling study. Prog. Oceanogr. 79: 167–176.

Edwards, K. F., M. K. Thomas, C. A. Klausmeier, and E. Litchman. 2015. Light and growth in marine phytoplankton: allometric, taxonomic, and environmental variation. Limnol. Oceanogr 60: 540–552. doi:10.1002/lno.10033

Edwards, K. F., M. K. Thomas, C. A. Klausmeier, and E. Litchman. 2016. Phytoplankton growth and the interaction of light and temperature: A synthesis at the species and community level. Limnol. Oceanogr. 61: 1232–1244. doi:10.1002/lno.10282

Fawcett, S. E., and B. B. Ward. 2011. Phytoplankton succession and nitrogen utilization during the development of an upwelling bloom. Mar. Ecol. Prog. Ser 428: 13–31. doi:10.3354/meps09070

Fernández, C., L. Farías, and M. E. Alcaman. 2009. Primary production and nitrogen regeneration processes in surface waters of the Peruvian upwelling system. Progr.Oceanogr. 83: 159–168. doi:10.1016/j.pocean.2009.07.010

Franz, J., H. Hauss, U. Sommer, T. Dittmar, and U. Riebesell. 2012a. Production, partitioning and stoichiometry of organic matter under variable nutrient supply during mesocosm experiments in the tropical Pacific and Atlantic Ocean. Biogeosciences **9:** 4629–4643. doi:10.5194/bg-9-4629-2012

Franz, J., G. Krahmann, G. Lavik, P. Grasse, T. Dittmar, and U. Riebesell. 2012b. Dynamics and stoichiometry of nutrients and phytoplankton in waters influenced by the oxygen minimum zone in the eastern tropical Pacific. Deep Sea Res. Part I Oceanogr. Res. Pap **62:** 20–31. doi:10.1016/j.dsr.2011.12.004

Hu, S., and W. O. Smith. 1998. The effects of irradiance on nitrate uptake and dissolved organic nitrogen release by phytoplankton in the Ross Sea. Continental Shelf Research **18**: 971–990. doi:10.1016/S0278-4343(98)00021-1

Harrison, W. g., T. Platt, R. Calienes, and N. Ochoa. 1981. Photosynthetic Parameters and Primary Production of Phytoplankton Populations off the Northern Coast of Peru, p. 303–311. In Coastal Upwelling. American Geophysical Union (AGU).

Hutchins, D. A., C. E. Hare, R. S. Weaver, and others. 2002. Phytoplankton iron limitation in the Humboldt Current and Peru Upwelling. Limnol. Oceanogr. **47:** 997–1011. doi:10.4319/lo.2002.47.4.0997

Jones, C. T., S. E. Craig, A. B. Barnett, H. L. MacIntyre, and J. J. Cullen. 2014. Curvature in models of the photosynthesis-irradiance response. J. Phycol. **50:** 341–355. doi:10.1111/jpy.12164

Kämpf, J., and P. Chapman. 2016. The Functioning of Coastal Upwelling Systems, p. 31–65. In J. Kämpf and P. Chapman [eds.], Upwelling Systems of the World: A Scientific Journey to the Most Productive Marine Ecosystems. Springer International Publishing.

Kiefer, D. A., R. J. Olson, and O. Holm-Hansen. 1976. Another look at the nitrite and chlorophyll maxima in the central North Pacific. Deep-Sea Res. Oceanogr. Abstr. **23:** 1199–1208. doi:10.1016/0011-7471(76)90895-0

Kittu, L. R., A. J. Paul, M. Fernández-Méndez, M. J. Hopwood, and U. Riebesell. 2023. Coastal N_2 Fixation Rates Coincide Spatially With Nitrogen Loss in the Humboldt Upwelling System off Peru. Global Biogeochem. Cycles **37:** e2022GB007578. doi:10.1029/2022GB007578

MacIsaac, J. J., and R. C. Dugdale. 1972. Interactions of light and inorganic nitrogen in controlling nitrogen uptake in the sea. Deep-Sea Res. Oceanogr. Abstr. **19:** 209–232. doi:10.1016/0011-7471(72)90032-0

Mackey, D. J., H. W. Higgins, M. D. Mackey, and D. Holdsworth. 1998. Algal class abundances in the western equatorial Pacific: Estimation from HPLC measurements of chloroplast pigments using CHEMTAX. Deep Sea Res. Part I: Oceanogr. Res. Pap. **45:** 1441–1468. doi:10.1016/S0967-0637(98)00025-9

Messié, M., and F. P. Chavez. 2015. Seasonal regulation of primary production in eastern boundary upwelling systems. Prog. Oceanogr. **134:** 1–18. doi:10.1016/j.pocean.2014.10.011

Messié, M., J. Ledesma, D. D. Kolber, R. P. Michisaki, D. G. Foley, and F. P. Chavez. 2009. Potential new production estimates in four eastern boundary upwelling ecosystems. Progr. Oceanogr. **83**: 151–158. doi:10.1016/j.pocean.2009.07.018

Meyer, J., C. R. Löscher, G. Lavik, and U. Riebesell. 2017. Mechanisms of P* Reduction in the Eastern Tropical South Pacific. Front. Mar. Sci**. 4**. doi:10.3389/fmars.2017.00001

Morris, A. W., and J. P. Riley. 1963. The determination of nitrate in seawater. Anal. Chim. Acta. **29:** 272–279. doi:10.1016/S0003-2670(00)88614-6

Muggli, D. L., and W. O. Smith. 1993. Regulation of nitrate and ammonium uptake in the Greenland Sea. Marine Biology **115**: 199–208. doi:10.1007/BF00346336

NASA/JPL. 2020. MODIS Aqua Level 3 SST Thermal IR Annual 4km Daytime V2019.0.doi:10.5067/MODSA-AN4D9

Paul, A. J., L. T. Bach, J. Arístegui, and others. 2022. Upwelled plankton community modulates surface bloom succession and nutrient availability in a natural plankton assemblage. Biogeosciences **19:** 5911–5926. doi:10.5194/bg-19-5911-2022

Pennington, J. T., K. L. Mahoney, V. S. Kuwahara, D. D. Kolber, R. Calienes, and F. P. Chavez. 2006. Primary production in the eastern tropical Pacific: A review. Prog. Oceanogr. **69:** 285–317. doi:10.1016/j.pocean.2006.03.012

Platt, T., S. Sathyendranath, I. Joint, and M. J. R. Fasham. 1993. Photosynthesis characteristics of the phytoplankton in the Celtic Sea during late spring. Fish. Oceanogr. **2:** 191–201. doi:10.1111/j.1365-2419.1993.tb00135.x

Platt, T., S. Sathyendranath, G. N. White, T. Jackson, S. Saux Picart, and H. Bouman. 2017. Primary Production: Sensitivity to Surface Irradiance and Implications for Archiving Data. Front. Mar. Sci. **4.**

Redfield, A. C. 1958. The biological control of chemical factors in the environment. Am. Sci. **46:** 205–221.

Sasai, Y., S. L. Smith, E. Siswanto, H. Sasaki, and M. Nonaka. 2022. Physiological flexibility of phytoplankton impacts modelled chlorophyll and primary production across the North Pacific Ocean. Biogeosciences **19:** 4865–4882. doi:10.5194/bg-19-4865-2022

Shiozaki, T., Ken Furuya, Taketoshi Kodama, and Shigenobu Takeda. 2009. Contribution of N_2 fixation to new production in the western North Pacific Ocean along 155°E. Mar. Ecol. Progr.Ser. doi:10.3354/meps07837

Slawyk, G., Y. Collos, and J.-C. Auclair. 1977. The use of the ^{13}C and ^{15}N isotopes for the simultaneous measurement of carbon and nitrogen turnover rates in marine phytoplankton1. Limnol. Oceanogr. **22:** 925–932. doi:10.4319/lo.1977.22.5.0925

Thomas, A. C., P. Brickley, and R. Weatherbee. 2009. Interannual variability in chlorophyll concentrations in the Humboldt and California Current Systems. Prog. Oceanogr. **83:** 386–392. doi:10.1016/j.pocean.2009.07.020

Tyrrell, T. 1999. The relative influences of nitrogen and phosphorus on oceanic primary production. Nature **400:** 525. doi:10.1038/22941

Westberry, T., M. J. Behrenfeld, D. A. Siegel, and E. Boss. 2008. Carbon-based primary productivity modelling with vertically resolved photoacclimation. Global Biogeochem. Cycles. **22:** GB2024. doi:10.1029/2007GB003078

Wilkerson, F. P., and R. C. Dugdale. 1987. The use of large shipboard barrels and drifters to study the effects of coastal upwelling on phytoplankton dynamics1, 2. Limnol. Oceanogr.**32:** 368–382. doi:10.4319/lo.1987.32.2.0368

Acknowledgements

This doctoral dissertation was carried out within the framework of the Project BioTip, subproject: Humboldt Tipping (01LC1823B), funded by Bundesministerium für Bildung und Forschung (BMBF). This doctoral work is part of Work Package 1 of Humboldt Tipping directly supervised by Dr. Allanah J. Paul and Prof. Dr. Ulf Riebesell. In addition, this dissertation work has also benefited from the BMBF project Coastal Upwelling in a Changing Ocean (CUSCO, FKZ03F0) as well as collaborations and research stays at Instituto Del Mar del Peru (IMARPE, Peru) and the University of Southern Denmark (SDU, Odense). I am grateful for the financial support and wonderful collaboration I benefitted from in this project.

Seven years ago, I started my academic career at GEOMAR Helmholtz Centre for Ocean Research as a master's student. The last four years of this time make up the great challenging and exhilarating endeavour of my doctoral studies journey. If you are lucky, as I have been, you can only accomplish this journey with the help and support of people from whom you learn and channel the strength to power on. This is one of the sections of this dissertation I was looking forward to write, so I apologize in advance for the length but I believe I cannot use a few formal sentences to express my gratitude.

To the almighty God, in whom my faith has grounded me over the course of the last four years, I give the glory.

I am enormously grateful to my advisor Prof. Dr. Ulf Riebesell with whom I have had the pleasure and privilege to learn and exchange ideas with over the last 7 years of knowing him. As my lecturer, you re-ignited my fascination for the ocean and all things marine biogeochemistry. You gave me the opportunity as a master's student to learn and explore this path while visiting different parts of the world's ocean. Later, as my doctoral advisor, you provided me with scientific freedom and financial security that allowed me to broaden my scientific expertise. As a member of your research group, you challenged me to always take on new tasks and responsibilities that have nurtured me professionally and personally. I will always have fond memories of our inspiring conversations on science and life. Thank you for providing me with all these opportunities over the years. It will take at least another seven years if not more for me to realize how much I have learnt from you and through it all, I remain forever grateful.

Dr. Allanah Paul, you are my gift that kept giving. You have been not only my supervisor but also instrumental support, personally and mentally during this time. Thank you for always making time for me. I am grateful for your patience in introducing me to the wonderful world of the Nitrogen we cannot breathe but need, I am utterly fixated ☺!! You taught me all I had to learn during my master's thesis to get me started on this journey. During my doctoral work, you created room for me to think independently and be creative with my ideas as I developed my scientific research skills. Thank you for pausing your life in Kiel to travel with me back and forth to Peru and supporting this project that has had its fair share of challenges. Your dedication and positive outlook through the professional challenges kept me afloat. Our professional and personal conversations were always inspiring and I hope they remain that way. Thank you for showing me that you can be a great scientist and teach with humility. As a friend, you lent me a listening ear and held my hand firm through the downs of my graduate

and doctorate timeline. Truly, words cannot fully describe my gratitude, to put it humbly, in the words of Paulo Coelho, *"a teacher is someone who inspires the student to give her best in order to discover what she already knows"*, you have been my teacher.

I would like to thank Prof. Dr. Maren Voss, Prof. Dr. Andreas Oschlies and Prof. Dr. Silvia Sanders. Even though it is your professional duty, I count myself privileged to have you as part of my doctoral thesis committee. Thank you for answering my request email and for taking the time off your busy schedules to read the defendable dissertation draft and attend my defence.

Dr. Caroline Löscher, Dr. Mar Fernandez-Mendez, Dr. Mark Hopwood, and Dr. Michelle Graco, so far yet so near. Working and knowing all of you has been a luxury. I am grateful for your time to discuss research ideas and life. Caro and Mar, through you, I got an unfiltered preview into all thing's women in science, the good and bad. I channel you when I think of fierce women in this profession and I know I can always count on your support. Caro, thank you for hosting me in your lab at SDU-Odense and introducing me to a vibrant team of researchers. For your helpful comments on my first manuscript and for entertaining my crazy ideas on cryptic nitrogen fixation and trace metals. It was all a pleasure and I hope to work together again in the future. Mar and family Sieben-Fernandez, what can I say, you welcomed me to your wonderful family. Mar, thank you for being a personal and professional friend and for being there any time I needed your help in this journey. I hope to make it to more concerts and *chiringitos* with you now that all this is done and you hopefully have an assistant and daycare ☺!!. Mark, thank you for being part of my professional growth from the beginning when I walked into your office asking for your opinion about the role of iron in the ocean and I walked out with a bottle of iron to take on my cruise. With you, I had a crash course on trace metals and scientific writing. You not only gave me iron but also great ideas that have helped refine my second manuscript and I keep drawing from them to develop my research focus. Michelle, thank you for your support on the Peruvian cruises and for hosting me at IMARPE.

I recognize the support of the captains, crew members, and scientists onboard the MSM80 cruise of the German R/V Maria S Merian which was instrumental to my work this far. Specifically, I thank Dr. Allanah Paul, Dr. Mar Fernanadez-Mendez, Dr. Joaquin Ortiz, Dr. Rainer Kiko, and Dr. Michael Meyerhöfer for assisting with onboard sampling and Kastriot Quelaj for nutrient sampling and analysis. Our great team spirit on board made the seven weeks bearable.

To past and present members of the FB2-BI group, thank you for the welcoming attitude you created in the group. The opportunities to travel with the KOSMOS team have surely added to my perspective of what great team effort can accomplish. Through the uniqueness of this group and the members that have crossed my path, I have built strong friendships that I hope will last the test of time and the mobility in this career that sometimes keeps us apart. *Mi Arbeitskollegen especiales*, Dr. Joaquin Ortiz and Nicolas Sanchez, "puchis", thank you for making this journey a full experience. No life topic was taboo to us. In a society where so much is censored and unsaid, you provided a safe and free environment for some raw and difficult conversations of our time, and we had fun while at it. I always laughed loudest when with you either in room 214 or the comfort of our homes. Our time together fed my intellectual appetite in ways no book would. Let's do this at least once a year in some corner of the world with good coffee and food. Just no Udon noodles again please!!!!. Antonia, even though for a limited time, thank you for sharing your brilliance with me and for the constant supply of chocolate. My next-door office neighbours Dr. Carsten Spisla and Dr. Moritz Baumann and Dr. Michael

Sswat just one floor above, the coffees and chats were a highlight of my work days, thank you. Micha thank you for taking your time to revieing my summary, your attention to detail helped refine it. Dr. Silvan Goldenberg, I am grateful for your support as a colleague and friend, especially during the height of the pandemic. Thank you for always being ready to help, teach and advise. Dr. Giulia Faucher, while you came towards the end, your timing was perfect. Your friendship has kept me sane over this past year. Your optimism, objectivity and perspective have been a breath of fresh air, *"Lo apprezzo molto"*. None of the N_2 fixation rates I report here would have been realised without the mass spectrometry expertise of Kerstin Nachtigall. Your help in the lab these past years has been vital to my work, thank you for literally dissecting the mass spectrometer to teach me everything you know. Dr. Silke Lischka, thank you for your kind listening ear and motivating chats. Silvana Gagliardi and Monika Peschke, I am grateful for your support in taking over most of the administrative obligations, which gave me time to focus on my work.

Throughout my doctoral studies, I have enjoyed and appreciated necessary distractions from friends in Kenya, Kiel and elsewhere in the world. Waithira and Mercy, I wouldn't have done any of it without you. Your encouragement, companionship and unconditional support have kept me grounded; I remain forever grateful. A special thanks to Clarissa, Salma, Alba, Mirian, Mariana, TianFei, Gregor and Elsa for the good times and great conversations we had. Thank you to all the PhD students at SDU-Odense, especially Christian who made me feel part of them from the first day. I will not forget the good times and cakes I had with you all.

I wish to extend my gratitude to Dr.Sabine Milde of the graduate centre at CAU, Dr. Avan Antia and the former ISOS team for supporting doctoral students throughout their journey. I have benefitted from the high-quality courses and talks on soft and hard skills and funding opportunities that have been provided through your respective programs. I consider myself equipped to navigate the professional field because of what I learnt through your work. Dr. Sabine, thank you for offering the Zeitschreibtische where I could retreat and work on my manuscripts and dissertation without distractions over the last year. It made a big difference to have this privilege.

The glue that holds me together, my family. Mama, the greatest blessing and support of my life, you opened and keep opening doors for me, through your prayers and thoughts. Truly this is your phD. Dad, your unconditional love and support meant everything to me. My siblings Hammy, Francois, Andy and Cindy thank you for your warmth and unconditional love and support. Luca my blessing, these last 2 years have been a rollercoaster and you probably will never believe me again when I say I will be done with something in half a year ☺. I am grateful for your love, laughter, understanding, encouragement and raw advice. Thank you for making sure I ate and drank during these last weeks of finishing this dissertation and your helpful critique and translation of my summary. For opening the doors to your life and sharing your family with me, I now have a second family, *Asante sana!!*

Last but not least, thank you to me for following my dreams and sticking through the challenging and good times. As I look back and connect the dots, I am convinced, it has all been worth it.

Eidesstattliche Erklärung

Hiermit erkläre ich, dass die vorliegende Dissertation mit dem Titel:

Assessing the biogeochemical role and controls of nitrogen fixation in the Eastern Tropical South Pacific

von mir selbstständig verfasst worden ist und keine weiteren Quellen und Hilfsmittel als die angegebenen verwendet wurden. Die vorliegende Arbeit ist unter Einhaltung der Regeln guter wissenschaftlicher Praxis der Deutschen Forschungsgemeinschaft entstanden und wurde weder im Rahmen eines Prüfungsverfahrens an anderer Stelle vorgelegt noch veröffentlicht. Veröffentlichte oder zur Veröffentlichung eingereichte Manuskripte wurden kenntlich gemacht. Ich erkläre ebenfalls, dass mir zu keinem Zeitpunkt ein akademischer Grad entzogen worden ist.

Ich erkläre mich einverstanden, dass diese Arbeit an die Bibliotheken des GEOMAR Helmholtz-Zentrum für Ozeanforschung Kiel und der Christian-Albrechts-Universität zu Kiel weitergeleitet wird.

Kiel: 10.07.2023 Leila Richards Kittu, MSc.